Investigating the effect of *RICTOR*-deficiency in mTORC2 assembly/activity and its impact on human embryonic stem cell properties

Yueh-Ho Chiu

Thesis submitted towards the fulfilment of the degree of

Doctor of Philosophy

Institute of Reproductive and Developmental Biology
Department of Metabolism, Digestion and Reproduction
Faculty of Medicine
Imperial College London

October 2019

Abstract

The mechanistic target of rapamycin (mTOR) signalling plays crucial roles in controlling mammalian cell behaviour and function, and thereby maintains tissue homeostasis and organism health. This signalling functions through two distinct multi-protein complexes, mTOR complex 1 (mTORC1) and mTOR complex 2 (mTORC2). Both complexes are essential in embryo development as deficiency of either one in mouse leads to embryonic lethality. Considerable knowledge has been obtained regarding to mTORC1 while much less is known about mTORC2, including its function in human embryonic development. In the current study, I utilise CRISPR/Cas9 technology to generate *mTORC2*-deficient HEK 293T cells and human embryonic stem cells (hESCs) by disrupting one of the mTORC2 key components, *RICTOR* gene. With these *RICTOR*-knockout cell model systems, I explored the relationship between the two key subunits (RICTOR and mSIN1) of mTORC2 and their functions in mTORC2 assembly/activity. In particularly, I investigated the effect of *mTORC2*-deficiency on human pluripotent stem cell properties.

Using *RICTOR*-KO 293T cells, I have demonstrated that the protein expression of mSIN1 is substantially diminished upon *RICTOR*-deficiency and so does the mTORC2 activity. Further analyses demonstrate that RICTOR/mTORC2 is crucial for mSIN1 protein stability, which may be partly attributed to the mTORC2-associated phosphorylation on mSIN1-Ser260/270 residues. More importantly, this phosphorylation may also affect substrate recognition of mTORC2, suggesting that mTORC2 may have an auto-regulatory function which affects its substrate selection. In addition to the 293T cells, my data in hESCs reveal that mTORC2 signalling may be dispensable for the hESC self-renewal but may have a function in their cell fate determination, particularly in the differentiation of the mesendoderm lineages. Collectively, my findings advance our understanding in both regulation and function of RICTOR/mTORC2 and knockout cells generated from this work are valuable cell models for the further studies on this important signalling pathway, which will provide potential insights for both new therapies development and regenerative applications.

Statement of Originality

All the experiments in this thesis were conducted by me unless otherwise stated in the text.

Copyright Declarations

The copyright of this thesis rests with the author and is made available under a Creative Commons Attribution Non-Commercial No Derivatives licence. Researchers are free to copy, distribute or transmit the thesis on the condition that they attribute it, that they do not use it for commercial purposes and that they do not alter, transform or build upon it. For any reuse or redistribution, researchers must make clear to others the licence terms of this work.

2019

Acknowledgements

First of all, I would like to express my sincere gratitude to my adviser, Dr. Wei Cui, for supervising and supporting me in the last four years. Her patience, encouragement and immense knowledge in science helped me in all the time of research. For me, Dr. Wei Cui is more than an equal partnership than a supervisor to student throughout the time of my PhD.

Besides my supervisor, I would like to show my appreciation to my colleagues in the lab, past and present, Dr. Shuchen Zhang, Dr. Siti Aminah Muhammad Imran, Huihan Zhi, Jiaxi Zheng, Manjari Triverdi, Karishma Valand and Faiza Batool. All of you have been there to support me and made this experience truly memorable. My sincere thanks also goes to Dr. Veronique Azuara and her group, who generously helped and provided insightful suggestions on my research. With a special mention to my accessors of early and late stage review: Dr. Olivier Emmanuel PARDO and Dr. Navaratnam Naveenan, for their invaluable comments that broaden my research topic from various perspectives. All gratitude and thanks to my Viva examiners, Dr. Aylin C. Hanyaloglu and Prof. Majlinda Lako, for giving their valuable comments and suggestions on this thesis.

A special thanks to all my friends in London and Taiwan who always have my back. With their encouragement and accompany (and provision of alcohol), I achieved my important goal in my life and had a wonderful time during this long journey.

Last but not least, to my beloved family, especially my parents. Words cannot express how grateful I am for their love and support. They are my cheerleaders, my supporters, my strongest shield against any difficulties and the reason that sustained me thus far. I love you all, sincerely.

誌謝

我是一個幸運到自己想哭的人。

18 歲的我也許無法想像自己會有拿到博士學位的一天，畢竟我當時一心一意只想穿著曉明校服在一中街的水利大樓前溜滑板車[1]。回首博士班這 4 年的日子，和許多同樣是在博士班這片真理汪洋中載浮載沉的人相比起來，我何其幸運的一路以來得到許多人的支持與幫助，讓我可以順利的在 30 歲以前完成這個學位。

感謝我的博士班指導教授 Dr. Wei Cui 在學術以及精神上的各種支持。若不是 Dr. Wei Cui 無私傳授各種學術研究的相關知識及經驗，也許在第一年博士班資格考過後我就會選擇休學回大甲開洗衣店[2]。我想，被一位負責任的老師指導應該是所有博士班學生最夢寐以求的事情，而我很幸運的有一位超級負責任的指導教授訓練我獨立思考以及完成各種實驗的能力。當我實驗進度不如預期的時候，謝謝 SCD 及 VA 實驗室同事們的鼓勵及擁抱，因為有你們才讓這條似乎看不到盡頭的漫漫長路多少可以忍受。另外，感謝碩士班指導教授陳宏文老師在畢業那麼多年後依然與我保持聯繫，並且在我每年回台灣時給予我在選擇人生方向上的寶貴建議。

謝謝這幾年來願意以各種方式參與在我生活中的各路朋友，無論是在台灣、倫敦還是世界上的哪個角落。特別感謝那些在我寫論文期間不定時會被我用五音不全的歌聲轟炸「要是能重來，我不要唸博班～」[3] 的朋友；謝謝湘雯、竹馬、廷伃、怡中、示涵和婷資透過通訊軟體無時差的幫我打氣以及各種抒(講)發(垃)心(圾)情(話)；感謝天祺、Duke、倫敦溫柔鄉傅涵、澍琛、淳敬、Joanne 和嘉誼讓我的負面情緒有一個正當的出口；謝謝我的酒精及歡樂供應商中島美家® Rick、Ariel 和 Johnnie，有你們在的倫敦好像也變得有那麼一點可愛。

最要感謝的是我的父母，邱敏昌先生以及陳桂滿女士。謝謝爸爸媽媽無私的愛與包容讓我得以在沒有經濟壓力的情況下完成我人生中的一個大目標。我知道自己不是一個完美的孩子，但我很幸運的有一對一百分的父母。另外，謝謝我的妹妹越庭、越珉及弟弟哲皓，你們的陪伴讓我堅信無論發生什麼事，我都還有一個你們都在的家。I love you all, sincerely.

最後，我想要謝謝那個從高中以來就一直沒有放棄的自己。曾經有那麼多個瞬間覺得自己笨的很過份，有那麼多個夜晚只想蹲在房間的角落抱著自己痛哭，即使妳明白這條路遠比妳想像中的還窒礙難行，但妳沒有被寂寞和生活打敗，堅持的走完了。

妳真的很棒，辛苦了。

---

[1] 邱家著名的「滑板車事件」，時至今日邱先生和陳女士只要想到還會拿這件事出來數落我。

[2] 台中市大甲區順天路上有一家名為「衣博士」的連鎖洗衣店。

[3] 改編自李榮浩的經典歌曲《李白》。

This thesis is dedicated to my beloved parents

Mr. Chiu and Mrs. Chen

For their endless love and support

Table of Contents

Abstract i

Statement of Originality ii

Copyright Declarations iii

Acknowledgements iv

誌謝 v

Table of Contents vii

Tables and Figures x

Abbreviations xii

Chapter One 1

1.1 The mTOR signalling pathway 2

1.1.1 Molecular composition of mTOR complexes 3

1.1.2 The regulation and downstream targets of mTOR signalling 5

1.1.3 mTOR signalling pathway in early embryonic development 11

1.2 The key factors in mTOR complex 2 12

1.2.1 RICTOR 13

1.2.2 mSIN1 16

1.3 mTOR signalling pathway in pluripotent stem cells 20

1.3.1 Derivation of hESC lines 20

1.3.2 The regulation of self-renewal and pluripotency in hESCs 21

1.3.3 Gene targeting tools for hESCs research 26

1.3.4 Role of mTOR signalling in regulation of hESC self-renewal and pluripotency 29

1.4 Aims and Objectives 31

Chapter Two 32

2.1 Cell culture 33

2.1.1 Materials 33

2.1.2 Methods 36

2.2 Molecular Biology - DNA/RNA techniques 40

2.2.1 Materials 40

2.2.2 Methods 45

2.3 Molecular Biology – Protein techniques 54

2.3.1 Materials 54

2.3.2 Methods 59
2.4 Software and Online Tools 62
Chapter Three 63
3.1 Introduction 64
3.2 Results 66
3.2.1 Design and cloning of sgRNA to target human RICTOR 66
3.2.2 Knockout (KO) validation of RICTOR-sgRNAs in HEK 293T cells 69
3.2.3 Dual sgRNA-directed *RICTOR*-KO and clonal isolation of HEK 293T cells 71
3.2.4 Targeted gene editing at *RICTOR* gene locus in human embryonic stem cells (hESCs) by lipofection 74
3.2.5 Targeted deletion of *RICTOR* in hESCs by electroporation 76
3.2.6 Clonal isolation and verification of successful *RICTOR*-KO hESCs 78
3.3 Conclusions and Discussion 82
Chapter Four 86
4.1 Introduction 87
4.2 Results 89
4.2.1 Deletion of *RICTOR* abolishes the activity of mTORC2 but not mTORC1 and PI3K 89
4.2.2 *RICTOR* deficiency leads to decreased cell proliferation and viability 90
4.2.3 RICTOR/mTORC2 regulates mSIN1 at post-translational levels via protein degradation 92
4.2.4 The stability of mSIN1 might be regulated by both RICTOR-mSIN1 interaction and mTORC2-mediated phosphorylation 96
4.2.5 The mTORC2-mediated phosphorylation of mSIN1-Ser260/270 plays a role in mSIN1 stability 100
4.2.6 Phosphorylation of mSIN1-S260/270 may differentially regulates PKCα phosphorylation 103
4.3 Conclusions and Discussion 105
Chapter Five 108
5.1 Introduction 109
5.2 Results 111
5.2.1 RICTOR/mTORC2 is dispensable for the maintenance of self-renewal/pluripotency in hESCs 111
5.2.2 RICTOR/mTORC2 signalling pathway might be required for the conversion of primed hESCs to naïve state via 5iLAF 115
5.2.3 Deletion of *RICTOR* abolishes mTORC2 activity as well as mSIN1 expression 118
5.2.4 Disruption of RICTOR/mTORC2 signalling might induce cellular adaptation in hESCs 120
5.2.5 *RICTOR* depletion impaired the formation of embryonic bodies from hESCs 122
5.2.6 The deficiency of *RICTOR* exhibits a poor differentiation potential in hESCs 127

5.3 Conclusions and Discussion 131
Chapter Six 135
6.1 Plasmid-based CRISPR-Cas9 system: an efficient approach for gene-knockout in mammalian cells 137
6.2 Important roles of RICTOR/mSIN1 in mTORC2 assembly and function 139
6.3 mTORC2 signalling may have a role in mesendodermal differentiation of hESCs 141
6.4 Future Perspective 144
6.4.1 RICTOR's function in mTORC2 activity: from the aspect of protein structure and cellular localisation 144
6.4.2 Phosphorylation of mSIN1: How is it regulated and what is the impact of it? 145
6.4.3 *mTORC2*-deficiency in differentiation: Assessing the *RICTOR*-KO hESCs in directed lineage-specific differentiation 145
6.4.4 Exploring the underlying mechanisms: Gene expression profile of *mTORC2*-deficiency hESCs 146
Reference 148

Tables and Figures

Chapter One

Figure 1.1 Components of the mTOR complexes ... 4
Figure 1.2 Simplified signalling pathway of mTORC1 ... 7
Figure 1.3 Regulation of mTORC2 signalling pathway ... 10
Figure 1.4 Protein structure and regulatory sites in RICTOR ... 14
Figure 1.5 Functional domains of mSIN1 isoforms and the regulatory sites ... 17
Figure 1.6 Summary of signalling pathways involved in hESCs self-renewal and differentiation ... 24
Figure 1.7 The mechanism of the CRISPR-Cas9 system ... 28
Figure 1.8 Aims and objections ... 31

Chapter Three

Table 1. Potential sgRNAs in exon 4 and 5 on *RICTOR* gene locus ... 67
Table 2. Selected sgRNAs in exon 4 and 5 with potential off-target sites ... 67
Figure 3.1 sgRNA design and the construction of sgRNA expression vectors ... 68
Figure 3.2 Validation of single sgRNA-mediated *RICTOR*-targeting in HEK 293T cells ... 70
Table 3. Summary of analysis in dual *RICTOR*-KO HEK 293T clones ... 72
Figure 3.3 Generation and clonal isolation of dual sgRNA-mediated *RICTOR*-KO in HEK 293T cells ... 73
Figure 3.4 Introduction of Cas9-sgRNA expression plasmid into hESCs via lipofection ... 75
Figure 3.5 Electroporation of EGFP and Cas9-sgRNA expression plasmids into hESCs ... 77
Figure 3.6 Clonal isolation and validation of *RICTOR*-KO hESCs ... 79
Figure 3.7 Isolate successful *RICTOR*-KO clones via double serial clonal dilution ... 81

Chapter Four

Figure 4.1 *RICTOR*-deficiency abolishes mTORC2 activity in HEK 293T cells ... 89
Figure 4.2 Characterisation of HEK 293T *RICTOR*-KO cells ... 91
Figure 4.3 The deficiency of *RICTOR* is accompanied by the decreased expression of mSIN1 and mTORC2 activity ... 93
Figure 4.4 The presence of RICTOR suppresses mSIN1 from proteasome-mediated degradation in HEK 293T cells ... 95
Figure 4.5 The PS region of RICTOR is dispensable for the stabilisation of mSIN1 ... 98

Figure 4.6 RICTOR/mTORC2 may have dual roles in stabilising mSIN1 99
Figure 4.7 The phosphomimetic mutants of mSIN1 at S260D and S270D overcomes the instability of mSIN1 in *RICTOR*-KO cells 102
Figure 4.8 Phosphorylation of mSIN1 at S260/270 are required for PKCα-S657 phosphorylation 104

Chapter Five

Figure 5.1 RICTOR/mTORC2 is not necessarily required for hESC self-renewal 112
Figure 5.2 hESCs remained undifferentiated after knockout of *RICTOR* 114
Figure 5.3 *RICTOR*-deficiency affects the transition from primed-to-naïve hESCs 117
Figure 5.4 *RICTOR*-deficiency diminishes the activity of mTORC2 and affects its downstream signalling cascades in hESCs 119
Figure 5.5 Characterisation of early- and later-passage *RICTOR*-KO hESCs 121
Figure 5.6 *In vitro* differentiation of H1 WT EBs 123
Figure 5.7 *RICTOR*-KO hESCs display poor efficiency of EBs formation 124
Figure 5.8 The present of ROCK inhibitor enhances EBs formation *in vitro* 126
Figure 5.9 Assessing the differentiation potential of the *RICTOR*-KO hESCs 128
Figure 5.10 Deletion of *RICTOR* leads to defective mesendoderm differentiation 130

Chapter Six

Figure 6.1 Proposed diagram of how mTOR signalling affects hESC cell-fate determination 143

Abbreviations

ATF2	Activating transcription factor-2
Ala, A	Alanine
AMPK	AMP-activated kinase
Asp, D	Aspartic acid
BBS	Bardet-Biedl syndrome
bFGF	Basic FGF
BCA	Bicinchoninic Acid Assay
BMP4	Bone morphogenetic protein-4
BSA	Bovine Serum Albumin
CPSII	Carbamoyl phosphate synthetase II
C-CS	Central conserved region
CQ	Chloroquine
CRISPR	Clustered regularly interspaced short palindromic repeats
Ccdc28b	Coiled-coil domain-containing protein 28B
Co-IP	Co-immunoprecipitation
CM	Conditioned medium
CS5	Conserved domain 5
CRIM	Conserved region in middle
Cas9	CRISPR associated protein 9
crRNA	CRISPR RNA
CHX	Cycloheximide
DAPI	4’,6 diamidino-2-phenylindole
DEPTOR	DEP domain containing mTOR-interacting protein
DEPC	Diethyl pyrocarbonate
DMSO	Dimethyl sulfoxide
DTT	Dithiothreitol
DSB	Double-strand break
DMEM	Dulbecco’s modified Eagle medium
4EBP1	eIF4E binding protein 1
EBs	Embryoid Bodies
ESCs	Embryonic stem cells
ECL	Enhanced chemiluminescence substrate
EMT	Epithelial-mesenchymal transition
EGTA	Ethylene glycol tetraacetic acid

EDTA	Ethylenediaminetetraacetic acid
eIF4E	Eukaryotic translation initiation factor 4E
ECM	Extracellular matrices
FBXW7	F-box and WD repeat domain containing 7
FGF2	Fibroblast growth factor 2
FACS	Fluorescence-Activated Cell Sorting
FBS	Foetal Bovine Serum
FcεRI	High-affinity receptors for IgE
FLCN	Folliculin
FOXO1	Forkhead transcription factor 1
FL	Full-length
FKBP12	12kDa FK506-binding protein
Gadd45β	Growth arrest and DNA damage-inducible 45β
GRB10	Growth factor receptor-bound protein 10
HDR	Homology directed repair
HRP	Horseradish peroxidise
HEPES	4-(2-hydroxyethyl)-1-piperazineethanesulfonic acid
hESCs	Human ESCs
HUVEC	Human umbilical vein endothelial cell
HM	Hydrophobic motif
iMEFs	Inactivated mouse embryonic fibroblast
ICE	Inference of CRISPR Edits
ICM	Inner cell mass
indel	Insertion-deletion
IRS1	Insulin receptor substrate 1
IGF1	Insulin-like growth factor 1
ILK	Integrin-linked kinase
KD	Knockdown
KO	Knockout
KSR	Knockout Serum Replacement
LIF	Leukemia inhibitory factor
mLST8	Mammalian lethal with SEC thirteen 8
mSIN1	Mammalian stress-activated protein kinase (SPARK)-interacting protein 1
mTOR	Mechanistic/mammalian target of rapamycin
MEKK2	Mitogen-activated protein kinase kinase kinase 2
MAPKAP1	Mitogen-activated protein kinase-associated protein 1

MEFs	Mouse Embryonic Fibroblasts
mESCs	Mouse ESCs
mTORC1	mTOR complex 1
mTORC2	mTOR complex 2
PS	Multiple phosphorylation sites containing region
mut	Mutant
Myo1c	Myosin 1c
NEAA	Non-essential Amino Acids
NHEJ	Non-homologous end joining
NP-40	Nonidet P-40
NSCLC	Non-small-cell lung carcinoma
N-CS	N-terminal conserved domain
NTD	N-terminal domain
OSN	OCT4, SOX2 and NANOG
MAPK14	p38MAPK
S6K1	p70S6 kinase 1
PMSF	Phenylmethanesulfonylfluoride
$PI(3,4,5)P_3$	Phosphatidylinositol (3,4,5)-trisphosphate
$PI(4,5)P_2$	Phosphatidylinositol (4,5)-bisphosphate
PI3K	Phosphatidylinositol 3 kinase
pH3	Phospho-H3
PDK1	Phosphoinositide-dependent kinase-1
PSP	PhosphoSitePlus®
PH	Pleckstrin homology
PCBP2	Poly(rC)-binding protein-2
PCR	Polymerase chain reaction
PVDF	Polyvinylidene fluoride
Pdcd4	Programmed cell death 4
PRAS40	Proline-rich AKT/PKB substrate 40 kDa
PI	Propidium iodide
PKB/AKT	Protein kinase B
PKC	Protein kinase C
Protor1/2	Protein observed with Rictor-1/2
PAM	Protospacer adjacent motif
RIPA	Radio Immunoprecipitation Assay Buffer
RICTOR	Rapamycin-insensitive companion of mTOR

REM	Ras exchange motif
Rheb	Ras homolog enriched in brain
RBD	Ras-binding domain
REDD1	Regulated in DNA damage and development 1
RAPTOR	Regulatory-associated protein of mTOR
ROCKi	Rho Kinase Inhibitor/p160 rho-associated coiled-coil kinase inhibitor
RhoGDI2	Rho-GDP dissociation inhibitor 2
RNP	Ribonucleoprotein
RICTOR-KO	*RICTOR*-knockout
RNAi	RNA interference
RPMI	Roswell Park Memorial Institute
SGK1	Serum and glucocorticoid induced kinases 1
SCID	Severe combined immunodeficiency
STAT3	Signal transducer and activator of transcription 3
sgRNA	Single guide RNA
SDS	Sodium dodecyl sulphate
SSEA	Stage-specific embryonic antigen
SREBP1/2	Sterol regulatory element binding protein 1/2
SAPK	Stress-activated protein kinase
T7E1	T7 endonuclease I
TEMED	Tetramethylethylenediamine
TNFR	TNF receptor
tracrRNA	Trans-activating crRNA
TALENs	Transcription activator–like effector nucleases
TFEB	Transcription factor EB
TGFβ	Transforming growth factor β
TBS-T	Tris Buffered Saline with Tween-20
TSC1/2	Tuberous sclerosis complex
TNFα	Tumour necrosis factor α
TRA	Tumour-related antigen
TM	Turn motif
ULK1	Unc-51 like autophagy activating kinase 1
WT	Wild-type
ZFNs	Zinc-finger nucleases

01

Introduction

1.1 The mTOR signalling pathway

The mechanistic target of rapamycin (mTOR), also known as mammalian target of rapamycin, is an evolutionarily conversed serine/threonine protein kinase, which belongs to the phosphatidylinositol 3 kinase (PI3K)-related kinase family. Its initial identification and cloning was reported in 1994 (Brown et al., 1994; Chiu et al., 1994; Sabatini et al., 1994), shortly after the discovery of two yeast orthologous genes, *TOR1* and *TOR2*. *TOR1* and *TOR2* were identified in a genetic screening that confer resistance to the immunosuppressant drug rapamycin in *Saccharomyces cerevisiae* (Helliwell et al., 1994; Kunz et al., 1993). Rapamycin, which is an antifungal compound, was originally found and isolated from the bacterium *Streptomyces hygroscopicus* in a soil sample from the Rapa Nui islands in 1972 (Vezina et al., 1975). In mammalian cells, rapamycin was found to have the properties of anti-proliferation and immunosuppressive effects, thus it has been shown to be used in the treatment of many diseases (Chung et al., 1992; Kuo et al., 1992; Price et al., 1992). In order to suppress cell proliferation, rapamycin forms a complex with the 12kDa FK506-binding protein (FKBP12), and this complex acts as an allosteric inhibitor to block the mTOR activity when it is in the complex of mTORC1 as the catalytic subunit (Brown et al., 1994; Sabatini et al., 1994).

It has been increasingly recognized that the mTOR signalling pathway plays many critical roles in controlling mammalian cell behaviours and functions in response to environmental changes, and thereby it is important for maintaining tissue homeostasis and organism health. Disturbance of this signalling frequently results in abnormal cell proliferation, differentiation and metabolism, which leads to many health problems and diseases, including type II diabetes, obesity and cancer (Saxton and Sabatini, 2017).

1.1.1 Molecular composition of mTOR complexes

The mTOR signalling functions through two distinct multi-protein complexes known as mTOR complex 1 (mTORC1) and mTOR complex 2 (mTORC2), which are different in their constituent components and substrate specificities. Although the catalytic subunit mTOR interacts with DEP domain containing mTOR-interacting protein (DEPTOR) and mammalian lethal with SEC thirteen 8 (mLST8) in both complexes, mTORC1 specifically associates with regulatory-associated protein of mTOR (RAPTOR) and proline-rich AKT/PKB substrate 40 kDa (PRAS40). RAPTOR is an adapter protein that binds strongly with mTOR to its effectors, substrates and regulators, and thus modulating the activity of mTORC1 in response to various signals (Foster et al., 2010; Hara et al., 2002; Kim et al., 2002; Nojima et al., 2003; Schalm et al., 2003); while PRAS40 and DEPTOR have been characterised as distinct negative regulators of mTORC1, which may not be necessarily required for mTORC1 activity (Peterson et al., 2009; Sancak et al., 2007; Vander Haar et al., 2007; Wang et al., 2007). The main function of mLST8 is to mediate protein–protein interactions, however, it remains to be elucidated whether it is necessarily required for mTORC1 activity even though it is vital for mTORC1 complex formation *in vitro* (Aylett et al., 2016; Guertin et al., 2006; Kim et al., 2003).

In mTORC2, apart from mTOR, DEPTOR and mLST8, the complex contains rapamycin-insensitive companion of mTOR (RICTOR) and mammalian stress-activated protein kinase (SPARK)-interacting protein 1 (mSIN1, also known as mitogen-activated protein kinase-associated protein 1 [MAPKAP1]) (Frias et al., 2006; Sarbassov et al., 2004; Shiota et al., 2006). RICTOR is a scaffold protein in mTORC2 similar to RAPTOR in mTORC1, which acts as a key component in mTORC2 for its assembly and function (Ikenoue et al., 2008; Sarbassov et al., 2004). mSIN1 is considered to be important for mTORC2 assembly and recruiting the substrate to the mTORC2 (Frias et al., 2006; Yang et al., 2006). Similar to its role in mTORC1, DEPTOR is described as a natural mTOR inhibitor in mTORC2 (Peterson et al., 2009). However, unlike mTORC1, the scaffolding function of mLST8 appears to be critical for the assembly and activity of mTORC2 complex both *in vitro* and in *vivo*, as the disruption of mLST8 specifically impair the stability and activity of mTORC2 (Guertin et al., 2006; Hwang et al., 2019; Stuttfeld et al., 2018). In addition to the core components of mTORC2, protein observed with RICTOR-1/2 (Protor-1/2) has been identified as a direct binding partner with

RICTOR in forming mTORC2 (Pearce et al., 2007; Woo et al., 2007). Although in comparison with other components in mTORC2, the functional role of Protor-1/2 in mTORC2 is less well understood, but it has been implicated that it may affect substrate recognition of mTORC2 (Gan et al., 2012; Pearce et al., 2011) (Figure 1.1).

The distinct protein composition in the two complexes might account for their divergence in rapamycin response, regulation of activation and cellular functions (Populo et al., 2012; Sancak et al., 2010). For instance, mTORC1 is acutely sensitive to the rapamycin-induced inhibition, whereas mTORC2 is resistant to acute rapamycin exposure and can only reduce its activity after long-term treatment of rapamycin in certain cell types (Shimobayashi and Hall, 2014).

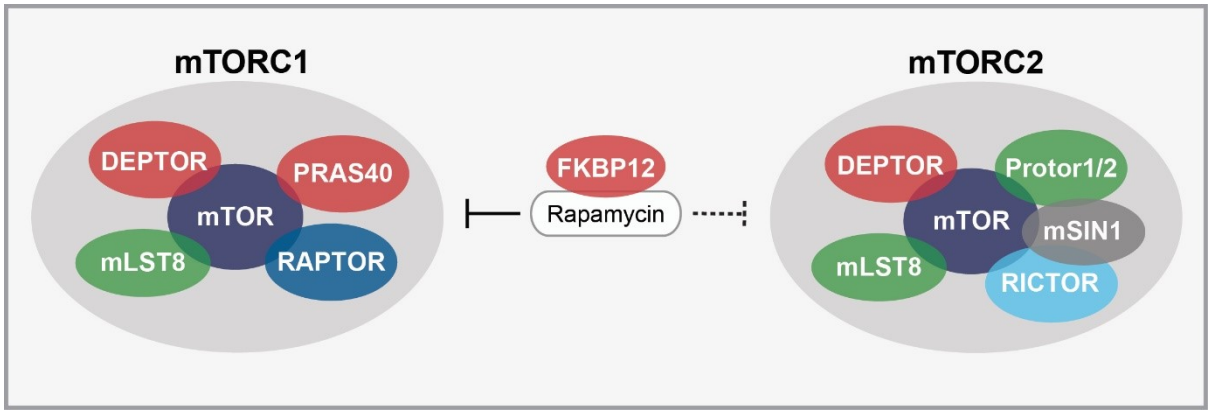


Figure 1.1 Components of the mTOR complexes

*Schematic of different components in **(Left)** mTORC1 and **(Right)** mTORC2. mTORC1 and mTORC2 share common subunits: the catalytic subunit mTOR, negative regulator DEPTOR and the positive regulator mLST8. mTORC1 additionally associates with RAPTOR and PRAS40, while mTORC2 contains RICTOR, mSIN1 and Protor1/2. Rapamycin forms a complex with FKBP12, which inhibits the kinase activity of mTORC1, whereas mTORC2 is resistant to acute rapamycin exposure and can only reduce its activity after long-term treatment. Positive regulators in each complex are shown in green and negative regulators in red, respectively.*

1.1.2 The regulation and downstream targets of mTOR signalling

i. mTORC1

Since the discovery of mTOR in 1994, researchers have been mainly focused on the regulation and the function of mTORC1. The mTORC1 signalling pathway plays critical roles in cell growth, nucleotide and protein synthesis, lipid metabolism and autophagy (Saxton and Sabatini, 2017). Previous studies have revealed that the activity of mTORC1 can be regulated through different mechanisms and by regulatory inputs, such as growth factors, nutrients, cellular energy status and stress.

The mTORC1 signalling pathway is activated by growth factors and cytokines such as insulin through PI3K/AKT signalling cascade. The transduction of the insulin signal leads to the PI3K-mediated conversion of phosphatidylinositol (4,5)-bisphosphate ($PI(4,5)P_2$) to phosphatidylinositol (3,4,5)-trisphosphate ($PI(3,4,5)P_3$), which then recruits AKT to the cell membrane and activates it through phosphorylation by PDK1 and mTORC2. This active AKT is able to inhibit the mTORC1 negative regulator, tuberous sclerosis complex (TSC1/2), releasing the GTPase protein, Ras homolog enriched in brain (Rheb) that directly binds and activates mTORC1 (Inoki et al., 2002; Kim and Guan, 2019; Manning et al., 2002). Other growth factor pathways can also active mTORC1 via the inhibition of TSC1/2, including WNT and the inflammatory cytokine tumour necrosis factor α (TNFα) (Inoki et al., 2006; Lee et al., 2007). Amino acids, especially leucine, arginine, and glutamine, stimulate mTORC1 via the Rag GTPases, a heterodimer protein composed of four related small GTPases (RagA or RagB with RagC or RagD) (Bar-Peled et al., 2012; Sancak et al., 2010). RAPTOR binds with the active Rags in an amino acid-dependent manner, leading to the recruitment of mTORC1 to the outer surface of lysosomes and the interaction between mTORC1 and Rheb, which promotes the kinase activity of mTORC1 on the surface of lysosomes (Kim et al., 2008; Sancak et al., 2010; Sancak et al., 2008). mTORC1 activity is also tightly regulated by cellular energy status and hypoxia-induced energy stress through the AMP-activated kinase (AMPK) pathway. When the AMP:ATP ratio increases, TSC2 is activated by AMPK via phosphorylation at a residue differing from that by PI3K/AKT and this AMPK-mediated TSC2 phosphorylation, subsequently inhibits mTORC1 signalling (Corradetti et al., 2004; Inoki et al., 2003). Active AMPK can also reduce mTORC1 activity by directly phosphorylating RAPTOR in response to

energy depletion (Gwinn et al., 2008). In addition, oxygen deprivation can stimulate the expression of regulated in DNA damage and development 1 (REDD1), resulting in the inhibition of mTORC1 signalling via TSC2 (Brugarolas et al., 2004).

To control cellular functions in response to different environmental and intracellular conditions, mTORC1 regulates cell growth and metabolism mainly by phosphorylating its downstream signalling effectors. For example, mTORC1 participates in the process of protein synthesis via the phosphorylation of two well-characterised substrates: p70S6 kinase 1 (S6K1) and eIF4E (eukaryotic translation initiation factor 4E) binding protein 1 (4EBP1). mTORC1 phosphorylates S6K1 on its hydrophobic motif site (Thr389) to initiate and enhance mRNA translation efficiency through the induction of ubiquitin-mediated PDCD4 degradation (an inhibitor of eIF4A(F)) and the interaction with SKAR (a component of exon-junction complexes) (Dorrello et al., 2006; Holz et al., 2005; Ma et al., 2008). The activation of S6K1 also increases mRNA biogenesis and nucleotides synthesis through regulating its effectors like carbamoyl phosphate synthetase II (CPSII) (Ben-Sahra et al., 2013). The direct phosphorylation of 4EBP1 by mTORC1 leading to its dissociation from the cap-binding protein eIF4F, which results in the assembly of eIF4E complex and initiates the 5'-cap-dependent translation (Brunn et al., 1997; Gingras et al., 1999). In addition, several studies have shown that acute mTORC1 inhibition not only decreases general mRNA translation but also increases overall protein degradation (Selman et al., 2009; Zhao et al., 2015). mTORC1 also participates in lipogenesis by phosphorylating Lipin1 to prevent its translocation into the nucleus, leading to the upregulation and activation of sterol regulatory element binding protein 1/2 (SREBP1/2), the transcription factors that control numerous genes involved in fatty acid and cholesterol synthesis (Peterson et al., 2011). As a negative regulator of autophagy, mTORC1 controls cell growth by regulating protein catabolism. mTORC1 phosphorylates Unc-51 like autophagy activating kinase 1 (ULK1, an autophagy-initiating kinase) to inhibit the autophagosome formation under nutrient replete conditions (Kim et al., 2011). Furthermore, the phosphorylation of transcription factor EB (TFEB) by mTORC1 blocks its nuclear translocation and also downregulates the expression levels of genes that related to lysosomal biogenesis (Martina et al., 2012; Roczniak-Ferguson et al., 2012; Settembre et al., 2012) (Figure 1.2).

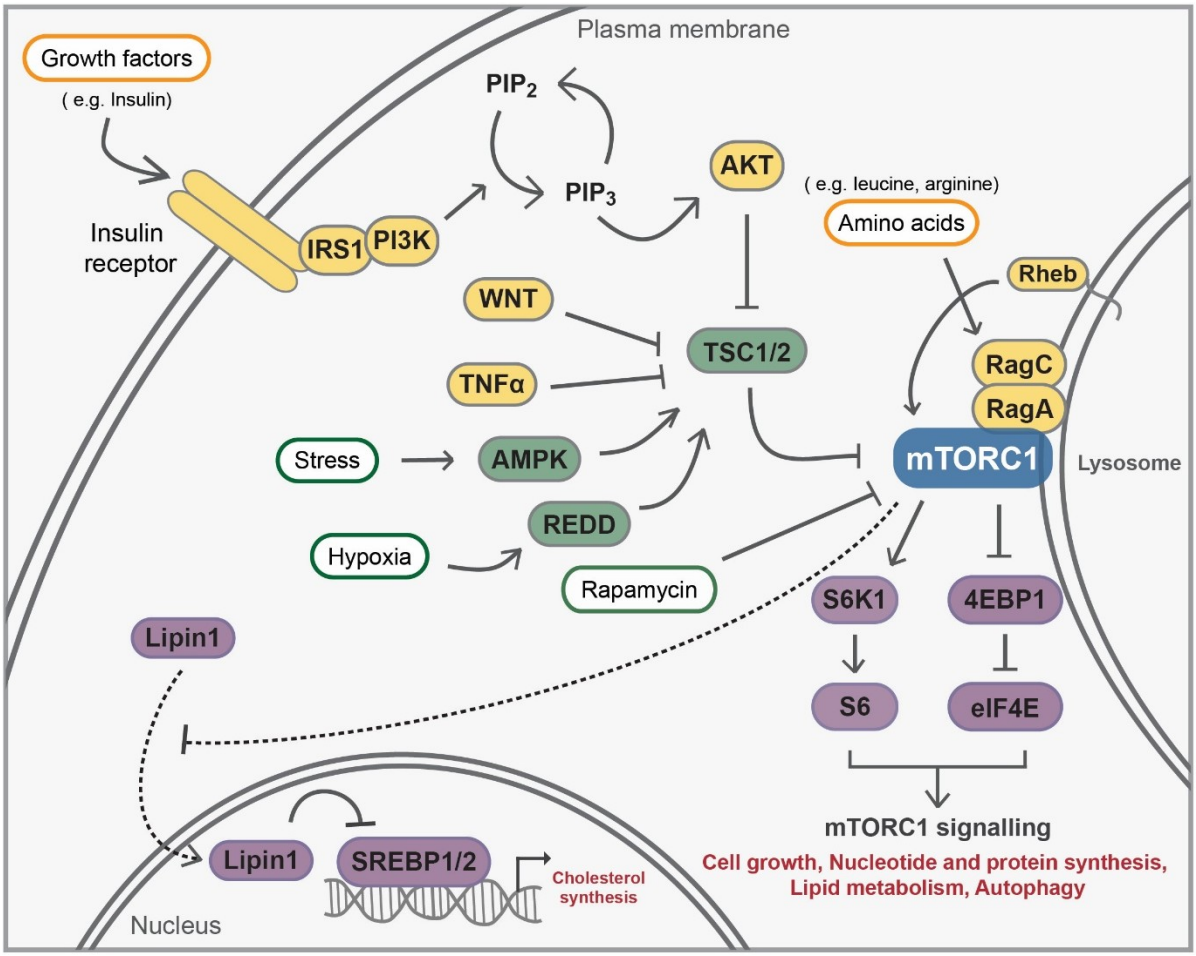


Figure 1.2 Simplified signalling pathway of mTORC1

The upstream regulators and downstream effectors of mTORC1. Multiple inputs, such as growth factors, amino acids, cellular stress and hypoxia, regulate the activity of mTORC1 through the mechanisms shown. mTORC1 signalling participates in cell growth, nucleotide and protein synthesis, lipid metabolism and autophagy. Positive regulators of mTORC1 signalling are shown in yellow, negative regulators are represented in green while the downstream effectors are shown in purple.

ii. mTORC2

In comparison with mTORC1, the regulation and function of mTORC2 are less well understood. It has been assumed that mTORC2 appears to be insensitive to nutrients, however, *Tato et al.* demonstrated that the activation of mTORC2 signalling can be stimulated by amino acids via PI3K/AKT pathway (Tato et al., 2011). Growth factors, such as insulin and insulin-like growth factor 1 (IGF1), have been thought to activate mTORC2 via a poorly defined PI3K-dependent mechanism in which ribosomes are involved (Zinzalla et al., 2011). It has been reported that PI3K phosphorylates PIP_2 to generate PIP_3 and recruits mTORC2 to plasma membrane via the mSIN1-PH domain. This subsequently releases mSIN1 inhibition on the mTOR kinase domain, leading to mTORC2 activation (Liu et al., 2015). However, Ebner and colleagues recently suggest that mTORC2 might be constitutively active at the plasma membrane in a PI3K- and growth factor-independent manner. The PI3K signalling is only required for the recruitment of the substrate AKT to the plasma membrane, where it can be phosphorylated by mTORC2 (Ebner et al., 2017). Some recent studies suggest that AKT and mTORC1 might also be involved in the regulation of mTORC2. AKT promotes the activation of mTORC2 via phosphorylates mSIN1-Thr86, which in turn enhances mTORC2 kinase activity and forms a positive feedback loop (Yang et al., 2015). Unexpectedly, by inhibiting the insulin/PI3K pathway, mTORC1 could function as a negative regulator of mTORC2. These actions are mediated by the activation of growth factor receptor-bound protein 10 (GRB10) via mTORC1 and the phosphorylation-dependent degradation of insulin receptor substrate 1 (IRS1) via S6K1 (Harrington et al., 2004; Hsu et al., 2011; Shah et al., 2004; Yu et al., 2011). In addition to growth factors, recent study also provides the evidence that the energy sensor, AMPK, could directly interact and phosphorylate mTORC2 in response to acute energetic stress (Kazyken et al., 2019).

So far, the downstream effectors of mTORC2 are less characterised than mTORC1 and only three groups of mTORC2 substrates have been clearly identified, which are all belonging to the AGC protein kinase family, including AKTs, serum and glucocorticoid induced kinases 1 (SGK1) and some members of protein kinase C family (PKC), such as PKCα (Saxton and Sabatini, 2017). AKT, also known as protein kinase B (PKB), has three isoforms, AKT1, AKT2 and AKT3, encoded by three different genes (Vanhaesebroeck and Alessi, 2000). AKT1 (AKT hereafter) is the most well-characterised target of mTORC2, which promotes cell survival and

growth (Manning and Cantley, 2007; Song et al., 2005). The full kinase activation of AKT requires the phosphorylation of two key residues on AKT, hydrophobic motif (HM, Ser473) and activation loop (Thr308) (Alessi et al., 1996). mTORC2 is responsible for the phosphorylation of AKT-Ser473 residue whilst the primary AKT-Thr308 kinase is phosphoinositide-dependent kinase-1 (PDK1). Notably, in the absence of mTORC2, AKT can still be phosphorylated at Thr308 by PDK1 for partial activation and regulates some of its downstream targets (Guertin et al., 2006; Jacinto et al., 2006; Shiota et al., 2006). In addition to AKT-Ser473, another well-conserved threonine residue in the turn motif (TM) of AKT, Thr450, has also been reported to be phosphorylated by mTORC2. However, the AKT-Thr450 phosphorylation is likely to be performed through a co-translational mechanism which ribosomes are involved (Zinzalla et al., 2011).

Similar to AKT, the activation of SGK1 is mediated by both mTORC2 and PDK1 via phosphorylation of the Ser422 residue and Thr256 residue, respectively (Kobayashi and Cohen, 1999; Park et al., 1999). SGK1 plays key roles in regulating diverse cellular processes, one of which is stimulating sodium transport into epithelial cells (Loffing et al., 2006). It is known that loss of mTORC2 components (either RICTOR, mSIN1 or mLST8) in cells diminished SGK1 activity, even though mTORC1 activity is maintained (Garcia-Martinez and Alessi, 2008; Laplante and Sabatini, 2012). And finally, mTORC2 also controls actin cytoskeleton arrangement and cell shape by regulating PKC activation (Jacinto et al., 2004; Sarbassov et al., 2004). Although the first identified substrate of mTORC2 in PKC family was PKCα, other PKC members, including PKCδ, PKCζ PKCγ and PKCε were also shown to be activated by mTORC2, indicating that mTORC2 modulates cytoskeleton organization and cell migration with various aspects (Gan et al., 2012; Li and Gao, 2014; Thomanetz et al., 2013) (Figure 1.3).

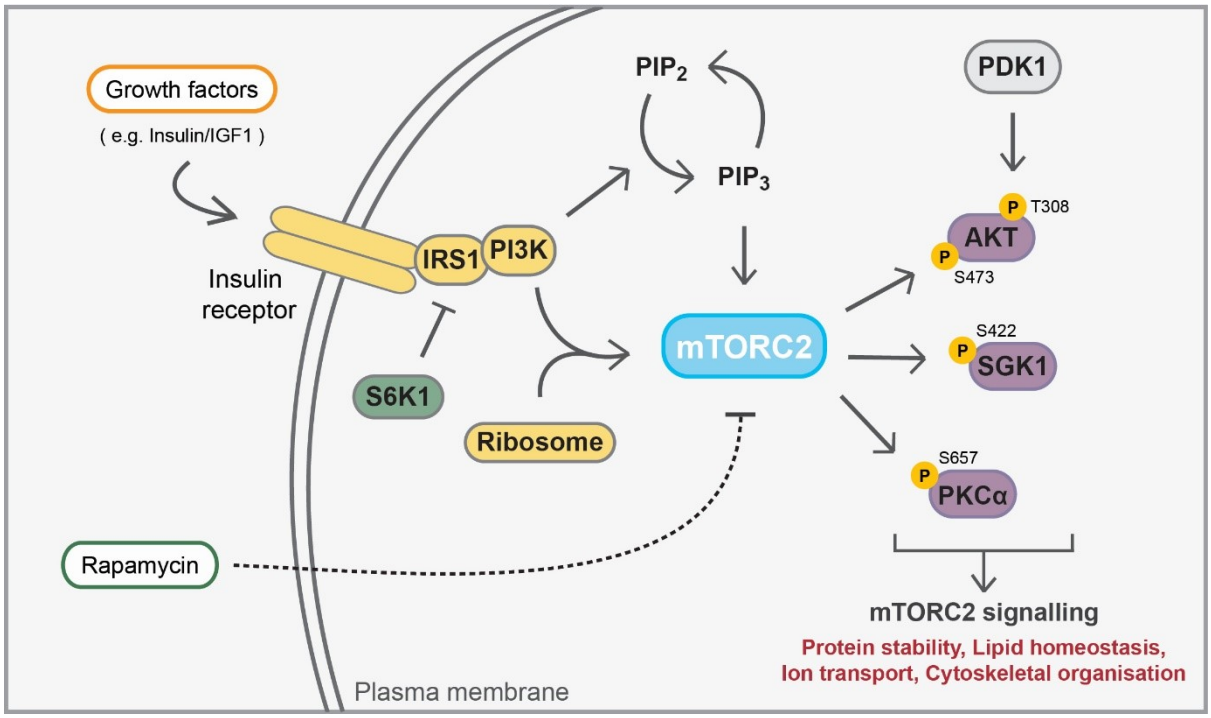


Figure 1.3 Regulation of mTORC2 signalling pathway

The upstream regulators and downstream effectors of mTORC2. mTORC2 appears to be sensitive to growth factor signals like insulin, and being activated by them through a poorly defined PI3K-dependent mechanism in which ribosomes are involved. The activation of mTORC2 regulates protein stability, lipid homeostasis, ion transport and cytoskeletal organisation. Positive regulators of mTORC2 signalling are shown in yellow, negative regulators are represented in green while the downstream effectors are shown in purple.

1.1.3 mTOR signalling pathway in early embryonic development

To dissect the roles of mTORC1 and mTORC2 in the early mouse embryonic development, knockout mice were generated with the disruption of *mTor* (Gangloff et al., 2004; Guertin et al., 2006; Murakami et al., 2004), *Raptor*, *mLst8* (Guertin et al., 2006), *Rictor* (Guertin et al., 2006; Shiota et al., 2006; Yang et al., 2006) and *mSin1* (Jacinto et al., 2006) individually in the mouse germlines. All these knockout mice exhibit embryonic lethality, demonstrating a critical role of mTOR signalling in embryonic development and growth.

In these knockouts, the *mTor*- and *Raptor*-null embryos die shortly after implantation at E5.5-6.5 with failure of proliferation in the inner cell mass (ICM) and trophoblast cells (Gangloff et al., 2004; Guertin et al., 2006; Murakami et al., 2004). On the other hand, genetic ablation of *Rictor* or *mSin1* exhibit phenotypes of embryonic lethality around E10.5 to E12.5, with *Rictor*$^{-/-}$ embryos showing marked cardiovascular and placental defects (Guertin et al., 2006; Shiota et al., 2006). The *mLst8*-deficient embryos die around E10.5, resulting from the improper development of the foetal vascular system and placenta, a phenotype similar to that of *Rictor*-null embryos (Guertin et al., 2006). These results suggest that mTORC1 and mTORC2 have different functions in early embryonic development with *mTORC1*-deficient embryos dying earlier than *mTORC2*-deficient embryos. Notably, *mLst8*-deficency recapitulates the phenotype of *mTORC2*-knockout rather than *mTORC1*-knockout, which is different from that of *mTor*, even though both of them are the core components in both mTOR complexes. Collectively, these results clearly indicated that mTORC1 activity is indispensable in driving cell proliferation during early embryonic development, whilst mTORC2 is required at a later stage, possibly associated with cardiovascular development, whose function is necessary for embryo survival during the mid-gestation stage (from E9.5 to E14.5).

In addition to genetic manipulation, the application of inhibitors is another strategy that is commonly used by researchers to study the effect of mTOR signalling in early embryonic development. Murakami and colleagues provide the evidence that rapamycin treated mouse embryos display lethality at E5.5, which mimicking the effect of *mTor* and *Raptor* deletion. However, interestingly, *Bulut-Karslioglu A et al*. showed that partial inhibition of mTOR with its inhibitor INK128 or RapaLink-1 on mouse blastocysts induced them into diapause for more

than 10 days, which remain pluripotent and competent for further development (Bulut-Karslioglu et al., 2016; Murakami et al., 2004). Thus, the role of mTOR signalling in regulating the development of preimplantation mouse embryos is unclear and the detailed molecular and biological mechanisms underlying these phenotypes remain to be elucidated.

1.2 The key factors in mTOR complex 2

Given that the regulation and structures of mTORC2 are still largely unknown, therefore, no specific inhibitor for mTORC2 has been developed. Most of the studies on mTORC2 rely on manipulating its defining subunits, RICTOR and mSIN1. Previous studies have shown that genetic disruption of *RICTOR* dramatically decreased the protein level of mSIN1, indicating that the mSIN1 protein stability depends on the protein expression of RICTOR (Frias et al., 2006; Jacinto et al., 2006; Yang et al., 2006). However, conflicting results were reported regarding the protein stability of RICTOR in the absence of *mSIN1*. Some studies suggested that the deficiency of *mSin1* resulted in the reduction of Rictor protein (Frias et al., 2006; Jacinto et al., 2006; Yang et al., 2006), whereas others revealed that the protein expression of RICTOR/Rictor was unaffected in mSIN1 RNAi knockdown or *mSin1*-knockout cells (Yao et al., 2017).

Genetic studies have shown that both RICTOR and mSIN1 are required for mTORC2 activity and ablating any of them can lead to mTORC2 disability (Guertin et al., 2006; Shiota et al., 2006). RICTOR-mSIN1 are able to form a complex to maintain their stability and thus building the structure for mTORC2 (Frias et al., 2006; Jacinto et al., 2006; Yao et al., 2017). The interaction between RICTOR and mSIN1 is detergent insensitive as they were still able to associate with each other while mTOR was dissociated from the complex by employing harsher detergents, which suggests that the interaction between RICTOR and mSIN1 is independent of mTOR (Yao et al., 2017). Moreover, the recent studies in human mTORC2 structure have revealed that the tight interaction between RICTOR and mSIN1 generates a steric effect and thereby obstructing the binding of FKBP12-rapamycin to mTOR. As a result, mTORC2 forms a more compact conformation (compared to mTORC1) and this might be the

possible underlying mechanism of why mTORC2 is resistant to acute rapamycin treatment (Chen et al., 2018; Stuttfeld et al., 2018).

1.2.1 RICTOR

RICTOR, the mammalian orthologue of AVO3 in budding yeast *Saccharomyces cerevisiae*, was the first identified specific subunit in mTORC2 (Jacinto et al., 2006; Sarbassov et al., 2004). Although most of the studies on RICTOR have linked its function closely with mTORC2, recent evidence also indicated that RICTOR may have functions independent of mTORC2 (Smrz et al., 2014).

RICTOR locus is located on chromosome 5 in the human genome, comprising of 38 exons. The translated RICTOR protein contains 1,708 amino acids with a predicted molecular weight of 190 kDa. Without any previously identified domain or motifs, RICTOR protein consists of several sections which have been found conserved in many eukaryotes from yeast to human (Jacinto et al., 2004; Sarbassov et al., 2004). In the pfam database, the human RICTOR protein contains following pfam domains: an N-terminal conserved domain (N-CS), central conserved region (C-CS), Ras exchange motif (REM), conserved domain 5 (CS5) and multiple phosphorylation sites (PS) containing region (http://pfam.xfam.org/protein/Q6R327) (Fig 1.4A). However, another analysis identified two highly conserved regions in the RICTOR orthologues across different species, which are located at N and C terminal region of the protein as shown in Fig 1.4B (Dibble et al., 2009). Interestingly, the sequences between the N and C regions has approximately 21 potential phosphorylation sites which is only conserved among vertebrates (Dibble et al., 2009). Moreover, it is widely supported that the phosphorylation status at these sites, such as Thr1135, might provide a potential link between the two mTOR complexes (Boulbes et al., 2010; Dibble et al., 2009; Gao et al., 2010; Julien et al., 2010; Treins et al., 2010).

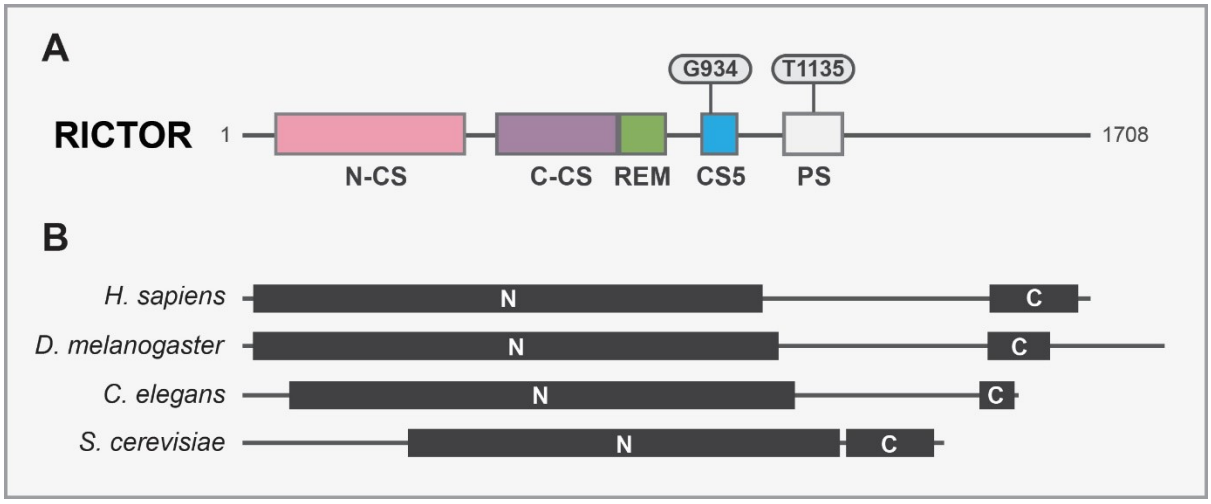


Figure 1.4 Protein structure and regulatory sites in RICTOR

(A) *Schematic of RICTOR conserved regions and regulatory sites. These two regulatory sites (G934 and T1135) do not affect mTORC2 activity but may affect other properties. N-CS = N-terminal conserved domain; C-CS = central conserved region; REM = Ras exchange motif; CS5 = conserved domain 5 and PS = region containing multiple phosphorylation sites.* ***(B)*** *Schematic diagram of full-length RICTOR orthologs from different species are indicated. There are two major regions, the highly conserved region located at its N-terminal portion (N) and another relatively less-well-conserved region at C-terminal region (C).*

i. mTORC2-dependent function of RICTOR

The functional study of RICTOR have been mostly related to its role as an essential component of mTORC2. At the molecular-cell level, RICTOR is required for the phosphorylation of the mTORC2 substrates. Inactivation of the *RICTOR* gene by loss-of-function methods (either knockdown or knockout) in different human cancer cell types diminished the mTORC2 kinase activity (Sarbassov et al., 2005). It has been shown that the deletion of either N-terminus or C-terminus of RICTOR lead to the failure of mTORC2 assembly and function, indicating that an intact full-length of RICTOR protein might be required for both integrity and activity of mTORC2 (Aimbetov et al., 2012; Glidden et al., 2012; Huang et al., 2009). Furthermore, several regulatory sites, such as Gly934 and Thr1135, have been identified in RICTOR protein, to play a role in modulating the assembly or other properties of mTORC2. However, the exact mechanisms remain controversial and unclear (Aimbetov et al., 2012; Bhattacharya et al., 2016; Boulbes et al., 2010; Dibble et al., 2009).

The role of mTORC2 in embryonic development was studied in mouse models through germline deletion of *Rictor* and the *Rictor*-knockout mice exhibited embryonic lethality around E10.5 (Guertin et al., 2006; Shiota et al., 2006). Histological analysis showed that this might be as a result of cardiovascular and placenta defects, suggesting that RICTOR/mTORC2 is an essential regulator for mouse embryo development. Interestingly, all the tissue-specific *Rictor*-knockout mice showed milder phenotypes, manifested mainly as smaller size and metabolic disorders (Bentzinger et al., 2008; Cybulski et al., 2009; Kumar et al., 2010; Siuta et al., 2010). For example, conditional ablation of *Rictor* in the central nervous system resulted in smaller neurons and small brain (Thomanetz et al., 2013). The only exception is the elimination of *Rictor* in mesendoderm during early embryonic development, which showed similar phenotype as that in germline-null mice (Zhao et al., 2014). However, it remains largely unknown about how mTORC2 functions in this process and the molecular mechanisms underlying these phenotypes. Since all these works were done in mouse models, there is limited information about whether mTORC2 plays any role in the human development.

ii. mTORC2-independent function of RICTOR

Recent evidence suggest that RICTOR might also have functions that are independent of mTORC2, possibly through the association with other proteins or complexes which do not contain mTOR. In particular, RICTOR has been shown to control the stability of the SGK1 or cell cycle proteins (c-Myc and cyclin E) via regulating the function of an E3 ubiquitin ligase complex through interacting with Cullin-1 or F-box and WD repeat domain containing 7 (FBXW7) (Gao et al., 2010; Guo et al., 2012). In addition, RICTOR, but not mSIN1, has been found to be involved in the regulation of cell migration and epithelial-mesenchymal transition (EMT) by associating with the regulators of cell morphology, such as myosin 1c (Myo1c) and Rho-GDP dissociation inhibitor 2 (RhoGDI2), indicating that this function of RICTOR is independent of mTORC2 (Agarwal et al., 2013; Hagan et al., 2008). The biological activities of RICTOR can also expand to immunology. mTOR and RICTOR have been reported to participate in a mTOR kinase activity–independent regulation of neutrophil chemotaxis, and RICTOR regulates high-affinity receptors for IgE (FcεRI)-mediated degranulation independently of mTORC2 (He et al., 2013; Smrz et al., 2014). Furthermore, RICTOR can facilitate integrin-linked kinase (ILK)-mediated AKT-Ser473 phosphorylation without the

involvement of mTOR in some cancer cells to promote their survival (McDonald et al., 2008). Collectively, all these studies provide the evidence that RICTOR is a multifunctional signalling regulator and thus it is important to know which functions of RICTOR acts through mTORC2-dependent mechanisms and which ones do not.

1.2.2 mSIN1

mSIN1 (MAPKAP1), encoded by the *MAPKAP1* gene, was first identified as a Ras partner protein before it was known as an essential component of mTORC2 (Frias et al., 2006; Jacinto et al., 2006; Schroder et al., 2007; Yang et al., 2006). The *MAPKAP1* gene maps to chromosome 9 in the human genome containing 13 exons. mSIN1 was predicted to have five multiple alternative splicing isoforms, named mSIN1.1-mSIN1.5 (Fig 1.5). However, only four of them have been detected in human cells, while mSIN1.3 is undetectable (Frias et al., 2006).

The longest mSIN1 isoform, mSIN1.1 is a protein of 522 amino acids with a predicted molecular weight of 59 kDa. It contains four possible domains: N-terminal domain (NTD), conserved region in middle (CRIM), Ras-binding domain (RBD), and pleckstrin homology (PH) like domain. The role of NTD has been identified as a key domain which affects the interaction between mSIN1 and other mTORC2 components (Cameron et al., 2011; Schroder et al., 2005). As such, except mSIN1.4, which lacks the N-terminal 192 amino acids, the other three isoforms (mSIN1.1, mSIN1.2 and mSIN1.5) can interact with mTOR to form three distinct mTORC2 complexes (Frias et al., 2006; Schroder et al., 2004). The CRIM domain, which is a highly conserved section from yeast to human, is located at the middle part of mSIN1 and has an ubiquitin-like fold structure (Tatebe et al., 2017). Additionally, the CRIM domain has been clearly demonstrated as an important factor for the substrate recognition of mTORC2 (Cameron et al., 2011; Kataoka et al., 2015; Tatebe et al., 2017). RBD is known to interact with Ras protein while the PH domain is responsible for mediating membrane localisation of mSIN1 (Yuan et al., 2015) (Figure 1.5).

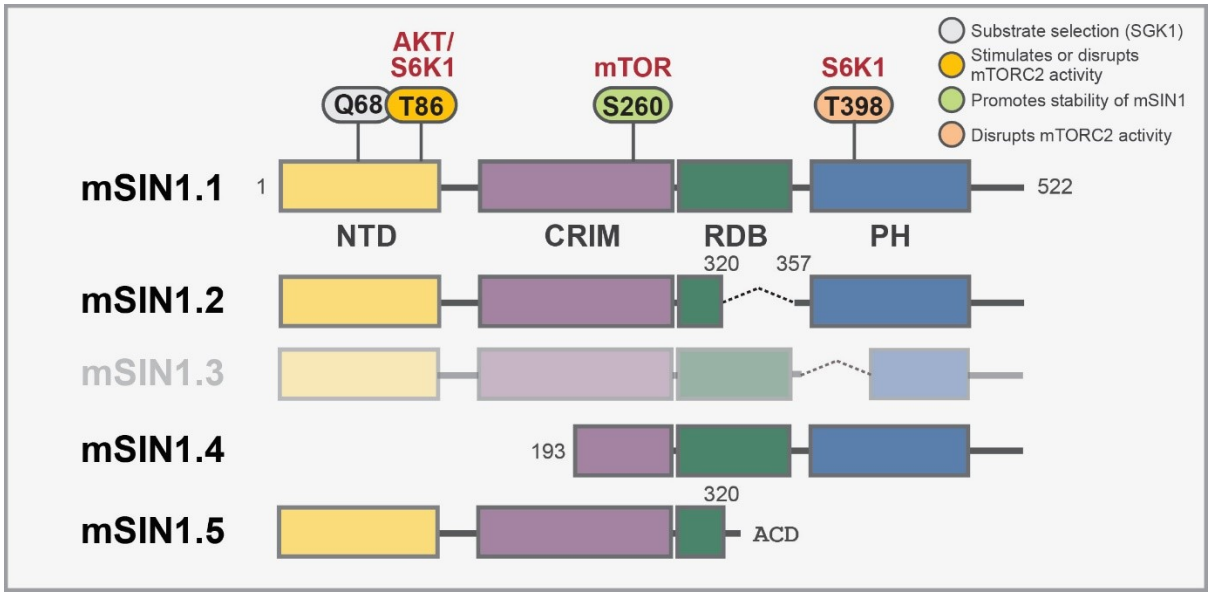


Figure 1.5 Functional domains of mSIN1 isoforms and the regulatory sites

Schematic representation of five predicted mSIN1 isoforms (mSIN1.1-1.5), four (excluding mSIN1.3) of them can be detected in human cells. Full-length of mSIN1 (mSIN1.1) has four domains: N-terminal domain (NTD), conserved region in middle (CRIM), Ras-binding domain (RBD), and pleckstrin homology (PH) like domain. The function of the regulatory sites and their corresponding kinase(s) are also indicated.

i. Function of mSIN1 in mTORC2 signalling

Similar to mTOR and RICTOR, mSIN1 is widely expressed in human tissue (Frias et al., 2006; Yuan et al., 2015). As an essential component of mTORC2, mSIN1 is required for the complex formation and activity (Yang et al., 2006). Due to the structural difference between different mSIN1 isoforms, it has been suggested that different mSIN1 isoforms may form distinct mTORC2 complexes that have diverse subcellular localisation and respond differently to the upstream stimulations. For instance, as the PH domain of mSIN1 plays a key role in the activation of mTORC2 by insulin (Liu et al., 2015). Hence, only the mTORC2 complexes which incorporated with mSIN1.1 and mSIN1.2, but not the mSIN1.5-containing mTORC2, are sensitive to insulin stimulation (Frias et al., 2006; Yuan et al., 2015).

It has been reported that the deficiency of *mSIN1* in various cell types led to the decrease protein level of RICTOR, which subsequently disrupted the interaction between RICTOR and mTOR and therefore attenuated the mTORC2-dependent phosphorylation AKT at Ser473 (Frias et al., 2006; Jacinto et al., 2006; Yang et al., 2006). In addition to participating in the

complex integrity, mSIN1 is also considered to function as a direct binding partner for the recruitment of the substrates to mTORC2. According to the analyses from both yeast and human, the highly conserved CRIM domain of mSIN1 was associated with the ability to select target proteins and, moreover, the CRIM domain of Sp Sin1 alone, an orthologue of mSIN1 in fission yeast, appears to be sufficient for the substrate-recruiting function in fission yeast. Therefore, the CRIM domain of mSIN1 is important for mTORC2 to act on its substrates (Cameron et al., 2011; Kataoka et al., 2015; Tatebe et al., 2017).

The underlying mechanisms of how mTORC2 controls and activates different substrates have rarely been investigated. The functional study of mSIN1 indicated that the assembly and substrate recognition of mTORC2 can be affected by the regulatory sites on mSIN1. For instance, Gln68 on mSIN1 mediates the interaction and activation between mTORC2 and SGK1, but not AKT (Lu et al., 2011). Moreover, the phosphorylation of Ser260 by mTOR enhances the intermolecular interactions within mTORC2 complex and thereby promotes the stability of mSIN1 and integrity of mTORC2 (Chen et al., 2013).

Given that several studies have demonstrated that mSIN1 is necessarily required for the mTORC2 activity, it is conceivable that mSIN1 has biological role in regulating cellular function during mouse embryo development and tumour progression. Similar to *Rictor*-deficient mice, homozygous *mSin1*-knockout mice were also embryonic lethal due to early developmental abnormalities, indicating an important role of mSIN1 in the proper mouse embryo development (Jacinto et al., 2006). In addition to embryo development, it has been found that a tumour invasion suppressor, programmed cell death 4 (PDCD4), inhibits mSIN1 translation which diminishes the phosphorylation of AKT and by that suppresses cell invasion (Wang et al., 2017). Furthermore, overexpress mSIN1 in non-small-cell lung carcinoma (NSCLC) cells significantly promotes cell migration and invasion through the induction of EMT process (Hu et al., 2017). Thus, mTORC2 controls cell growth, metabolism and many other processes through direct activates its downstream targets, but precisely how mTORC2 utilise mSIN1 as a selective adapter to target its substrates remains to be studied.

ii. Function of mSIN1 outside mTORC2 signalling

Before its prominent role related to the mTORC2 signalling pathway has been identified, mSIN1 was mainly known as a binding partner of proteins that are involved in counteracting environmental stress, which include MEKK2, Ras, ATF2, p38 and the interferon receptor (Oh and Jacinto, 2011). It has been reported that mSIN1 acts as a negative regulator in the dimerization of mitogen-activated protein kinase kinase kinase 2 (MEKK2) which in turn blocks the activation of MEKK2 downstream targets (Cheng et al., 2005); mSIN1 also inhibits the activation of ERK and JNK signalling pathways via interacting with activated Ras (Schroder et al., 2007). The study of protein-protein interaction mediated by the Src-SH3 domain indicated that mSIN1 may act as a scaffold molecule, facilitating the formation of multiprotein complexes which participate in cellular stress responses (Alexandropoulos and Baltimore, 1996). For example, Ghosh and colleagues suggest that mSIN1 provides a link between poly(rC)-binding protein-2 (PCBP2) and the TNF receptor (TNFR), leading to stimulation of p38MAPK (MAPK14) pathway and by which protects stressed cells from apoptosis (Ghosh et al., 2008). mSIN1 also contributes to stress-activated protein kinase (SAPK) signalling, acting as a scaffold molecule to positively regulate the phosphorylation of activating transcription factor-2 (ATF2) by p38 in response to the stress. This in turn enhances the transcription of growth arrest and DNA damage-inducible 45β (Gadd45β), one of the ATF-2 downstream targets that has been identified to involve apoptotic cell death (Makino et al., 2006). Furthermore, a Bardet-Biedl syndrome (BBS)-related protein, coiled-coil domain-containing protein 28B (Ccdc28b), has been shown to modulate ciliogenesis through its interaction with mSin1 but independently from mTorc2 in zebrafish (Cardenas-Rodriguez et al., 2013). All these findings further substantiate that apart from being a subunit of mTORC2, mSIN1 could perform different functions in varied biological processes which depends on its interacting partners.

1.3 mTOR signalling pathway in pluripotent stem cells

To date, even though the animal models are instrumental for illustrating the RICTOR/mSIN1/mTORC2 functions during embryonic development, they have a limitation for further elucidation of molecular mechanisms underlying these phenotypes due to material availability, animal welfare and long procedure for genetic modifications. In addition, the extracted fibroblasts from knockout embryos gave limited information for the detailed functions of mTORC2 in the differentiation and developmental processes. As such, embryonic stem cells (ESCs), particularly human ESCs (hESCs) act as an alternative model system, overcoming some of the shortfalls of the animal model systems, and therefore, present a great cell resource to study the function and molecular mechanism of RICTOR/mSIN1/mTORC2 in embryo development, especially human embryo development.

1.3.1 Derivation of hESC lines

The successful isolation of human embryonic stem cells (hESCs) (Thomson et al., 1998) presented an unlimited and powerful cell resource not only for potential clinical application but also for human biological and biomedical researches in the past 20 years. hESCs are derived from the inner cell mass (ICM) of human blastocyst, an early-stage preimplantation embryo. Like all ESCs, hESCs possess two unique characteristics, unlimited self-renewal and pluripotency, having the ability to amplify themselves to indefinite numbers and meanwhile retaining their capacity to give rise to all embryonic tissues, including the germ cells (Keller, 2005). Therefore, hESCs provide a valuable cell model for the studies of gene function and molecular mechanisms during human development and cell fate determination.

1.3.2 The regulation of self-renewal and pluripotency in hESCs

The self-renewal and pluripotency of hESCs are governed by two sets of factors: intrinsic transcription factors and extrinsic factors, which work coordinately to maintain epigenetic configuration for proper hESC properties (Zhao and Jin, 2017).

i. Intrinsic factors

Extensive researches have revealed that hESCs dependent on the delicate regulatory network involving both intrinsic and extrinsic factors to maintain their capacity of self-renewal and pluripotency (Yilmaz and Benvenisty, 2019) (Figure 1.6). The core transcriptional regulatory circuitry contains transcription factors OCT4, SOX2 and NANOG (OSN) that are the key intrinsic factors in responsible for maintaining self-renewal and pluripotency in both mouse and human ESCs. These factors form a complex and function together in a network to support each other's expression and to prevent the ESC differentiation by repressing the activation of lineage-specific genes (Boyer et al., 2005; Chambers et al., 2003; Chew et al., 2005; Fong et al., 2008; Mitsui et al., 2003; Nichols et al., 1998). Due to the ethical issues associated with the use of human embryos, most of the functional studies on OSN associated with human development were performed on hESCs (Wang et al., 2012). Several studies have revealed that a reduction in any of the OSN protein levels in hESCs would result in loss of the undifferentiated stem cell state and differentiated into trophectoderm or primitive endoderm lineages (Adachi et al., 2010; Babaie et al., 2007; Fong et al., 2008; Hay et al., 2004; Hyslop et al., 2005; Zaehres et al., 2005). Although the role of OSN is mostly described as the repressors of differentiation, it has also been shown that that each factor can collaborate with other signalling pathways to control specific cell fates in hESCs. For example, OCT4 induces hESCs differentiate toward extraembryonic fates in a bone morphogenetic protein-4 (BMP4)-dependent manner (Wang et al., 2012).

Notably, the very first study of gene function in human embryos was published in 2017 (Fogarty et al., 2017). With the advent of gene-editing technology CRISPR-Cas9, Norah and colleagues suggest the expression of OCT4 may be required in the first few days during human embryo development, which further supports the idea that the OCT4 is indispensable for maintaining the self-renewal and pluripotency of ESCs.

ii. Extrinsic factors

Extrinsic factors refer to the growth factors, cytokines and extracellular matrices (ECM) in the culture dish, which function through signal transduction pathways to crucially affect the expression of intrinsic factors, thereby controlling self-renewal and differentiation in hESCs. In general, the signalling pathways contribute in modulating hESCs identity can be divided into two types of pathways: self-renewal-supporting signals and differentiation-inducing signals (Zhao and Jin, 2017).

Unlike mESCs, hESCs are not dependent on leukemia inhibitory factor (LIF) and its downstream signal transducer and activator of transcription 3 (STAT3) to sustain their ability of self-renewal and pluripotency (Daheron et al., 2004). Instead, it has been established that the intracellular signalling pathways which are activated by the signalling ligand molecules, TGFβ (transforming growth factor β) /Activin A/Nodal and FGF2 (fibroblast growth factor 2), are important and also be responsible for maintaining the undifferentiation state of hESCs (Zhao and Jin, 2017). The TGFβ/Activin A/Nodal-mediated signalling maintains hESC self-renewal through the activation of their cell membrane receptors and the downstream effectors, SMAD2 and SMAD3 (Beattie et al., 2005; Xiao et al., 2006). The activated SMAD2/3 proteins translocate into the nucleus and positively regulate the transcriptional activity of NANOG by direct binding to its proximal promoter region (Bertero et al., 2015; Pauklin and Vallier, 2015; Vallier et al., 2009; Xu et al., 2008). Despite the essential role in supporting self-renewal, high levels of Activin A (Activin hereafter) has also been found to drive lineage specification toward mesendoderm in hESCs, which is particularly efficient when the level of PI3K/AKT signalling is low (McLean et al., 2007; Singh et al., 2012), suggesting that Activin can function to either enhance or repress hESC self-renewal in a context-dependent manner. In addition to TGFβ/Activin/Nodal, hESCs also heavily rely on FGF2 signalling to maintain their self-renewal and to prevent their differentiation. FGF2, also known as basic FGF (bFGF), induces the activation of PI3K/AKT and MEK/ERK pathways which subsequently restrains differentiation-inducing activity in hESCs (Armstrong et al., 2006; Greber et al., 2007; Kang et al., 2005; Li et al., 2007).

On the other hand, the activation of BMP and WNT signalling are known to drive the transition of hESCs from a self-renewal state to differentiation. The mechanisms by which BMP signalling, mainly triggered by BMP4, induces hESCs to differentiate into multiple lineages including mesoderm and trophoblast (Pauklin and Vallier, 2015). Several independent studies reported that BMP4 induces hESCs differentiation to trophoblast without the formation of mesoderm (Amita et al., 2013; Xu et al., 2002), whereas other studies demonstrated that hESCs differentiate to mesodermal cell types which expressed high levels of mesoderm markers in the presence of BMP4 (Bernardo et al., 2011; Richter et al., 2014). A study presented by *Kuerk et al*. further revealed that BMP might be involved in the differentiation of both trophoblast and mesodermal lineages depending on other signalling pathways. For instance, WNT signals appear to be critical for the BMP-dependent cell fate decision (Kurek et al., 2015). In comparison with BMP signalling pathway, the exact role of WNT signalling in hESC self-renewal and differentiation remains in disagreement (Blauwkamp et al., 2012; Pauklin and Vallier, 2015; Singh et al., 2012). The WNT signalling seems to function differently under various cellular conditions, depending on the time course and its subcellular localisation. It has been shown that short-term upregulation of WNT signalling enhances hESC self-renewal, whereas long-term elevated WNT signalling promotes hESCs differentiate toward mesendodermal lineages (Huang et al., 2015; Zhou et al., 2016). Moreover, the nucleus or cytoplasm localisation of β-catenin in canonical WNT signalling pathway leads to opposite effects on hESC differentiation or self-renewal, respectively (Kim et al., 2013). Taken together, these findings provide insights that the two unique characteristics of hESCs are regulated by the crosstalk between multiple extracellular signal-regulated pathways, and thus should be precisely controlled to prevent differentiation.

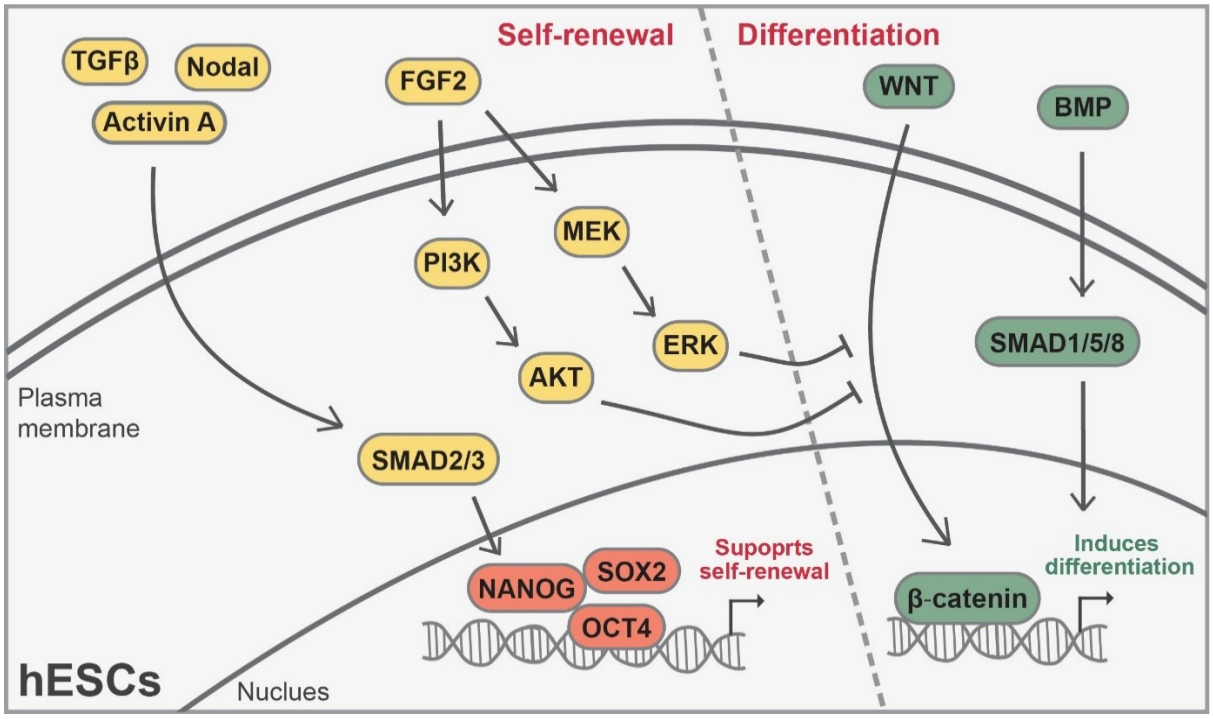


Figure 1.6 Summary of signalling pathways involved in hESCs self-renewal and differentiation

hESCs rely on both intrinsic and extrinsic factors to regulate self-renewal and differentiation. The core transcriptional regulatory circuitry, OCT4, SOX2 and NANOG, are intrinsic factors that are critical for maintaining self-renewal and pluripotency in hESCs. Signalling pathways which activated by TGFβ/Activin A/Nodal and FGF2 are known to support self-renewal in hESCs, whereas BMP and WNT drive differentiation. The nucleus-positioned core transcription factors are shown in red. Extracellular signals and the components of signalling pathways which maintain the pluripotency or induce differentiation of hESCs are indicated in yellow and green, respectively.

1.3.3 Different States of Pluripotency

i. Primed and naïve states

It becomes evident that pluripotency is not restricted to the cells at a specific developmental stage, rather it is a property of cells in the early embryonic development, spanning from the inner cell mass (ICM) of preimplantation blastocysts to postimplantation epiblast cells. However, there are distinct differences in gene expression profile and epigenetic configuration of these cells at various developmental stages, even though they are all pluripotent (Nichols and Smith, 2009). mESCs derived from the ICM of preimplantation blastocysts and cultured in 2i conditions exhibit genomic DNA hypomethylation and high levels of Nanog expression, which resemble that in the ICM (Collier and Rugg-Gunn, 2018). These mESCs have the ability to efficiently contribute to blastocyst chimeras (Duggal et al., 2015; Honda et al., 2013; Nichols and Smith, 2009, 2011; Ying et al., 2008) and are named naïve ESCs. By contrast, mouse stem cells, EpiSCs derived from post-implantation epiblast and culture in FGF and Activin supplemented condition, reveal higher DNA methylation and lower levels of Nanog, named primed ESCs (Brons et al., 2007; Tesar et al., 2007; Ying et al., 2008).

Interestingly, although both derived from the ICM of the blastocysts, mESCs and hESCs require different culture environment and exhibit distinct cell properties which indicated that mESCs and hESCs are at two distinct states even though they were isolated from embryos at the equivalent developmental stages (Martin, 1981; Thomson et al., 1998). Furthermore, the culture conditions of hESCs are almost the same as that for EpiSCs and both cell types also exhibit similar cell morphology, epigenetic state and transcriptional expression of genes (Chandrasekaran et al., 2017; Festuccia et al., 2013; Takahashi et al., 2018). Therefore, hESCs and hPSCs in most of the cultures are classified as in primed state (Nichols and Smith, 2009; Weinberger et al., 2016).

ii. The conversion between primed and naïve states

It has been shown that the naïve and primed states of mESCs are interchangeable in response to the culture conditions (Dutta et al., 2011, Li et al., 2011; Ying et al., 2008). Therefore, several groups have developed protocols, with either transgene-dependent or -independent

approaches, to convert hPSCs into naïve state using gene expression profile and epigenetic signature as markers (Hanna et al., 2010; Chan et al., 2013; Gafni et al., 2013; Theunissen et al., 2014; Takashima et al., 2014; Guo et al., 2016)

Unlike naïve mESCs, naïve hESCs conversion is more complex, requiring more exogenous factors in addition to the 2i/LIF required for naïve mESCs, which involve multiple signalling pathways, such as MEK/ERK, BMP, etc (Hanna et al., 2010; Gafni et al., 2013; Chan et al., 2013; Theunissen et al., 2014). Moreover, most of these naïve hPSC culture conditions still require the use of feeder cells (mouse embryonic fibroblasts, MEF) to support the conversion and/or maintenance of naïve hESCs. Notably, by analysing the transcriptomes, Warrier and colleagues showed that the naïve-like hESCs have similar transcriptional profiles despite they were obtained from different protocols and that they are distinct from primed hESCs (Warrier et al., 2017). For example, they expressed higher levels of REX1, TCL1B, ESRRB and PRDM14. Importantly, the study identified PI3K/AKT/mTOR signalling, particularly the mTORC2 pathway, may play a crucial role in the induction of naïve state of hESCs (Warrier et al., 2017).

1.3.4 Gene targeting tools for hESCs research

Study of gene function and mechanisms in hESCs has been hampered by the difficulties in genetic modification in these cells due to low transfection and targeting efficiency. However, the recent advance in gene targeting technique using clustered regularly interspaced short palindromic repeats (CRISPR) with its associated nuclease CRISPR associated protein 9 (Cas9) has greatly improved the efficiency of gene modification in hESCs (Liang et al., 2015). CRISPR was firstly described in 1987 in bacterium *Escherichia coli* by Nakata's group (Ishino et al., 1987), and it showed that certain DNA sequences that are associated with CRISPR repeats could be unwind or cut by CRISPR associated nuclease, named Cas nuclease (Jansen et al., 2002). It is believed that the CRISPR-Cas system functions as an immune system in prokaryotes to protect them from invading foreign genetic elements such as plasmids and phages (Bhaya et al., 2011).

Further studies demonstrated that one of the CRISPR-Cas systems, CRISPR-Cas9, not only functions in prokaryotes but also can be engineered to function as a gene targeting tool in eukaryotes, even in mammalian cells (Bauer et al., 2015; Liang et al., 2015; Wu et al., 2014). In details, CRISPR-Cas9 system functions through Cas9 nuclease together with a single guide RNA (sgRNA). sgRNA is an artificial chimeric molecule consisting of a 20-bp CRISPR RNA (crRNA) that fused with trans-activating crRNA (tracrRNA) via a linker loop (Jinek et al., 2012). The targeting specificity of Cas9 nuclease is determined by the 20-bp guide sequence on crRNA, therefore, this 20-bp is necessarily required to be identical to the genomic DNA sequence following by a protospacer adjacent motif (PAM) sequence at the 3' downstream region in the genomic DNA. The suitable PAM sequence is dependent upon the species of Cas9 (e.g. 5′-NGG-3′ for *Streptococcus pyogenes* Cas9) and it is essential for the specific DNA cleavage by Cas9-sgRNA complex (Figure 1.7).

Like zinc-finger nucleases (ZFNs) and transcription activator–like effector nucleases (TALENs), Cas9 promotes genome editing by introducing a double-strand break (DSB) in target DNA (Hsu and Zhang, 2012; Urnov et al., 2010). Repair of this DSB relies on two different DNA damage repair pathway: error-prone non-homologous end joining (NHEJ) pathway or the high-fidelity homology directed repair (HDR) pathway, both of which can be used to achieve a desired editing outcome. In 2012, Zhang Feng's research group revealed the mechanism of Cas9-mediated DNA targeting, and developed new strategy to reduce the off-target effect of Cas9 by modifying the Cas9 proteins and sgRNA design (Jiang et al., 2013; Jinek et al., 2012; Kleinstiver et al., 2016). For instance, combination of the HNH^{+}/$RuvC^{-}$ mutant (D10A) nickase of Cas9 (Cas9n) along with a pair of sgRNAs can cause a DNA double nicking and greatly reduces unwanted off-target effects (Ran et al., 2013a). The discovery and development of CRISPR-Cas9 system has considerably facilitated genetic modification in hESCs (Collinson et al., 2016; Li et al., 2018b; Yilmaz et al., 2018). Thus, makes hESCs easier to be used as a cell model to perform more comprehensive and detailed screening for identifying essential genes in human development.

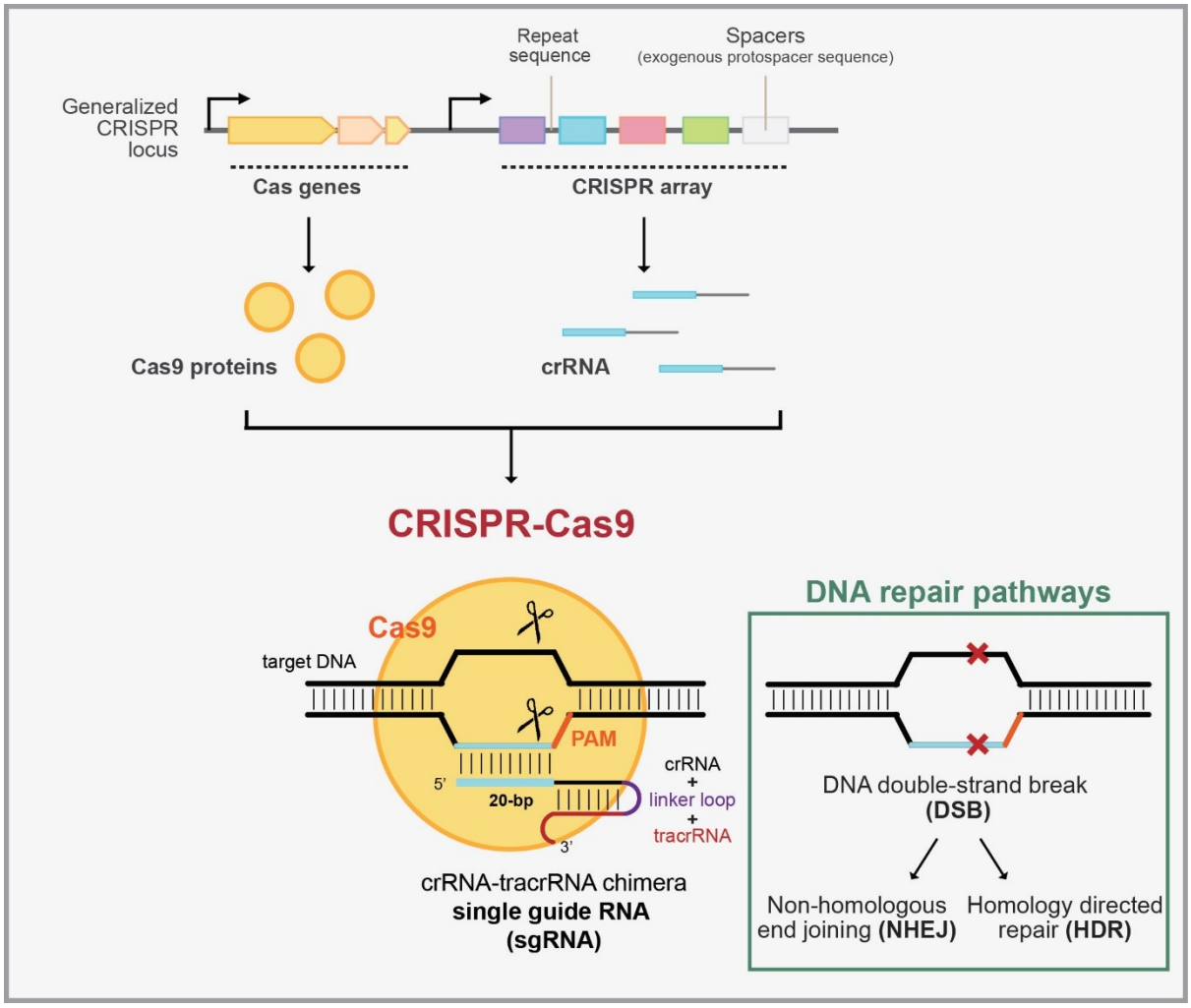


Figure 1.7 The mechanism of the CRISPR-Cas9 system

(Top) *CRISPR system was first described as an adaptive immunity in bacteria in 1980s. The CRISPR loci in bacteria is consisted of a clustered set of Cas genes followed by CRISPR array- a series of repeat sequences which interspaced by spacers that are identical to the sequences within foreign genetic elements (protospacers). Endonuclease Cas9 proteins are translated from the Cas genes and crRNAs are generated from the CRISPR array.* ***(Bottom)*** *Engineered CRISPR-Cas9 system can function as a gene targeting tool which composed of Cas9 protein and guide RNA (sgRNA, crRNA-tracrRNA chimera) with 20-bp guide sequences. The sgRNA enables Cas9 to recognise and introduce a DNA double-strand breaks (DSB) within the target DNA.* ***(Bottom right)*** *The resulting DSB is then subsequently repaired by either error-prone non-homologous end joining (NHEJ) or the high-fidelity homology directed repair (HDR) pathways. CRISPR, clustered regularly interspaced short palindromic repeats; Cas, CRISPR-associated; crRNA, CRISPR RNA; tracrRNA, trans-activating crRNA.*

1.3.5 Role of mTOR signalling in regulation of hESC self-renewal and pluripotency

Although intensive investigation has been carried out since the discovery of mTOR, limited information is available regarding the role of mTOR signalling in human development as most of the studies on mTOR signalling in development have been conducted on animal models. In addition, there are limited information about the function of mTOR signalling in the regulation of stem cells.

In neural stem cells (NSCs), the activity of mTOR kinase supports the proliferation and differentiation of NSCs as the formation of dendrites and dopaminergic neurons were significantly inhibited by mTOR inhibitors (Lee et al., 2016a, b; LiCausi and Hartman, 2018; Skalecka et al., 2016; Wahane et al., 2014). mTOR signalling is also participated and tightly regulated in the proper development of hematopoietic stem cells (HSCs) (Luo et al., 2014; Wang et al., 2016). Several studies have revealed that functional HSCs are dependent on the appropriate activity of the mTOR signalling pathway as hyperactivity of mTORC1 contributes to depletion of HSCs through the induction of tumour suppressor genes such as *TP53* (Lee et al., 2010; Signer and Morrison, 2013; Yilmaz et al., 2006). In consistent with this finding, the significantly enriched PI3K/AKT/mTOR pathway revealed to be corresponding with the rapid expansion of differentiated HSCs (Chen et al., 2015; Geest et al., 2009). Furthermore, commitment of mesenchymal stem cells (MSCs) to different lineages has been shown to be regulated by mTOR signalling. Although there is clear evidence that mTOR can promote adipogenesis through upregulation of the transcriptional and translational level of peroxisome proliferator-activated receptor gamma (PPARγ) (Cho et al., 2004; Zhang et al., 2009), several studies report that osteogenesis require inhibition of mTOR signalling (Isomoto et al., 2007; Lee et al., 2010c; Ogawa et al., 1998; Singha et al., 2008). More recent study has suggested that mTORC1 promotes adipocyte differentiation while mTORC2 suppresses adipogenesis and promotes osteogenesis (Martin et al., 2015), indicating that the two mTOR complexes may have distinct roles in MSC lineage determination.

In comparison with adult stem cells, although some recent studies have attempted to understand the physiological roles of mTOR complexes in hESCs, however, the contribution of PI3K/AKT/mTOR signalling in regulating of hESCs self-renewal and pluripotency still debate

as the previous studies showed contradictory results. Zhou and colleagues reported that mTOR signalling supports long-term self-renewal of hESCs, whereas other reports suggest that mTOR-mediated activation of S6K1 induces differentiation (Easley et al., 2010; Zhou et al., 2009). As the maintenance of the hESC characteristics is highly dependent on the extracellular signal-mediated pathways, conflicting results could be attributed to various culture conditions or even the cell lines used in the respective studies.

Interestingly, the functional roles of mTOR complexes that govern differentiation may act differently in hESCs and mESCs. Inhibition of mTORC1 by rapamycin in hESCs has been reported to induce a marked differentiation to mesendodermal lineages (Jung et al., 2016; Nazareth et al., 2016), whereas lacking of mTORC2 activity, but not mTORC1, resulted in a defective mesoderm specification in mESCs (Gomez-Salinero et al., 2016; Li et al., 2018a). Moreover, studies in naïve hESCs revealed that the expression of mTORC2 subunits, RICTOR and mSIN1, increased in naïve hESCs in comparison with primed state and this increase may have a function to prevent cell death in naïve hESCs (Warrier et al., 2017). This study provides evidence that mTORC2 signalling might also be involved in the maintenance of naïve state pluripotency. Nonetheless, Folliculin (FLCN), which is a key factor for promoting the exit from human naïve pluripotency, has been found to form a complex with mSIN1 and subsequently inhibits the functions of mTORC2 in the naïve state (Mathieu et al., 2019). All these findings indicated that the two mTOR complexes might play critical and divergent roles in regulating the capacity of self-renewal and pluripotency in hESCs.

As indicated above, it remains ambiguous about the regulation and exact molecular mechanisms by which the mTOR signalling implicates in hESC functions. This is particularly manifesting with mTORC2 for which there is no specific inhibitor that could be applied. Therefore, additional studies are necessary required to elucidate and distinguish the effects of RICTOR/mTORC2 from mTORC1 in the regulation of hESC biology, and thus might provide important information for the understanding of normal physiology and human disease.

1.4 Aims and Objectives

The overall aim of my project is to elucidate the molecular mechanisms by which mTORC2 is assembled, regulated and functioning in human cells. Given that there is no specific inhibitor for mTORC2, I aim to apply CRISPR-Cas9 system for the disable of RICTOR, which is a specific key subunit of mTORC2, in several human cell types. Since RICTOR is an essential factor in mTORC2, I anticipate that deciphering the role of RICTOR in mTORC2 assembly and function will greatly advance our understanding of mTORC2.

Specifically, I will aim to achieve the following objectives (Figure 1.8):

A. Generation and characterisation of *RICTOR*-deficient cells: such as HEK 293T cells and human embryonic stem cells (hESCs).
B. Investigate the role of RICTOR in cell functions and its underlying mechanisms.
C. Explore how RICTOR affects mTORC2 assembly and its relationship with other components in mTORC2 complex.
    a. How does RICTOR regulate mSIN1 expression?
    b. How does RICTOR regulate mTORC2 assembly and activity?
D. The function of RICTOR/mTORC2 in regulating hESC self-renewal and differentiation.

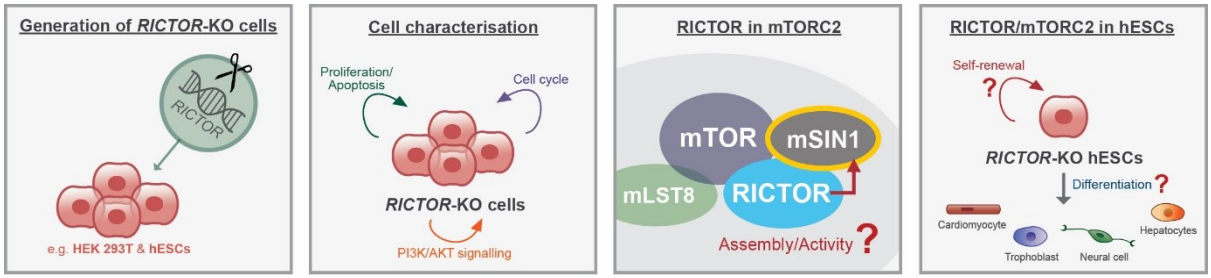


Figure 1.8 Aims and objections

02

Materials and Methods

2.1 Cell culture

2.1.1 Materials

2.1.1.1 Cell lines

All cells were cultured at 37 °C with 5% CO_2.

Cells	Source
H1 hESC (WA-01)	Male human ES cell line isolated by Thomson et al., 1998, distributed by WiCell.
H7 hESCs (WA-07)	Female human ES cell line isolated by Thomson et al., 1998, distributed by WiCell.
PC-3	Prostate adenocarcinoma cell line derived from a metastatic site in the bone, kind gift from Dr. Robert Krypta.
HEK 293T	Kidney cell line immortalised by T-antigen delivered by adenovirus, obtained from the ECACC.
RICTOR-control HEK 293T	Control HEK 293T cells for *RICTOR*-knockout HEK 293T cells.
RICTOR-knockout HEK 293T	Stable *RICTOR*-knockout HEK 293T generated by CRISPR-Cas9 system.
mSIN1-control HEK 293T *mSIN1*-null HEK 293T	*mSIN1*-Control and null HEK 293T cells were obtained from Professor McCormick from UCSF, USA.
Mouse Embryonic Fibroblasts (MEFs)	Wild-type MEFs isolated from E13.5 CD-1 mouse embryos.
Rictor-control MEFs	Control MEFs for *Rictor*-null kind gift from Prof. Mark Magnuson (Shiota et al., 2006).
Rictor-null MEFs	Immortalised MEFs with knockout of *Rictor* gene also from Prof. Mark Magnuson (Shiota et al., 2006).
RICTOR-control H1 hESCs	Control hESCs for *RICTOR*-knockout hESCs.
RICTOR-knockout H1 hESCs	Stable *RICTOR*-knockout hESCs generated by CRISPR-Cas9 system.

2.1.1.2 Growth Factors and Inhibitors

Reagent	Supplier	Working Concentration
Basic Fibroblast Growth Factor (bFGF)	R&D	10ng/ml
Puromycin	Sigma-Aldrich	1~2µg/ml
Rho Kinase Inhibitor (ROCKi)	Sigma-Aldrich	10µM
Chloroquine	Sigma-Aldrich	100µM
MG-132	Calbiochem	30µM
Cycloheximide	Abcam	20µg/ml
Rapamycin	R&D/Tocris	100nM
Torin-2 (Torin)	R&D/Tocris	15nM

2.1.1.3 Media Components

Reagent	Supplier
200mM L-Glutamine	Sigma-Aldrich
100X Penicillin-Streptomycin	Sigma-Aldrich
20% Bovine Serum Albumin (BSA)	Sigma-Aldrich
Dulbecco's Modified Eagle AQ Media (DMEM-AQ)	Sigma-Aldrich
Heat-inactivated Foetal Bovine Serum (FBS)	Sigma-Aldrich
Knockout DMEM	Life Technologies
Knockout Serum Replacement (KSR)	Sigma-Aldrich
Opti-MEM® Reduced Serum Medium	Life Technologies
Roswell Park Memorial Institute AQ-Media 1640 (RPMI-AQ)	Sigma-Aldrich
50mM β-mercaptoethanol	Life Technologies
Non-essential Amino Acids (NEAA)	Life Technologies

2.1.1.4 Media Recipes

Media	Components
Knockout Serum Replacement Medium (KSR-M)	**Knockout™ DMEM (KO-DMEM)** supplemented with: 20% Knockout™ Serum Replacement 1mM L-glutamine 1X NEAA 0.1M β-mercaptoethanol for tissue-culture 1X Penicillin-Streptomycin
MEF/HEK 293T medium	**DMEM-AQ** supplemented with: 10% FBS 1X Penicillin-Streptomycin
MEF-conditioned medium for hESCs (MEF-CM)	**MEF conditioned KSR-M** supplemented with: 1mM L-glutamine 1X Penicillin-Streptomycin 10ng/ml bFGF
PC-3 medium	**RPMI-AQ** supplemented with: 10% FBS 1X Penicillin-Streptomycin

2.1.1.5 Disassociation Enzymes

Enzyme	Supplier
Accutase	Sigma-Aldrich
Collagenase IV	Life Technologies
Trypsin-EDTA	Sigma-Aldrich

2.1.1.6 Reagents, Chemicals and Kits

Reagent	Supplier
2% Gelatine in H_2O	Sigma-Aldrich
Calcium Phosphate Transfection Kit	Sigma-Aldrich
Dimethyl sulfoxide (DMSO)	Sigma-Aldrich
Lipofectamine™ LTX with PLUS™ Reagent	Life Technologies
Matrigel® Matrix Growth Factor Reduced	BD Bioscience
NEON™ Transfection System	Fisher Scientific

2.1.2 Methods

2.1.2.1 Culture and propagation of hESCs

I. Isolation of Mouse Embryonic Fibroblasts (MEFs)

Quick and humane sacrifice of pregnant female CD1 mice (E13.5), dissected out the uterine horns and briefly washed with PBS containing 2X Penicillin/Streptomycin (Pen/Strep). Separated each embryo from surrounding membranes and washed with PBS to remove as much blood as possible. After removed the heart and liver, finely minced and dissociated the mouse embryos into single cells by incubating with trypsin at 37^{o}C in Bijou tubes for 10 minutes. Meanwhile, tissues were vortexed during the incubation in order to break up any large clumps of cells. Neutralized the cells with MEF medium (see section 2.1.1.4 for MEF medium recipe) then transferred the suspension into T75 flasks. Approximately 2-3 days later, cells were collected and frozen down in MEF medium supplemented with 10% DMSO and labelled as P0 (passage 0) when they reached 80-90% confluency. A recommended number of cells per cryovial is 1x10^{7} cells.

II. Generation of Mouse Embryonic Fibroblast-Conditioned Medium (MEF-CM)

Frozen MEFs were quickly thawed in a warm water bath and expanded up to 3 or 4 passages in MEF medium. Cells were collected by trypsinization and inactivated with gamma irradiation at 40 grays to stop their further proliferation, then seeded appropriate number (2 x 10^{7}) of irradiated cells into T225 flask which coated with 0.5% gelatin in advance. The following day, replaced MEF medium with 150ml of Knockout Serum Replacement Medium (KSR-M) (see section 2.1.1.4 for KSR-M recipe) supplemented with 4ng/ml bFGF (0.4µl/ml). Collected the medium, now considered MEF-conditioned medium (MEF-CM), from the T225 flask after 24 hours of conditioning into collection bottle and stored at -80^{o}C until use. Another 150ml KSR-M supplemented with 4ng/ml bFGF (0.4 µl/ml) was added back into the T225 flask, repeated the same procedure for up to seven days in a row. At the time of use, defrosted and filtered MEF-CM to remove cellular debris and supplemented with 2mM L-glutamine and 1X Penicillin-Streptomycin. MEF-CM was kept at 4^{o}C and to be used within one week after defrosting.

III. Preparation of Matrigel®-coated plates

Stock Matrigel® should be thawed overnight, or for a few hours at least, on ice at cold room (Matrigel® solidifies at room temperature). Diluted Matrigel® 1 in 2 with cold Knockout DMEM and the mixture was aliquoted into 15ml tubes (1ml/tube). Stored the aliquoted Matrigel® at -20°C or used it immediately. To create working stocks, slowly thawed the 1ml aliquots overnight at 4°C and diluted 1 in 18 in cold Knockout DMEM. For 6-well plate, 1ml of Matrigel® working stock was added in each well to cover the whole surface and followed by sealing with a layer of Parafilm® around the edge of the 6-well plate to prevent evaporation. Plate was allowed to set overnight at 4°C or for at least 4 hours at room temperature. Matrigel® solution was aspirated immediately before use.

IV. Routine culture and maintenance of Human Embryonic Stem Cells (hESCs)

H1 hESCs were cultured in MEF-CM and freshly supplemented it with additional 10ng/ml of bFGF on Matrigel®- coated plates. Medium was changed daily for the maintenance of hESCs, passaged as small colonies routinely when cells were 90-100% confluent (normally 5-7 days). For passaging hESCs by mechanical dissociation, aspirated the medium from the well and washed once with PBS. Treated the cells with 200U/ml Collagenase type IV, which dissolved in Knockout DMEM, and incubated at 37°C for 5-7 minutes. When the edge of the hESCs colonies started to pull away from the plate, aspirated the Collagenase type IV solution and rinsed the plate with PBS. Colonies were broke up and detached by manual scraping with a 5ml pipette in 1ml MEF-CM, colonies could be further broke up by pipetting cells up and down before they were transferred into a new plate. The split ratio is generally between 1:2 and 1:4 depending on the cell conditions.

V. Formation of Embryoid Bodies (EBs) from hESCs

Aspirated medium from hESCs, treated cells with 1ml/well of Collagenase type IV (200U/ml) and incubated 5-7 minutes at 37°C. Removed Collagenase type IV and gently washed once with 1ml PBS. Added 2ml of differentiation medium (KSR-M, medium formulations are listed in section 2.1.1.4) into each well and scraped cells with a 5ml pipette manually. Transferred 2 wells of cells into low attachment T25 flask in a total volume of 4-5ml of differentiation medium. After overnight culture in suspension, ES cells form floating aggregates known as embryoid

bodies (EBs). Changed the media every 2-3 days by transferring EBs into a 15ml tube and let the aggregates settled for 5 minutes. Removed the supernatant and replaced with fresh differentiation medium, then placed the EBs back to low attachment T25 flask for further culture. Alternatively, EBs at different stages can be transferred to tissue culture plates for further induction of differentiation.

2.1.2.2 Culture and propagation of HEK 293T and PC-3 cells

Cells were routinely cultured at 37°C in a 5% CO_2 incubator with a humidified atmosphere. HEK 293T cells were maintained in Dulbecco's modified Eagle medium (DMEM) containing 10% FBS and 1X Pen/Strep and PC-3 cells were incubated in Roswell Park Memorial Institute (RPMI) 1640 medium supplemented with 10% FBS and 1X Pen/Strep. When cells had reached ~90-100% confluency, aspirated the medium from the tissue culture vessels and gently washed the cells with 1X PBS. Cells were then dissociated by incubating with trypsin-EDTA at 37°C for 5-10 minutes. Stop the trypsinization by adding growth medium and split the cells in a ratio from 1:5 to 1:10. For long-term storage, $1x10^6$ cells were suspended in 1ml freezing medium which composed of 90% fresh medium and 10% DMSO. Cell suspension were then transferred in cryovial and stored in liquid nitrogen for long term preservation.

2.1.2.3 Culture and propagation of *Rictor*-Control and *Rictor*-Null MEF

The spontaneously immortalized control and *Rictor*-null MEFs were cultured in Dulbecco's modified Eagle medium (DMEM) supplemented with 10% FBS and 1X Pen/Strep. The propagation procedures of MEFs were similar to those described for HEK 293T and PC-3 cells (see section 2.1.2.2). Notably, as *Rictor*-null MEFs presents a slower growing rate in culture than control MEFs, the subculture of *Rictor*-null MEFs were perform at split ratio no greater than 1:3 to reduce senescence associated cell death, whereas the control MEFs were passaged at 1:3 to 1:10 splitting ratio. Both MEF cell lines were frozen at $3x10^6$ cells per cryovial in freezing medium composed of 90% DMEM and 10% DMSO.

2.1.2.4 Inhibitor assays

The inhibitors were dissolved in either deionized water or DMSO for the indicated stock concentrations. Allowed the cells to grow to the desired density before the treatment of inhibitors. Cells were treated with different inhibitors at the indicated working concentrations/time points and collected for the following analysis.

2.1.2.5 Genetic manipulation of cell lines

I. Calcium Phosphate Transfection

Cells were seeded in 10-cm tissue culture dishes with 10ml of medium for 24 hours and they should be about 70-80% confluent at the time of transfection. Growth medium was aspirated and replaced with 6ml of fresh medium before transfection. The transfection mix was prepared into two tubes, one with 2X HeBS (tube A) and another with DNA and $CaCl_2$ (tube B), up to 15 to 20μg DNA can be used for one 10-cm plate. Tube A and tube B were then mixed by slowly dropping the DNA and $CaCl_2$ mixture while aerating the 2X HeBS with 1ml pipet. The mixture was stood in room temperature for 20 minutes then dropped evenly over the cell culture medium on the plate and mixed gently. 12 to 16 hours post-transfection, gently removed the medium from the plate and replaced with 10ml of pre-warmed fresh medium.

II. Lipofection

Transient transfection of hESCs and tumour cell lines (PC-3 cells) with plasmid DNA was achieved by lipofection. Cells were plated at an appropriate density according to different surface areas of tissue culture vessels and cells should be about 70-80% confluent at the time of transfection. Take 12-well plate for example, 1μg of DNA plasmid together with 1μl of PLUS™ Reagent were diluted in 50μl of OptiMEM® (typically 1/20 volume of total medium) and 2μl of Lipofectamine™ LTX reagent was suspended in another 50μl of OptiMEM® in a separate tube. Each tube was incubated for 5 minutes then mixed gently by pipetting up and down. After incubated at room temperature for 20 minutes, the DNA-lipid complex was added to the cells and the cell culture medium was replaced with fresh medium 16-18 hours post-transfection.

III. Electroporation

Gene editing of H1 hESCs was conducted using the Neon™ Transfection and plasmid-based CRISPR-Cas9 system. After pre-treated with Rho Kinase inhibitor (ROCKi) for 24 hours, culture medium was removed from the plates and cells were washed with PBS and then treated with accutase for 5-10 minutes at 37°C to form a single cell suspension. The cells were centrifuged at 1000 rpm for 5 minutes, and following supernatant removal, cell pellet was then washed with PBS. Pelleted the cells by centrifugation again and re-suspended cell pellet in Buffer-R which contained CRISPR-Cas9 plasmids. The cells were transfected with the Neon™ Transfection system at 1050 V, 30 ms and 2 pulse. After electroporation, the cells were gently plated on Matrigel®-coated plates with MEF-CM medium (without Penicillin-Streptomycin) supplied with bFGF and ROCKi. Puromycin selection (0.5μg/ml) was started 48 hours post-transfection. After 3 days selection, colonies were dissociated with accutase and plated at a low density in puromycin-free culture for the isolation of H1 *RICTOR*-knockout clonal cell lines.

2.2 Molecular Biology - DNA/RNA techniques

2.2.1 Materials

2.2.1.1 Reagents, Chemicals and Kits

Reagent	Supplier
2-Log DNA ladder	NEB
50 bp DNA ladder	NEB
6X DNA loading	NEB
Agarose (molecular biology grade)	Sigma-Aldrich
Ampicillin	Sigma-Aldrich
Chloroform:Isoamyl alcohol 24:1	Sigma-Aldrich
Phenol:Chloroform:Isoamyl Alcohol 25:24:1	Sigma-Aldrich
DH5α Competent *E. coli*	Sigma-Aldrich
Ethanol	VWR
Ethidium Bromide	Sigma-Aldrich
Ethylenediaminetetraacetic acid (EDTA)	Sigma-Aldrich
HiSpeed Midiprep Kit	Qiagen
Isopropanol	VWR

Magnesium chloride ($MgCl_2$), anhydrous	Sigma-Aldrich
Molecular Grade Water	Sigma-Aldrich
Murine RNAse Inhibitor	NEB
$Oligo(dT)_{12-18}$	Thermo Fisher
NEB Monarch Gel extraction kit	NEB
SYBR® Green Jumpstart™ *Taq* Ready Mix	Sigma-Aldrich
Tri Reagent ®	Sigma-Aldrich
Tris Base	Sigma-Aldrich
Sodium chloride (NaCl)	Sigma-Aldrich
Hydrochloric acid (37%)	Sigma-Aldrich
Sodium dodecyl sulfate (SDS)	Sigma-Aldrich
Propidium iodide (PI)	Sigma-Aldrich
RNase A	Fisher
Proteinase K	Sigma-Aldrich
Triton X-100	Sigma-Aldrich

2.2.1.2 Buffers and Solutions

Buffers	Components
50X Tris-Acetate-EDTA Buffer (TAE)	242g Tris Base 57.1ml Acetic Acid 18.6g EDTA Autoclaved water to 1L
Tris-EDTA Buffer (TE)	1ml Tris-HCL pH 8.0 (10mM) 200µl of 0.5M EDTA pH 8.0 (1mM) Autoclaved water to 100ml
TNE buffer	100mM Tris-HCl pH 7.4 5mM EDTA 0.2% SDS 200mM NaCl
Lysogeny Broth (LB) Medium	10g Bacto-tryptone 5g Yeast extract 10g NaCl Autoclaved water to 1L
LB Agar	5g Bacto-tryptone 2.5g Yeast extract 5g NaCl 7.5g Agar Autoclaved water to 500ml
P1 Resuspension Buffer (Qiagen)	50mM Tris-HCl pH 8.0 10mM EDTA 100µg/ml RNAse A

P2 Lysis Buffer (Qiagen)	200mM NaOH 1% Sodium Dodecyl Sulphate (SDS)
P3 Neutralisation Buffer (Qiagen)	3M Potassium acetate pH 5.5

2.2.1.3 DNA Modifying Enzymes

Enzyme	Supplier
Antarctic Phosphatase	NEB
DNAse I	Sigma
Jumpstart™ *Taq* Polymerase	Sigma
ProtoScript II Reverse Transcriptase	NEB
Q5® High Fidelity Polymerase	NEB
Restriction endonucleases	NEB
T4 ligase	NEB
T4 polynucleotide kinase (PNK)	NEB
T7 endonuclease I (T7EI)	NEB

2.2.1.4 Plasmids

Recombinant plasmids used in this project are shown in the following table:

Recombinant plasmid	Vector	RE site*	Insert
eSpCas9(1.1)-2A-Puro	pSpCas9(BB)-2A-Puro	AgeI, KfII	eSpCas9(1.1)
eSpCas9(1.1)-2A-Puro-RICTOR Exon4-1	eSpCas9(1.1)-2A-Puro	BbsI	RICTOR sgRNA-Exon 4-1
eSpCas9(1.1)-2A-Puro-RICTOR Exon4-2	eSpCas9(1.1)-2A-Puro	BbsI	RICTOR sgRNA-Exon 4-2
eSpCas9(1.1)-2A-Puro-RICTOR Exon5-1	eSpCas9(1.1)-2A-Puro	BbsI	RICTOR sgRNA-Exon 5-1
eSpCas9(1.1)-2A-Puro-RICTOR Exon5-2	eSpCas9(1.1)-2A-Puro	BbsI	RICTOR sgRNA-Exon 5-2
eSpCas9(1.1)-2A-Puro-RICTOR Exon5-3	eSpCas9(1.1)-2A-Puro	BbsI	RICTOR sgRNA-Exon 5-3
pCAG-Puro-3XHA-DsRed	**(L106)** pCAG-Puro-2A-3XHA-SOX2	BsrGI, Bsu36I	DsRed
pCAG-Puro-3XHA-RICTOR	pCAG-Puro-3XHA-DsRed	FseI, Bsu36I	RICTOR Full-length
pCAG-Puro-3XHA-RICTOR ΔN-CS (Δ1-500)	pCAG-Puro-3XHA-DsRed	FseI, Bsu36I	RICTOR Δ1-500 aa

pCAG-Puro-3XHA-RICTOR ΔC-CS+REM (Δ501-860)	pCAG-Puro-3XHA-DsRed	FseI, Bsu36I	RICTOR Δ501-860 aa
pCAG-Puro-3XHA-RICTOR ΔCS5 (Δ861-1000)	pCAG-Puro-3XHA-DsRed	FseI, Bsu36I	RICTOR Δ861-1000 aa
pCAG-Puro-3XHA-RICTOR ΔPS (Δ1001-1200)	pCAG-Puro-3XHA-DsRed	FseI, Bsu36I	RICTOR Δ1001-1200 aa
pCAG-Puro-3XHA-RICTOR ΔC-ter (Δ1201-1708)	pCAG-Puro-3XHA-DsRed	FseI, Bsu36I	RICTOR Δ1201-1708 aa
pMSCV-mSIN1.1-myc	Addgene Plasmid #12576		
pMSCV-mSIN1.4-myc	Addgene Plasmid #12578		
pMSCV-mSIN1.5-myc	Addgene Plasmid #12579		
pCMV-FLAG-EGFP	**(L75)** pCMV-Flag-OCT4	EcoRI, MluI	EGFP
pCMV-mSIN1.1-FLAG	pCMV-FLAG-EGFP	EcoRI, MluI	mSIN1.1 Full length
pCMV-mSIN1.1 S260D-FLAG	pCMV-FLAG-EGFP	EcoRI, MluI	mSIN1.1 S260D
pCMV-mSIN1.1 S270D-FLAG	pCMV-FLAG-EGFP	EcoRI, MluI	mSIN1.1 S270D
pCMV-mSIN1.1 S260/270D-FLAG	pCMV-FLAG-EGFP	EcoRI, MluI	mSIN1.1 S260/270D
pCMV-mSIN1.1 S260/270A-FLAG	pCMV-FLAG-EGFP	EcoRI, MluI	mSIN1.1 S260/270A
pCMV-mSIN1.1 Δ260-270	pCMV-FLAG-EGFP	EcoRI, MluI	mSIN1.1 Δ260-270 aa
pRK5-HA-Ubiquitin	Addgene Plasmid #17608		

*RE site: restriction enzyme cleavage sites

2.2.1.5 Primers for sgRNAs

I. Oligo sequence for sgRNA

Oligo name	Forward strand	Reverse strand
RICTOR Exon 4-1	CACCGGCCACAGTGAAGAAAAACT	AAACAGTTTTTCTTCACTGTGGCC
RICTOR Exon 4-2	CACCGAAAACTGGGCTTTCACTATG	AAACCATAGTGAAAGCCCAGTTTTC
RICTOR Exon 5-1	CACCGCAAAAGAAGTGCGAGCAGC	AAACGCTGCTCGCACTTCTTTTGC
RICTOR Exon 5-2	CACCGAGACTCCAGTATTCTCCAGA	AAACTCTGGAGAATACTGGAGTCTC
RICTOR Exon 5-3	CACCGTAGCACCTTCTGGAGAATAC	AAACGTATTCTCCAGAAGGTGCTAC

II. First and Nested primers sequence for sgRNA

First primer	Forward strand	Reverse strand
RICTOR Exon 4	TGTGAGATTCTGGCATTGAGG	GCCTCTATTAGTGTGCATGGG
RICTOR Exon 5	CCAGGTAGGCAGAGAGAGGA	ACGTCCAACACACAATGCTC
Nested primer	**Forward strand**	**Reverse strand**
RICTOR Exon 4	ACTGGCAGGTCAAATGAGAA	ACTAAAATCTGAAAGGGATGGGA
RICTOR Exon 5	GGTAAGAATGTACTAAGGAGGCA	TCTATACACTTTATGGCAGGCAT

2.2.1.6 Primers for qRT-PCR

Primers	Forward strand	Reverse strand
mTOR	AGGCCGCATTGTCTCTATCAA	GCAGTAAATGCAGGTAGTCATCCA
RICTOR	GGAAGCCTGTTGATGGTGAT	GGCAGCCTGTTTTATGGTGT
mSIN1	TCCACAGACTGCGATTCACAACC	TCTTCAGCAAGGTCACAGGCACA
Cas9	AGCTGATCCGGGAAGTGAAA	GATTTCCTGCTCGCTCTTGG
OCT4	TCGAGAACCGAGTGAGAGGC	CACACTCGGACCACATCCTTC
SOX2	GCCGAGTGGAAACTTTTGTCG	GCAGCGTGTACTTATCCTTCTT
NANOG	AGTCCCAAAGGCAAACAACCCACTTC	TGCTGGAGGCTGAGGTATTTCTGTCTC
REX1	TCACAGTCCAGCAGGTGTTT	GCCATCACATAAGGCCCACA

PAX6	CCAGGGCAATCGGTAGT	ACGGGCACTCCCGCTTATAC
SOX1	AACACTTGAAGCCCAGATGGA	GCAGGCTGAATTCGGTTCTC
Brachyury	TGCTTCCCTGAGACCCAGTT	GATCACTTCTTTCCTTTGCATCAAG
TBX6	AAGTACCAACCCCGCATACA	TAGGCTGTCACGGAGATGAA
GATA6	ACTTGAGCTCGCTGTTCTCG	CAGCAAAAATACTTCCCCCA
SOX7	ACGCCGAGCTCAGCAAGAT	TCCACGTACGGCCTCTTCTG
SOX17	GGCGCAGCAGAATCCAGA	CCACGACTTGCCCAGCAT
β-actin	AGAGCTACGAGCTGCCTGAC	AGCACTGTGTTGGCGTACAG
RPL22	TCGCTCACCTCCCTTTCTAA	TCACGGTGATCTTGCTCTTG

2.2.2 Methods

2.2.2.1 Recombinant plasmid construction

I. PCR primer design and amplification

a. Primer design

The primer pairs were designed with Primer3 website (http://bioinfo.ut.ee/primer3/) based on the gene of interest. Appropriate restriction enzyme sites were incorporated in the primer pairs. The gene of interest was amplified from genomic DNA, a cDNA library or vector DNA by running a PCR (polymerase chain reaction) before inserted into an expression vector.

b. PCR (polymerase chain reaction)

Set up the PCR reactions with Q5® High-Fidelity PCR Kit as below in a 0.2ml PCR microtubes. Gently mixed the reactions and transferred PCR tubes to a thermocycler to begin the cycling program.

Component	Volume
5X Q5 Reaction Buffer	10µl
10mM dNTP	1µl
10µM Forward Primer	2.5µl
10µM Reverse Primer	2.5µl
Template DNA	Variable
Q5 High-Fidelity DNA Polymerase	0.5µl
Nuclease-Free Water	to 50µl

98°C	30 sec	
98°C	5-10 sec	25-35 cycles
50-72°C	10-30 sec	
72°C	20-30 sec	
72°C	2 min	
4°C	∞	

II. Restriction enzyme digestion and DNA fragment purification

a. Restriction enzyme(s) digestion

Digested DNA substrate (either PCR product or plasmid DNA) with restriction enzyme(s) with appropriate reaction buffer by reading the instructions for the enzyme(s). Assembled the components (DNA substrate, restriction enzyme(s), reaction buffer and Nuclease-Free Water) in a sterile tube and mixed gently by pipetting, incubated tube at appropriate temperature (usually 37°C) for 1.5-2 hours depending on the application and the amount of DNA in the reaction. After DNA digestion, treated the digested recipient vector with Antarctic phosphatase for 30 minutes at 37°C to prevent re-circularization of the vector.

b. Agarose gel electrophoresis and DNA fragment purification

Decided the concentration of agarose gel required and weighed the right amount agarose powder, added appropriate amount of 1X TAE buffer and dissolved the agarose powder by heating in a microwave. Cooled the solution and added ethidium bromide (EtBr) to a final concentration of 5µg/ml and poured the agarose solution into a cast gel tray, inserted the comb and left it at room temperature to set. Mixed DNA sample with 6X DNA loading dye and loaded into the wells of agarose gel, ran the gel at a voltage of 100V for 20-30 minutes and cut out the target band on an open UV box. To purify DNA fragment, followed the manufacturer's instructions to isolate the DNA from the gel by using NEB Monarch Gel extraction kit.

III. DNA ligation and transform

Set up the reaction mix (10X T4 DNA Ligase Buffer, Vector DNA, Insert DNA, T4 DNA Ligase and Nuclease-Free Water) in a tube on ice, gently mixed the reaction by pipetting. Incubated at 16^{o}C overnight or room temperature for an hour. Took competent cells (DH5α) out of -80°C and thawed on ice (approximately 20-30 minutes). Reaction mix (10µl) was added to 100µl of competent cells in a 1.5ml eppendorf tube and the mixture was incubated on ice for 30 minutes. Heat-shock the mixture at 42^{o}C for 30 seconds, chilled on ice for 2-3 minutes followed by adding 1ml LB medium and incubated at 37^{o}C for 1 hour. Pelleted the cells by centrifuging at 5000 rpm for 30 seconds and poured off 900µl supernatant, re-suspended cell pellet in the residual medium and gently spread on LB-agar plates which contained 50µg/ml ampicillin. The

plates were inverted and incubated overnight at 37°C and the bacterial colonies were visible by eye 16-18 hours later.

IV. Mini and midi preparation of plasmid DNA

Small scale DNA purification is used for sub-cloning. Picked individual bacterial colony and placed into universal tube which contained 5ml LB medium supplemented with 50μg/ml ampicillin. Incubated the universal tube at 37°C in a shaker overnight. After incubating, transferred 3ml of bacteria liquid to a 1.5ml tube and pelleted the cells at 14000 rpm for 1 minute in the microcentrifuge. Removed the growth medium by pouring out the supernatant and resuspened the bacteria pellet in 200μl of Buffer P1, vortexed until everything was completely dissolved. Added 200μl of Buffer P2, inverted the tube 5 times then incubated in room temperature for 3 minutes. Do not vortex, as this will result in shearing of genomic DNA and contaminate the DNA preparation. After the incubation, added 300μl of Buffer P3 and mixed gently by inverting the tube several times, then the mixture was placed on ice for 20 minutes. Centrifuged at 14000 rpm for 10 minutes and transferred supernatant to a fresh tube, added equal volume of isopropanol (700μl), vortexed and immediately spun at 14000 rpm for 1 minute. After centrifuging, washed the DNA pellet with 70% ethanol then centrifuged again. Removed supernatant and dissolved the DNA pellet in 30-50μl of TE buffer (or molecular grade water).

Large scale of DNA amplification is normally used for mammalian cell transfection.Tthe bacteria liquid from mini preparation was added into 200ml LB broth medium supplemented with 50μg/ml ampicillin and this large volume of bacterial suspension was incubated at 37°C in a shaker overnight. Cells were pelleted down the following day by centrifugation at 4000 rpm for 15 minutes and subjected to the purification using HiSpeed Midiprep kits.

The DNA concentration was quantified by NanoDrop™ Spectrophotometer 1000 (Thermo Fisher) at A260/280 and the plasmids were further verified by Sanger sequencing.

2.2.2.2 Gene expression analysis

I. RNA isolation and extraction

For gene expression analysis, lysed at least $1x10^6$ cells or one ~90% confluent well of hESCs/tumour cells directly in 6-well plate by adding 1ml TRI Reagent. Pipetted the cells up and down several times or scraped the well briefly. Collected the lysate into a 1.5ml eppendorf tube and allowed samples to stand for 5 minutes at room temperature. Added 0.2ml of chloroform:Isoamyl alcohol and shook vigorously for phase separation. Centrifuged the mixture at 12000xg for 15 minutes at 4°C and carefully transferred the aqueous phase to a fresh tube. Mixed the aqueous phase with 0.5ml of isopropanol and left at room temperature for 5 minutes to precipitate RNA. Centrifuged the samples at 12000xg for 20 minutes and washed the RNA pellet with 1ml of 75% ethanol. A final centrifugation was performed at 7500xg for 5 minutes to pellet the washed RNA pellet, poured off the ethanol and dried the RNA pellet for 15 minutes by air drying on bench. Re-suspended the RNA pellet in 16µl of either diethylpyrocarbonate (DEPC)-treated water or TE buffer.

II. DNase treatment

2U of DNase I and 2µl of 10X Reaction buffer were added to each RNA sample. The mixture was incubated at room temperature for 15 minutes. Followed by adding 2µl of Stop solution and incubated for 10 minutes at 70°C to stop DNase I reaction. Measured DNase treated RNA concentration by using NanoDrop™ Spectrophotometer 1000.

III. Reverse transcription

1-2µg of total RNA was used as template to generate cDNA or use in gene expression analysis under most circumstances. RNA samples were initially incubated with primer Oligo $d(T)_{12-18}$ in a RNAse-Free microfuge tube at 65°C for 5 minutes to denature the RNA/primer.

Component	Volume
RNA template	1-2µg
50µM Primer (Oligo $d(T)_{12-18}$)	2µl
10mM dNTP	1µl
Nuclease-Free Water	To 12µl

After the initial annealing reaction, mixed the following components by vortexing:

Component	Volume
5X ProtoScript II RT Reaction buffer	4µl
0.1M DTT	2µl
Murine RNAse inhibitor	1µl
ProtoScript II Reverse Transcriptase	1µl
Final volume	20µl

*Note: Made up two tubes for each sample, one served as the RT reaction (RT+) and the other, the non-RT control (RT-), was used as negative control.

Incubated the 20µl cDNA synthesis reaction at 42^{o}C for an hour, then inactivated the enzyme at 80^{o}C for 5 minutes. After completion of cDNA synthesis, the cDNA solutions were diluted 1 in 10 with the addition of 180µl of molecular grade water and stored at -20^{o}C until used.

IV. Semi-quantitative Polymerase Chain Reaction (PCR)

The quality of the cDNA was checked by standard PCR prior to quantitative real-time analysis. Housekeeping genes such as β-actin and RPL22 were used to ensure that cDNA synthesis was successful. The quality of newly designed primers can also be assessed by standard PCR to ensure their specificity.

A typical reaction contains:

Component	Volume
cDNA template	1-2µl
10X JumpStart™ *Taq* reaction buffer	1µl
10mM dNTP	0.5µl
20mM Forward primer	0.25µl
20mM Reverse primer	0.25µl
JumpStart™ *Taq* DNA Polymerase	1.25U
Nuclease-Free Water	To 25µl

Reaction mixtures were incubated in the thermocycler with the following cycling conditions:

Step	Temperature	Time
Initial Denaturation	94°C	1 minute
Denaturation Annealing Extension	94°C 55-68°C 72°C	30 seconds 30 seconds 1 minute
25-35 Cycles		
Final Extension	72°C	1 minute
Hold	4-10°C	∞

The melting temperature (T_m) of a primer is typically designed in a range of 60-65°C and the annealing temperature (T_a) of the primer is about 3-5° below the T_m. 6X DNA loading buffer was mixed with the reactions followed by running through a 1% TAE gel. The PCR product should appear as a clean single band that around 100-200 bp in size.

V. Quantitative Real-Time PCR (qRT-PCR)

After confirmed the quality of cDNA, the reaction of qRT-PCR was set up as below:

Component	Volume
SYBR green® JumpStart™ *Taq* Ready Mix	15µl
cDNA template	2µl
100µM Forward Primer	0.9µl
100µM Reverse Primer	0.9µl
Nuclease-Free Water	11.2µl

Each reaction was set up in triplicate and vigorously mixed the reaction followed by centrifuging to collect contents to the bottom of the 96-well PCR plate. Ran the reactions on Bio-Rad Opticon2™ DNA Engine Real-time fluorescence thermocycler with the following conditions:

Step	Temperature	Time
Initial Denaturation	94°C	2 minute
Denaturation Annealing Extension Real-time fluorescence read/sec	94°C 60°C 72°C 75-84°C	15 seconds 30 seconds 30 seconds +3°C/sec
40 Cycles		
Melting curve read/sec	67-91°C	+0.3°C/sec

The final result was analysed and performed by Opticon™ Monitor 3 and Comparative Ct Method ($2^{-\Delta\Delta C(t)}$ Method). In brief, raw Ct value of the sample was normalized to the Ct value of endogenous housekeeping gene, such as RPL22 or β-actin, to generate the ΔCt value. For the ΔΔCt calculation, ΔCt was further normalized to the control. The relative gene expression "fold-change" was calculated by taking the ΔΔCt value as the exponential function of 2. The standard deviation was calculated from at least three qRT-PCRs from three independent experiments. Primer sequences are listed in section 2.2.1.6.

2.2.2.3 Cell cycle analysis

hESCs and HEK 293T cells were grown under routine culture conditions in 6-well plate. After cells reached 70–80% confluence, harvested the cells in appropriate manner. Centrifuged the cells at 1200 rpm at 4°C for 5 minutes then fixed the cells in 1ml cold 70% ethanol. Fixed cells for at least 1 hour at 4°C, the fixed cells can be store at 4°C for several days prior to propidium iodide (PI) staining and FACS analysis. The fixed cells were washed twice with PBS then incubated with 0.25% Triton X-100 in PBS on ice for 15 minutes. Centrifuged the cells at 12000 rpm at 4°C for 5 minutes and removed the supernatant, re-suspended cell pellet in 0.5ml of PBS containing RNase A (final concentration 0.2mg/ml) and incubated at 37°C for 30 minutes. Pelleted the cells by centrifuging and re-suspended the cell pellet with 350µl of PBS containing 50µg/ml PI, kept the cells in the dark and incubated at room temperature for 30 minutes. The cells were ready for analysis by flow cytometry with a BD FACSCalibur™ (BD Bioscience) after incubation. Each cell cycle phase (sub-G1, G0/G1, S and G2/M) was determined by the cellular DNA content profile and the analysis of cell cycle distribution were calculated with CellQuest software (evaluated as %). At least three independent experiments were performed and the results are presented as means ± SD.

2.2.2.4 Statistical Analysis

Each experiment was conducted at least three times and results are presented as mean ± standard deviation (SD). Normal distribution was tested before comparisons. The comparisons of means between groups were analysed with two-tail unpaired Student's t-test. P-value < 0.05 was considered statistically significant.

2.2.2.5 Design sgRNA (single guide RNA)

I. Target selection for sgRNA

Online CRISPR sgRNA design tools (http://crispr.mit.edu/, https://www.deskgen.com/landing/) provide genomic sequence of interest and identify suitable target sites. After determined the target sequence of sgRNA, incorporated 19 bp of the selected target sequence into two partially complementary oligonucleotides with 4 nucleotides (nt) overhangs that compatible for cloning into the expression plasmid:

```
5′ – CACCGNNNNNNNNNNNNNNNNNN      – 3′
3′ –      CNNNNNNNNNNNNNNNNNNNCAAA – 5′
```

II. Oligo annealing and cloning into expression vectors

Set up the phosphorylation and annealing mixture for generating sgRNA:

Oligo 1 (100mM)	1µl
Oligo 2 (100mM)	1µl
10X T4 Ligation Buffer (NEB)	1µl
T4 PNK (NEB)	0.5µl
ddH_2O	until 10µl

Anneal in a thermocycler using the following parameters:

37°C	30 minutes
95°C	5 minutes then ramp down to 25°C at 5°C/minutes

Meanwhile, set up the digestion reaction for expression plasmid (eSpCas9(1.1)-2A-Puro) with *BbsI* and incubated the reaction at 37°C for at least an hour. Purified digested plasmid by agarose gel electrophoresis and extracted the linearize plasmid with NEB Monarch Gel extraction kit. Ligated the sgRNA with linearize plasmid, incubated the ligation reaction at room temperature for 1 hour, then transformed the final product into the competent cells.

2.2.2.6 Preparation of genomic DNA from cell culture

hESCs and HEK 293T cells were harvested from 6-well plate and pelleted by centrifuging at 1500 rpm for 5 minutes. Disrupted the cells with 700µl of TNE buffer supplied with proteinase K (100µg/ml) and RNase A (20µg/ml) and incubated overnight at 37°C. Transferred cell lysate to a pre-spun (centrifuged at 13000 rpm for 20-30 seconds) 2ml PLG tube and added 700µl of Phenol-Chloroform. Mixed thoroughly by inverting tubes several times to form a transiently homogenous suspension, then centrifuged at 14000 rpm for 5 minutes. Carefully transferred

the upper aqueous layer to a fresh 1.5ml eppendorf and mixed with 50% volume (350µl) of cold isopropanol, incubated at -20°C for at least 2 hours up to overnight. After the incubation, pelleted genomic DNA by centrifuging at 14000 rpm for 20 minutes at 4°C, and washed the pellet with 1ml 70% ethanol, spun down and removed ethanol. Briefly air-dried the genomic DNA pellet before re-suspending it in 50-150µl of TE buffer (dependent on the size of DNA pellet).

2.2.2.7 T7 endonuclease I (T7E1) assay

Genomic DNA was extracted from HEK 293T cells which were transfected with Cas9 plasmids expressing sgRNA. PCR was performed using primers (First and Nested primers) and approximately 100ng of genomic DNA was used as template to yield cleavage products between 200-800 bp. PCR products were then heated and cooled in a thermocycler to form heteroduplexes:

PCR products (WT/WT, WT/MUT)	10µl
10X NEBuffer 2	2µl
Nuclease-Free Water	7µl
Total volume	19µl

Anneal in a thermocycler using the following parameters:

95°C	10 minutes
95-85°C	ramp rate of -2°C/sec
85-25°C	ramp rate of -0.1°C/sec

Added 1µl (10U) of T7E1 and incubated the digestion at 37°C for 25 minutes. Stopped the reaction by adding 2ul of 0.25M EDTA and the digested DNA was separated on 2-2.5% agarose gels. After quantified the intensity of DNA bands, the percentage (%) of indel (insertion-deletion) mutations were calculated by using the following formula:

$$\% \text{ Modification} = 100 \times [1-(1-\text{fraction cleaved})^{1/2}]$$

$$\text{Where fraction cleaved} = \frac{\text{concentration of digested products}}{(\text{concentration of digested products} + \text{concentration of undigested band})}$$

2.3 Molecular Biology – Protein techniques

2.3.1 Materials

2.3.1.1 Reagents, Chemicals and Kits

Reagent	Supplier
30% Acrylamide/Bis	Sigma-Aldrich
4-(2-hydroxyethyl)-1-piperazineethanesulfonic acid (HEPES)	Sigma-Aldrich
4',6 diamidino-2-phenylindole (DAPI)	Sigma-Aldrich
Adenosine triphosphate (ATP)	Sigma-Aldrich
Ammonium persulfate (APS)	Sigma-Aldrich
Bicinchoninic Acid Assay (BCA) Protein Quantification Kit	Thermo Fisher
Bromophenol blue	Sigma-Aldrich
Bovine Serum Albumin (BSA)	Sigma-Aldrich
CHAPS	Calbiochem
CL-Xposure film	Scientific Labs
Dithiothreitol (DTT)	Sigma-Aldrich
Donkey serum	Sigma-Aldrich
Clarity Western Enhanced chemiluminescence substrate (ECL)	Bio Rad
Ethylene glycol tetraacetic acid (EGTA)	Sigma-Aldrich
Glycerol	Sigma-Aldrich
Glutathione magnetic beads	Sigma-Aldrich
Goat serum	Sigma-Aldrich
Immobilon® polyvinylidene fluoride (PVDF) membrane	Millipore
Luminate Forte Enhanced ECL substrate	Millipore
Methanol	VWR
Mowiol 4-88	Sigma-Aldrich
Nonidet P-40 (NP-40)	Anachem
PageRuler Plus Protein Ladder	Thermo Fisher
Pierce™ 16% Formaldehyde	Thermo Fisher
Phenylmethanesulfonyl Fluoride (PMSF)	Sigma-Aldrich
Phosphatase Inhibitor Cocktail 2	Sigma-Aldrich
Protease Inhibitor Cocktail	Sigma-Aldrich
Protein A/G Dynabeads®	Life Technologies
Skim milk powder	Sigma-Aldrich
Sodium azide (NaN_3)	Sigma-Aldrich

Sodium deoxycholate	Sigma-Aldrich
Sodium fluoride (NaF)	Sigma-Aldrich
Sodium dodecyl sulphate (SDS)	Sigma-Aldrich
Sodium orthovanadate (Na_3VO_4)	Sigma-Aldrich
Tetramethylethylenediamine (TEMED)	Sigma-Aldrich
Triton X-100	Sigma-Aldrich
Tween-20	Sigma-Aldrich
β-mercaptoethanol	Sigma-Aldrich
Mouse IgG−Agarose	Sigma-Aldrich
Monoclonal Anti-HA−Agarose antibody produced in mouse	Sigma-Aldrich
ANTI-FLAG® M2 Affinity Gel	Sigma-Aldrich

2.3.1.2 Buffers and Solutions

Immunoblotting

Buffers	Components
Radio Immunoprecipitation Assay Buffer (RIPA)	25ml 1M Tris-HCl pH 8.0 (50mM) 15ml 5M NaCl (150mM) 5ml NP-40 (1% v/v) 2.5g Sodium deoxycholate (0.5% w/v) 0.5g SDS (0.1% w/v) Autoclaved water to 500ml
2X Sample buffer	2.5ml 0.5M Tris-HCl pH 6.8 (125mM) 2ml glycerol (20% v/v) 4ml 10 % SDS (4% w/v) 160µl 1.25% bromophenol blue (0.02 % w/v) 500µl β-mercaptoethanol (715mM) Autoclaved water to 10ml
5X Sample buffer	1.25ml 0.5M Tris-HCl pH 6.8 (50mM) 2.5ml glycerol (25 % v/v) 2ml 10% SDS (2% w/v) 400µl 0.5% bromophenol blue (0.02 % w/v) 500µl β-mercaptoethanol (715mM) Autoclaved water to 10ml
4% Polyacrylamide Stacking Gel	2.5ml 0.5M Tris-HCl pH 6.8 (125mM) 1.3ml 30% Acrylamide/Bis (4% v/v) 100µl 10% SDS (0.1 % w/v) 50µl 12% APS (0.06 % w/v) 12µl TEMED (0.12 % v/v) Autoclaved water to 10ml
8% Polyacrylamide Running Gel	2.5ml 0.5M Tris-HCl pH 6.8 (125mM) 2.7ml 30% Acrylamide/Bis (6% v/v) 100µl 10% SDS (0.1 % w/v)

	75µl 12% APS (0.075 % w/v) 18µl TEMED (0.18 % v/v) Autoclaved water to 10ml
10X SDS Running Buffer	30.3g Tris base (250mM) 144.2g Glycine (1.9M) 50ml 20% SDS (1%) Autoclaved water to 1L
Transfer Buffer	5.82g Tris base (48mM) 2.93g Glycine (39mM) 3.75ml 10% SDS (0.04% w/v) 200ml methanol (20% v/v) Autoclaved water to 1L
Tris Buffered Saline with Tween-20 (TBS-T)	20ml Tris-HCl pH 7.6 (20mM) 26ml NaCl (130mM) 1ml Tween-20 (0.1 % v/v) Autoclaved water to 1L

Immunoprecipitation

Buffers	Components
2X Non-denaturing CS lysis buffer	1ml 1M Tris-HCl pH 7.5 (20mM) 1.5ml 5M NaCl (150mM) 100µl 0.5M EDTA pH 8.0 (1mM) 400µl 0.125M EGTA pH 8.0 (1mM) 500µl NP-40 (1% v/v) Autoclaved water to 25ml
mTOR Complex IP buffer	10ml 1M Tris-HCl pH 8.0 (50mM) 6ml 5M NaCl (150mM) 0.8ml 0.5M EDTA pH 8.0 (2mM) 20ml Glycerol (10% v/v) 0.6g CHAPS (0.3% v/v) Autoclaved water to 200ml
Protein purification buffer	10ml 1M Tris-HCl pH 8.0 (50mM) 6ml 5M NaCl (150mM) 0.8ml 0.5M EDTA pH 8.0 (2mM) 20ml Glycerol (10% v/v) 2ml TritonX-100 (1% v/v) Autoclaved water to 200ml
Protein elution buffer	1XTBS TBS 10X For 1 L; 24.23g Trizma® HCl 80.06g NaCl Dissolve in 800mL distilled water pH to 7.6 with HCl Top up to 1L

Immunocytochemistry

Buffers	Components
Fixation buffer	4g paraformaldehyde dissolved in 90ml autoclaved water at 60°C 10M NaOH added dropwise till solution clears 10ml 10X DPBS Adjust pH to 7.2 with 9.61M HCl acid Adjust volume to 100ml with autoclaved water
Fixation buffer	Diluted 16% PFA solution with PBS
Blocking/permeablising buffer	1ml goat/donkey serum (10% v/v) 0.25g BSA (2.5% w/v) 30µl Triton X-100 (0.3% v/v) DPBS to 10ml
Mowiol mounting solution	12ml 200mM Tris-HCl pH 8.5 (135mM) 6g glycerol 2.4g Mowiol 4-88 6ml autoclaved water Heat tubes at 60°C to dissolve Mowiol

Fluorescence activated cell sorting

Buffers	Components
Staining buffer	2ml FBS (2% v/v) 0.4ml 0.5M EDTA pH 8.0 (2mM) Autoclaved water to 100ml
Blocking buffer	40% Goat serum in Staining buffer

2.3.1.3 Antibodies

Antigen	Supplier	Application and dilution
Brachyury	R&D System, #AF2085	IB 1:1000
SOX17	R&D System, #AF1924	IB 1:500
OCT4	Cell Signaling, #2750	IB 1:1000
SOX2	R&D System, #AF2018	IB 1:1000
Cas9 (clone 7A9)	Millipore, #MAC133	IB 1:2000
RICTOR	Bethyl Laboratories, A300-459A	IB 1:4000
mTOR	Cell Signaling, #2972	IB 1:1000
mSIN1 (D7G1A)	Cell Signaling, #12860	IB 1:1000
pAKT S473 (D9E, XP)	Cell Signaling, #4060	IB 1:1000
pAKT T450	St John's, STJ90168	IB 1:1000
pAKT T308 (D25E6)	Cell Signaling, #13038	IB 1:1000
AKT	Cell Signaling, #9272	IB 1:1000
GBL (mLST8)	ThermoFisher, #MA5-14993	IB 1:1000
pPKC alpha S657	abcam, #ab180848	IB 1:1000
PKC alpha (Y124)	abcam, #ab32376	IB 1:1000
pp70-S6K T421/S424	Cell Signaling, #9204	IB 1:2000
p70-S6K	Cell Signaling, #9202	IB 1:2000
pGSK3α/β S21/9	Cell Signaling, #9331	IB 1:1000
GSK3α/β	Santa Cruz, sc-71190	IB 1:1000
Phospho-Histone H3 (S10)	St John's, STJ90289	IB 1:1000
Cleaved-Caspase-3 p17 (D175)	St John's, STJ90026	IB 1:1000
Ubiquitin (P4D1)	Biolegend, #646301	IB 1:1000
LC3 (APG8B) (N-term)	ABGENT, #AP1802a	IB 1:1000
FLAG® M2, Clone M2	Sigma, #F1804	IB 1:2000, IF 1:200
HA	Sigma, #H6908	IB 1:2000, IF 1:100
Myc-Tag (9B11)	Cell Signaling, #2276	IB 1:1000
Tra-1-81	ThermoFisher, #MA1-024	FACS 1:100
SSEA1 (MC-480)	ThermoFisher, #MA1-022	FACS 1:100
SSEA4 (MC-813-70)	ThermoFisher, #MA1-021	FACS 1:100
Mouse IgG3	Sigma, #M3645	FACS 1:100
Mouse IgM	Sigma, #M3795	FACS 1:100
Mouse IgG3-FITC	Southern Biotechnologie, #1102-02	FACS 1:100

Mouse IgM-PE	Southern Biotechnologie, #1022-09	FACS 1:100
β-actin	Sigma, #A5316	IB 1:5000
Goat IgG-HRP	Santa Cruz, #2020	IB 1:5000
Mouse IgG-HRP light chain	Stratech, #115-035-174	IB 1:10000
Rabbit IgG-HRP light chain	Stratech, #211-032-171	IB 1:10000
Rabbit IgG (H+L)-HRP	Thermo, #31460	IB 1:10000
Rabbit IgG-Alexa Fluor 488	Life Technologies, #A11055	IF 1:400
Rabbit IgG-Alexa Fluor 568	Life Technologies, #A11011	IF 1:400
Mouse IgG-Alexa Fluor 488	Life Technologies, #A11001	IF 1:400
Mouse IgG Alexa Fluor 568	Life Technologies, #A11004	IF 1:400

2.3.2 Methods

2.3.2.1 Protein extraction and quantification

Discarded the medium in culture dishes and washed the cells with 1X ice-cold PBS. Removed PBS and added ice-cold RIPA buffer supplemented with phosphatase and protease inhibitors. Scraped the cells with plastic cell scraper to collect the cell lysate then transferred the cell lysate in 1.5ml eppendorf. Centrifuged the eppendorf at 14,000 rpm for 20 minutes at 4°C in order to separate cell supernatant and pellet. After the centrifugation, collected the supernatant in fresh eppendorf for the following analysis. Protein concentration was determined by BCA Assay Protein Quantification Kit.

2.3.2.2 Immunoblotting

Typically, 10 to 20μg of protein was mixed with 5X sample buffer and water to bring the total volume to 15-30μl. Boiled the samples at 95°C for 3-5 minutes to denature proteins, cooled it down at room temperature then carefully loaded into the wells of SDS-pages. Equivalent amounts of protein were resolved at 100V for 1 hour 30 minutes through 8% Bis-Tris polyacrylamide gels immersed in SDS running buffer before being transferred onto PVDF membranes. Proteins were then transferred from SDS-pages to PVDF membranes using wet transfer method. In a wet transfer, the SDS-pages and membranes were clamped tightly with sponge and filter papers (sandwich). The sandwich was entirely submerged under transfer buffer in the transfer tank and transferred at constant voltage of 100V for 1 hour at 4°C. After blocked with appropriate blocking buffer for at least 30 minutes, membranes were incubated with specific primary antibody for overnight at 4°C and followed by horseradish peroxidise

(HRP) conjugated secondary antibodies for 1 hour at room temperature. The reactions were detected by ECL substrate and exposure onto CL-XPosure film. Primary and secondary antibodies used in immunoblotting are listed in section 2.3.1.3.

2.3.2.3 Quantitation and statistical analysis of immunoblotting

The densitometry of immunoblotting bands were measured and quantified with Image J software. To compare protein expression levels between samples, the values of target protein were normalised to the house-keeping protein (β-actin) and then calculated as fold change to the control. All the results are presented as the average values ± SD from three independent biological samples. The statistical analysis was assessed by two-tail unpaired Student's t-test and p-value < 0.05 was considered statistically significant.

2.3.2.4 Co-immunoprecipitation (Co-IP)

HEK 293T cells were transiently transfected with either Flag or HA-tag fused protein for 48 hours and lysed in pre-chilled IP buffer containing protease and phosphatase inhibitors. Scraped the cells and collected into a clean eppendorf, broke the cells using a syringe with 25G needle. Centrifuged the cells lysate at 14000 rpm for 20 minutes at 4°C then transferred the supernatant to another new eppendorf. To eliminate the non-specific binding proteins, pre-cleared the cell lysate with normal mouse IgG agarose beads on shaker for an hour at 4°C. Removed the normal mouse IgG agarose beads via centrifugation at 5000 rpm for 40 seconds and quantified the protein concentration with BCA assay or other methods. Typically, 1-2mg of protein was used for performing Co-IP in eppendorf with 1ml of IP buffer. Added appropriate amount of either anti-Flag or anti-HA agarose beads for precipitation and rotated at 4°C for overnight. Pelleted the agarose beads via centrifugation at 5000 rpm for 40 seconds and washed the agarose beads with 1ml pre-chilled IP buffer, repeated it for 3-5 times. Eluted the interaction proteins from agarose beads with 2X sample buffer and boiled it at 95°C for 5 minutes and subjected to immunoblotting. Light-chain specific HRP conjugated secondary antibodies (listed in section 2.3.1.3) were used to overcome the masking effect.

2.3.2.5 Ubiquitination assay

For *in vivo* ubiquitination assay, Flag-tag fused protein and HA-ubiquitin were co-transfected into HEK 293T cells for 48 hours. Before harvesting, cells were treated with 30μM of MG132

(proteasome inhibitor) to enrich the ubiquitination signal. Cells were lysed in pre-chilled CS lysis buffer supplemented with protease and phosphatase inhibitors. 1-2mg of protein was used for performing immunoprecipitation at 4°C for overnight. Immunocomplexes were washed 3 times with CS lysis buffer to remove the non-specific binding protein and terminated by boiling for 5 minutes in 2X sample buffer. Taking the mSIN1 ubiquitination assay as example, mSIN1 was immunoprecipitated with Flag antibody and analysed by immunoblotting with either HA or ubiquitin antibodies to examine ubiquitin ladder formation.

2.3.2.6 Immunostaining of hESCs

hESCs or EBs were split and grown on Matrigel® pre-coated coverslips until they reached the desired confluency. Cells were washed 3 times with cold 1X PBS and fixed with 4% fresh paraformaldehyde solution at room temperature for 10 minutes. The fixed cells were washed again with cold 1X PBS and incubated with blocking buffer at room temperature for an hour and followed by an overnight incubation with appropriate diluted primary antibodies at 4°C. After 3 times washings with PBS, cells were incubated with appropriate fluorophore-conjugated secondary antibody for an hour in the dark and followed by an incubation of DAPI for 5 minutes. Coverslips with stained cells were mounted in Mowiol 4-88 solution and analysed by Leica SP5 II confocal fluorescent microscope. Primary and secondary antibodies applied in immunostaining are listed in section 2.3.1.3.

2.3.2.7 Fluorescence activated cell sorting

hESCs were harvested and dissociated into single cells by accutase. Pelleted the cells via centrifugation at 1300 rpm for 5 minutes, discarded the supernatant and re-suspended the cell pellets in 50µl of blocking buffer. Incubated the cell suspension on ice for 10-15 minutes. Added appropriate primary antibodies or the isotype-matched IgG (negative controls) into the tubes and incubated on ice for 30 minutes. Cells were then washed with staining buffer and centrifuged at 1300 rpm for 5 minutes. Removed the supernatant and mixed the cells with appropriately diluted secondary antibody in staining buffer and placed the cells on ice for 30 minutes for incubation. After the incubation, added 3ml of 1X PBS in each tube to wash away the extra antibody and pelleted the cells via centrifugation at 1300 rpm for 5 minutes. Discarded the supernatant then re-suspended the cell pellet with 0.5-1ml of 1X PBS and kept the cells on ice before analysis. Data were acquired on a FACSCalibur flow cytometer (BD

Biosciences) and analysed using CellQuest software. The gating parameters between the positive and negative cell population were determined and set for the inclusion of 3% of the isotype-matched controls.

2.4 Software and Online Tools

Computer Software
Leica LAS AF Lite
Image J
SnapGene
CellQuest
Serial Cloner
Opticon Monitor 3

Online Tools Website	
Basic Local Alignment Search Tool (BLAST)	http://blast.ncbi.nlm.nih.gov/Blast.cgi
NEB Double Digest Finder	https://www.neb.com/tools-andresources/ interactive-tools/double-digestfinder
CRISPR DESIGN	http://crispr.mit.edu/
DESKGEN™ CRISPR Libraries	https://www.deskgen.com/landing/
Reverse Complement	http://www.bioinformatics.org/sms/rev_comp.html
COMMON DNA SEQUENCES	http://www.algosome.com/resources/common-sequences.html#t7
NEBioCalculator™	http://nebiocalculator.neb.com/#!/main
NEBcutter V2.0	http://nc2.neb.com/NEBcutter2/
Primer 3 (version 4.1.0)	http://bioinfo.ut.ee/primer3/
Inference of CRISPR Edits (ICE)	https://ice.synthego.com/#/

03

Generation of *RICTOR*-knockout HEK 293T and Human Embryonic Stem cells (hESCs)

3.1 Introduction

In the last decade, mTOR signalling pathway has emerged as a master regulator in cell growth and metabolism (Kim and Guan, 2019; Saxton and Sabatini, 2017; Xie et al., 2018). The mTOR signalling performs its functions via two compositionally and functionally distinct complexes, mTORC1 and mTORC2. In general, mTORC1 is associated with cell mass growth, while mTORC2 is involved in cell proliferation and survival (Laplante and Sabatini, 2012). Great advances have been made over the last decades in mTORC1 on its structure, regulation and function, which are partly attributed to the discovery and use of its inhibitor rapamycin. However, unlike mTORC1, the lack of specific inhibitor has impeded our understanding in the regulation and function of mTORC2, which mainly rely on the genetic manipulation of mTORC2-specific factors, RICTOR or mSIN1 as depicted in the Chapter 1. In these studies, the exhibition of embryonic lethal phenotypes in *Rictor*- and *mSin1*-knockout mice suggest that mTORC2 may have an important role in controlling mouse embryonic development (Guertin et al., 2006; Jacinto et al., 2006; Shiota et al., 2006; Yang et al., 2006). Since mTOR signalling is conserved in all mammals, it is possible that mTORC2 signalling also plays a vital role in human embryonic development. Nonetheless, it remains unclear how mTORC2 affects embryonic development. Thus, elucidating the regulation and molecular mechanisms of mTORC2 in human cells will be essential for understanding its function and it could also provide some new insights into the development of new therapeutic intervention.

RICTOR is a scaffold protein of mTORC2 and the expression of RICTOR not only is essential for mTORC2 assembly, but may also control the stability of some of the other components within the complex (Frias et al., 2006; Ikenoue et al., 2008; Jacinto et al., 2006; Sarbassov et al., 2004; Yao et al., 2017). Hence, I propose that deciphering the molecular mechanisms underlying the structure, regulation and function of RICTOR is crucial for the understanding of mTORC2 signalling and for the development of new methods to interfere this signalling network.

To avoid the interference of endogenous RICTOR and explore the functions of RICTOR in human cells, *RICTOR*-knockout (*RICTOR*-KO) clonal cell lines were established in two different human cell types, H1 hESC line and HEK 293T cells, by taking the advantage of

CRISPR-Cas9 technology. A successful gene targeting experiment with CRISPR-Cas9 system influenced by various parameters, including the choice of cell types, the design of sgRNA and the nucleic acid delivery methods (Liang et al., 2015). Gene editing in human cells, especially in hESCs, has been notoriously difficult due to the low transfection efficiency and the poor cell viability (Czerwinska et al., 2019). Therefore, I took the strategy to determine the sgRNA targeting efficacy in HEK 293T cells before applying them to hESCs. In this chapter, I described different strategies and optimisation methods for generating *RICTOR*-KO HEK 293T cells and hESCs by single plasmid-mediated CRISPR-Cas9 gene disruption. The successful generation of these *RICTOR*-KO clonal cell lines were achieved, which enabled us to investigate different functions of RICTOR/mTORC2 in different cell types. For instance, *RICTOR*-KO HEK 293T cells are useful for studying fundamental questions in molecular cell biology of RICTOR/mTORC2, while the *RICTOR*-KO hESCs are suitable for investigating the function of RICTOR/mTORC2 in human development.

3.2 Results

3.2.1 Design and cloning of sgRNA to target human *RICTOR*

My targeting strategy to generate *RICTOR*-KO was: 1) selecting the first few exons in the coding region as putative target sites to reduce the possibility of generating truncated, partial functional proteins (Wang et al., 2016); 2) simultaneously targeting two sites in genomic DNA for a deletion of over 1000 bp, so that a screening by DNA PCR could be relatively easy to identify the targeted clones. The human *RICTOR* gene consists of 38 exons and in considering that the first 5 exons of the *RICTOR* gene are all very small, which range from 48 bp (exon 2) to 132 bp (exon 5), it was difficult to identify two targeting sites spanning over 100 bp within the same exon (Fig. 3.1A). Thus, I decided to target two exons instead of one. To avoid large introns, I confined the targeting region to exon 4 and 5 of the *RICTOR* gene as they encode protein sequences near N-terminus and with the intron 4 of 891 bp. Since efficient gene targeting by CRISPR-Cas9 system requires complete homology between sgRNA including its downstream trinucleotide PAM sequence (5'-NGG-3') and the targeted genomic DNA sequences, genomic DNA isolated from both HEK 293T cells and H1 hESCs were amplified by PCR on the region cross exons 4 to 5 and sequenced, which confirmed that they are identical to the published sequences (data not shown).

Two different online tools, "CRISPR DESIGN" (http://crispr.mit.edu/) and "DESKGEN" (https://www.deskgen.com/landing/), were used to design the potential sgRNAs that target exon 4 and 5 of the *RICTOR* gene. The results identified 6 and 9 potential sgRNAs in exon 4 and 5, respectively (Table 1). These CRISPR design tools provided both sgRNA sequences and the computationally predicted off-target sites elsewhere in the genome. In considering both predicted score of on-target activity and the potential off-target sequences, I selected 2 sgRNAs targeting exon 4 (purple) and 3 sgRNAs targeting exon 5 (light blue) to be subcloned into the expression vector for further validation (Table 2 and Figure 3.1A).

A variety of plasmids have been reported to express CRISPR-Cas9 as well as sgRNA into cells/animals and to generate gene-knockouts successfully (Bording et al., 2019; Fogarty et al., 2017; Song et al., 2019; Vilarino et al., 2017). I selected the "all-in-one" expression plasmid, pSpCas9(BB)-2A-Puro generated by Feng Zhang's lab (Ran et al., 2013), which

express both Cas9 and the sgRNA despite under different promoters. Furthermore, the Cas9 cDNA is linked in-frame with puromycin resistant gene via 2A peptide to ensure that all surviving cells after puromycin treatment will express Cas9. The same lab also invented a new modified Cas9, Cas9(1.1), which has been reported to increase the specificity and to reduce off-target activity by mutating three residues (K848A/K1003A/R1060A) (Slaymaker et al., 2016). Therefore, I decided to replace the original Cas9 in the pSpCas9(BB)-2A-Puro with this modified Cas9(1.1) to create eSpCas9(1.1)-2A-Puro, which contains higher fidelity Cas9(1.1) and puromycin resistance marker (Fig. 3.1B). eSpCas9(1.1)-2A-Puro was generated from pSpCas9(BB)-2A-Puro and eSpCas9(1.1) by digesting with two restriction enzymes, *Age*I and *Kfl*I, which separated Cas9 and Cas9(1.1) from pSpCas9(BB)-2A-Puro and eSpCas9(1.1), respectively. The *Age*I-*Kfl*I fragment of Cas9(1.1) was then inserted into the pSpCas9(BB)-2A-Puro to replace the original Cas9, and the diagnostic restriction enzyme digest with *Hae*II was used for verifying the resulting plasmids (Fig. 3.1C). After the construction of expression plasmid, the synthesized partially complementary sgRNA oligos were annealed and inserted between the *Bbs*I sites of eSpCas9(1.1)-2A-Puro plasmid (Fig. 3.1D). The resulting sgRNA plasmids were verified by sequencing from the U6 promoter using the U6-Fwd primer (Fig. 3.1E).

Table 1. Potential sgRNAs in exon 4 and 5 on *RICTOR* gene locus

Exon 4	Target sequence	PAM	CRISPR DESIGN	DESKGEN
Guide #1	AAAACTGGGCTTTCACTATG	AGG	54	55
Guide #2	AGCCCAGTTTTTCTTCACTG	TGG	47	65
Guide #3	GGCCACAGTGAAGAAAAACT	GGG	44	62
Guide #4	TGGCCACAGTGAAGAAAAAC	TGG	30	32
Guide #5	TGACAGCTTCTTTGTGATAT	TGG	-	31
Guide #6	ACTATGAGGATATCATAATT	TGG	-	25

Exon 5	Target sequence	PAM	CRISPR DESIGN	DESKGEN
Guide #1	GCAAAAGAAGTGCGAGCAGC	AGG	73	34
Guide #2	TAGCACCTTCTGGAGAATAC	TGG	70	44
Guide #3	CAAAAGAAGTGCGAGCAGCA	GGG	67	65
Guide #4	CTTTCAATTTTAGCACCTTC	TGG	62	24
Guide #5	AGACTCCAGTATTCTCCAGA	AGG	62	62
Guide #6	TCTGGAGAATACTGGAGTCT	TGG	55	46
Guide #7	GAAGGTGCTAAAATTGAAAG	TGG	49	60
Guide #8	GTTTGTTTTCATACAGTTTG	CGG	-	47
Guide #9	AAGTGGACTATTTAATAGCT	AGG	-	47

Table 2. Selected sgRNAs in exon 4 and 5 with potential off-target sites

Name	Target sequence	PAM	CRISPR DESIGN	DESKGEN	Potential off-target sites	PAM	Score	Mismatches	Locus
Exon 4-1	GGCCACAGTGAAGAAAAACT	GGG	44	62	CTCCACAGAGAAGAAAAACT	GAG	1.6	[1, 2, 9]	chr3: -9974228
					GGCCTCGGGGAAGAAAAACT	GGG	1.0	[5, 7, 9]	chr2: -1318038
Exon 4-2	AAAACTGGGCTTTCACTATG	AGG	54	55	CAGACTGGTCTTTCACTATG	CAG	1.6	[1, 3, 9]	chrY: -2463664
					CAGACTGGTCTTTCACTATG	CAG	1.6	[1, 3, 9]	chrY: +2424202
Exon 5-1	GCAAAAGAAGTGCGAGCAGC	AGG	73	34	GACAAAGAAGTACGAGCAGC	AGG	1.4	[2, 3, 12]	chr5: +6505882
Exon 5-2	AGACTCCAGTATTCTCCAGA	AGG	62	62	AGTTGCCAGCATTCTCCAGA	TGG	1.3	[3, 4, 5, 10]	chr11: -588209
Exon 5-3	TAGCACCTTCTGGAGAATAC	TGG	70	44	TACCACCTTCTGGAGATTAA	AGG	0.5	[3, 17, 20]	chr16: +251438
					TATCACCTTCTGGAGAAGAG	AGG	0.3	[3, 18, 20]	chr3: -1234527

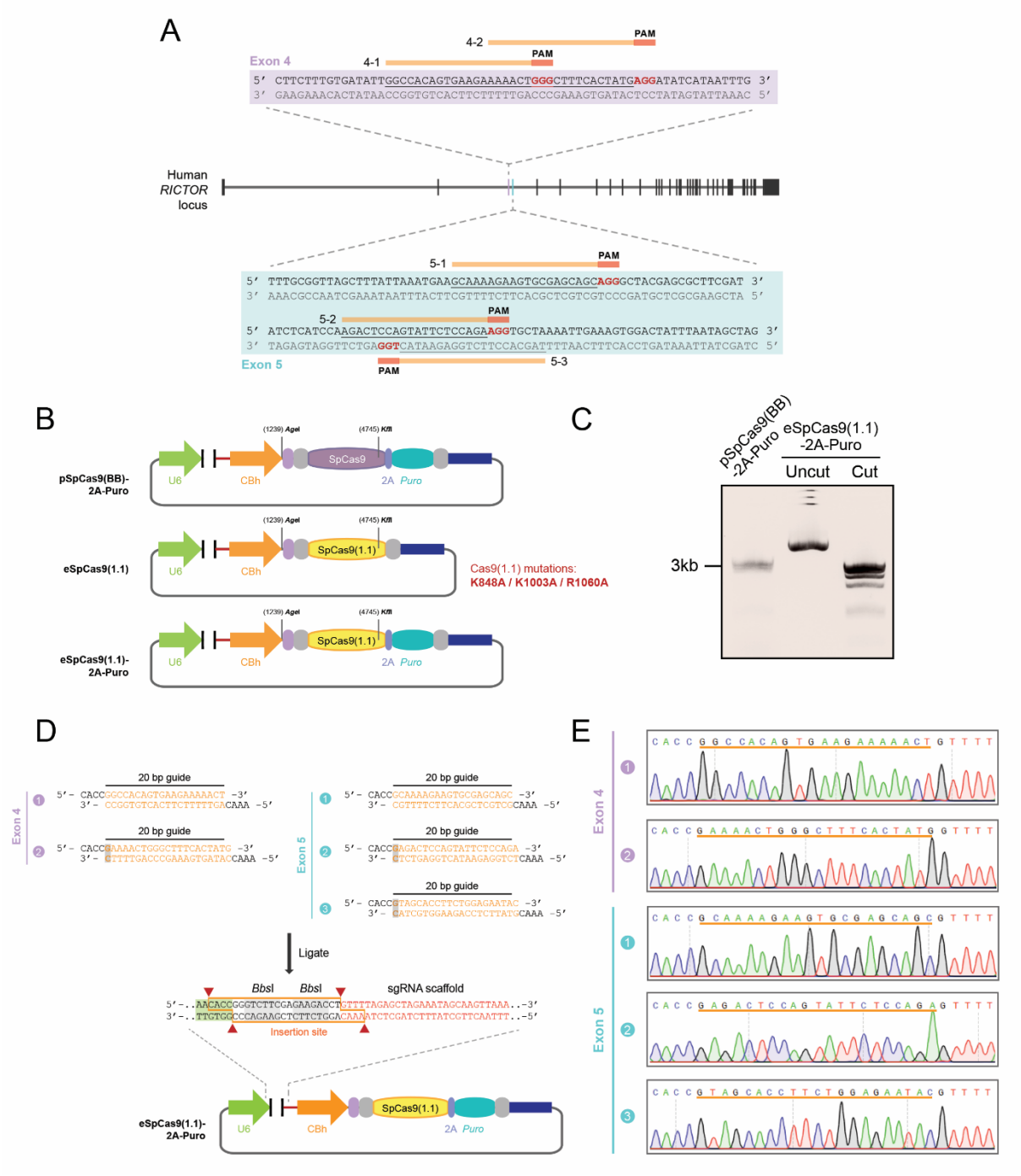


Figure 3.1 sgRNA design and the construction of sgRNA expression vectors

*(**A**) Schematic illustration of the human RICTOR gene and the sequences of its exon 4 and 5. The sequences underlined are the sgRNA sequences with the protospacer adjacent motif (PAM) highlighted in red. (**B**) Schematic diagram of three different CRISPR-Cas9 plasmids. pSpCas9(BB)-2A-Puro and eSpCas9(1.1) were combined to generate eSpCas9(1.1)-2A-Puro. (**C**) The eSpCas9(1.1)-2A-Puro plasmid with and without digestion by HaeII restriction enzyme were shown. (**D**) Digested eSpCas9(1.1)-2A-Puro with restriction enzyme BbsI (restriction sites were highlighted in grey blocks) and cloned the sgRNA (pair of annealed oligos) into the eSpCas9(1.1)-2A-Puro before sgRNA scaffold. For sgRNA 4-2, 5-2 and 5-3, an additional guanine nucleotide was added to the 5′ of 20-bp in order to increase the targeting efficiency. (**E**) Results from DNA sequencing by using U6-Fwd primer (5'-GAGGGCCTATTTCCCATGATTCC-3'). Sequencing results showed that each sgRNA was successfully constructed into eSpCas9(1.1)-2A-Puro.*

3.2.2 Knockout (KO) validation of RICTOR-sgRNAs in HEK 293T cells

After successfully constructing the Cas9 plasmids expressing various RICTOR sgRNAs, I next examined the targeting efficiency of these sgRNAs in HEK 293T cells. The plasmids contain Cas9 and different RICTOR-sgRNA were transfected into HEK 293T cells individually by calcium-phosphate co-precipitation and the Cas9 plasmid without sgRNA was used as a control (Fig. 3.2A). Transfected cells were selected for 5 days with 2μg/ml and then surviving cells were harvested for targeting analysis. First, I applied T7 Endonuclease I (T7E1) assay to quantify the insertion-deletion (indel) mutations in these cells and to compare their cleavage efficiency between different RICTOR sgRNAs (Fig. 3.2B). Depending on the exon being targeted by specific sgRNAs, DNA fragments were amplified by the primers of exon 4 (primer 4F/4R) or exon 5 (primer 5F/5R) (Fig. 3.2C top). The agarose gel electrophoresis of the PCR products showed a single band of the expected size, indicating high specificity of these primers (Fig. 3.2C bottom). The results showed that among 5 different RICTOR-targeting sgRNAs, sgRNA 4-1 or 5-2 showed a relatively high percentage of indel mutations (Fig. 3.2D). RICTOR protein expression levels were also verified in these cells by immunoblotting with anti-RICTOR antibody, which showed consistent results with T7E1 assay. The cells transfected with sgRNA 4-1 or sgRNA 5-2 exhibited the lowest RICTOR protein expression (Fig. 3.2E). The phosphorylation of AKT-Ser473, a well characterised mTORC2 substrate, was reduced in *RICTOR*-targeted cells and similar reduction was detected in the expression of mSIN1, another essential component of mTORC2 (Fig. 3.2E). As expected, all the transfected cells expressed Cas9, albeit at different levels (Fig. 3.2E and F). The targeting efficacy, however, did not show a clear correlation with the Cas9 expression, indicating that Cas9 is not a sole factor that determine the targeting efficiency. Taken together, these data indicated that sgRNAs 4-1 and 5-2 may have better targeting effect than the rest.

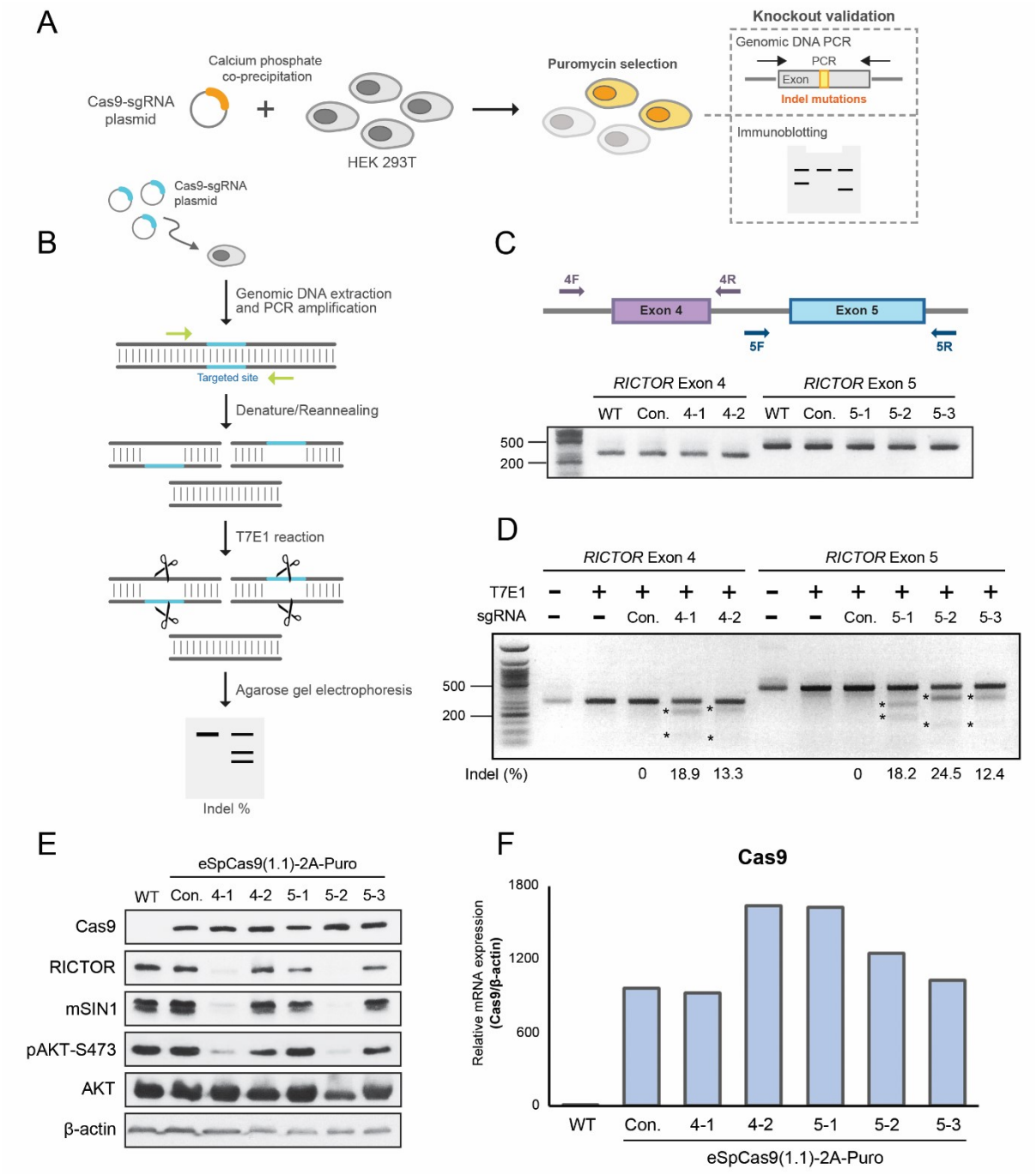


Figure 3.2 Validation of single sgRNA-mediated *RICTOR*-targeting in HEK 293T cells

(A) *Schematic depicts the experimental procedure to validate sgRNA efficacy in HEK 293T cells.* ***(B)*** *A workflows of T7 Endonuclease I (T7E1) assay. Briefly, genomic DNA was extracted from the sgRNA transfected HEK 293T cells, and the target sites (indicated in blue) were amplified by PCR. The wild-type and edited DNA PCR products were then denatured and reannealed to form heteroduplexes (mismatches) which can be digested by T7E1 endonuclease. After quantified the intensity of DNA bands on agarose gel, the percentage of indel mutations can be calculate with formula.* ***(C)*** *PCR amplification of targeted fragments. Primer sites on RICTOR are indicated by arrows* ***(Top)*** *and amplified PCR products in gel electrophoresis are shown* ***(bottom)****.* ***(D)*** *T7E1 assay results. Asterisks indicate expected fragment sizes upon success RICTOR-targeting and number at the bottom indicate the % of indel mutations. sgRNAs and T7E1 treatment are also indicated.* ***(E)*** *Immunoblotting with indicated antibodies on cell lysates from sgRNA-transfected HEK 293T cells.* ***(F)*** *Cas9 mRNA levels in HEK 293T cells described in E.*

3.2.3 Dual sgRNA-directed *RICTOR*-KO and clonal isolation of HEK 293T cells

Several studies have reported that the gene targeting efficiency (or induce genomic DNA-fragment deletion) could be potentially increased by introducing two DNA double-strand breaks (Bressan et al., 2017; Erard et al., 2017; Liu et al., 2016). In order to quickly and efficiently identify targeted *RICTOR*-KO cells by DNA PCR, 3 different RICTOR sgRNAs, 4-1, 5-1 and 5-2 were selected and paired according to their individual target efficiency and cleavage site (see section 3.2.1). Each pair of sgRNAs (i.e. 4-1/5-1 and 4-1/5-2) was combined in a way that both exon 4 and 5 would be targeted simultaneously and induce a ~1 kb deletion in *RICTOR* gene, which could evaluate the mutation efficiency by observing the size of the PCR products (Fig. 3.3A). The Cas9 expression vectors containing each pairs of the sgRNAs were co-transfected into HEK 293T cells, total 11 and 13 clones were successfully isolated from these two different sgRNAs transfections, and 5 clones were collected from controls. The *RICTOR* disruption and *RICTOR*-KO were analysed by DNA PCR amplification/sequencing and immunoblotting, respectively.

Of the 24 potential targeting clones, results from immunoblotting showed that RICTOR and AKT-Ser473 phosphorylation could still be detected in some clones (i.e. D, G and J from 4-1/5-1 targeting) (Fig. 3.3B top), indicating that they might contain at least one wild-type allele (WT or monoallelic mutation). As expected, the PCR products that were amplified from the genomic DNA crossing *RICTOR* exons 4 and 5 with primer 4F/5R displayed different knockout genotypes (Fig. 3.3B bottom). Take 4-1/5-2 targeting clones as examples, although the size of the PCR product from clone C was very similar to that of wild-type (~1347 bp), the lack of RICTOR protein expression indicated that all the alleles contained small indels (multiallelic mutations, heterozygous deletion). In comparison, PCR amplicons for clone L resulted in a single band with an estimated size of 400 bp, indicating that clone L was multiallelic homozygous deletion. In summary, the 11 clones obtained from 4-1/5-1 targeting contained 37% (4/11) wild-type or monoallelic mutation with residual RICTOR protein, 64% (7/11) multiallelic mutation and 18% (2/11) of them were homozygous deletion. On the other hand, all the 13 clones isolated from 4-1/5-2 targeting had multiallelic mutation and 15% (2/13) of them were identified with homozygous deletion (Table 3).

Further analysis was focused on 4 multiallelic homozygous deletion clones (*RICTOR*-KO 4-1/5-1 F, H and 4-1/5-2 F, L) and the PCR products were directly sent for Sanger sequencing. As predicted, the sequencing results showed a clear and defined large deletion in each sequenced clones and the large deletion had significantly altered the genomic-sequence of *RICTOR* in each clone (Fig 3.3C). These results not only confirmed the successful establishment of *RICTOR*-KO 293T cells by CRISPR-Cas9 system, but also with high efficiency and over 15% of homozygous deletion rates. Nonetheless, *RICTOR*-KO 293T clonal cells could serve as a valuable cell model for exploring the fundamental questions in molecular cell biology of RICTOR/mTORC2.

Table 3. Summary of analysis in dual *RICTOR*-KO HEK 293T clones

sgRNA	Approx. deletion size (bp)	WT or Monoallelic Mutation	Multiallelic Mutation: Heterozygous deletion	Multiallelic Mutation: Homozygous deletion	Total
-	0	5	0	0	**5**
4-1 + 5-1	967	4	5 (45%)	2 **(18%)**	**11**
4-1 + 5-2	1016	0	11 (85%)	2 **(15%)**	**13**

* Number of clones

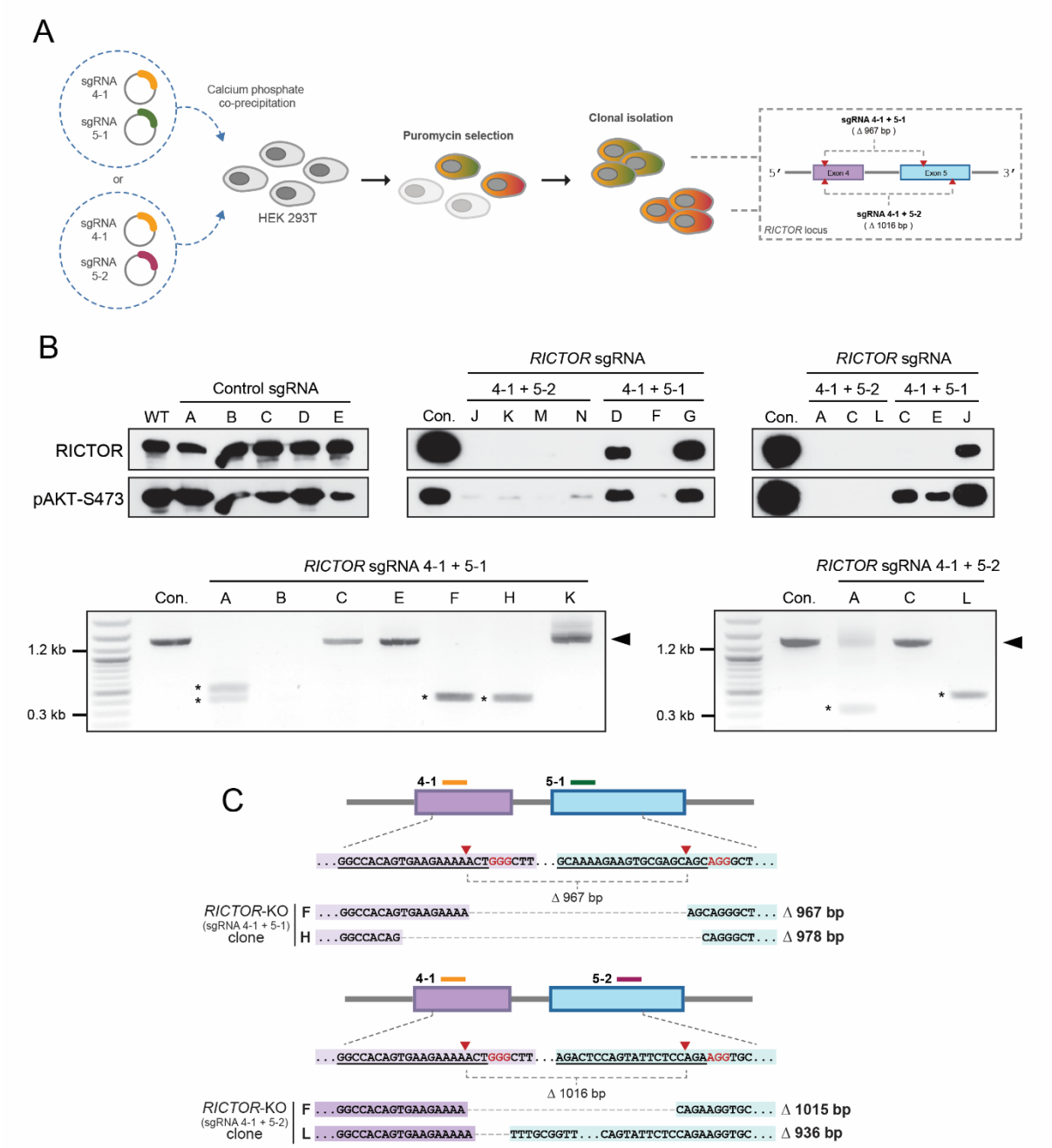


Figure 3.3 Generation and clonal isolation of dual sgRNA-mediated *RICTOR*-KO in HEK 293T cells

*(**A**) Schematic of the experimental strategy for generating dual sgRNA-mediated RICTOR-KO HEK 293T cells. (**B**) Representative immunoblotting images **(top)** and PCR products of genomic DNA extracted from potential targeted clones were visualised in 2% agarose gel by electrophoresis **(bottom)**. Black arrows show the expected size of wild-type PCR products and the smaller PCR products are marked with black asterisks. (**C**) Sequencing results of the four possible RICTOR homozygous deletion clones.*

3.2.4 Targeted gene editing at *RICTOR* gene locus in human embryonic stem cells (hESCs) by lipofection

After the initial attempt at screening the RICTOR sgRNAs and the experience of establishing *RICTOR*-KO 293T clonal cells, next I aimed to generate *RICTOR*-KO hESCs for the purpose of investigating the role of RICTOR/mTORC2 in human early embryonic development. There are several methods that can be used to transfect hESCs such as lipofection, lentiviral transducion and electroporation (Eiges et al., 2001; Gropp et al., 2003; Lakshmipathy et al., 2004; Xiong et al., 2005; Zwaka and Thomson, 2003). Given that lipofection can be quickly accomplished and based on the previous experience in our lab, I applied lipofection to introduce Cas9-sgRNA 4-1 plasmid into hESCs for the initial try. Briefly, hESCs were dissociated and re-suspended in conditional media (CM) together with the lipofection reagent and Cas9-sgRNA plasmids mixture. At the time point of 48 hours post-transfection, 1.6μg/ml of puromycin was added for selection of stable colonies in the following 10 days (Fig 3.4A). After puromycin selection, total 9 clones were isolated, and the selection pressure was maintained by keeping 1μg/ml puromycin in the culture medium. However, RICTOR protein could be detected in all 9 potential knockout clones by immunoblotting and the results from DNA sequencing revealed that the *RICTOR* gene in all 9 clones had sequences identical to wild-type sequences (only two of them were shown in the Figure 3.4B and C), suggesting that the generation of stably transfected hESCs clones by liposome method was difficult and inefficient as the results showed that none of these clones were successfully knockout (Fig 3.4B and C).

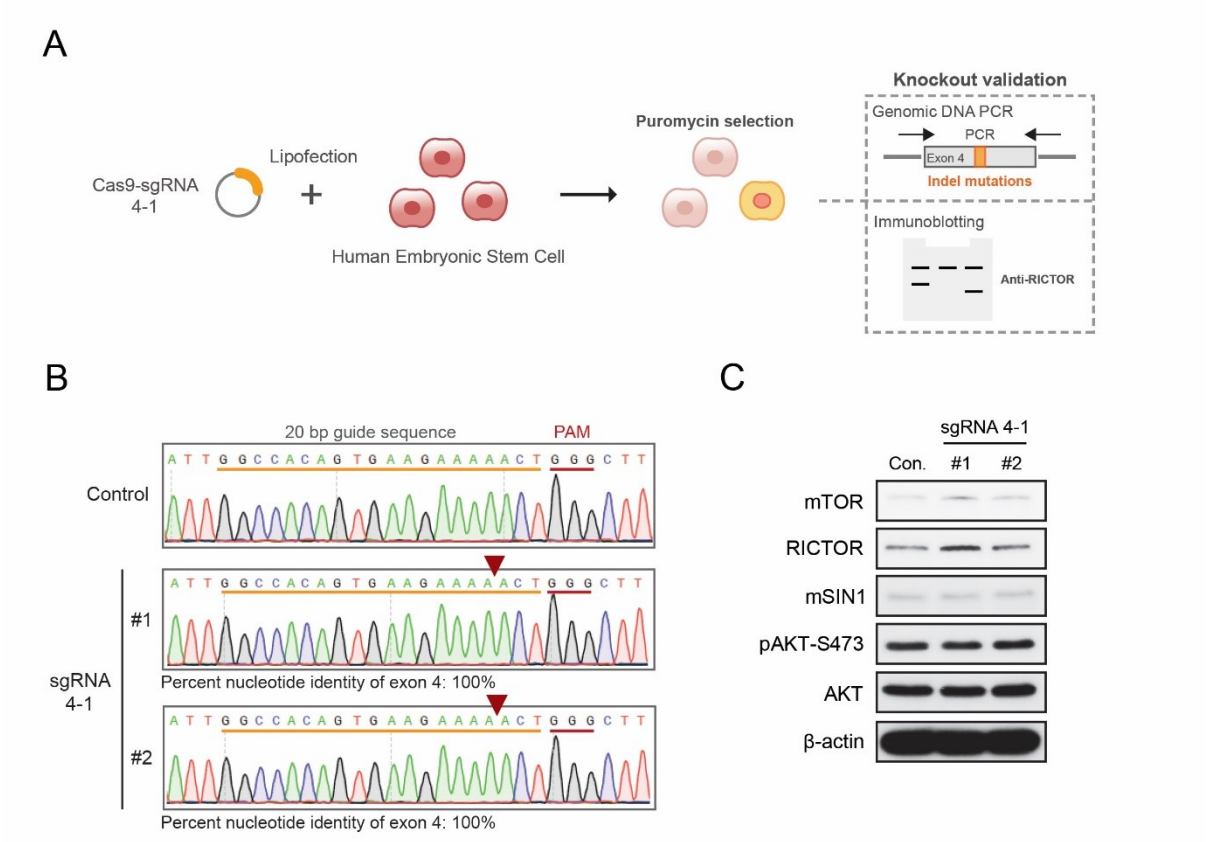


Figure 3.4 Introduction of Cas9-sgRNA expression plasmid into hESCs via lipofection

(A) Overview of the experimental process for generating RICTOR-KO hESCs via lipofection. (B) Sanger sequencing of control and two RICTOR potential targeted clones showed identical sequences. The 20-bp guide sequences on exon 4 of RICTOR were marked with orange line, PAM were underlined in red and the red triangles indicate the expected cleavage sites. (C) Cell lysates extracted from control and two RICTOR potential targeted clones (sgRNA 4-1 #1 and #2) were analysed by immunoblotting and probed with indicated antibodies. Representative images from one experiment are also shown.

3.2.5 Targeted deletion of *RICTOR* in hESCs by electroporation

Even though the lipid-mediated cell transfection method is probably the simplest and easiest way to achieve genetic manipulation, my results from last section (3.2.4) indicated that this method was not efficient enough for generating gene-knockout hESCs with plasmid-based system. This conclusion is also supported by a previous report which published in Journal of Biotechnology, 2015 (Liang et al., 2015), no conditions were found for efficient Cas9 plasmid delivery via lipid-based reagents in hESCs. Since most of the stable gene modification in hESCs were done by electroporation (Martinez et al., 2015; Merkle et al., 2015; Ranganathan et al., 2014), thus, I next performed electroporation with the Neon™ Transfection system to deliver Cas9-sgRNA expression plasmids into hESCs (Fig 3.5A).

To optimise the transfection conditions and also maximise the gene targeting efficiency, the transfection of EGFP encoding plasmid into hESCs was used as an initial model in the searching for suitable parameters. Total 24 different electroporation parameters were applied to hESCs with the same amount of EGFP plasmid, and the transfection efficiency was analysed by light and fluorescence microscopy at the time point 48 hours post-transfection. Results from fluorescence microscopy showed that, although the transfection efficiency was low in hESCs, the EGFP signal could still be detected in 4 out of 24 conditions (Fig 3.5B). After deciding the best condition for hESCs transfection, next I transfected hESCs with 3 different RICTOR sgRNAs in two different pairs (sgRNAs 4-1/5-1 or 4-1/5-2) together with Cas9 for the disruption of *RICTOR*. hESCs transfected with Cas9 but without sgRNA were used as controls, and the same optimisation protocol (1050V, 30ms pulse width, 2 pulses) was applied for EGFP transfection as an efficiency indicator. 48 hours post-transfection, puromycin (0.5μg/ml) was added to the cells from day 3 to day 5 only for a short period of selection (Fig 3.5C), and the drug-resistant colonies were maintained in the same well with puromycin-free medium for another 20 days before they were picked and expanded for the clonal isolation (Fig 3.5D).

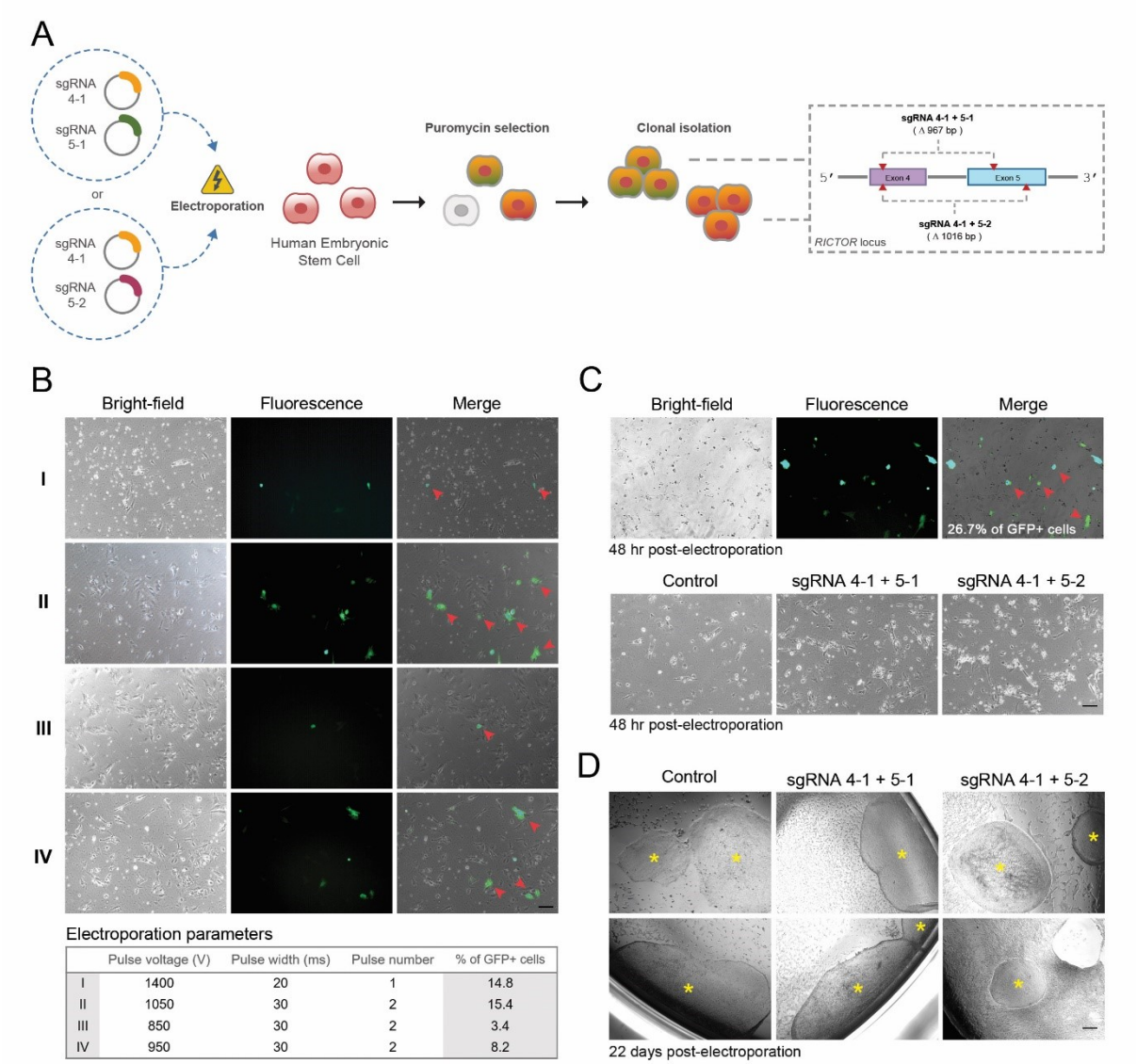


Figure 3.5 Electroporation of EGFP and Cas9-sgRNA expression plasmids into hESCs

(A) *Overview of the experimental process for generating RICTOR-KO hESCs via electroporation.* ***(B)*** *The bright-field and fluorescence images of the electroporation parameters optimisation. hESCs (H1) were transfected with 0.5μg of EGFP-encoding plasmid by the Neon™ transfection system. Red arrows indicate the hESCs which expressed EGFP. Scale bar, 100μm.* ***(C)*** *The bright-field and fluorescence images of electroporated cells (1050V, 30ms pulse width, 2 pulses). Scale bar, 100μm.* ***(D)*** *Bright-field images of control and RICTOR targeted cell colonies. The hESCs colonies are marked with yellow asterisks. Scale bar, 500μm.*

3.2.6 Clonal isolation and verification of successful *RICTOR*-KO hESCs

After delivered CRISPR-Cas9 system in hESCs via electroporation, the next step is to isolate the targeted clones from the transfected population. The cells were dissociated into single cells with accutase when the cell colonies grew to a visible size. Single cells (cell numbers ranging from 15,000 to 50,000 per 10-cm dish in general) were plated onto 10-cm culture dishes, which coated with matrigel in advance, and allowed the cells to grow for 10-12 days before the clones were manually picked into 24-well plates. Remarkably, I observed that the colonies of potential *RICTOR*-KO hESCs grew much slower than that of the controls. For initial screening of *RICTOR*-KO clones, genomic DNA and the whole cell lysate were extracted from a small number of cells and validated by both Sanger sequencing and immunoblotting. Genomic DNA was collected from selected clones (clone P2, P3 from 4-1/5-2 targeting and control C1) for the detection of genome editing at the human *RICTOR* locus. PCR products (crossing *RICTOR* exons 4 and 5, primer 4F/5R) were sent for Sanger sequencing, and the sequencing results showed that a mixed sequence content was present around the expected break sites in both clone P2 and P3 but not in control genomic DNA, indicating that the Cas9-sgRNA complex efficiently induced indel mutations in *RICTOR* gene (Fig 3.6A). The Sanger sequencing results of *RICTOR*-KO clone P2 and P3 were further analysed with the online bioinformatics tool- Inference of CRISPR Edits (ICE), which can help to quantify the frequency of small mutations in a pool of cells and can also be informative about the number of clones that need to be screened for the desired genotype. As shown in Fig 3.6B, the results of analysing genomic profile in both clone P2 and P3 showed that around 60% of the genomic DNA sequences were identical to the wild-type, indicating that both clone P2 and P3 might still be mixed clones. However, the results also showed that 30% of the genomic DNA sequences had frameshift mutations in both P2 and P3, suggesting that 3 out of 10 clones might possibly be *RICTOR*-deficiency.

Additionally, I found that among all puromycin-resistant potential *RICTOR*-KO clones which I have isolated, different levels of RICTOR protein could be detected in all potential KO clones by immunoblotting after a long exposure time (Fig 3.6C). Most likely, this could be due to the presence of small subpopulation of *RICTOR* heterozygotes, which indicated that the clonal

isolation might not be purely clonal. Although the Cas9-sgRNA expression plasmids had been successfully delivered into hESCs and the *RICTOR* gene interruption was confirmed by genomic DNA sequencing, the majority of potential *RICTOR*-KO clones were actually heterogenous polyclonal populations which could be due to the contamination of heterozygously targeted *RICTOR* cells or contamination of parental non-edited cells.

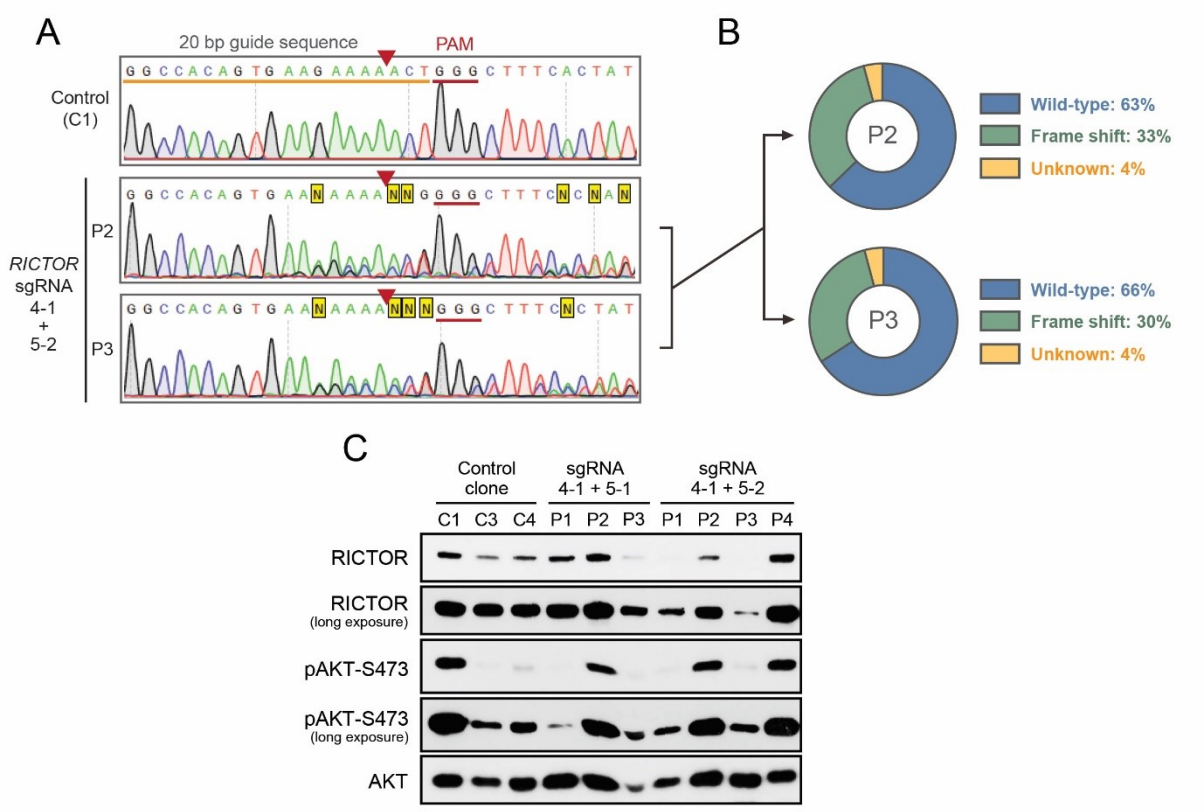


Figure 3.6 Clonal isolation and validation of *RICTOR*-KO hESCs

(A) *Sequencing results of control and RICTOR potential knockout clones (P2 and P3 from 4-1/5-2 targeting). The 20-bp guide sequences on exon 4 of the RICTOR gene were marked with orange line, PAM were underlined in red and the red triangles indicate the expected cleavage sites.* ***(B)*** *The pie charts summarised the indel mutations in RICTOR-KO clone P2 and P3. Wild type, no indel; frame shift, 3N+1 or 3N+2; Unknown, cannot identified.* ***(C)*** *Immunoblotting analysis of control and RICTOR-KO clones with indicated antibodies. Representative images from one experiment are also shown.*

Therefore, a second round of clonal isolation was carried out by plating cells (P3 population, which retained the lowest level of RICTOR protein) at low density. Total 24 potential *RICTOR*-KO clones were obtained from P3 population and an anti-RICTOR immunoblotting was performed (Fig 3.7A). As shown in Figure 3.7A, the expression of RICTOR protein was detectable in control clone but completely absent in all 24 putative *RICTOR*-KO clones, even after a long exposure time. To identify indel mutations, genomic DNA were extracted from clone #1 and #5 and amplified by the primer sets (Fig. 3.2C primer 4F/5R) flanking the two cleavage sites. The 1.3 kb PCR products from clone #1 and #5 were individually inserted into the pGEM®-T Easy vector and at least 5 colonies for each PCR fragment were randomly selected and sent for sequencing to detect indel mutations. Upon analysis of the TA cloning results (Figure 3.7B), all the sequences showed deletions and no wild-type sequence was recognised, despite that deletions were generated at multiple sites and in multiple sizes even within the same clonal cells. These results provide the information that even each cell colony was originated from a single cell, the cells could possibly keep re-targeting by the Cas9-sgRNA complex until the 20 bp targeting sequences are not identified. Collectively, these data suggest that even the transfection efficiency of plasmid-based electroporation system is extremely low in hESCs (<10%), disruption of the target sequence in hESCs is achievable with suitable conditions by electroporation.

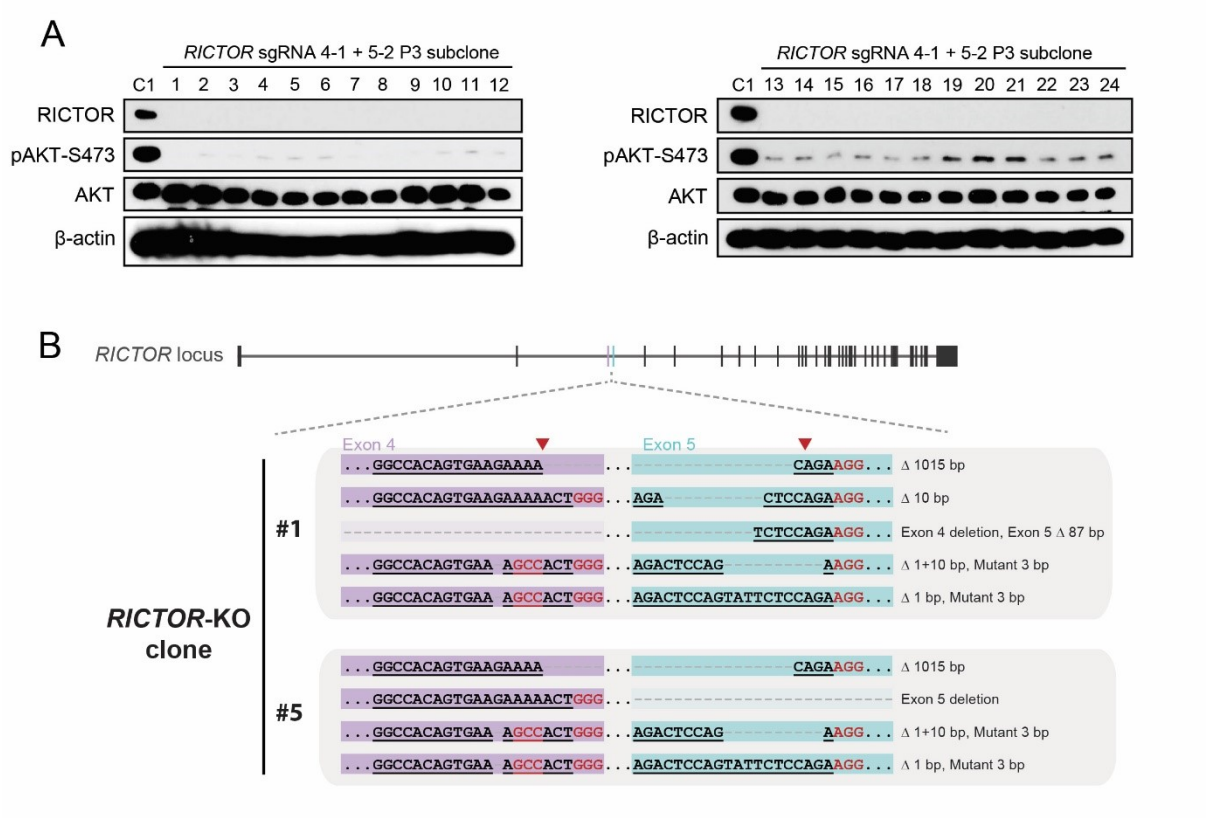


Figure 3.7 Isolate successful *RICTOR*-KO clones via double serial clonal dilution

(A) *Immunoblotting with indicated antibodies in total 24 RICTOR-KO clones. The protein expression of control clone (C1) was used as positive control. All clones were checked in one experiment as shown, but several of these clones (e.g. 1, 5, 9) have been validated several times by western (data not shown).* ***(B)*** *Summary of Sanger sequencing results from subcloned PCR products.*

3.3 Conclusions and Discussion

The advancement of CRISPR-Cas9 system provides a powerful tool for researchers to determine the function of uncharacterised genes. Several considerations and experimental setting should take into account when generating knockout cell lines. In my study, to clarify the regulation and biological function of RICTOR/mTORC2 in human cells, functional *RICTOR* knockout studies using CRISPR-Cas9 system in various cell models were created for different objectives. In this chapter, I have described the procedure for the generation of *RICTOR*-deficient clonal cell lines from the design and cloning of sgRNA to the final knockout validation.

For the design of sgRNA, a number of online tools are available to identify potential sgRNA sequences. As the specificity of Cas9 largely depends on the sequence of sgRNA, it is highly recommended that more than one online design tools should be used as reference in order to identify the optimum sgRNAs. With regards to the previous works in *Rictor*-null mice, *Rictor* gene function can be ablated by targeting the first few exons in the coding region (exon 1 to 3) (Guertin et al., 2006; Shiota et al., 2006; Yang et al., 2006). Hence, several computationally predicted sgRNAs in exon 4 and 5 were selected for my following experiments. Using HEK 293T cells as an initial cell model, I then compared the efficiency of plasmid-based gene editing among different sgRNAs. Although I have demonstrated that single sgRNA is sufficient to disrupt RICTOR expression in HEK 293T cells, single sgRNA introduced by liposome-mediated transfection to hESCs was not success. Considering the low targeting efficiency in hard-to-transfect hESCs, dual-sgRNA expression method was also applied in HEK 293T cells for the purpose of screening the best sgRNA pairs and allowed me to maximise the chance to obtain *RICTOR*-KO hESC clones. Notably, applied multiple sgRNAs into the cells may induce an increased level of off-target mutagenesis, thus, it is required to introduce different combinations of sgRNAs and carefully validate their phenotypes.

According to the cell types and experiment objectives, the CRISPR-Cas9 system can be delivered to the cells via several strategies and methods. The generation of *RICTOR*-KO hESCs showed consistent results as previous findings, the electroporation-mediated transfection has a relatively high transfection efficiency than lipid-based delivery vehicles (Liang et al., 2015). Apart from the transfection methods, it has been shown that the editing

efficiencies in hESCs can be enhanced by the pre-assembled Cas9 protein/sgRNA ribonucleoprotein (RNP) complexes (Farboud et al., 2018; Kim et al., 2014). Plasmid-mediated genome editing method often leads to permanent expression of Cas9, which might possibly accumulate the off-targeting events. In my study, results show that among all 6 selected HEK 293T cell lines (including both controls and *RICTOR*-KO), 4 of them showed constitutive expression of Cas9, while the others were silenced by unknown mechanism. The extended expression of Cas9 in the cells could bring some difficulties for the following experimental design, for instance, the phenotypic rescue experiments. Thus, several of these problems can be overcome by replacing the Cas9 plasmid delivery with the short persistence and less toxic Cas9 RNP.

In addition to detecting on-target indel mutations and enhancing the targeting efficiency, a successful CRISPR-Cas9 gene editing in cell lines should not affect overall genomic stability in the cells and have no off-target effects. Particularly, genetic mutations may occur due to the long and stressful process during the generation of gene-modified cells (Baker et al., 2016). Therefore, it is important to characterise the targeted cells not only on their cell properties (e.g. self-renewal and differentiation potency for hESCs) but also on their genomic DNA. To assess genetic stability in *RICTOR*-KO cells, the most informative method is whole genome sequencing to compare any difference in cells prior and after the gene-editing. However, this approach is very costing. Alternatively, karyotyping will inform any chromosomal changes as an indication of genomic stability.

To analyse off-target effects, there are numerous strategies, either biased or unbiased, can be applied to detect CRISPR-Cas9 off-target effects currently (Anderson et al., 2018; Martin et al., 2016). Biased methods relied on bioinformatics algorithms (i.e. CRISPR DESIGN and DESKGEN) which identify and predict potential off-target sites. Although these computational predictions may be the most practical and easiest way to analyse off-target mutations, unintended mutations anywhere in the genome could be hindered by the biased approaches. Therefore, genome-wide unbiased technologies have been developed, such as Integrative-Deficient Lentiviral Vectors (IDLV) capture, Whole Genome Sequencing (WGS) and Genome-wide Unbiased Identification of Double-stranded breaks Enabled by Sequencing (GUIDE-seq), to overcome the limitations of biased methods and enhance the accuracy and precision

of off-target sites detection (Gabriel et al., 2011; Smith et al., 2014; Tsai et al., 2015). However, the later approaches are expensive. Alternatively, it might be possible to generate multiple clones with different sgRNAs. If they show similar phenotypes/effects, it is likely that these phenotype/effects are not resulted from off-target mutations. Thus, even though we have carefully designed and selected the sgRNA target sites to minimise any unintended modification, generation of more clones with different sgRNAs could help us to minimise the off-target effects.

The selection of suitable clonal cell lines from cell populations could be really challenging as there is no standard protocol and more likely to rely on the experience of the operator. Although the heterogeneous population with high knockout efficiencies might be a good option for investigating gene function, the percentage of knockout cells could gradually decrease due to the proliferation rate difference. Indeed, the isolation of *RICTOR*-KO clonal cells is indispensable in my study because loss of RICTOR has been reported to suppress cell proliferation (Babaev et al., 2018; Bian et al., 2017; Wang et al., 2015). Since there is no reporter gene product such as EGFP in my CRISPR-plasmid transfected hESCs, cells were isolated by serial dilution cloning instead of Fluorescence-Activated Cell Sorting (FACS), alternatively. The single cell-derived clonal isolation can be really challenging as the plating of single cell or cells at low density generates a significant stress on cells, which may lead to selective pressures, especially for hESCs. I observed a great proportion of *RICTOR*-KO hESCs that were incapable of maintaining an undifferentiated state during the long process of single cell expansion, even going into growth arrest or cell death, which was possibly due to the cellular stress by clonal isolation or the effect of deficiency of *RICTOR*. As such, the clonal isolated cells are likely to contain a small number of non-targeted or partially targeted cells, it is better to carry out at least two round of clonal isolation procedure to ensure the gene of interest has been completely targeted in all cells.

However, there are some other important factors that need to be considered during clonal isolation, particularly clonal variability which could possibility lead to incomplete or incorrect results. For instances, low clonogenicity of cancer cell populations is regarded as one of the major obstacles in treating cancer patients (Schneider et al., 2017). It has been reported that some established cell lines, especially genetic-unstable cell types (such as hESCs), exhibit

significant inter-clonal heterogeneity (McGranahan and Swanton, 2017). Given that both genome-editing and clonal expansion are stressful processes which may result in genetic aberrations, it is absolutely crucial to generate and analyse more than one independent knockout clone to confirm that any unexpected result is not due to clonal artifact. Therefore, in order to investigate the role of *RICTOR*-deficiency in cell properties, two independent *RICTOR*-KO clones with different sgRNA combinations were utilised to avoid, or minimise, the possibility of clonal variability in this project (chapter four and five). Similarly, it is also important to isolate two control clones to minimise any clonal variability. However, if any phenotypes appear to be more clonal variable, it might be necessary to obtain extra clones to insure that any phenotypic effects are indeed as a result of deficiency/mutation of the target gene.

In sum, proper experimental design and effective strategies are necessarily required for the establishing CRISPR-Cas9 mediated gene editing in human cells. Given that RICTOR/mTORC2 signalling pathway has drawn much attention recently because its crucial involvement in cell proliferation, differentiation and metabolism, the generation of *RICTOR*-KO 293T and hESC clonal cell lines provides us with valuable cell models for characterising the function of the *RICTOR* gene and for exploring the biological roles of RICTOR/mTORC2 in human cells. The *RICTOR*-KO clonal cells characterisation and their underlying mechanisms are described in the following chapters.

04

Phosphorylation of mSIN1-CRIM domain affects protein stability and substrate selectivity

4.1 Introduction

Although increasing evidence indicate that mTORC2 may have functions in many physiological process, the role of RICTOR/mTORC2 in human cells is mostly described as an important mediator which regulates cell proliferation and survival (Laplante and Sabatini, 2012). Furthermore, abnormal RICTOR/mTORC2 signalling is often associated with cancer cells and the overexpression of RICTOR has been discovered in a large proportion of cancer types which promotes mTORC2 activity (Gkountakos et al., 2018; Masri et al., 2007; Xie et al., 2018). Several studies, both *in vivo* and *in vitro*, have demonstrated that depletion of RICTOR with either siRNA or shRNA leads to an inhibitory effect on cancer cell growth (Bian et al., 2017; Driscoll et al., 2016; Masri et al., 2007; Schmidt et al., 2017), which is also consistent with the slower cell growth that I had observed during the process of generating *RICTOR*-KO cells. Previous studies have shown that the hyperactivation and amplification of RICTOR/mTORC2 signalling is commonly associated with cancer, and the inactivation of RICTOR/mTORC2 pathway has been shown to be implicated in degenerative diseases, such as Alzheimer's disease and ischemic tissues (e.g. heart and liver) (Hwang and Kim, 2011; Lee et al., 2017; Volkers et al., 2013; Xu et al., 2018). Notably, although it has been indicated by numerous studies that dysfunctional RICTOR/mTORC2 signalling leads to a variety of human diseases partly through dysregulations of its downstream targets (Dazert and Hall, 2011; Saxton and Sabatini, 2017), the specific molecular mechanisms underlying diverse physiological or pathological functions remain largely unknown and need to be further elucidated.

In order to explore how mTORC2 selects and recruit its targets, it is important to understand the structure of mTORC2 itself and the function of each core components in mTORC2 assembly and function. Although it is well characterised that mTOR is the kinase subunit that catalyses the transfer of phosphate group to its substrates (Mendoza et al., 2011), the accessibility of catalytic subunit and the substrate selections are thought to be controlled by other components of mTORC2. Recent studies on mTORC2 structure and through gene-knockout of specific subunits indicate that RICTOR and mSIN1 are important for mTORC2 assembly and substrate recruitment, in which RICTOR mainly functions as a scaffold protein while mSIN1 has a crucial role in substrate selection (Cameron et al., 2011; Karuppasamy et

al., 2017; Lu et al., 2011; Stuttfeld et al., 2018; Tatebe et al., 2017; Zinzalla et al., 2011). Furthermore, some studies found that the expression of mSIN1 requires the expression of RICTOR and *vice versa*, while the other reports showed that expression of RICTOR did not change much in the absence of mSIN1 (Frias et al., 2006; Jacinto et al., 2006; Yang et al., 2006; Yao et al., 2017). Therefore, several questions remain to be answered: 1) the relationship between RICTOR and mSIN1; 2) the exact mechanisms by which RICTOR regulates mSIN1 expression; 3) how mTORC2 utilises mSIN1 as a selective adaptor to target its substrates.

The *RICTOR*-KO HEK 293T clonal cell lines that I have generated have provided us with a suitable cell model for deciphering all these fundamental questions at molecular and cellular biological levels for RICTOR/mTORC2. In this chapter, I characterised the phenotypic alterations of *RICTOR*-deficiency in HEK 293T cells and described the results of a series of experiments which not only address the research questions that I have mentioned above but also validated some of the findings previously reported, such as the relationship between mTORC1 and mTORC2.

4.2 Results

4.2.1 Deletion of *RICTOR* abolishes the activity of mTORC2 but not mTORC1 and PI3K

To decipher the fundamental biological mechanisms, I comprehensively characterised the *RICTOR*-KO HEK 293T clonal cell lines that were generated by CRISPR/Cas9 system as described in Chapter 3. As shown in Fig. 4.1A, ablation of RICTOR in 293T cells completely eliminated mTORC2 activity as shown by the absence of phosphorylation on Ser473 and Thr450 of AKT, which are similar to that in *Rictor*-null MEF (Guertin et al., 2006; Shiota et al., 2006) (Fig 4.1B). In contrast, there is no clear change on AKT phosphorylation at Thr308, which is associated with PDK1/PI3K activity, indicating that RICTOR might not be involved in these pathways. However, the phosphorylation of S6K, a marker of mTORC1 activity, showed a slight increase in *RICTOR*-KO cells compared to that in control cells (Fig 4.1A), possibly due to the disruption of mTORC2 complex assembly, which subsequentially releases mTOR and increases the availability of mTOR protein. All these findings are consistent with previous reports on *RICTOR*-knockdown in various cell types (Das et al., 2011; Rosner et al., 2009; Sarbassov et al., 2004). Thus, these results indicate that *RICTOR*-deficiency specifically hampered the activity of mTORC2 but not mTORC1.

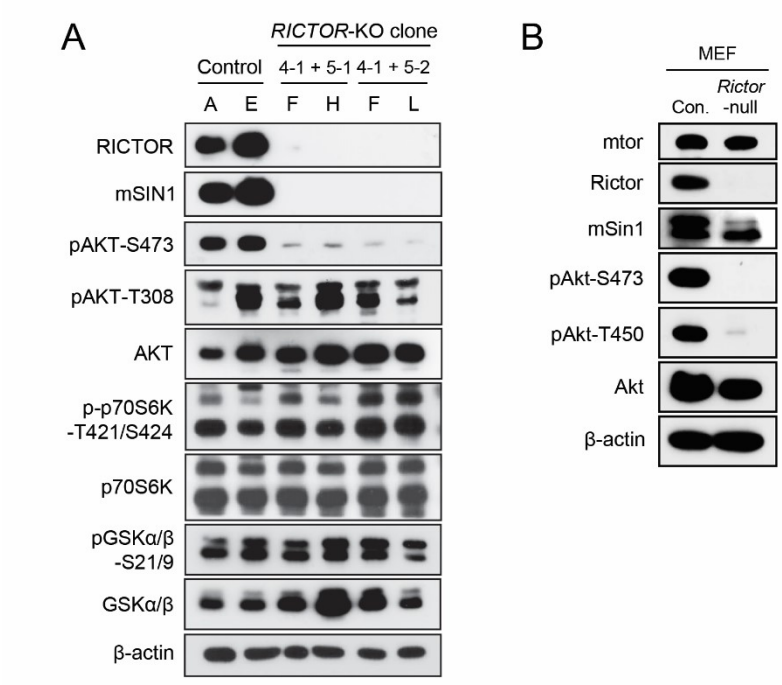


Figure 4.1 *RICTOR*-deficiency abolishes mTORC2 activity in HEK 293T cells

(A, B) *Immunoblotting analysis of control and RICTOR-KO 293T clones* ***(A)*** *with indicated antibodies and Rictor-null MEF was used as positive control* ***(B)****. The experiment was conducted three times and representative images are shown.*

4.2.2 *RICTOR* deficiency leads to decreased cell proliferation and viability

Next, I investigated whether *RICTOR*-deficiency affect cell morphology and growth. Firstly, I noticed that in comparison with controls, *RICTOR*-KO clones exhibited a more 'dome-shaped' morphology, and they were more easily to detach from the plates in the routine culture conditions (Fig 4.2A). These seem to agree with the previous report that the disruption of mTOR signalling suppresses cell adhesion and that RICTOR/mTORC2 might regulate cell adhesion in an AKT-independent manner (Chen et al., 2015). Secondly, during the generation and culture of these *RICTOR*-KO cells, I also observed that wild-type control 293T appeared to reach confluency quicker than the knockout cells even though they were plated at similar numbers. To validate this observation, I examined the cell growth in both control and *RICTOR*-KO cells using trypan blue staining and cell counting. The viable cell numbers were plotted (Fig 4.2B) and statistically analysed according to their RICTOR status, which showed that cell growth of the *RICTOR*-KO cells were significantly reduced compared to the controls (Fig 4.2C). In order to address whether this difference in cell growth resulted from the difference in their proliferation or apoptosis, the protein levels of phospho-H3 (pH3, a proliferation marker) and cleaved-caspase 3 (an apoptosis marker) were examined by immunoblotting (Fig 4.2D). The results showed that the pH3 levels were obviously lower in the *RICTOR*-KO cells than in the controls, whereas the *RICTOR*-KO cells exhibited considerably higher levels of cleaved-caspase 3. These results indicate that the reduced cell growth in *RICTOR*-KO cells is likely a combined effect of decreased proliferation and increased apoptosis. To further explore the role of RICTOR in cell proliferation and apoptosis, I analysed the cell cycle in these cells by flow cytometry (Fig 4.2E). In comparison with the controls, the *RICTOR*-KO cells showed an increased population of cells in the sub-G0/G1 phase, suggesting a higher rate of apoptosis in them. In addition, *RICTOR*-KO cells displayed a clear enrichment of cell populations in G1 phase and a reduction in S/G2/M phases, indicating that deficiency of *RICTOR* might lead to a prolonged G0/G1 phase, even G1 arrest that in addition to increased apoptosis. Collectively, these phenotypic alterations demonstrate that the deficient of RICTOR attenuates cell growth by decreasing cell proliferation and increasing cell death.

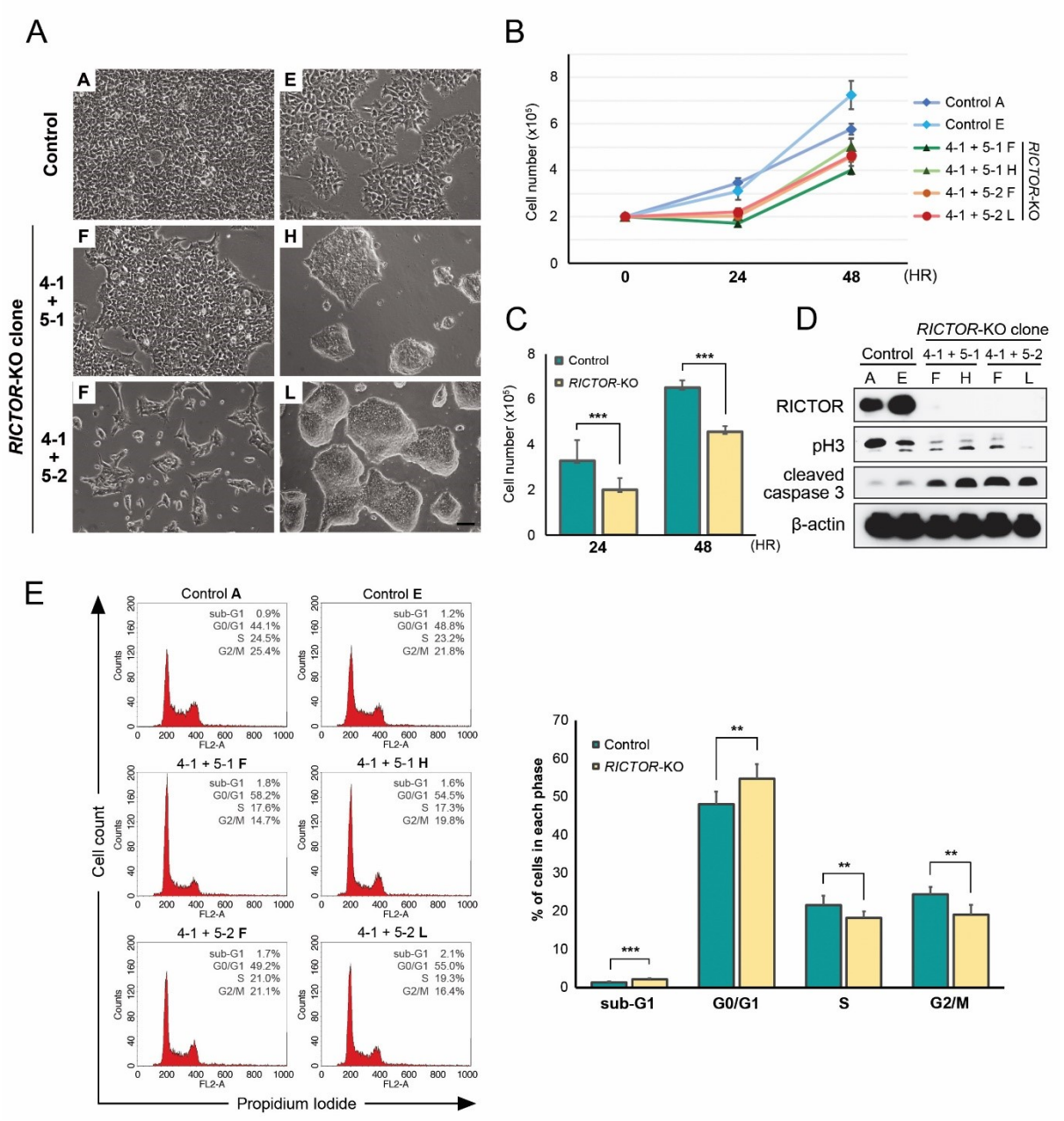


Figure 4.2 Characterisation of HEK 293T *RICTOR*-KO cells

(A) *Representative phase-contract images of control and RICTOR-KO clones. Scale bar, 100μm.* ***(B)*** *Cell proliferation assay of control and RICTOR-KO cells. Cells were counted at 24 and 48 hours post plating with trypan blue staining. Number of live cells were plotted as means ± SD (n=3).* ***(C)*** *Histogram showing average cell growth in combined control and RICTOR-KO clones, respectively. Data are represented as the means ± SD (n = 6 for controls and n = 12 for RICTOR-KO) (***p < 0.001 by two-tail unpaired t-test).* ***(D)*** *Immunoblotting with proliferation and apoptosis markers as phospho-Histone H3 (pH3) and cleaved-caspase 3 antibodies, respectively. Representative images from three independent experiments.* ***(E)*** *Cell cycle analysis using flow cytometry in control and RICTOR-KO cells, and the distribution of each cell cycle phase (sub-G1, G0/G1, S, G2/M) is presented as bar chart. Data are represented as the means ± SD (n = 6 for controls and n = 12 for RICTOR-KO) (**p<0.01, ***p < 0.001 by two-tail unpaired t-test).*

4.2.3 RICTOR/mTORC2 regulates mSIN1 at post-translational levels via protein degradation

Given that mTORC2 is a multi-protein complex and that RICTOR has an essential role in mTORC2 assembly and functions, I further investigated the relationship between RICTOR and other core components of the mTORC2 complex, such as mTOR, mSIN1 and mLST8. Interestingly, diminishing *RICTOR* substantially decreased mSIN1 expression without a clear effect on the expression of mTOR and mLST8 (Fig 4.3A). This reduced mSIN1 expression could be rescued by introducing RICTOR expression back to the cells, at least partly, indicating that RICTOR has a positive regulatory effect on mSIN1 expression (Fig 4.3B). This was further supported by the facts that a dramatic reduction of mSIN1 protein expression was also detected in other *RICTOR*-KO cell types such as PC-3 cells (Fig 4.3C) and hESCs (Chapter 5), indicating that *RICTOR*-depletion-induced reduction in mSIN1 expression is not cell type specific. It has been suggested that RICTOR and mSIN1 proteins may stabilise each other through the formation of a binary complex, and thereby in the absence of one, the other will be degraded (Frias et al., 2006; Yang et al., 2006). However, other reports showed that the protein expression of RICTOR was unaffected in mSIN1 RNAi-knockdown or *mSin1*-knockout cells (Jacinto et al., 2006; Yao et al., 2017). To further examine the effect of RICTOR and mSIN1 on each other, we obtained *mSIN1*-KO HEK 293T cells from Professor McCormick's laboratory in the USA and examined the expression of RICTOR protein in these cells by immunoblotting. Although both AKT-Ser473 and Thr450 failed to be phosphorylated in these cells, similar to that in *RICTOR*-KO cells, there was no clear difference detected on the expression of RICTOR (Fig 4.3D). The results suggest that the stabilisation between RICTOR and mSIN1 might not be a mutual effect, rather RICTOR has a regulatory effect on mSIN1 expression, while mSIN1 hardly affects RICTOR expression, at least in 293T cells.

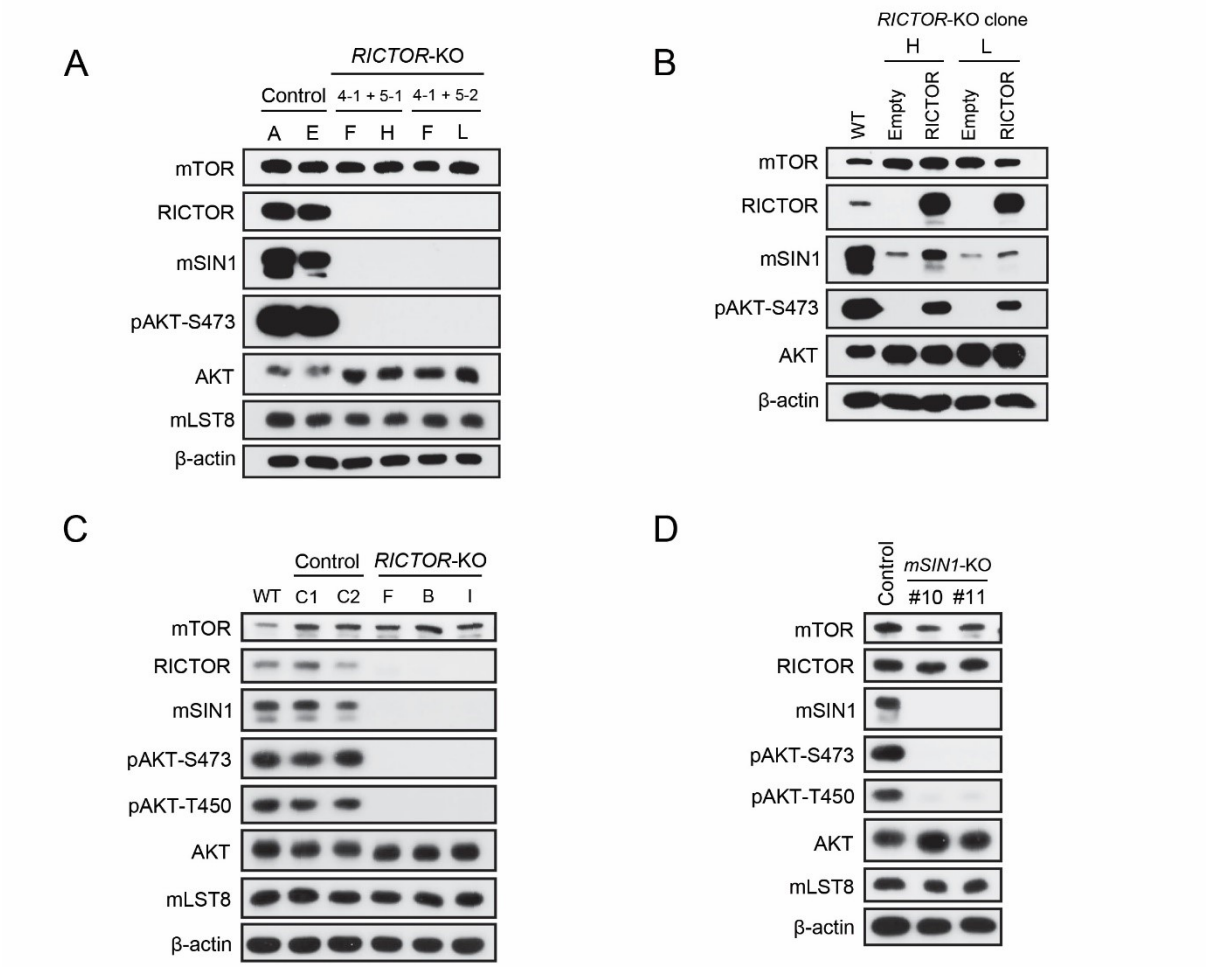


Figure 4.3 The deficiency of *RICTOR* is accompanied by the decreased expression of mSIN1 and mTORC2 activity

(A) *Immunoblotting analysis with indicated antibodies in HEK 293T control and RICTOR-KO clones. Representative images from four independent experiments.* ***(B)*** *Immunoblotting showing re-expression of RICTOR in RICTOR-KO clones rescued mSIN1 expression. RICTOR-expressing vector was transfected into indicated RICTOR-KO clones and cells were harvested for immunoblotting after 48 hours. Representative images from three independent experiments.* ***(C)*** *Immunoblotting with indicated antibodies in PC-3 control and RICTOR-KO clones. Representative images from three independent experiments.* ***(D)*** *Protein expression of control and mSIN1-KO clones were analysed by immunoblotting with indicated antibodies. Representative images from two independent experiments.*

To investigate the molecular mechanisms by which RICTOR affects mSIN1 expression, I compared the mSIN1 transcript expression in *RICTOR*-KO to the control cells and revealed that mSIN1 mRNA was expressed at similar levels in both cell types (Fig 4.4A). This suggests that the reduction of mSIN1 protein expression in *RICTOR*-KO cells occurred at post-transcriptional levels, possibly at post-translational levels via protein degradation as RICTOR has been shown to directly interact with mSIN1.

Therefore, I presumed that RICTOR may stabilise mSIN1 by preventing it from degradation. To address my hypothesis, I first examined whether the reduction of mSIN1 in *RICTOR*-KO cells indeed resulted from degradation by treating cells with MG132 and chloroquine (CQ) to inhibit proteasome and lysosome activity, respectively (Fig 4.4B). In RICTOR wild-type cells, no clear change was detected in both RICTOR and mSIN1 expression 6 hours after inhibiting protein synthesis by cycloheximide (CHX), and similarly, no clear change was detected after inhibition of both protein degradation pathways (Fig 4.4C). These results implied that both RICTOR and mSIN1 were very stable in 293T cells. Next, I carried out similar experiments in *RICTOR*-KO cells to identify the pathway by which mSIN1 is degraded in the absence of RICTOR. Surprisingly, neither inhibition of proteasome nor inhibition of lysosome degradation pathway showed any increase in mSIN1 protein levels within regular cell lysates produced with RIPA buffer. To exclude any possibility that *RICTOR*-deficiency might lead to mSIN1 accumulated in insoluble fraction prior to degradation, the insoluble pellets were further dissolved with SDS sample buffer and performed immunoblotting with mSIN1 antibody. Interestingly, I found that the proteasome inhibitor, but not lysosome inhibitor, induced a clearly noticeable mSIN1 in the insoluble fraction of *RICTOR*-KO cells (Fig 4.4D). These findings indicate that RICTOR might not only be involved in stabilising mSIN1 protein from proteasome-mediated degradation, but also affect its solubility.

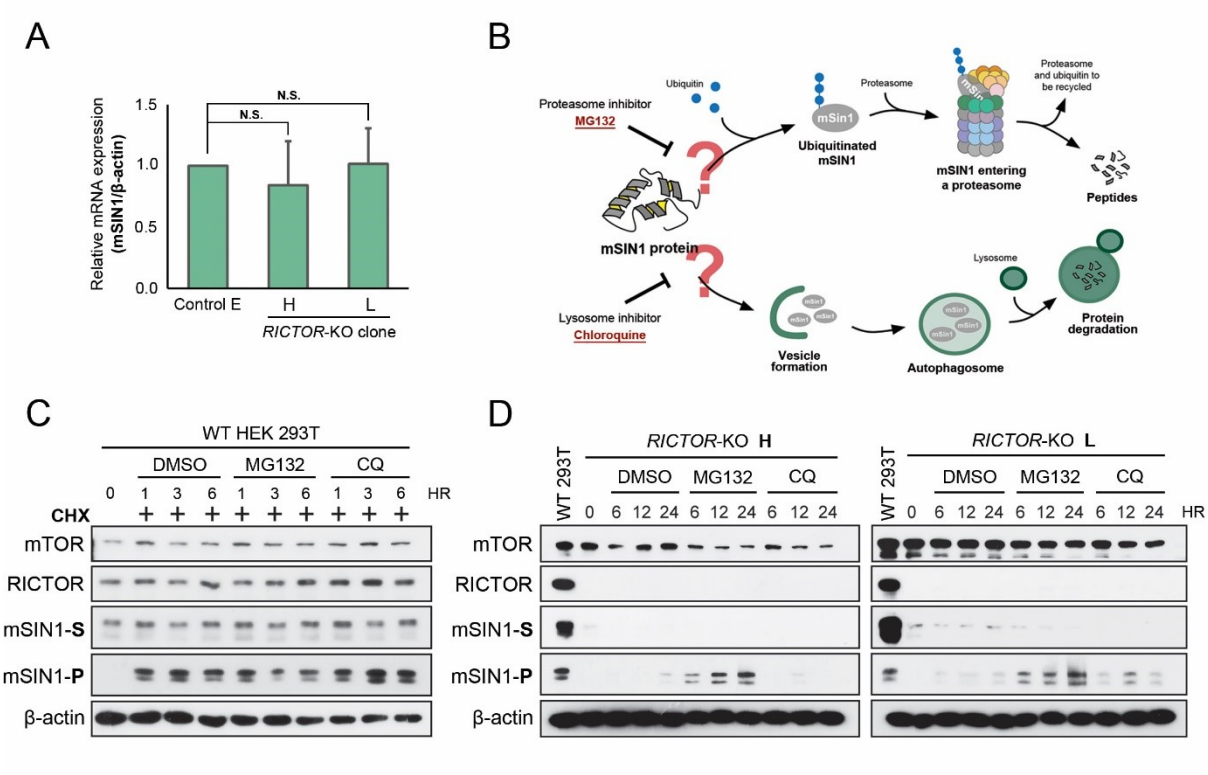


Figure 4.4 The presence of RICTOR suppresses mSIN1 from proteasome-mediated degradation in HEK 293T cells

(A) *qRT-PCR analysis of mSIN1 mRNA expression in indicated RICTOR-KO clones. Data are represented as the means ± SD (n = 3) relative to the wild-type control.* ***(B)*** *Schematic of the experimental strategy for identifying the possible degradation pathway of mSIN1 protein.* ***(C)*** *Protein degradation assay for RICTOR and mSIN1 in HEK 293T wild-type cells. 293T cells were treated with 20μg/ml cycloheximide (protein synthesis inhibitor, CHX) with either 30μM MG132 (proteasome inhibitor) or 100μM chloroquine (lysosome inhibitor, CQ) for indicated time points before they were lysed and analysed by immunoblotting with indicated antibodies. Representative images from two independent experiments.* ***(D)*** *Expression of mSIN1 protein in RICTOR-KO 293T clones in response to inhibition of protein degradation by immunoblotting. Cells were treated as in* ***(C)*** *for the indicated time and were fractionated into soluble (S) and insoluble (P) fractions after lysed in RIPA buffer. Representative images from two independent experiments.*

4.2.4 The stability of mSIN1 might be regulated by both RICTOR-mSIN1 interaction and mTORC2-mediated phosphorylation

In the previous section I have demonstrated that RICTOR functions to suppress proteasome-mediated degradation of mSIN1 and solubility of the mSIN1 protein. As such, I anticipate that RICTOR might stabilise mSIN1 through two potential mechanisms: via the RICTOR-mSIN1 interaction or the RICTOR/mTORC2-mediated function.

To further explore my hypothesis, I first investigated the role of RICTOR-mSIN1 interaction in mSIN1 stabilisation. Although RICTOR was the first identified specific subunit in mTORC2 (Jacinto et al., 2006; Sarbassov et al., 2004), it remains ambiguous about the function and structure of RICTOR in the regulation of mTORC2 assembly and activity. Therefore, to elucidate how RICTOR functions in mTORC2 activity and mSIN1 expression, I generated five different HA-tagged RICTOR expression constructs that contain distinct RICTOR deletions in each one, based on the sequences and conserved regions of RICTOR (Fig 4.5A). These constructs were transiently transfected into *RICTOR*-KO cells individually and a HA-tagged full-length *RICTOR* expression vector was used as a control. By immunoblotting, the expression of all the RICTORs were confirmed by their expected size with HA antibody (Fig 4.5B). Remarkably, transfection of RICTOR-Δ1001-1200 construct, which contains a deletion of the PS region, restored the mSIN1 expression and phosphorylation of AKT-Ser473 to similar levels as that of RICTOR-full-length (FL) in *RICTOR*-KO 293T cells, whereas transfection of other RICTOR-mutated vectors failed to restore mSIN1 expression and mTORC2 activity (Fig 4.5B). On the other hand, there was no significant effect on either mTORC2 activity or mSIN1 expression when these constructs were overexpressed in the control cells (Fig 4.4C). These results demonstrated that the region of 1001-1200 aa is not necessarily required for RICTOR to stabilise mSIN1 and to assemble mTORC2 and that the stabilisation of mSIN1 is correlated with the restoration of mTORC2 activity.

Several studies have claimed that an intact full-length of RICTOR protein is required for the activity and assembly of mTORC2 (Aimbetov et al., 2012; Glidden et al., 2012; Huang et al., 2009). To validate that the RICTOR mutant with a deletion in the multiple phosphorylation sites region (PS region, 1084-1188 aa) is still able to interact with other core components of mTORC2, HA co-immunoprecipitation assays were performed using extracts isolated from wild-type HEK 293T cells that had been transiently transfected with various HA-RICTOR-deletion constructs. Results from immunoblotting showed that endogenous mSIN1 protein could be immunoprecipitated with either RICTOR-FL or RICTOR-Δ1001-1200 proteins but not the RICTOR proteins lacking either N-terminal or C-terminal regions. Similarly, mTOR and mLST8 were also only detected in the immunoprecipitates of RICTOR-FL or RICTOR-Δ1001-1200 proteins. These results suggest that the interaction between RICTOR and mSIN1 plays a critical role in stabilising mSIN1 as well as mTORC2 assembly (Fig 4.5D). Taken above, these findings demonstrate that the association between RICTOR and mSIN1 might play important role in regulating mSIN1 stability, and the multiple phosphorylation sites (PS region) of RICTOR is dispensable for stabilising mSIN1 expression as well as recovering mTORC2 activity.

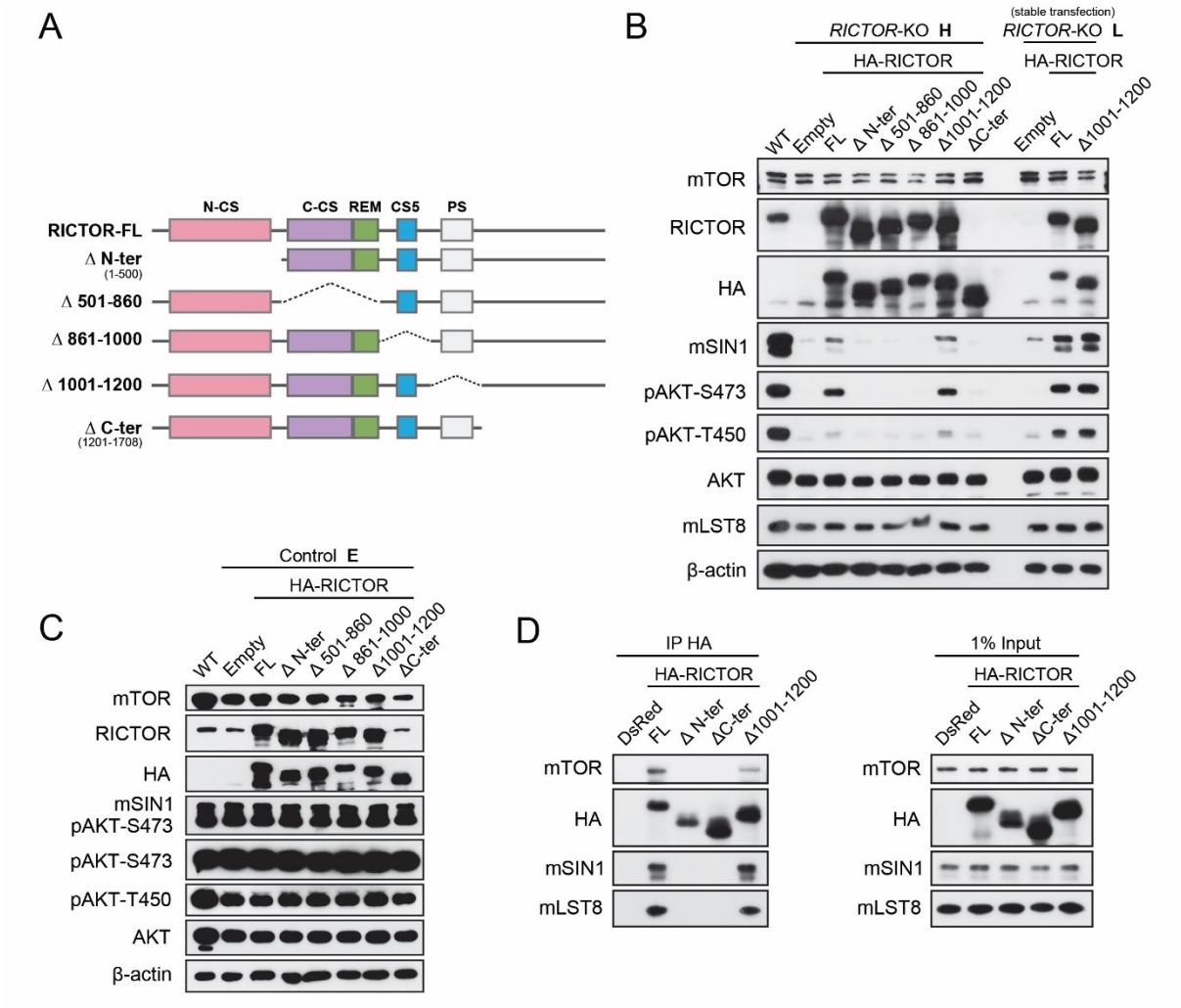


Figure 4.5 The PS region of RICTOR is dispensable for the stabilisation of mSIN1

(A) *Schematics show various RICTOR expression constructs. N-CS = N-terminal conserved domain; C-CS = central conserved region; REM = Ras exchange motif; CS5 = conserved domain 5 and PS = region containing multiple phosphorylation sites.* ***(B, C)*** *Effect of RICTOR mutants in RICTOR-KO 293T cells* ***(B)*** *and control* ***(C)****. Cells were either transiently or stably transfected with indicated vectors then lysed for immunoblotting with indicated antibodies. Representative images from two independent experiments.* ***(D)*** *Immunoblotting analysis of whole-cell lysate (1% Input) and anti-HA immunoprecipitates (IP HA) derived from different HA-RICTOR mutants transfected wild-type 293T cells. The empty vector (HA-DsRed) was used as a negative control. Representative images from one experiment.*

To study whether mSIN1 stability is simply dependent on RICTOR-mSIN1 interaction and to identify which part of mSIN1 plays a role in the regulation by RICTOR, I expressed the three naturally occurred human mSIN1 protein isoforms (mSIN1.1, 1.4 and 1.5) into *RICTOR*-KO and control 293T cells. The mSIN1.1 isoform is a full length mSIN1 protein, while mSIN1.4 lacks the N-terminal region and mSIN1.5 does not contain C-terminal PH domain (Frias et al., 2006; Schroder et al., 2004). According to the previous studies, if the interaction between RICTOR and mSIN1 was the sole factor for mSIN1 stability, I assumed that the expression of mSIN1.4 isoform would not show any difference between control and *RICTOR*-KO cells as the N-terminal region of mSIN1 is mainly responsible for the RICTOR-mSIN1 interaction (Cameron et al., 2017; Liu et al., 2013; Yao et al., 2017). Thereby, plasmids which expresses myc-tagged mSIN1.1, mSIN1.4 and mSIN1.5 were transfected into both control and *RICTOR*-KO cells and their expression were examined by immunoblotting (Fig 4.6A). The results clearly showed that all three mSIN1 isoforms, including mSIN1.4, were detected at lower levels in *RICTOR*-KO cells than that in controls (Fig 4.6B). Since both control and *RICTOR*-KO cells have similar transfection efficiency as confirmed by the expression of EGFP, these results suggest that RICTOR might have a function to stabilise all three isoforms. Collectively, my findings indicate that the stabilisation of mSIN1 might not exclusively dependent on RICTOR-mSIN1 interaction, other factors may also be involved.

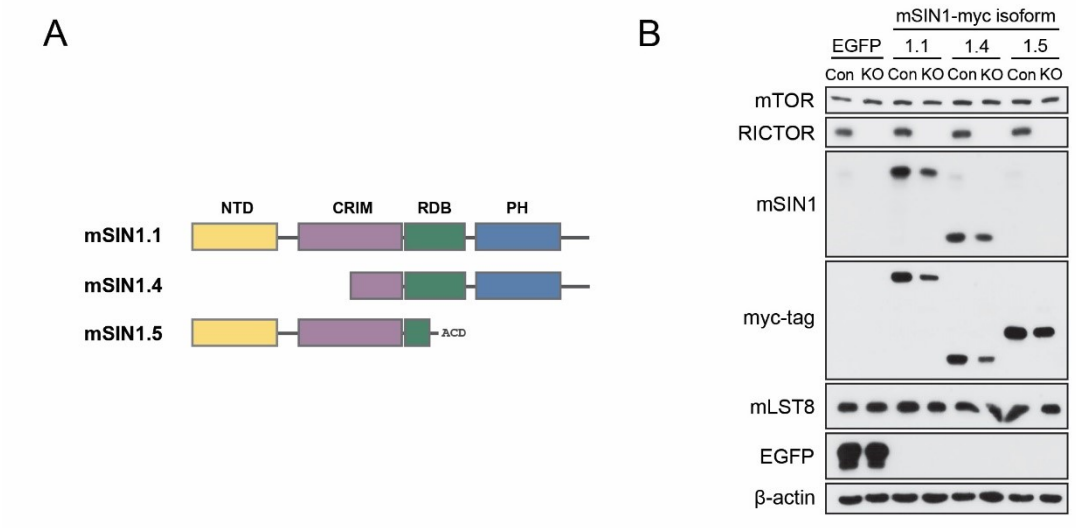


Figure 4.6 RICTOR/mTORC2 may have dual roles in stabilising mSIN1

(A) *Schematic of different mSIN1 isoforms. NTD = N-terminal domain; CRIM = conserved region in middle; RBD = Ras-binding domain and PH = pleckstrin homology like domain.* ***(B)*** *Immunoblotting with indicated antibodies of whole-cell lysate derived from control and RICTOR-KO cells that transfected with different myc-tagged mSIN1 isoforms. Representative images from two independent experiments.*

4.2.5 The mTORC2-mediated phosphorylation of mSIN1-Ser260/270 plays a role in mSIN1 stability

Interestingly, by introducing RICTOR back into *RICTOR*-KO cells, a slower migratory form of mSIN1 could only be detected in the presence of RICTOR/mTORC2 (Fig 4.7A). As mTOR is a well-known kinase and mSIN1 has been reported as a substrate of mTOR (Chen and Sarbassov dos, 2011; Saxton and Sabatini, 2017), it is likely that mTORC2-mediated phosphorylation of mSIN1 may be another factor that will regulate the stability of mSIN1. Since the expression level of all three isoforms (mSIN1.1, 1.4 and 1.5) were affected by *RICTOR*-deficiency, it is plausible that the mTORC2-associated phosphorylation might target the common region shared by all three isoforms. Notably, this common region contains approximately 128 amino acids (aa193-320 of Q9BPZ7), which constitutes the C-terminal part of the CRIM domain and the N-terminal region of RBD (Fig. 4.7B). Given the importance of CRIM domain in mSIN1 and the C-terminal region of the CRIM domain contains a PEST (proline (P), glutamic acid (E), serine (S), and threonine (T)) sequence that acts as a signal peptide for protein degradation (Rogers et al., 1986; Tatebe et al., 2017), I further focused on the C-terminal CRIM region (aa193-277) of mSIN1. A search in the public available dataset, PhosphoSitePlus® (PSP) (Hornbeck et al., 2015), revealed that two potential phosphorylation residues in this region are serine 260 and 270. To characterise the effect of Ser260 and Ser270 phosphorylation in the stabilisation of mSIN1, a series of Flag-tagged mSIN1 mutation or deletion (Δ260-270) expression constructs were generated. The serine residues at position 260 and 270 were individually converted to phosphomimetic aspartic acid (Asp, D) or non-phosphorylatable alanine (Ala, A) residues using site directed mutagenesis as illustrated in Figure 4.7B.

The deleted or point-mutated variants of Flag-mSIN1 were ectopically expressed in both wild-type (WT) and *RICTOR*-KO cells and their expression were examined by immunoblotting. It showed that the individual phosphomimetic mutant of mSIN1 (S260D or S270D) slightly increased protein expression compared to the wild-type mSIN1 in the absence of RICTOR, whilst the expression of mSIN1 protein levels were significantly increased by the co-substitution of both residues to the phosphomimetic (S260/270D, SD) and that these differences were not observed in 293T WT cells (Fig. 4.7C). On the other hand, deletion of

the region from S260 to S270 (Δ260-270), or phosphodefective mutants (S260/270A, SA) of mSIN1 showed similar expression levels as that of mSIN1-WT in *RICTOR*-KO cells. Thus, these data have implied that apart from the interaction between RICTOR-mSIN1, the mTORC2-associated phosphorylation may also affect the stability of mSIN1, and this stabilisation was found to depend on the phosphorylation status of Ser260 and Ser270, which located in its CRIM domain.

Since the phosphorylation of mSIN1-Ser260/270 has been shown above to clearly affect mSIN1 expression, I hypothesised that this phosphorylation may directly suppress the ubiquitin-proteasome-mediated degradation of mSIN1 to stabilise the protein. To validate my hypothesis, I performed *in vivo* ubiquitination assay to analyse the ubiquitination status on these mSIN1 mutants. Different Flag-mSIN1 mutants together with HA-tagged ubiquitin vector were co-transfected into *RICTOR*-KO 293T cells, and the EGFP vector was used as a negative control. The transfected cells were treated with the proteasome inhibitor MG132 for 3 hours before the cell lysates were collected. The whole-cell extracts were then subjected to immunoprecipitate with anti-Flag M2 agarose beads and followed by immunoblotting with anti-ubiquitin (Fig 4.7D). The analysis from immunoblotting revealed that the phosphomimetic mutants of mSIN1 (S260/270D, SD) led to decreased ubiquitination, whereas the phosphodefective mSIN1 (S260/270A, SA) showed a slightly higher level of ubiquitination than that of mSIN1-WT. This analysis suggests that under the condition of *RICTOR*-deficiency, mSIN1 is degraded faster when the two potential phosphorylation sites are both replaced with alanine, while the ubiquitin level of mSIN1 can be suppressed with a serine to aspartic acid substitution at both position 260 and 270.

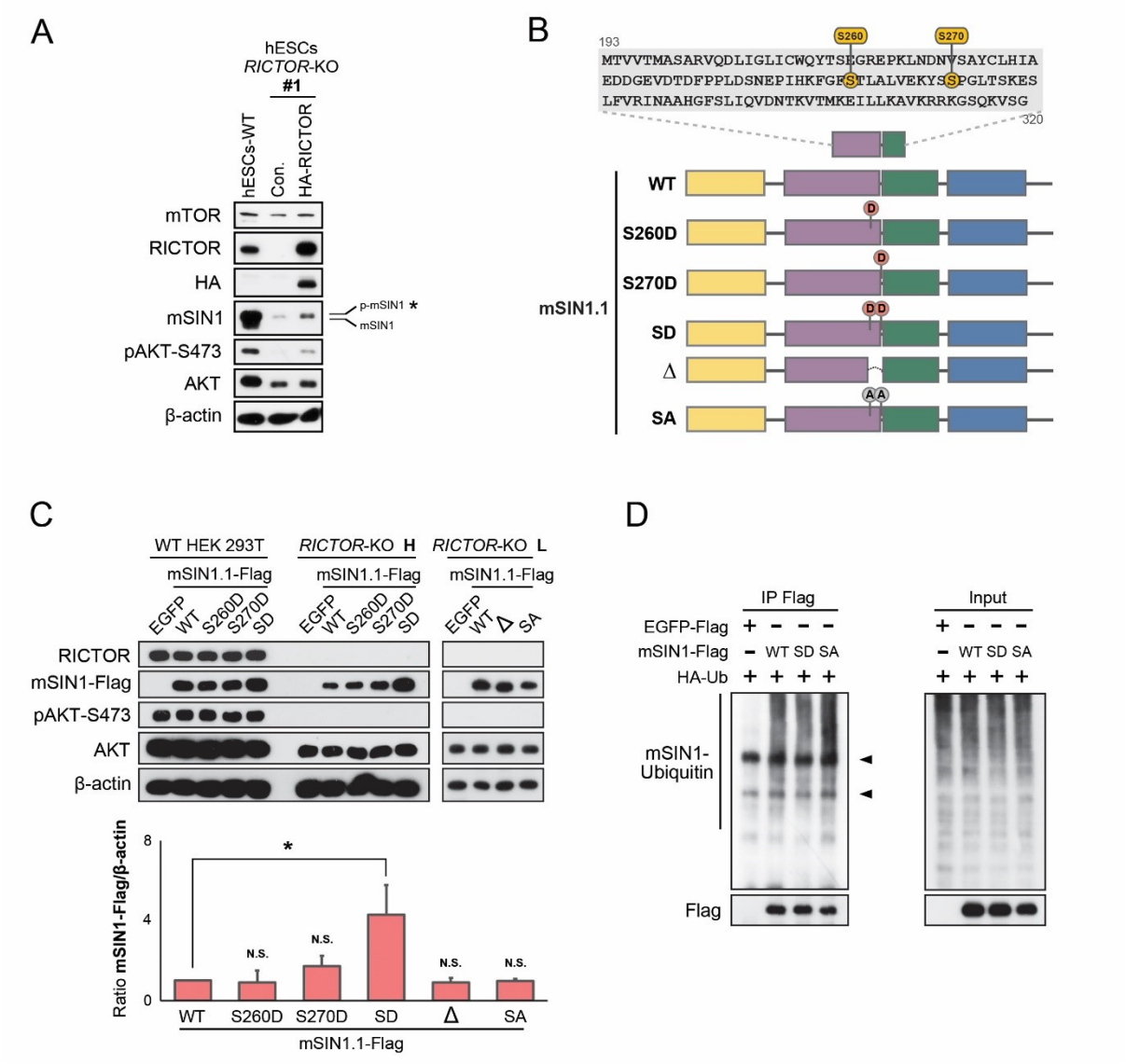


Figure 4.7 The phosphomimetic mutants of mSIN1 at S260D and S270D overcomes the instability of mSIN1 in RICTOR-KO cells

(A) *RICTOR-KO hESCs were transiently transfected with HA-RICTOR, followed by immunoblotting with indicated antibodies. Cells transfected with empty vector (HA-DsRed) were used as negative control.* ***(B)*** *Schematic of different mSIN1 mutated variants. S = serine; D = aspartic acid and A = alanine.* ***(C)*** *Different Flag-tagged mSIN1 mutation constructs were transiently transfected into wild-type and RICTOR-KO 293T cells, respectively. The total cell lysates were collected and analysed by immunoblotting with indicated antibodies* ***(top)*** *and the expression levels of mSIN1-Flag are represented as bar chart* ***(bottom)*** *(*p<0.05, n = 3). Representative images from three independent experiments.* ***(D)*** *RICTOR-KO cells were transfected with indicated vectors and treated with MG132. The cell lysates were then subjected to IP by using Flag M2-agarose beads and immunoblotting as indicated. Black arrows indicate the heavy chain of the Flag-IgG used for immunoprecipitation. Representative images from two independent experiments.*

4.2.6 Phosphorylation of mSIN1-S260/270 may differentially regulates PKCα phosphorylation

Since the phosphorylation status of serine 260 and 270 on mSIN1 has profound effect on its stability in *RICTOR*-KO cells but not in the presence of RICTOR, it is difficult to conclude that these phosphorylation have a pivotal role in mSIN1 stability due to the close association of RICTOR and mTORC2. Thus, a crucial question is whether these seine phosphorylation on mSIN1 protein has any effect on mSIN1 function and mTORC2 signalling pathway. Hence, I first inspected whether the phosphorylation of mSIN1 affects the expression of other components in mTORC2 complex. Different variants of Flag-mSIN1 were individually transfected into both WT and *mSIN1*-KO 293T cells, and the whole cell lysate was extracted and analysed by immunoblotting with different mTORC2 subunits' antibodies. Results from immunoblotting analysis showed that neither phosphomimetic (SD) nor phosphodefective (SA) mutant of mSIN1 altered the expression levels of other mTORC2 members (mTOR, RICTOR and mLST8) (Fig 4.8A). Next, I investigated whether phosphorylation of mSIN1-S260/270 plays a role in mTORC2 assembly. To determine the association with mTORC2 complex, wild-type or different mutants Flag-tagged mSIN1 were ectopically expressed in *mSIN1*-KO 293T cells, and anti-Flag immunoprecipitates were analysed for co-precipitation of other members in mTORC2 complex by immunoblotting. All the core components of mTORC2 were shown in the Flag-mSIN1 immunoprecipitates even with the deletion of S260-S270 region although the affinity might be varied, whereas no specific co-precipitated was detected in the EGFP negative control (Fig 4.8B). The results may indicate that the all three mSIN1 mutants could be successfully incorporated into the endogenous mTORC2 that could be validated by further experiments.

Since mSIN1 is known as a selective adaptor for mTORC2 to target its substrates (Cameron et al., 2011; Kataoka et al., 2015; Tatebe et al., 2017) and it have also been shown that different mSIN1 isoforms may form distinct mTORC2 complexes which have diverse response to upstream stimulations (Frias et al., 2006; Yuan et al., 2015). Therefore, to gain further insight into the functional role of these residues, I evaluated whether the phosphorylation status of mSIN1 on serine 260 and 270 has any impact on substrate specificity of mTORC2. *mSIN1*-KO 293T cells were transiently overexpressed with wild-type and different mutant

forms of mSIN1, including mSIN1-S260/270D (SD), mSIN1-S260/270A (SA) and mSIN1-Δ260-270 (Δ). At the time point 48 hours post-transfection, cells were lysed in RIPA buffer and the whole-cell lysates were resolved by SDS-page and immunoblotted with different mTORC2 downstream targets antibodies. Results from immunoblotting showed that all the mSIN1 variants, except mSIN1-Δ260-270 (Δ), were able to phosphorylate hydrophobic motif of AKT (AKT-Ser473), while the phosphorylation of turn motif, AKT-Thr450, could be detected in all variants, including mSIN1-Δ260-270 (Δ) (Fig 4.8C). Interestingly, mSIN1-S260/270D (SD) and mSIN1-S260/270A (SA) exhibited a differential phosphorylation pattern at the hydrophobic motif Ser657 of PKCα, in which only mSIN1-S260/270D (SD) showed a similar level of phosphorylation on PKCα-Ser657 as mSIN1-WT, whereas mSIN1-S260/270A (SA) showed lower levels of such phosphorylation. However, both of mSIN1 mutants were able to phosphorylate PKCα turn motif (PKCα-Thr638), while mSIN1-Δ260-270 (Δ) showed lower phosphorylation on both PKCα-Ser657 and Thr638 (Fig 4.8C). Taken together, these data indicated that the phosphorylation status of mSIN1-S260/270 might have important functional roles in the mTORC2 substrate recognition.

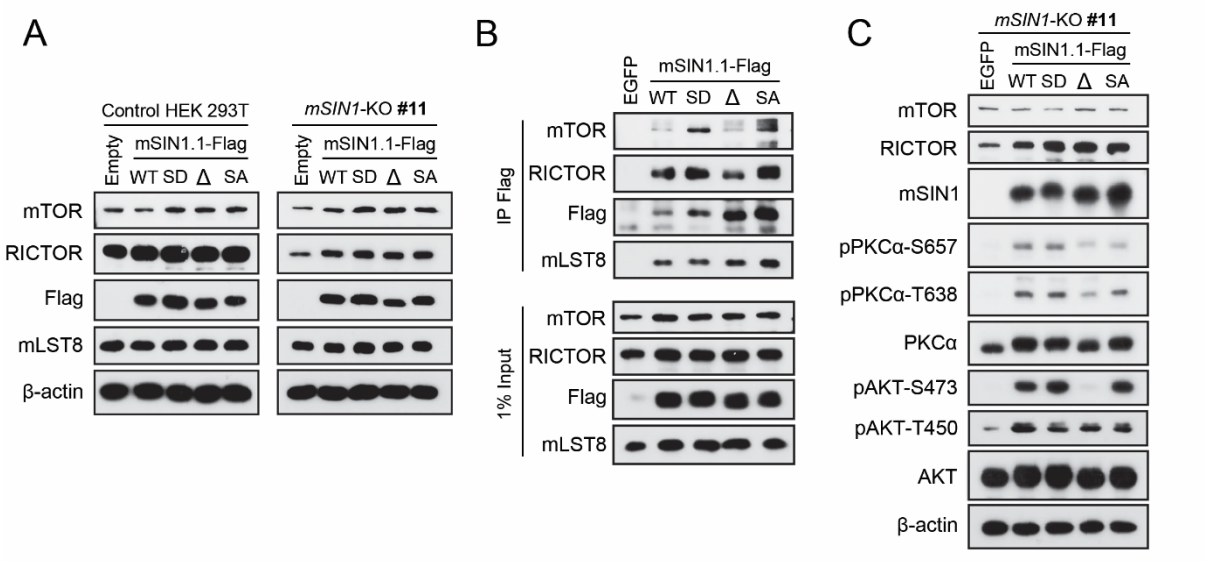


Figure 4.8 Phosphorylation of mSIN1 at S260/270 are required for PKCα-S657 phosphorylation

(A) *Control and mSIN1-KO cells were transiently transfected with indicated vectors and analysed by immunoblotting with indicated antibodies.* ***(B)*** *Immunoblotting analysis of whole-cell lysate (1% Input) and anti-Flag immunoprecipitates (IP Flag) derived from different mSIN1-Flag mutants transfected mSIN1-KO 293T cells. The empty vector (EGFP) was used as a negative control.* ***(C)*** *Different Flag-tagged mSIN1 mutation constructs were transiently transfected into mSIN1-KO 293T cells, respectively. Total cell lysates were then collected and analysed by immunoblotting with indicated antibodies. Representative images from two independent experiments.*

4.3 Conclusions and Discussion

To clarify the biological function of RICTOR/mTORC2 in human cells, in this chapter, I utilised *RICTOR*-KO HEK 293T cells to uncover the key roles played by RICTOR in the regulation of cell properties, mTORC2 complex stability and functions.

RICTOR is a core subunit of mTORC2 and it is required for mTORC2 assembly and activity. At the beginning of this chapter, I demonstrated that depletion of *RICTOR* in HEK 293T cells abolished the activity of mTORC2 but not mTORC1 (Fig 4.1A). The diminished activity of mTORC2, especially with the lack of AKT-Ser473 phosphorylation, might account for the decrease in the proliferative capabilities and the increase in cell apoptosis (Fig 4.2C). The functional roles of AKT have been mainly associated with the regulation of cell proliferation and apoptosis. Previous studies have reported that AKT promotes G1/S transition via directly phosphorylating its downstream substrates, such as GSK-3β and FOXOs. The phosphorylation of GSK-3 at Ser9 by AKT prevents the degradation of cyclin D1 while the AKT-mediated cytoplasmic-distribution of FOXOs decreases the transcriptional level of cyclin-dependent kinase (CDK) inhibitor, $p27^{KIP1}$ (Alao, 2007; Farhan et al., 2017; Huang and Tindall, 2007). Therefore, whether the reduced cell proliferation in *RICTOR*-KO cells is a consequence of cell cycle arrest, and whether the cell proliferation rate in *RICTOR*-KO cells can be rescued by the overexpression of phosphomimetic mutant of AKT (AKT-S473D) required to be evaluated. Interestingly, the deficiency of AKT-Ser473 phosphorylation could be detected in both *Rictor*- and *mSin1*-KO MEF cells and that the phosphorylation of AKT-Ser473 acts principally to control cell proliferation (Manning and Cantley, 2007; Song et al., 2005), one would expect that both *Rictor*- and *mSin1*-KO cells would show reduced cell proliferation. However, previous study revealed that the significant reduction in cell proliferation was only observed in the cells with loss of *Rictor* but not *mSin1* under routine culture conditions (Jacinto et al., 2006). Given that mSIN1 was firstly described as an associated protein that is involved in cellular stress response pathways (Alexandropoulos and Baltimore, 1996). Thus, it might be possible that the role of AKT-Ser473 phosphorylation in *mSin1*-KO MEF is mainly involved in regulating cell survival rather than cell proliferation.

I have demonstrated that RICTOR preserves the complex stability by stabilising another critical mTORC2 subunit, mSIN1. This is supported by the observation that the protein expression levels, but not mRNA levels, of mSIN1 was substantially diminished upon *RICTOR*-deficiency whilst the other subunits remained unaffected (Fig 4.3A and C). Several experimental studies have provided evidence that mSIN1 is an unstable protein upon dissociation from RICTOR/mTORC2 (Frias et al., 2006; Jacinto et al., 2006). However, other factors could also modulate mSIN1 stability as deletion of *RICTOR* resulted in an unstable mSIN1.4 in addition to mSIN1.1 and 1.5 (Fig 4.6B), indicating that the common region shared by different mSIN1 isoforms might contain sequences or residues that are required for their stabilisation. The phosphorylation of mSIN1 at Ser260 was previously reported to be done by mTOR, which maintains mSIN1 stability and enhances the activity of mTORC2 (Chen et al., 2013). However, it did not clearly identify which mTOR complex perform this. Here, I have found that both Ser260 and Ser270 of mSIN1 can be phosphorylated and that this dual-phosphorylation at Ser260/270 within the CRIM domain of mSIN1 led to a marked increase in mSIN1 expression levels (Fig 4.7C). Furthermore, these phosphorylation are very likely performed by mTORC2 itself, albeit further validation is required for this. Thus, my results strongly suggest that RICTOR might have dual but related functions to collaboratively stabilise mSIN1 protein: a direct binding-partner of mSIN1 and an essential factor of mTORC2 that phosphorylates mSIN1 via mTOR kinase. Further experiments, such as *in vitro* kinase assay, are necessary to validate this observation and confirm that mTORC2 is indeed able to phosphorylate mSIN1-Ser260/270. Moreover, the contribution of RICTOR/mTORC2 in mSIN1 degradation pathway still unclear as the results obtained from *RICTOR*-KO 293T cells showed that RICTOR prevents endogenous mSIN1 from proteasome-mediated degradation (Fig 4.4D), whereas other indicated that the regulation of protein expression of exogenous mSIN1 was controlled by lysosomal degradation in WT 293T cells (Chen and Sarbassov dos, 2011). One of the explanations of this contradictory observation in mSIN1 degradation pathways is that the endogenous and exogenous mSIN1 protein might possibility be degraded through different mechanisms in 293T cells.

As part of the mTORC2 complex, mSIN1 has been demonstrated to function as a substrate-adaptor for mTORC2 by physically interacting with the downstream targets through its CRIM domain (Cameron et al., 2011; Lu et al., 2011; Tatebe et al., 2017). On the other hand,

previous researches also suggested that the post-translational modifications such as phosphorylation of mSIN1 mediates the formation and regulates the function of mTORC2 complex (Chen et al., 2013; Liu et al., 2013; Yang et al., 2015). Here, I identified that the different phosphorylation status, or even deleted, of these two serine residues on mSIN1 (Ser260 and Ser270) did not dramatically affect the assembly of mTORC2 but might alter its activity (Fig 4.8B and C). mSIN1 with a small deletion on its CRIM domain (Δ260-270) abolished the mTORC2-mediated AKT-Ser473 phosphorylation, whereas mSIN1 with non-phosphorylatable alanine mutants (S260/270A, SA) formed a partially functional mTORC2 complex and selectively restored the phosphorylation at the hydrophobic motif (HM) of AKT (Ser473) but not PKCα (Ser657). Thus, my results suggest that mTORC2 may have an auto-regulatory function which might affect its substrate selection. Recently, it has been reported that a single amino acid (Q68) mutation or subcellular localisation of mSIN1 could specifically affect the phosphorylation of another mTORC2 substrate, SGK1 at its HM motif (Gleason et al., 2019; Lu et al., 2011). Conclusively, it appears that different mechanisms are used by mTORC2 for regulating the phosphorylation of its downstream substrates at HM motifs. Therefore, it will be interesting to investigate whether the phosphorylation status of these two residues (Ser260/270) on mSIN1 plays any roles in the RICTOR/mTORC2-dependent activation of SGK1.

Taken together, the results from this chapter show that the *RICTOR*-KO HEK 293T cells, which were generated via CRISPR-Cas9 system, present a great cell resource for the study of RICTOR/mTORC2 from cellular functions to molecular mechanisms. With these cells, the relationship between RICTOR and mSIN1 has been highlighted, which supports the idea that both RICTOR and mSIN1 are required for the assembly and function of mTORC2. RICTOR stabilises mSIN1 to prevent it from proteasome-mediated degradation by protein interaction and mTOR-mediated phosphorylation in mSIN1-CRIM domain. Notably, this auto-regulatory controlling mechanism of RICTOR/mTORC2 not only stabilises mSIN1 but may further affect mTORC2 substrate specificity.

05

Effect of mTORC2 signalling-deficiency on human embryonic stem cell properties

5.1 Introduction

Signalling transduction plays an essential role in embryogenesis, which controls not only the axis formation in the embryo but also the differentiation of various cell types. Several signalling pathways have been well characterised for their roles in embryogenesis, such as TGFβ/BMP, WNT and FGF (Zhao and Jin, 2017). Although limited studies were performed in an attempt to reveal the function of mTORC2 signalling in embryonic development, it has been shown that the RICTOR/mTORC2 signalling has vital functions in mouse developmental processes. Germline deletion of either *Rictor* or *mSin1* exhibited embryonic lethality at mid-gestation, which was thought as a result of cardiovascular defect (Guertin et al., 2006; Jacinto et al., 2006; Shiota et al., 2006). However, the underlying mechanisms of its role in embryonic development remain elusive, especially in human development because of the ethical issues associated with the use of human embryos. Given that embryonic stem cells (ESCs), including human ESCs (hESCs), have the properties of unlimited self-renewal and pluripotent differentiation and that their pluripotent features resemble that of the early embryos, these cells thus provide a great cell resource that can be used to study the function and molecular mechanism of RICTOR/mTORC2 in human embryo development.

To date, little information is available regarding the specific function of RICTOR/mTORC2 signalling in the regulation of hESC self-renewal and pluripotency. The limited data on mTOR signalling in hESCs showed conflicting results: one of the studies indicated that mTOR has a positive role in maintaining self-renewal of hESCs, whereas others suggested that mTOR-mediated activation of S6K1 negatively regulates pluripotency-associated genes which further induces differentiation (Easley et al., 2010; Zhou et al., 2009). Notably, previous studies showed that treating hESCs with rapamycin appears to enhance marked differentiation to mesendodermal lineages, which was thought to result from inhibition of mTORC1 (Jung et al., 2016; Nazareth et al., 2016). However, this treatment might also inhibit mTORC2 signalling as the application of rapamycin lasted over several days. Thus, it is difficult to dissect the contribution of individual mTOR complexes. On the other hand, results from mESCs with genetic modification approaches suggested that dysfunction of mTORC2 resulted in a defective mesoderm specification (Gomez-Salinero et al., 2016; Li et al., 2018). As there is no specific inhibitor for mTORC2 and the complexity of signalling crosstalk between the two

mTOR complexes, it still remains unclear that whether RICTOR/mTORC2 signalling is required for hESCs maintenance and whether the *mTORC2*-deficient hESCs have different propensity in lineage-specification. Hence, to advance our understanding, it is necessary to distinguish the individual effects of these two complexes in hESC self-renewal and differentiation.

Previously in our lab, RICTOR-knockdown hESCs were generated, which did not exhibit a clear effect on hESC-morphology although the proliferation was reduced (Yu et al., 2015). However, these cells are not suitable for differentiation studies because of the silencing of the shRNA in these cells, particularly during differentiation as a result of dramatic epigenetic remodelling (Hu and Rosenfeld, 2012). Thus, in this chapter, I utilised *RICTOR*-KO hESCs, which I have established by CRISPR-Cas9 system, as my cell model to explore the functions of RICTOR/mTORC2 in regulation of hESC self-renewal/pluripotency and differentiation.

5.2 Results

5.2.1 RICTOR/mTORC2 is dispensable for the maintenance of self-renewal/pluripotency in hESCs

To examine the effects of RICTOR interruption on self-renewal and differentiation of hESCs, two individual *RICTOR*-KO hESCs clones (clone #1 and #5) were selected for the following characterisation. Under routine MEF-CM culture conditions on matrigel, *RICTOR*-KO hESCs were generally indistinguishable in their morphology from control and parental wild-type (WT) hESCs (Fig 5.1A). *RICTOR*-KO hESC clones displayed typical hESC morphology features, including large nuclei and scant cytoplasm. Although there is no dramatic change in their morphology, the colonies formed by *RICTOR*-KO cells exhibited a relatively loose and flattened structure in the centre. To investigate these cells for their pluripotency status, several stemness markers were examined by qRT-PCT and immunoblotting. RNA expression analysis showed that both OCT4 and NANOG mRNAs were expressed at similar levels between WT controls and *RICTOR*-KO hESCs, while the expression of SOX2 in two *RICTOR*-KO clones exhibited a slightly higher level than the WT controls (Fig 5.1B). Consistently, the protein expression of OCT4 was similar to WT controls as that in the *RICTOR*-KO hESCs, whilst SOX2 protein revealed a higher expression in the *RICTOR*-KO hESCs (Fig. 5.1C). Notably, my results showed that the disruption of *RICTOR* resulted in a considerable downregulation of REX1 mRNA (also known as ZFP42) expression (Fig 5.1B).

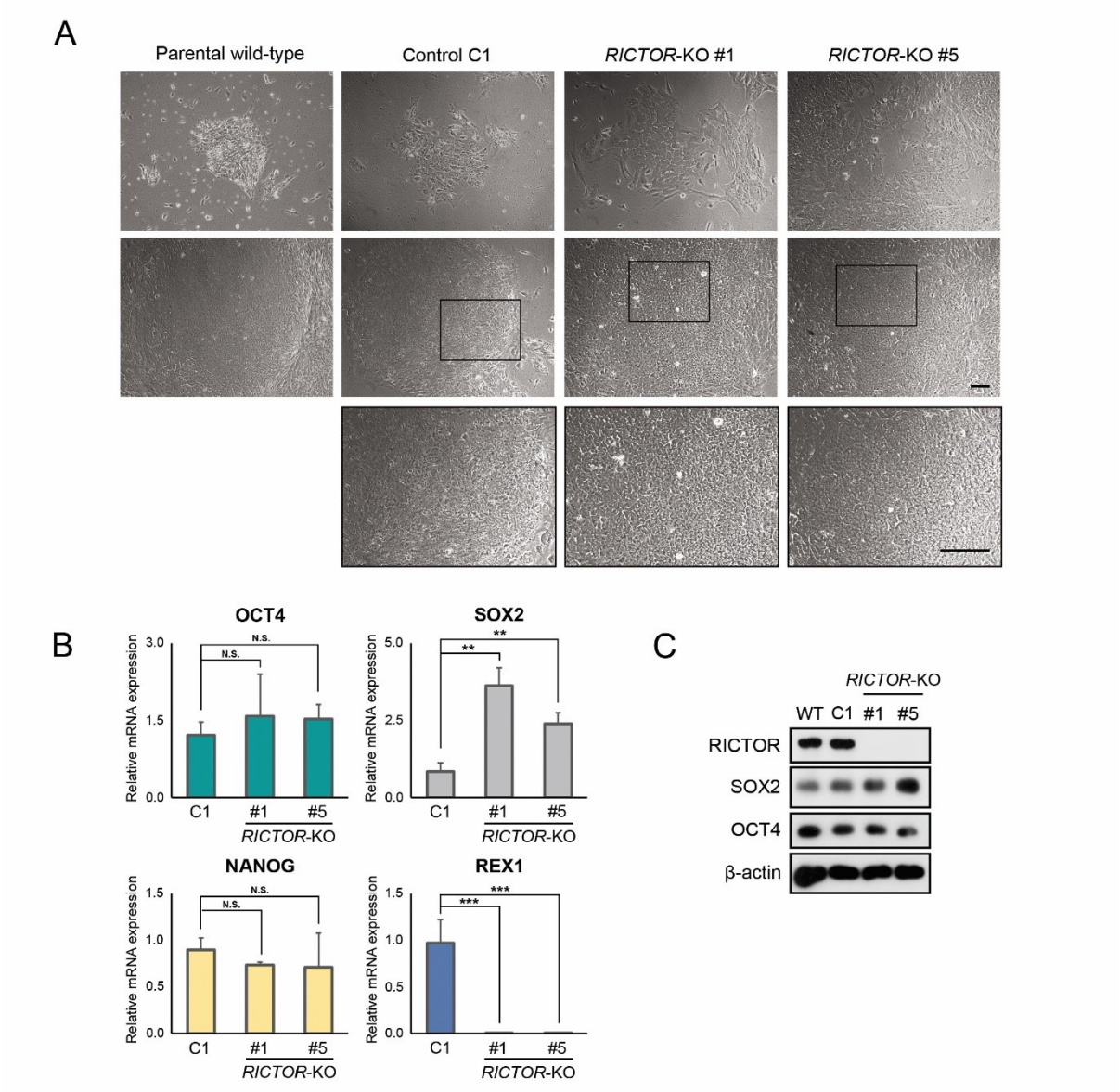


Figure 5.1 RICTOR/mTORC2 is not necessarily required for hESC self-renewal

(A) *Representative phase-contract images of parental WT, control C1 and RICTOR-KO hESCs. Scale bar, 100μm.* ***(B)*** *qRT-PCR analysis of pluripotency-related genes mRNA expression in control C1 and RICTOR-KO clones. Data are represented as the means ± SD (n = 3) relative to the C1 (**p<0.01, ***p < 0.001 by two-tail unpaired t-test).* ***(C)*** *Immunoblotting analysis of WT, control C1 and RICTOR-KO hESCs clones (clone #1 and #5) with indicated antibodies. Representative images from three independent experiments.*

To further validate the expression of the core pluripotency markers in *RICTOR*-KO hESCs, immunostaining was performed in these cells for OCT4 and SOX2 expression (Fig 5.2A). As expected, in WT controls, the expression of OCT4 was clearly positive in the undifferentiated cells but not in those spontaneously differentiated WT hESCs, and high levels of OCT4 and SOX2 were also detected in the majority of the *RICTOR*-KO hESCs. The results obtained from both immunostaining and flow cytometry analysis revealed that the loss of *RICTOR* in hESCs did not alter the proportion of cells expressing these hESC-specific surface antigens (Fig 5.2B and C), including the positively stained of pluripotency markers stage-specific embryonic antigen (SSEA)-4 and tumour-related antigen (TRA)-1-81, and with weak or no expression of the differentiation marker SSEA1. However, the intensity of TRA-1-81 and SSEA-4 expression in *RICTOR*-KO hESCs might be reduced. Given that this experiment was only done once, the results need to be further validated and the impact of this reduction, if consistent, requires further investigation. In addition, a certain percentage of WT and *RICTOR*-KO hESCs were positively stained with the SSEA1 antibody in these cultures, which might be due to spontaneous differentiation occurring in these cultures. As indicated above, since this experiment was only done once, more experiments are required for validation. Taken together, these results indicate that RICTOR/mTORC2 signalling pathway is dispensable for the maintenance of self-renewal in hESCs as ablation of *RICTOR* showed no detectable loss of undifferentiated morphology. Furthermore, established *RICTOR*-KO hESCs maintained their expression of pluripotency markers, except for REX1.

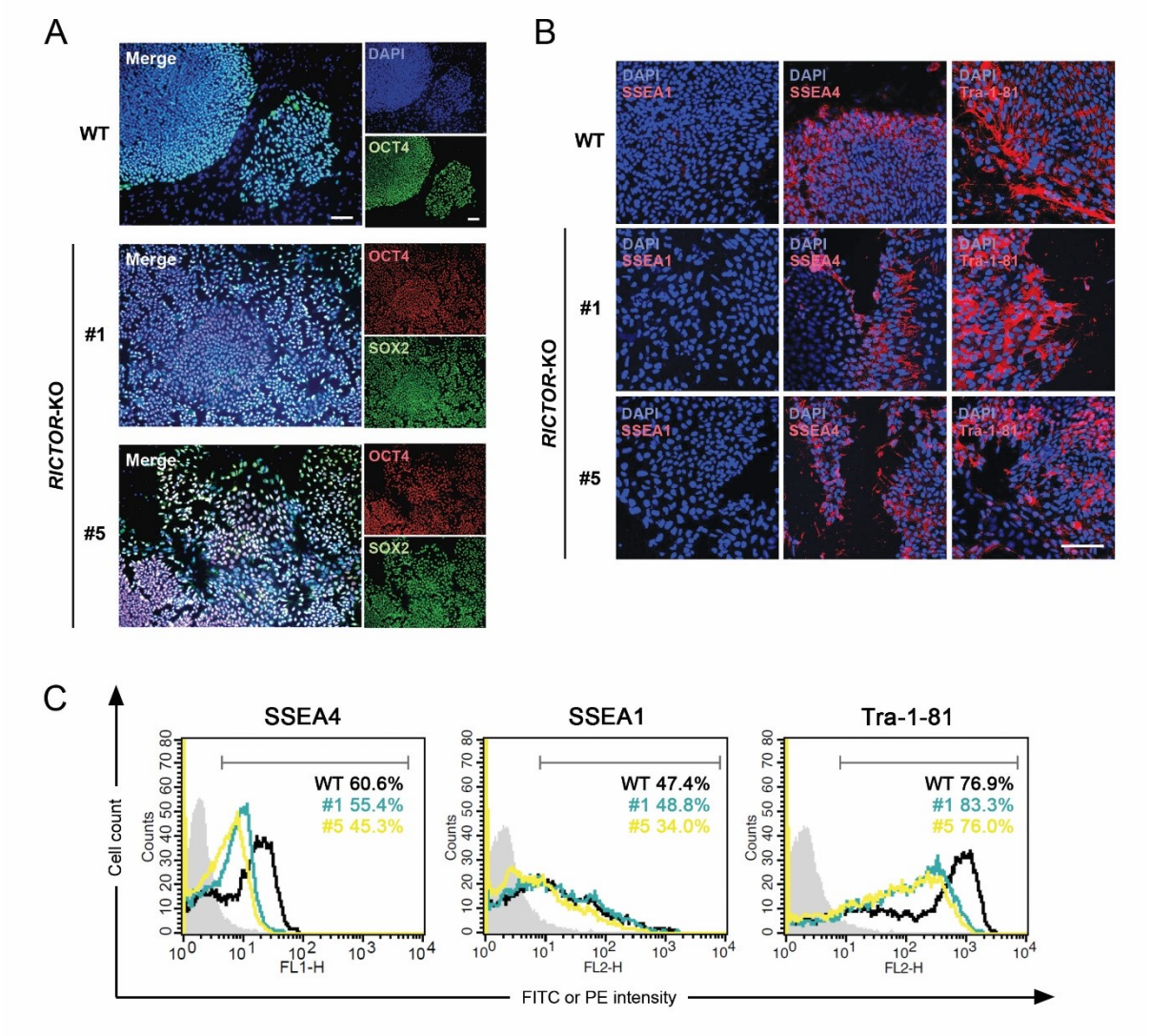


Figure 5.2 hESCs remained undifferentiated after knockout of *RICTOR*

(A) *Immunostaining with indicated antibodies in WT and RICTOR-KO clones. Scale bar, 100μm.* ***(B)*** *Immunofluorescent confocal microscopic analysis for markers (SSEA1, SSEA4 and Tra-1-81) characterising undifferentiated hESCs. Scale bar, 100μm.* ***(C)*** *Flow cytometry analysis of SSEA1, SSEA4 and Tra-1-81 expression in WT and RICTOR-KO clones. Grey solid filled represent the isotype controls; black lines represent WT; green lines represent RICTOR-KO clone #1 and the yellow line represent RICTOR-KO clone #5. For each histogram the positive gate (grey bar) was set for inclusion of 3% of the isotype.*

5.2.2 RICTOR/mTORC2 signalling pathway might be required for the conversion of primed hESCs to naïve state via 5iLAF

Although there is no clear change in the expression of the pluripotency factors OCT4 and NANOG in *RICTOR*-KO hESCs, the deficiency of *RICTOR* was accompanied by the significantly downregulated expression of REX1 at mRNA level in hESCs. Given that reduced REX1 expression has been reported in hESCs upon exiting from the naïve state, and further decreased upon differentiation (Eiges et al., 2001; Lee et al., 2013; Li et al., 2018; Rogers et al., 1991), REX1 has been used as a strong indicator for the successful conversion from primed-to-naïve state of hESCs (Nichols and Smith, 2009; Warrier et al., 2017). In addition, genome-wide expression analysis suggested that the PI3K/AKT/mTOR-signalling pathway facilitates the naïve sate in hESCs, particularly mTORC2 activity (Mathieu et al., 2019; Warrier et al., 2017). Therefore, to functionally identify the potential role of RICTOR/mTORC2 in hESCs' pluripotency, I asked whether the lack of RICTOR/mTORC2 activity affects the conversion of primed hESCs to the naïve state.

The primed-to-naïve conversion of hESCs can be achieved by either modifying culture conditions or genetic manipulation. Multiple research groups have established transgene-independent induction methods implicate in different cell culture media with specific combinations of cytokines or small molecules (Chan et al., 2013; Duggal et al., 2015; Gafni et al., 2013; Guo et al., 2016; Theunissen et al., 2014; Ware et al., 2014). In our lab, we utilised 5iLAF (inhibitors for MEK, GSK3, SRC, BRAF and ROCK, and growth factors LIF, Activin, and bFGF) culture conditions to convert the primed hESCs to the naïve state. Therefore, I plated the same numbers of WT and *RICTOR*-KO hESCs onto the feeder layer of inactivated mouse embryonic fibroblast (iMEFs) and cultured them with CM, which was similar to the routine hESC culture. Two days later, CM was replaced with 5iLAF medium and the medium was exchanged daily (Fig 5.3A). In WT hESCs, the application of 5iLAF medium led to a large amount of cell death within 48 hours, and then a small number of dome-shaped naïve hESC colonies started to emerge around day 10-12. By contrast, the two *RICTOR*-KO clones underwent massive cell death within 2 days after culturing with the 5iLAF medium and hardly any cells survived. By day 6, only the iMEFs could be observed in the tissue culture plates under the microscope (Fig 5.3B). Gene expression analysis of the naïve markers, REX1 and

NANOG, showed a clear upregulation at mRNA levels in WT hESCs after conversion to the naïve state, which corroborated with the observation in morphology, indicating the successful conversion of hESCs to naïve state. On the other hand, the loss of *RICTOR*-KO hESCs during the conversion process was supported by the greatly reduced, or even undetectable, expression levels of naïve markers (Fig 5.3C). Altogether, these results suggest that RICTOR/mTORC2 signalling pathway might be important for the conversion of naïve pluripotency state and further investigation are required to validate these results and to explore the underlying mechanisms.

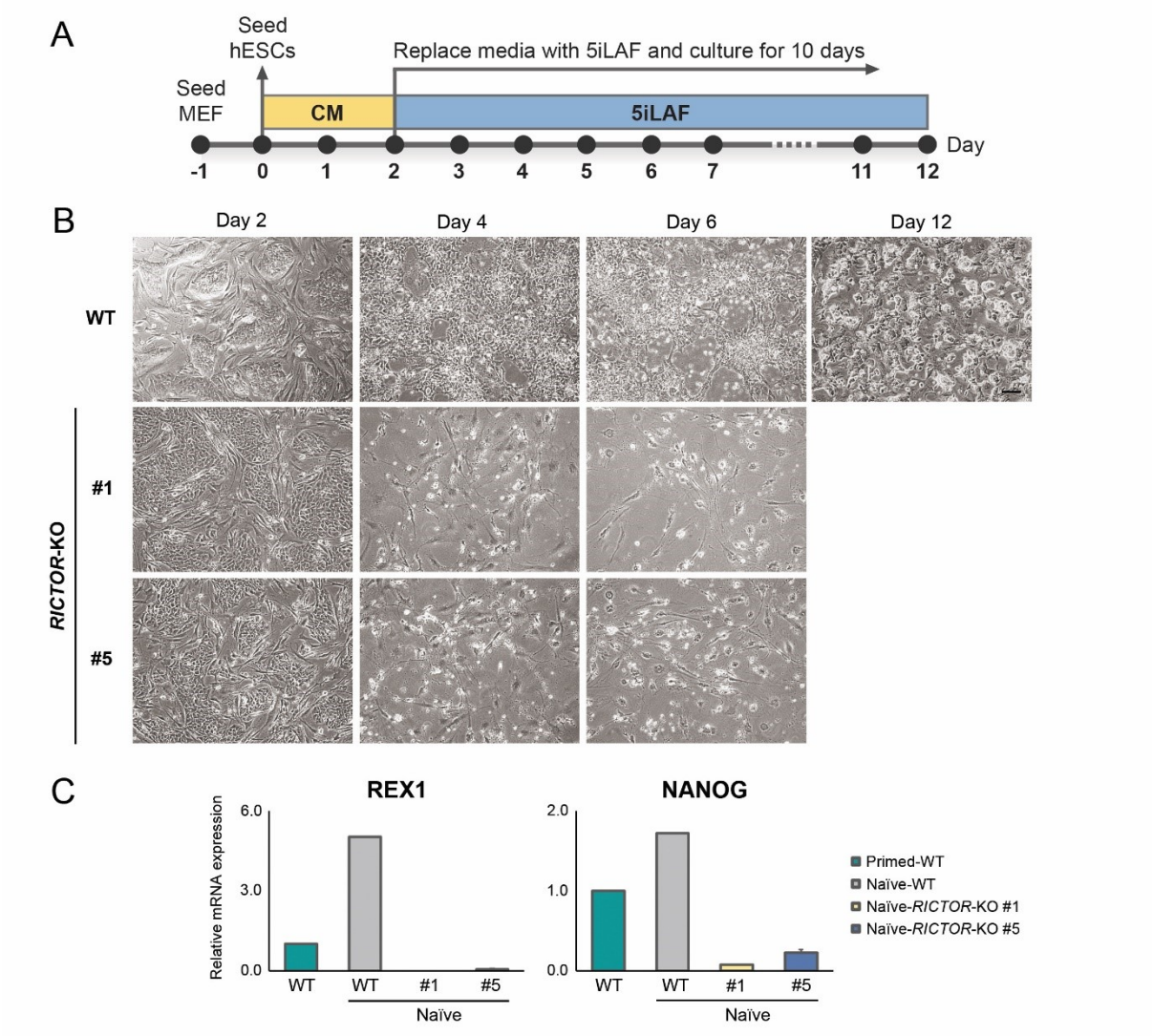


Figure 5.3 *RICTOR*-deficiency affects the transition from primed-to-naïve hESCs

(A) *Schematic diagram for naïve conversion of primed hESCs to naïve hESCs. CM, conditional medium.* ***(B)*** *Representative phase-contract images of hESCs converted from the primed condition (CM) to the naïve condition (5iLAF) for 12 days. Scale bar, 100μm. The WT hESCs conversion pictures are provided by Huihan, Zhi.* ***(C)*** *qRT-PCR analysis of REX1 and NANOG mRNA expression in converted WT and RICTOR-KO hESCs after 12 days naïve conversion. The mRNA level of WT hESCs cultured in CM was used as a control and data are represented relative to the control.*

5.2.3 Deletion of *RICTOR* abolishes mTORC2 activity as well as mSIN1 expression

I next investigated the effect of *RICTOR*-deficiency on the activity of mTOR signalling cascade in order to illustrate a more integrated study of mTOR pathways in hESC properties. The protein expression profile obtained from *RICTOR*-KO hESCs were similar to other different *RICTOR*-KO cell types which I have generated (Fig 4.3 A and B, Fig 5.4A). The deletion of *RICTOR* showed in a considerable reduction in mSIN1 protein expression but not other mTORC2 key components such as mTOR and mLST8. In comparison with WT and control hESCs, *RICTOR*-KO hESCs exhibited only very low, or even undetectable, levels of phosphorylation of AKT on its hydrophobic motif (Ser473) and turn motif (Thr450), but the total amount of AKT remained unchanged. By contrast, a severe reduction of total PKCα expression was detected in both *RICTOR*-KO clones, however, the phosphorylation of PKCα-Ser657, the hydrophobic motif of PKCα, was only reduced in clone #5 but not in clone #1. The immunoblotting also revealed that ablation of *RICTOR* led to a mild increase in the downstream of mTORC1 signalling as shown by phosphorylation of its substrate p70S6K, possibly due to the failure of mTORC2 complex assembly which released the mTOR protein sequestered by mTORC2, and thereby increasing the activity of mTORC1.

Moreover, the Forkhead transcription factor 1 (FOXO1) is known to be one of the downstream targets of AKT in which full activation of AKT is required (Hay, 2011). The phosphorylation of FOXO1 by AKT suppresses its translocation and accumulation in the nucleus, and thereby suppressing its transcriptional activity on its target genes, such as Bim-1 and FasL, genes participated in cell death; p27, gene involved in cell arrest, which then results in enhanced cell survival, growth and proliferation (van den Berg and Burgering, 2011; Zhang et al., 2011a; Zhang et al., 2011b; Zhang et al., 2011c). Immunostaining with anti-FOXO1 antibody revealed that FOXO1 was mostly localised in the cytoplasm in the WT hESCs, whereas FOXO1 was localised predominantly in the nuclei in the *RICTOR*-KO clones (Fig 5.4B). Collectively, these results demonstrate that the expression of RICTOR is required for mTORC2 activity, and loss of RICTOR/mTORC2 is accompanied by the nuclear accumulation of FOXO1 which might further restrict cell proliferation and induce apoptosis.

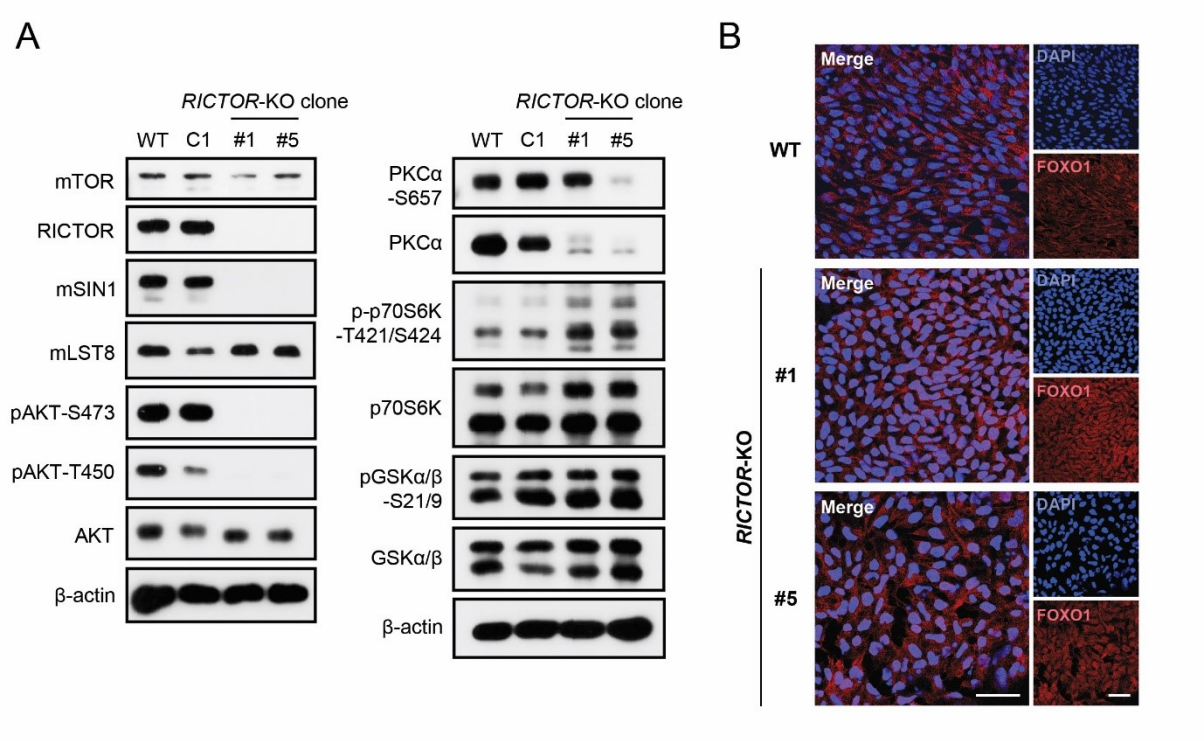


Figure 5.4 *RICTOR*-deficiency diminishes the activity of mTORC2 and affects its downstream signalling cascades in hESCs

(A) *Immunoblotting analysis in WT, C1 and RICTOR-KO hESC clones with indicated antibodies. Representative images from three independent experiments.* ***(B)*** *Fluorescence microscopic analysis of FOXO1 localisation in WT and RICTOR-KO clones. Scale bar, 50μm.*

5.2.4 Disruption of RICTOR/mTORC2 signalling might induce cellular adaptation in hESCs

During the isolation and initially expansion/culture of *RICTOR*-KO hESC clones, an obviously slow growth rate was observed in these cells as compared to the controls (early-passage cells, see section 3.2.6), which was similar to that observed in *RICTOR*-KO HEK-293T cells (see section 4.2.2). These observation was further supported by the reduced levels of pH3, a proliferation marker and the increased apoptotic marker cleavage-caspase 3 in *RICTOR*-KO hESCs (Fig 5.5A). To further explore the impact of *RICTOR*-deficiency in hESCs proliferation and apoptosis, the cell cycle distribution of WT and *RICTOR*-KO hESCs were determined by FACS analysis (Fig 5.5B). As presented in Fig 5.5B, the early-passage *RICTOR*-KO hESCs demonstrated an obvious increase in the number of cells in the sub-G1 phase, which indicated a higher rate of apoptosis. Moreover, *RICTOR*-KO hESCs accumulated at the G0/G1 phase with decreased cells proportion of G2/M phase compared to the WT hESCs, which is consistent with the lower proliferation rates observed in early-passage *RICTOR*-KO hESCs.

Interestingly, unlike the HEK 293T cells, the growth of *RICTOR*-KO hESCs were gradually accelerated after the initial slow growth, and, by passage 15, they appeared to have no obvious difference, and even faster in cell growth compared to either parental WT or control hESCs. The increased cell growth which observed in these later-passage cells was correspondingly accompanied by the alteration at molecular levels, exhibited as reduced levels of cleavage-caspase 3 and increased FOXO1-Ser256 phosphorylation (Fig 5.5C). It is conceivable that this phenotypic change in cell growth might be due to the signalling rewiring and cellular adaptation. For example, phosphorylation of FOXO1 was initially reduced in the *RICTOR*-KO hESCs compared to the WT hESCs, leading to their accumulation in the nucleus (Fig 5.4B), but this phosphorylation became higher in *RICTOR*-KO hESCs with the increase of passages (Fig. 5.5C), indicating that in the absence of mTORC2, other signalling pathway(s) might have altered their activity to compensate the loss of mTORC2. However, the exact compensating mechanisms remain to be elusive. Even more intriguingly, in the five RICTOR-KO cell types in our labs, including hESCs, HEK 293T, PC-3 (a prostate cancer cell line), MEF and HUVEC (human umbilical vein endothelial cell), this adaption change in cell growth was only observed in the *RICTOR*-KO PC-3 cell in addition to the *RICTOR*-KO hESCs.

All the other cell types did not show this alteration, for instance, *Rictor*-KO MEF still grow much slower than the WT controls even at over 140 passages.

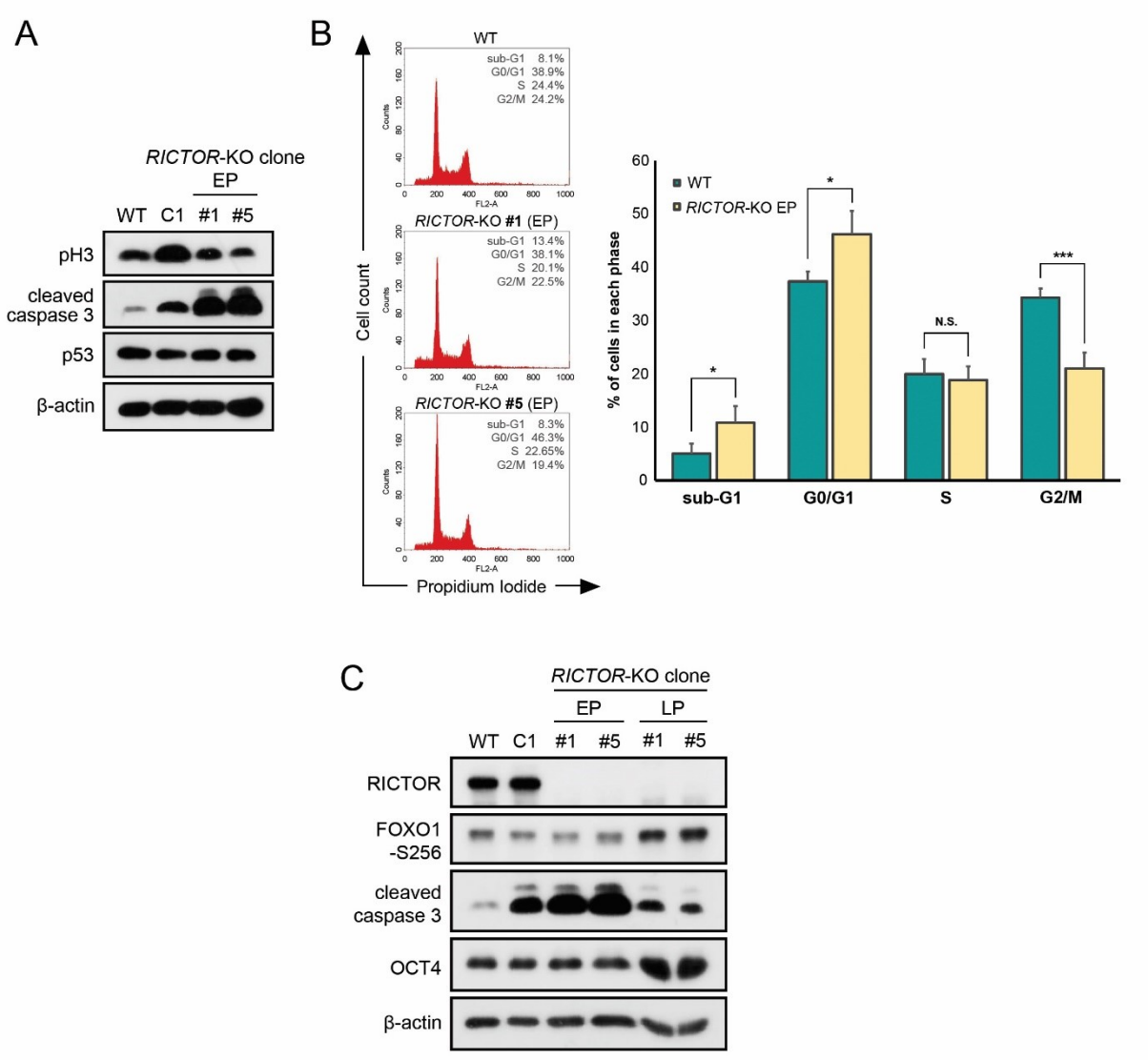


Figure 5.5 Characterisation of early- and later-passage *RICTOR*-KO hESCs

(A) *Immunoblotting analysis of proliferation and apoptosis antibodies, phospho-Histone H3 (pH3) and cleaved-caspase 3, in EP RICTOR-KO clones. EP, early-passage. Representative images from two independent experiments.* ***(B)*** *Cell cycle analysis using flow cytometry in WT and EP RICTOR-KO clones, and the distribution of each cell cycle phase (sub-G1, G0/G1, S, G2/M) is presented as bar chart. Data are represented as the means ± SD (n = 3 for WT and n = 6 for KO) (*p<0.05, ***p < 0.001 by two-tail unpaired t-test).* ***(C)*** *Protein expression of WT, C1, EP and LP RICTOR-KO clones were analysed by immunoblotting with indicated antibodies. LP, later-passage. Representative images from one experiment.*

5.2.5 *RICTOR* depletion impaired the formation of embryonic bodies from hESCs

Given that *RICTOR*-KO hESCs preserves the expression of core pluripotency transcription factors, next, I examined the pluripotency of *RICTOR*-KO hESCs by embryonic bodies (EBs) formation *in vitro*. Generally, three methods are commonly used to assess the overall differentiation propensity of stem cells: a) embryonic bodies (EBs) formation; b) teratoma; c) chimera. Among the three of them, EBs formation is the simplest *in vitro* approach to access the differentiation potential and to produce different cell lineages for further applications (Keller, 2005; Kurosawa, 2007; Pettinato et al., 2014). Therefore, I subjected WT, control and *RICTOR*-KO hESCs to the EB differentiation using a mechanical dissection method that generates irregular-sized hESCs clumps, which were then cultured in suspension for 10 days.

As shown in Fig 5.6A, in WT hESCs, spherical cell aggregates were spontaneously emerged within 2 days of suspension culture and continued to expand and differentiated. The EBs were collected at various time-points for the analysis of gene expression. It showed that the mRNA expression of pluripotent-associated genes, such as OCT4, SOX2 and NANOG, only exhibited a slight downregulation during cultural periods, while the expression of lineage-specific genes, including ectoderm (PAX6, SOX1), mesoderm (Brachyury, TBX6) and endoderm (SOX17 and GATA6), was increased and peaked at day 8 of EBs differentiation (Fig 5.6B), indicating that EBs formation led to hESC differentiation to all three germ-layer lineages. Given that I terminated the differentiation at 10 days, it was possible that the expression of the differentiated genes would continue to be increased while the pluripotent genes, such as OCT4 and NANOG would continue to be downregulated. All these findings were consistent with all previous observation from both our laboratory and researchers worldwide (Itskovitz-Eldor et al., 2000; Kurosawa, 2007; Son et al., 2011). Notably, during this EB differentiation process, the expression of mTORC2 components (mTOR, RICTOR, mSIN1 and mLST8) were generally stable with only minor fluctuations, and so did the mTORC2 activity as shown by the phosphorylation of the mTORC2 substrates (Fig 5.6C). Thus, I anticipated that the persistently expressing mTORC2-related genes as well as mTORC2 activity may have important function in preserving the differentiation capability of hESCs.

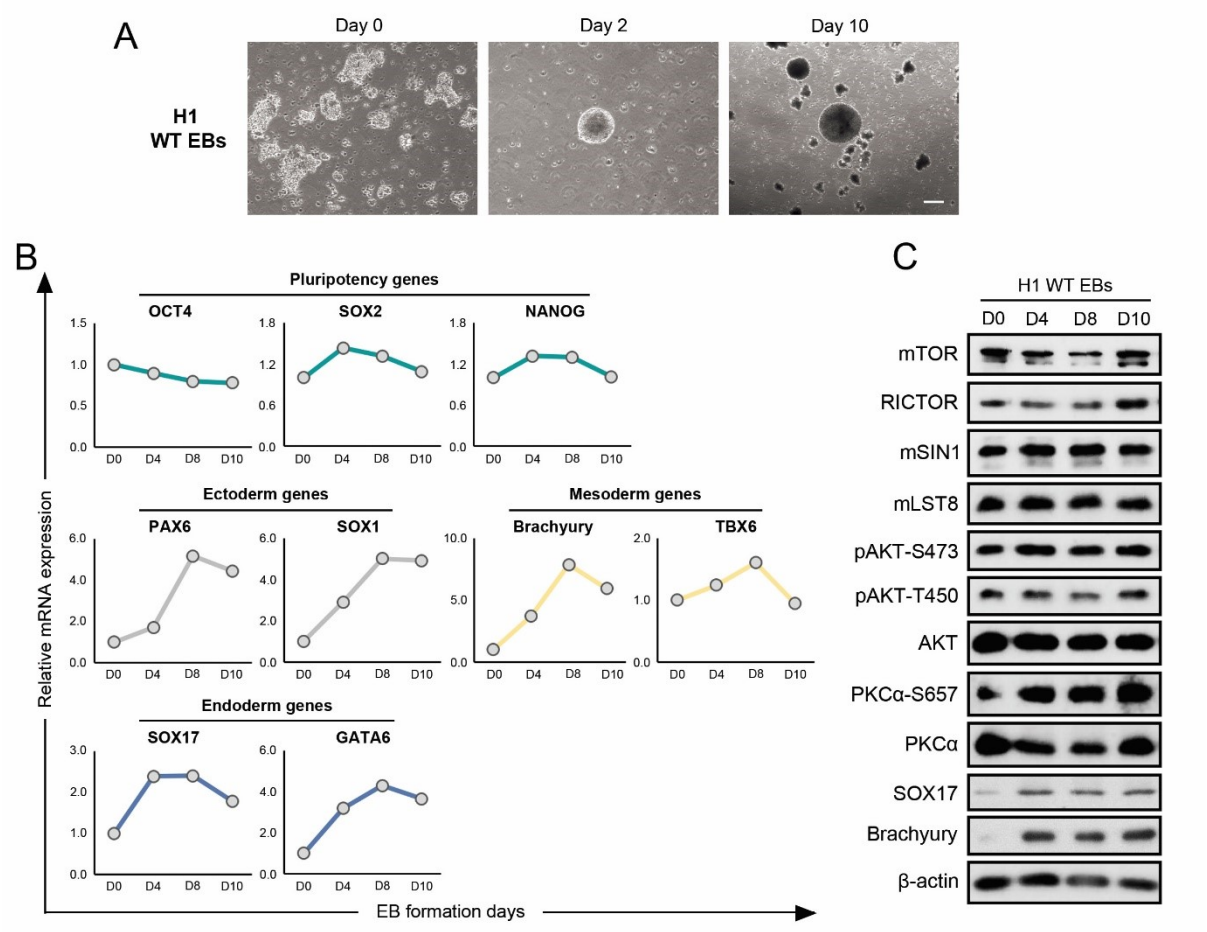


Figure 5.6 *In vitro* differentiation of H1 WT EBs

(A) *Bright-field images of representative EBs at indicated time points. Scale bar, 100μm.* ***(B)*** *qPCR analysis of spontaneous differentiation using markers of pluripotency (OCT4, SOX2 and NANOG) and the three germ layers [ectoderm (PAX6 and SOX1), mesoderm (Brachyury and TBX6), and endoderm (SOX17 and GATA6)] in H1 WT EBs.* ***(C)*** *H1 WT EBs were collected at indicated time points and lysed for immunoblotting with indicated antibodies. Representative images from one experiment.*

The hypothesis of RICTOR/mTORC2 signalling is important for hESC differentiation was further supported by the results of poorly established EB cultures in *RICTOR*-KO hESCs. Similar as the results obtained from WT hESCs, the formation of small spherical aggregates were observed from the control C1 hESCs when cultured in suspension *in vitro* within 48 hours, and the control C1 EBs increased in size during differentiation. However, although the shape of the mechanical-collected fragments of *RICTOR*-KO hESCs were indistinguishable compared to the control C1 at day 0, the *RICTOR*-KO hESCs failed to aggregate and were unable to produce large and cystic EBs throughout the culture duration (Fig 5.7A). Rather, massive cell death was observed during EB differentiation, which resulted in considerably fewer EBs in the *RICTOR*-KO culture than in the controls (Fig 5.7B).

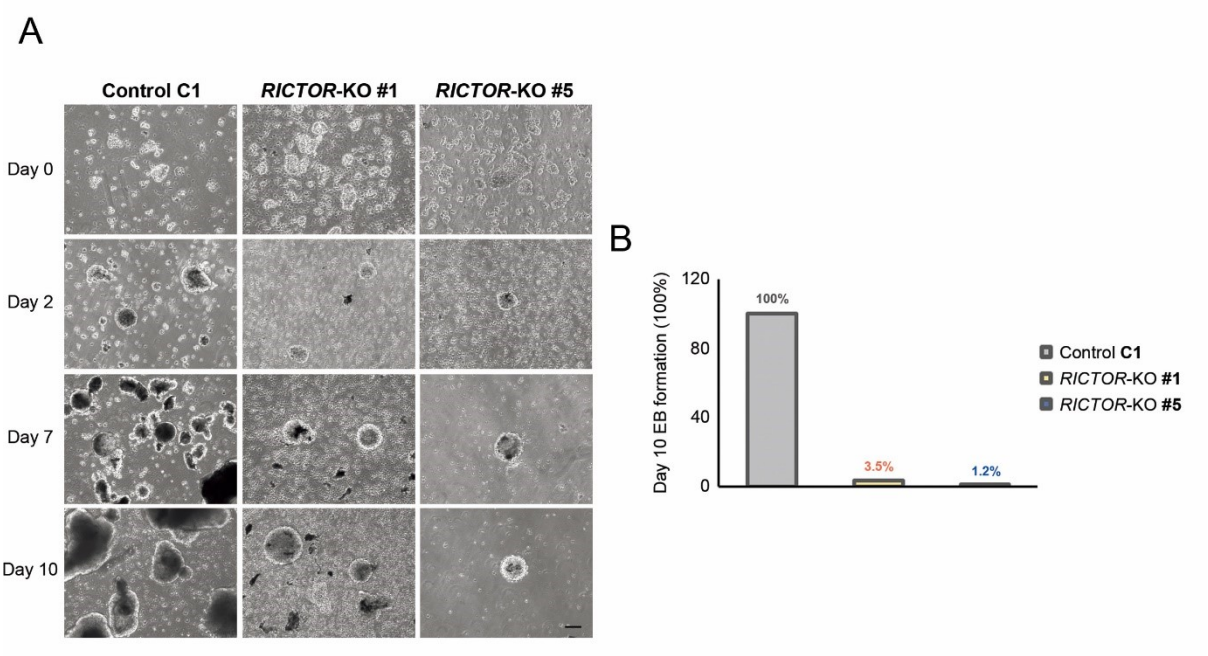


Figure 5.7 *RICTOR*-KO hESCs display poor efficiency of EBs formation

(A) *Representative phase-contract images of Control C1 and RICTOR-KO EBs at indicated time points. Scale bar, 100μm.* ***(B)*** *The presented percentage represents the number of C1 and RICTOR-KO spherical EBs relative to the number of C1 EBs after 10 days in suspension culture.*

Since cell aggregation is known to be largely dependent on cell-cell adhesion, and loss of cell-cell contact has been found to consequently induce anoikis (Hofmann et al., 2007; Wang et al., 2009). To overcome the poor efficiency of EB establishment in *RICTOR*-KO hESCs, EBs formation was performed in the medium supplemented with p160 rho-associated coiled-coil kinase inhibitor (ROCKi, Y-27632), which is used to block the dissociation-induced cell death and improve cell survival during EBs formation (Chen et al., 2010; Ohgushi et al., 2010; Watanabe et al., 2007). Both WT and *RICTOR*-KO EBs were differentiated into EBs for the first 2 days in the presence of the ROCKi in the suspension culture and the differentiation was terminated at day 10 (Fig 5.8A). Compared to the non-ROCKi-treated group, the positive effects of ROCKi was supported by the overall increase number of EBs in WT hESCs, indicating that the addition of ROCKi was beneficial for the EBs formation (Fig 5.8B). Although the size of the cell aggregates that generated from *RICTOR*-KO hESCs was significantly smaller than those derived from WT hESCs, the number of *RICTOR*-KO EBs was greatly elevated in the presence of ROCKi in comparison with the untreated *RICTOR*-KO EBs. However, the size and number of EBs were again markedly reduced and accompanied by massive cell death after withdrawal of ROCKi (Fig 5.8C). Taken together, these results indicate that the *RICTOR*-KO hESCs exhibited a defect in the formation of EBs.

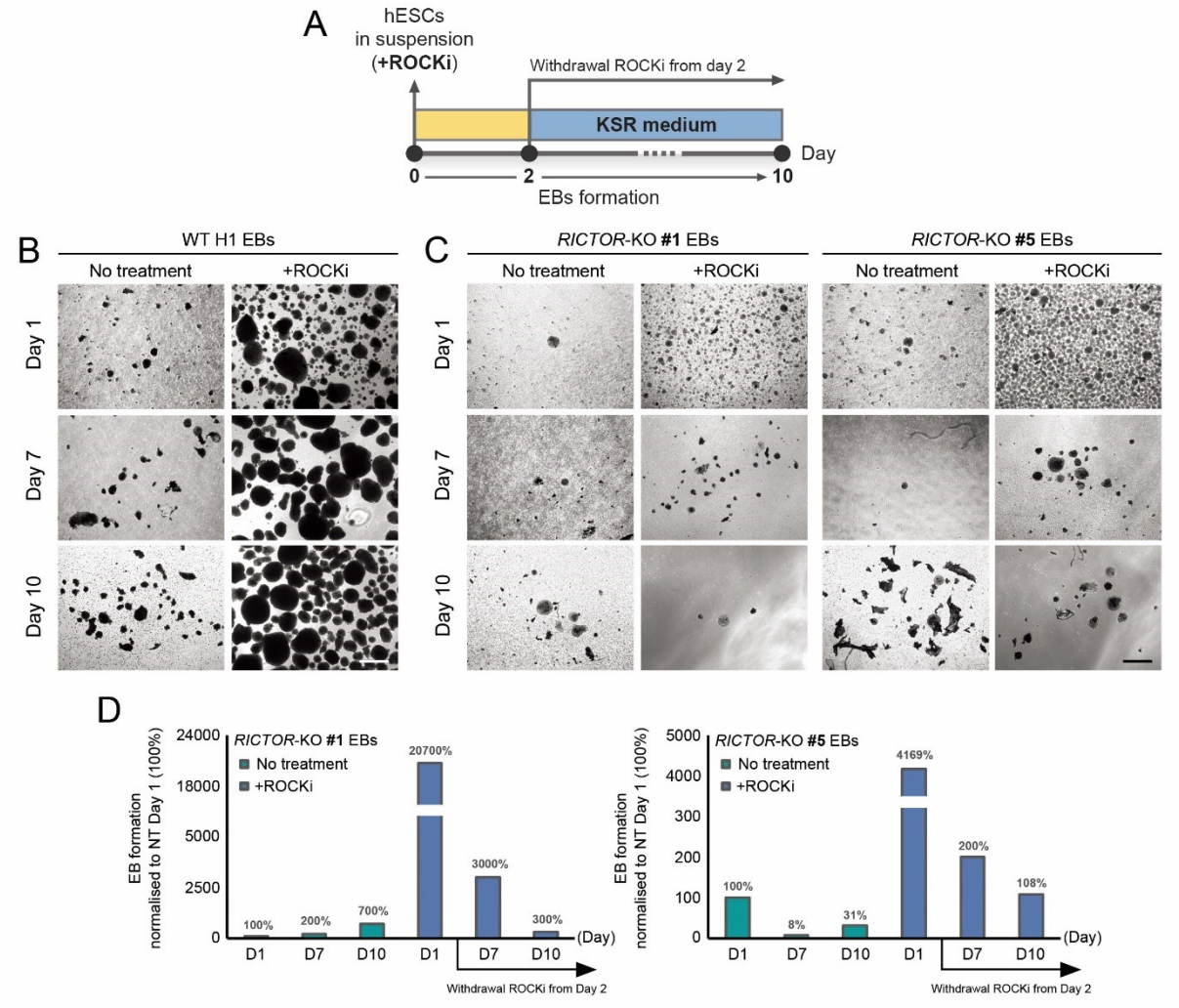


Figure 5.8 The present of ROCK inhibitor enhances EBs formation *in vitro*

(A) *Schematic overview of 10 days EBs formation. p160 rho-associated coiled-coil kinase inhibitor (ROCKi) was withdrawal from the differentiation medium (KSR medium) after day 2.* ***(B, C)*** *Representative phase-contract images of* ***(B)*** *WT and* ***(C)*** *RICTOR-KO EBs at indicated time points. Scale bar, 100μm.* ***(D)*** *Bar charts present the quantification results of the number of RICTOR-KO spherical EBs relative to the number of non-ROCKi-treated (NT) day 1 (D1) EBs.*

5.2.6 The deficiency of *RICTOR* exhibits a poor differentiation potential in hESCs

To gain additional insights into the developmental capability of *RICTOR*-KO hESCs, day 10 EBs from both WT and *RICTOR*-KO clones were then transferred to matrigel-coated plate and grown for another 12 days (Fig 5.9A). The outgrowth of differentiating cells was observed in the next few days and was highly heterogeneous in morphology. In comparison with the WT EBs, the limited *RICTOR*-KO EBs exhibited mainly neural progenitor morphology upon seeding into the adherent culture vessels (Fig 5.9B). The expression of several lineage-specific genes were measured in these cells at 12 days post-EB seeding (Day 10+12). Gene expression analysis of mRNA revealed that majority of the pluripotency-associated genes (OCT4, NANOG and REX1) were found reduced in both WT and *RICTOR*-KO EB-outgrowths, and the expression level of SOX2 in *RICTOR*-KO differentiated cells was slightly increased (Fig 5.9C). Moreover, as shown in Fig 5.9C, the elevated gene expression of three germ layers, including: PAX6 and SOX1 (ectoderm), Brachyury and TBX6 (mesoderm), SOX7 and GATA6 (endoderm) could be detected in Day 10+12 outgrowths of WT EBs, suggesting that they were able to spontaneously differentiate *in vitro*.

Intriguingly, although the EB differentiation and gene expression analysis was only done once and needs to be repeated, results from RT-PCR showed distinct the expression patterns for GATA6 and SOX7, two endoderm markers. GATA6 was detected in the outgrowths of *RICTOR*-KO EBs, while SOX7 was undetectable. Although the exact reasons for this differential expression are unclear, there are several possibilities. 1) GATA6 and SOX7 are reported to be sequentially expressed during primitive endoderm (PrE) formation in mouse embryo development (Artus et al., 2011). The expression of GATA6 is earlier than that of SOX7. 2) SOX7 might be only expressed in a sub-population of endodermal cells while GATA6 might be expressed in majority of endodermal cells (Artus et al., 2011). For example, SOX7 is found to be dispensable for the generation of PrE in mESCs (Kinoshita et al., 2015). 3) GATA6 and SOX7 might be expressed in different endoderm population and regulate differentiation of distinct cell types. Deficiency of *RICTOR* may only affect specific cell type differentiation through inactivation of SOX7. All these require further investigation.

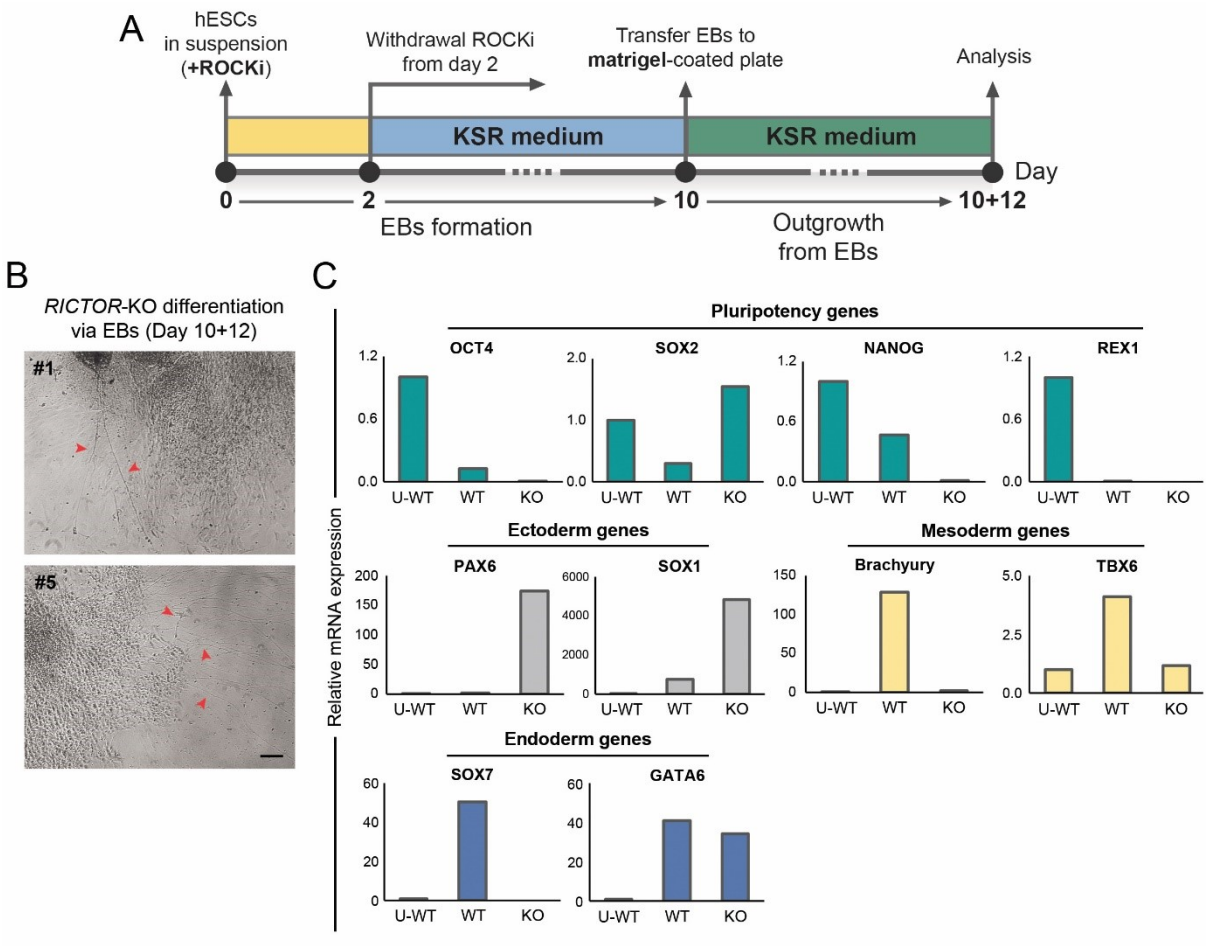


Figure 5.9 Assessing the differentiation potential of the *RICTOR*-KO hESCs

(A) *Overview of the strategy of 10+12 days EBs formation. ROCK inhibitor was only supplement in the differentiation medium (KSR medium) for the first 2 days and the EBs were cultured in suspension condition for total 10 days before they were allowed to outgrow on matrigel-coated plates.* ***(B)*** *Phase-contract images of differentiated RICTOR-KO hESCs. Red arrows indicate the neural-like morphology from the outgrowth of RICTOR-KO EBs. Scale bar, 100μm.* ***(C)*** *qPCR analysis of Day 10+12 EBs by using markers of pluripotency (OCT4, SOX2, NANOG and REX1) and the three germ layers [ectoderm (PAX6 and SOX1), mesoderm (Brachyury and TBX6), and endoderm (SOX17 and GATA6)] in WT and RICTOR-KO EBs. U-WT, undifferentiated-wild-type hESCs.*

All these findings were consistent with previous studies that the loss of pluripotency genes are concomitant with differentiation (Adachi et al., 2010; Babaie et al., 2007; Fong et al., 2008; Hay et al., 2004; Hyslop et al., 2005; Zaehres et al., 2005). Interestingly, among the examined germ layer markers, the *RICTOR*-KO EBs were mainly composed of ectoderm while the expression of mesodermal marker genes appeared to be most markedly downregulated, or even virtually undetectable, in the Day 10+12 outgrowths of *RICTOR*-KO EBs, indicating that *RICTOR*-KO hESCs were undergoing defective differentiation.

These outgrowing differentiated cells were further immunostained with antibodies against lineage-specific genes: class III β-tubulin (Tuj1, ectoderm), Brachyury (mesoderm) and SOX17 (endoderm). Results from immunostaining were consistent with the gene expression analysis, the outgrowing cells from WT EBs expressed markers characteristic for all three germ layers, which confirmed that the WT hESCs are pluripotent, having the potential to differentiate into a full spectrum of lineages associated with each germ layer (Fig 5.10A). In comparison with the WT EBs, when the *RICTOR*-KO EBs were allowed to adhere to a matrigel-coated surface, neuron-like outgrowths were observed from 2 to 3 days after plating. By examining the germ layer markers in the outgrowth of *RICTOR*-KO EBs, it was found that the great majority of the outgrowing cells stained positively for Tuj1 (ectoderm), whereas they expressed low levels of Brachyury (mesoderm) and SOX17 (endoderm) (Fig 5.10B), indicating that deficiency of *RICTOR* led to poor mesodermal and endodermal differentiation via EBs formation in hESCs. Collectively, these data imply that RICTOR/mTORC2 signalling pathway may have a crucial role in modulating hESC lineage propensity, particularly the mesendoderm lineages.

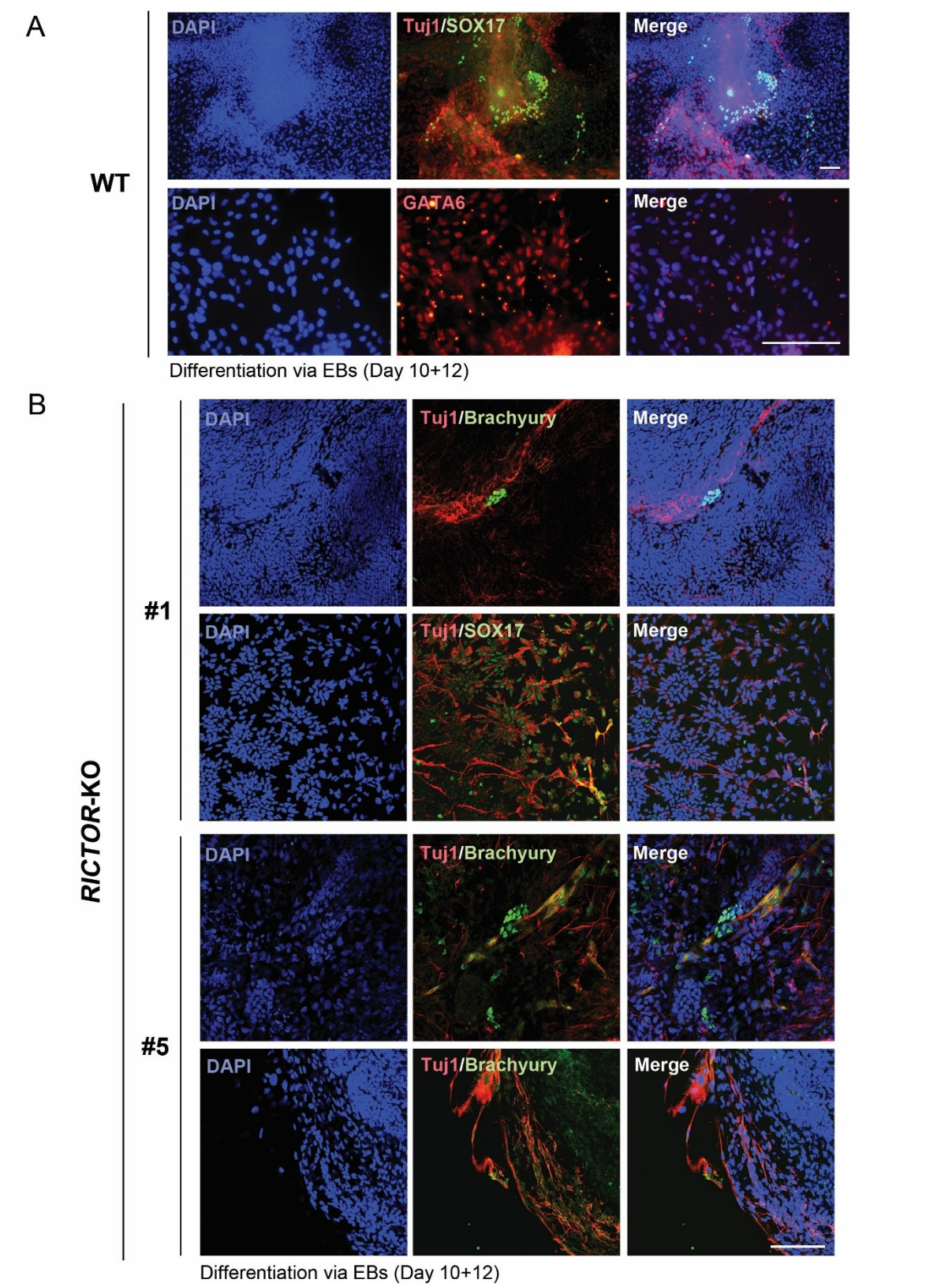


Figure 5.10 Deletion of *RICTOR* leads to defective mesendoderm differentiation

*Representative immunostaining images for Day 10+12 outgrowths of **(A)** WT and **(B)** RICTOR-KO EBs. The outgrowing differentiated cells were immunostained with Tuj1 (ectoderm), GATA6 (endoderm), SOX17 and Brachyury (mesoderm). Scale bar, 100µm.*

5.3 Conclusions and Discussion

RICTOR/mTORC2 has important functions during mouse early embryonic development. Mice with homozygous deletions of *Rictor* or *mSin1* results in embryonic lethality, which are considered to be attributed to the defects in cardiovascular function (Guertin et al., 2006; Jacinto et al., 2006; Shiota et al., 2006). The underlying molecular mechanisms of how RICTOR/mTORC2 regulates mouse development has not been fully elucidated to date, not to mention its role in human development. Thus, the establishment of *RICTOR*-KO hESCs provides us with a valuable resource to study the biological importance of RICTOR/mTORC2 signalling in human early embryonic development.

Previous studies have shown that long-term inhibition of mTOR signalling by rapamycin or Torin led to markedly decreased expression of pluripotency markers (OCT4, SOX2 and NANOG) and considerable reduction in the growth and survival of hESCs (Yilmaz et al., 2018; Zhou et al., 2012). However, I demonstrated in this chapter that RICTOR/mTORC2 might be dispensable for the self-renewal/pluripotency of hESCs as these cells are able to amplify themselves and meanwhile to generate cells of three embryonic germ layers (Fig 5.1 and 5.2). However, my preliminary data show that RICTOR/mTORC2 might be required for the conversion of hESCs to the naïve state in 5iLAF culture conditions (Fig 5.3B and C). Given that a successful naïve-to-primed conversion relies heavily on the high quality of undifferentiated hESCs, it will be interesting to further investigate that whether the failure of naïve conversion is truly a consequential effect of *RICTOR/mTORC2*-deficiency or due to the pluripotent state of *RICTOR*-KO hESCs. In considering that pluripotency may include a series of multiple states, spanning from naïve pluripotency to EpiSCs, rather than a specific fixed state, it is likely that the pluripotent state of *RICTOR*-KO hESCs might be more away from naïve pluripotent state than WT hESCs, based on the slightly morphological difference (Fig. 5.1A) and the result of SSEA4 and TRA-1-81 staining from flow cytometry (Fig. 5.2C). This is in consistent with the results from Rictor-KO mouse development, in which no clear defects are observed in tissue or organ formation (Guertin et al., 2006; Shiota et al., 2006). Further experiments, such as teratoma formation assay, will provide more evidence to conclude the role of RICTOR/mTORC2 signalling in hESC pluripotency. Interestingly, I also found that cell growth defect in hESCs as a result of *RICTOR/mTORC2* deficiency was able to be reversed

during long-term culture for which cellular adaptation might account for this. Intriguingly, not all the cell types have this adaption ability and underlying mechanisms remain to be explored. And finally, *RICTOR*-depleted hESCs form significantly fewer and smaller EBs than WT in suspension culture and display a defective differentiation potential, particularly for mesoderm fates *in vitro*.

Results from immunostaining revealed that reduced mTORC2/AKT activation was correlated with the increased nuclear localisation of FOXO1 in *RICTOR*-deficient hESCs (Fig 5.4B). By suppressing the mesendoderm lineage commitment and directly controlling the gene expression of OCT4 and SOX2, FOXO1 has been implied to be an important factor to regulate hESC pluripotency (Zhang et al., 2011c). Zhang and colleagues also revealed that a predominantly nuclear localisation of FOXO1 could be found in undifferentiated hESCs, which suggested that the subcellular localisation of FOXO1 might be an indicator of hESC pluripotent status. Therefore, I anticipate that the increased nuclear intensity of FOXO1 might possibly be the reason why *RICTOR*-KO hESCs displayed less spontaneous differentiation compared to WT hESCs under routine culture conditions (Fig 5.2A), and moreover, it might also play a role in the poorly differentiation toward mesendoderm lineage via EBs formation (Fig 5.9C). Whether cell fate determination of hESCs is directly mediated by the activity of RICTOR/mTORC2 or, alternatively, indirectly controlled via inhibiting other signalling pathways need to be elucidated.

Another interesting phenotypic change in *RICTOR*-KO hESCs was that the early-passage cells exhibited significantly higher cell apoptosis and reduced cell proliferation compared to the controls, which, however, were reversed in the later-passage *RICTOR*-KO hESCs (Fig 5.5). In comparison with other *RICTOR*-KO cell lines that we have generated, this reversed phenotypic change seemed to occur only in the hESCs and PC-3 cells, whereas HEK 293T, HUVECs and MEFs did not show this alteration. Inspecting the difference between these two groups of cells, the first group of cells share a distinct feature: tumorigenesis. Both PC-3 and hESCs, but not HEK 293T and HUVEC cells, are able to generate teratoma and prostate cancer, respectively, after they are implanted into the SCID (severe combined immunodeficiency) mice (Blum and Benvenisty, 2008; Nemeth et al., 1999). It has been known for some time that malignant cells have the ability to rewire their metabolism and molecular

circuitry, which might account for their drug resistance (Fodale et al., 2011). Since dysregulation of RICTOR/mTORC2 signalling often leads to diseases, including cancer (Saxton and Sabatini, 2017), and the development of cancer is a process of cellular adaptation (Ostrow et al., 2014). One of the explanations is that the deficiency of mTORC2 signalling might induce the derangement of intracellular signalling pathways as well as cell membrane molecules, and therefore leading to cellular adaptation. Although longer-term culture (later-passage) might also cause chromosomal abnormalities which is similar to those occurring in tumorigenesis (Baker et al., 2016; Lefort et al., 2008), it is less likely to be the case here unless *mTORC2*-deficiency increases the incidence of chromosomal abnomalities as control cells cultured for the same length of period did not exhibit similar proliferative changes. Given that it remains unclear why only tumorigenic cells have such adaptation ability, thus, *RICTOR*-KO hESCs might provide a cell model that facilitate our investigation on this issue.

I have demonstrated that knockout of *RICTOR* in hESCs preserves their stemness, as shown by the sustained expression of the core pluripotency transcription factors OCT4, SOX2 and NANOG (Fig 5.1C). However, the expression of REX1 was dramatically reduced at the transcriptional level in these *RICTOR*-KO hESCs. As one of the pluripotency-associated transcription factors, several reports have shown controversial results on the contribution of REX1 to pluripotency. Knockdown (KD) of REX1 in hESCs provided evidence that REX1 might participate in the regulation of both pluripotency and lineage specification (Son et al., 2013), while others studies performed on mouse ESCs and hESCs suggested that REX1 is only a pluripotency marker but has no functional role (Masui et al., 2008; Yilmaz et al., 2018). My results support the view that REX1 is not an essential factor for the maintenance of pluripotency in hESCs in terms of self-renewal/pluripotency capacity. Additionally, *RICTOR*-KO hESCs exhibited smaller EB sizes and changed their cell fate propensity during EB differentiation, which are similar to the results reported by *Son et al.* in their REX1-KD hESCs. It may be immature to conclude that these changes in *RICTOR*-KO hESCs are attributable to the downregulation of REX1 in these cells, therefore, further experiments are required to examine whether REX1 overexpression could restore the EB differentiation capacity. In addition, since the size of the EBs has been reported to be an important parameter that might affect ESC lineage specification, and mesendoderm differentiation has been reported to be enhanced in larger EBs (Bratt-Leal et al., 2009; Hwang et al., 2009; Karp et al., 2007; Mohr et

al., 2010), it is also possible that the alteration observed in cell fate in *RICTOR*-KO hESCs was resulted from poor cell proliferation after hESC differentiation.

In conclusion, results obtained from this chapter indicate that RICTOR/mTORC2 signalling might not be necessarily required for hESC self-renewal but might have a function in controlling cell fate determination. Thus, the establishment of *RICTOR*-KO hESCs can be further applied in comprehensive signalling studies and provide new insights into RICTOR/mTORC2 signalling in human early embryonic development.

06

General Discussion

As one the central controllers in regulating cell growth and homoeostasis, RICTOR/mTORC2 has been increasingly recognised to play many critical roles in mammalian cell behaviours and functions, particularly in response to environmental changes and stresses. Therefore, this signalling pathway is important for maintaining tissue homoeostasis and organism health in response to environmental changes, and thereby it is important for maintaining tissue homoeostasis and organism health (Saxton and Sabatini, 2017). To date, studies on RICTOR/mTORC2 signalling in mammalian cells have been relied on either inhibitors treatment (rapamycin or Torin) or RNA interference (RNAi)-mediated knockdown. Although these two methods are the most commonly used strategies, they do have shortfalls because the results of RNAi-based studies might be interfered by incomplete knockdown of the target protein and silencing of the siRNA in long-term experiments, while inhibitors often are not mTORC2-specific and might lead to cell type-dependent diverse biological responses (Lamming et al., 2012; Sarbassov et al., 2006; Schreiber et al., 2015). Hence, genetic knockout of RICTOR is an alternative and suitable approach which enable researchers to completely eliminate RICTOR protein and subsequently disable the mTORC2 function. In this study, several RICTOR-KO mammalian cell types were established via CRISPR-Cas9 system, by which I was able: **a)** to investigate the role of RICTOR in mTORC2 assembly and activity at molecular level and **b)** to assess the effect of *RICTOR/mTORC2*-deficiency on cell growth and differentiation.

6.1 Plasmid-based CRISPR-Cas9 system: an efficient approach for gene-knockout in mammalian cells

The development and application of CRISPR-Cas9 technology is broadening the landscape of genome editing, which facilitates the process of genetic modification across multiple model organisms (Ma and Liu, 2015). Since the first *in vitro* characterisation of CRISPR-Cas9 mechanism in 2012 (Jinek et al., 2012), researchers have dedicated to improve the conventional CRISPR-Cas9 technology from two main aspects: more efficient on-target genome editing and lower off-target effects. These goals can be achieved by several approaches including the modification of Cas9 and expression methods. To enhance the specific properties and reduce off-target edition, the residues on Cas9 protein which participate in the interaction with DNA were substituted with phosphodefective Alanine based on structural design principles (Kleinstiver et al., 2016; Slaymaker et al., 2016; Tan et al., 2019). Moreover, by fusing Cas9 protein with dihydrofolate reductase (DHFR), researchers generated a tightly regulated switched system to minimise the off-target rate by inducing a short period activation of Cas9 with the presence of trimethoprim (TMP) (Maji et al., 2017). And finally, to minimise the disruption to the genomic DNA other than specific target genes and to overcome the low transfection efficiency, pre-assembled Cas9 protein/sgRNA ribonucleoprotein (RNP) complexes have recently been developed to replace the constitutive Cas9 expression caused by plasmid-mediated expression (Farboud et al., 2018; Kim et al., 2014). The RNPs, which consists of Cas9 protein complexed with sgRNA, cleave the target chromosomal DNA within 24 hours and is degraded rapidly in cells, whereas the plasmid-based method usually requires at least 3 days after delivery and even integrate the plasmids into the genome (Liang et al., 2015; Ramakrishna et al., 2014). The less stressful RNP expression has been found to facilitate cell survival, which could largely increase the successful rate of genome editing (Kim et al., 2014; Ramakrishna et al., 2014). Furthermore, in comparison with plasmid transfection, the delivery of RNPs showed increase on-target editing and less off-target effects (Kim et al., 2014; Ramakrishna et al., 2014). More importantly, since this approach does not introduce external DNA into the genome except the target gene editing, it could be a better method in clinical application. Thus, as a new CRISPR technique, the application of RNPs holds immense potential in developing new therapeutic strategies.

In the present work, *RICTOR* gene was disrupted in different cell types via plasmid-based CRISPR-Cas9 system using conditions that were adapted from previously published methods (Liang et al., 2015; Ran et al., 2013). As mentioned above, this easy-to-manipulate DNA-based CRISPR-Cas9 system is widely used in genetic research as it remains several advantages over the RNA-based or RNP complexes, such as low cost, convenient and relatively stable (Liu et al., 2017). By confining the sgRNA target sites in exon 4 and 5 of the human *RICTOR* gene, my results demonstrate that calcium-phosphate transfection of plasmid-based Cas9-sgRNA system is sufficient to Cas9-mediated sequence-specific DNA break and subsequent NHEJ in HEK 293T cells, which then results in the *RICTOR* gene mutation/deletion and the ablation of RICTOR protein expression in those cells. Although the DNA-based system showed high targeting efficiency in HEK 293T cells, several issues are accompanied by the plasmid transfection of sgRNA and Cas9.

Firstly, targeting efficacies of plasmid-based system might be variable in different cell types due to their different efficiency on nucleus delivery of plasmids. For example, I found that it was very challenging to transfect plasmid-based CRISPR-Cas9 into hard-to-be transfected cell types, such as hESCs. Although the combination of effective delivery methods (e.g. viral-mediated delivery, electroporation and nucleofection) with plasmid-based CRISPR-Cas9 system could increase the low transfection efficiency in hESCs (Martinez et al., 2015; Merkle et al., 2015), these methods often simultaneously place a high degree of pressure onto cells, which induces significant cell death and therefore generates an obstacle for gene editing (Kim et al., 2014). Moreover, even if the CRISPR-Cas9 system has been successfully delivered into the nucleus, the plasmid DNA will randomly integrate into the genome of target cells, having a possibility to disrupt functional genes, another potential problem that is difficult to ascertain. Thirdly, the integrated CRISPR plasmids may be persistently expressed in target cells over time and the accumulation of Cas9 protein inside the transfected cells may produce substantial off-target effects, which is one of the most concerns of any plasmid-based CRISPR experiments (Liang et al., 2015). Indeed, some studies have reported that unintended edits were observed in transfected cells, particularly those with plasmid-based CRISPR-Cas9 system (Cradick et al., 2013; Fu et al., 2013). The application of CRISPR-Cas9 system in mammalian cells is a relatively new area which has only been reported since 2013 (Mali et al., 2013). Given that there is no previous study that specifically focus on the effect of Cas9 on

cell properties of mammalian cells, the constitutive Cas9 expression might possibility lead to any observable or unobservable phenotypic changes or could have harmful effects to the cells. Hence, it is crucial to analyse multiple independent knockout clones to ensure that the phenotypic effects are not caused by the unrevealed feature of Cas9.

Collectively, based on the cost-effectiveness ratio, gene editing in mammalian cells by introducing CRISPR components as plasmid-based system is the most straightforward, efficient and convenient method. Thus, we can utilise these benefits to provide preliminary and useful aspects for the following experiments. For example, the DNA-based CRISPR-Cas9 system could be used to rapidly compare the targeting efficiency among multiple sgRNA candidates, which can help researchers identify the ideal targeted sequences on the desire genes.

6.2 Important roles of RICTOR/mSIN1 in mTORC2 assembly and function

Much of the knowledge about mTORC2 has been obtained from the experimental results of its defining subunits, RICTOR and mSIN1. The expression and tight interaction between RICTOR and mSIN1 are known to be essential for mTORC2 activity as they provide the structural foundation for mTORC2 complex formation, thus, ablation either of them can lead to mTORC2 disability (Frias et al., 2006; Guertin et al., 2006; Jacinto et al., 2006; Shiota et al., 2006; Yao et al., 2017).

As the first identified subunit of mTORC2, structure and function of human RICTOR have been studied intensively, however, they still remains ambiguous (Jacinto et al., 2006; Sarbassov et al., 2004). Previous data have suggested that an intact full-length of RICTOR protein is required for preserving the integrity of mTORC2 (Aimbetov et al., 2012; Glidden et al., 2012; Huang et al., 2009). However, my results demonstrate that RICTOR mutant with a deletion (Δ1001-1200) around its multiple phosphorylation sites (PS region, 1084-1188 aa) was able to interact with other components of mTORC2 to restore the expression of mSIN1 and reconstitute the mTORC2 activity in *RICTOR*-KO HEK 293T cells (section 4.2.4). These

results suggest that this region is not necessarily required for RICTOR to assemble mTORC2. Interestingly, as indicated in section 1.2.1, this region of 200 amino acids is located within the section that is only conserved among vertebrates but not the yeast (Dibble et al., 2009; Hayashi et al., 2007). This could indicate that this region might be evolved in vertebrates and have a regulatory function to control mTORC2 formation and activity. This is supported by the findings that phosphorylation of two residues within this PS region of RICTOR, Thr1135 and Ser1162 by S6K and PLK1, respectively, negatively regulate assembly of mTORC2 (Bhattacharya et al., 2016; Shao and Liu, 2015). Therefore, it is envisaged that the RICTOR protein may have two key conserved regions located at its N and C terminal sides, respectively, which are connected by a regulatory linker region (Dibble et al., 2009).

Another finding of my study is RICTOR may regulate mSIN1 stability via more than one mechanism. My results show that *RICTOR*-deficiency reduces not only mSIN1.1 and 1.5 protein levels but also mSIN1.4 that does not have a RICTOR-interacting N-terminal domain, which indicate that apart from forming a heterodimer with RICTOR, mSIN1 could also be stabilised by other RICTOR/mTORC2-dependent mechanisms. My experiments of site-directed mutagenesis of Ser260 and Ser270 suggest that the mTORC2-mediated phosphorylation of mSIN1 may also contribute to its stability. More importantly, phosphorylation status of mSIN1-S260/S270 also plays functional roles in the mTORC2 substrate recognition, in particular, the activation of PKCα in HEK 293T cells.

So far, it remains unclear the underlying mechanisms by which mTORC2 selects and recognises its substrates for targeting. The mSIN1 protein has been proposed to be a subunit in mTORC2 for substrate selection and recognition (Cameron et al., 2011; Lu et al., 2011; Tatebe et al., 2017). Thus, whether and how the post-translational modification of mSIN1 modulate mTORC2 substrate specificity is an interesting question. Given that these two phosphorylation sites (S260/270) are located in the CRIM domain of mSIN1 which is thought to responsible for substrate recognition of mTORC2 (Cameron et al., 2011; Kataoka et al., 2015; Tatebe et al., 2017) and that mTORC2 has been reported to phosphorylate and activate its substrates by direct interaction (Cameron et al., 2011; Gan et al., 2011; Lu et al., 2011), it is conceivable that the decrease of negative charge on mSIN1 as a result of non-phosphorylation of S260/S270, might possibly alter the structure of CRIM domain that affects mTORC2 substrates binding. Since AKT and PKC are not competing for the same binding site

on mTORC2 (Gan et al., 2012), I anticipate that the structural change as a result of mSIN1-S260/270A (SA) in mTORC2 may only lead to a reduced binding affinity or a decreased frequency of encounter with PKCα, and thereby, only affects the regulation of PKCα-HM phosphorylation but not that of AKT. In addition to the post-translational modifications of mTORC2 subunits, other components in mTORC2 complex might also play a role in the substrate selection. Previously, the functional studies of Protor-1/2 revealed that by direct interaction with RICTOR/mSIN1, both Protor-1 and -2 are dispensable for the activation of AKT but play critical roles in the phosphorylation of SGK and PKCδ at their hydrophobic motifs, respectively (Gan et al., 2012; Pearce et al., 2011). Even though my results show that all different mSIN1 mutants (mSIN1-SD, SA and Δ) are able to incorporate into mTORC2 complex, it is unclear whether the phosphorylation status of mSIN1 affects mTORC2's association with Protor-1/2. Therefore further investigation is required.

6.3 mTORC2 signalling may have a role in mesendodermal differentiation of hESCs

Currently, studies based on inhibitor treatment only provide limited information about how mTOR signalling contributes to hESC cell fate determination. Rapamycin, as one of the most commonly used inhibitors, can efficiently diminish the activity of mTORC1 soon upon application without interfering mTORC2 pathway, whereas longer-term treatment of rapamycin has also been shown to reduce mTORC2 assembly and activity in certain cell types, which is considered as a result of exhaustion of functional mTOR (Lamming et al., 2012; Sarbassov et al., 2006; Schreiber et al., 2015). Considering that differentiation of pluripotent stem cells toward any specific cell lineages is not a quick procedure, inhibitor treatment might not be an ideal strategy to clearly dissect the functional roles of each of the mTOR complexes in hESC lineage specification. Therefore, in this study, I utilised CRISPR-Cas9 system to genetically disable the *RICTOR* gene, leading to complete elimination RICTOR expression. With this approach, I demonstrate that RICTOR/mTORC2 signalling may have an important function in regulating hESC lineage propensity, particularly the mesendoderm lineages.

Several studies have shown that the inactivation of mTORC1 by rapamycin treatment led to mesoderm and endoderm differentiation in hESCs (Nazareth et al., 2016; Zhou et al., 2012; Zhou et al., 2009), and this mesendoderm-enhancing effects of rapamycin could be phenocopied by RNAi-mediated knockdown of RAPTOR in both hESCs and mESCs (Nazareth et al., 2016; Zheng et al., 2017), suggesting that the neural-lineage specification of hESCs may require the activation of mTORC1. Yet, if we consider the long-term exposure (more than 24 hours) to rapamycin also affects, at least partially, the activity of mTORC2, it is possible to assume that the enhancing specification of mesendoderm might also be a result of dual inhibition of mTOR complexes (Fig 6.1). Although mTORC1 and mTORC2 are two distinct multi-protein complexes, several regulatory mechanisms have been unveiled between the mTOR complexes. By either competing binding with mTOR protein or the effects of negative regulatory phosphorylation, it has been found that specifically impairs one of them may often subsequently activate another in some cell types (Das et al., 2011; Dibble et al., 2009; Hua et al., 2019; Julien et al., 2010; Rosner et al., 2009; Sarbassov et al., 2004; Zheng et al., 2017). In consistent with published reports and my previous findings in *RICTOR*-KO HEK 293T and PC-3 cells (section 4.2.1), deletion of *RICTOR* in hESCs was observed with a slight increase of mTORC1 activity and decrease mTORC2 activity. Interestingly, by *in vitro* differentiation of hESCs via EBs formation, my data show that loss of *RICTOR* in hESCs, or more precisely, mTORC1 activity remained, led to the activation of ectodermal gene expression and induced neural differentiation. Therefore, as anticipated, mTORC1 and mTORC2 may have different roles in cell fate determination of hESC *in vitro*. mTORC1 activity appears to have a role in mediating ectoderm formation, whereas the activation of mTORC2 may possibility drive mesendoderm/endoderm commitment in the differentiation of hESCs.

In conclusion, a proper balance between mTORC1 and mTORC2 signalling pathways may be vital for early embryogenesis. The crosstalk between these two complexes tightly modulate the network of PI3K/AKT/mTOR signalling, and thus, retains the capacity of hESCs to differentiate into the full spectrum of the lineage.

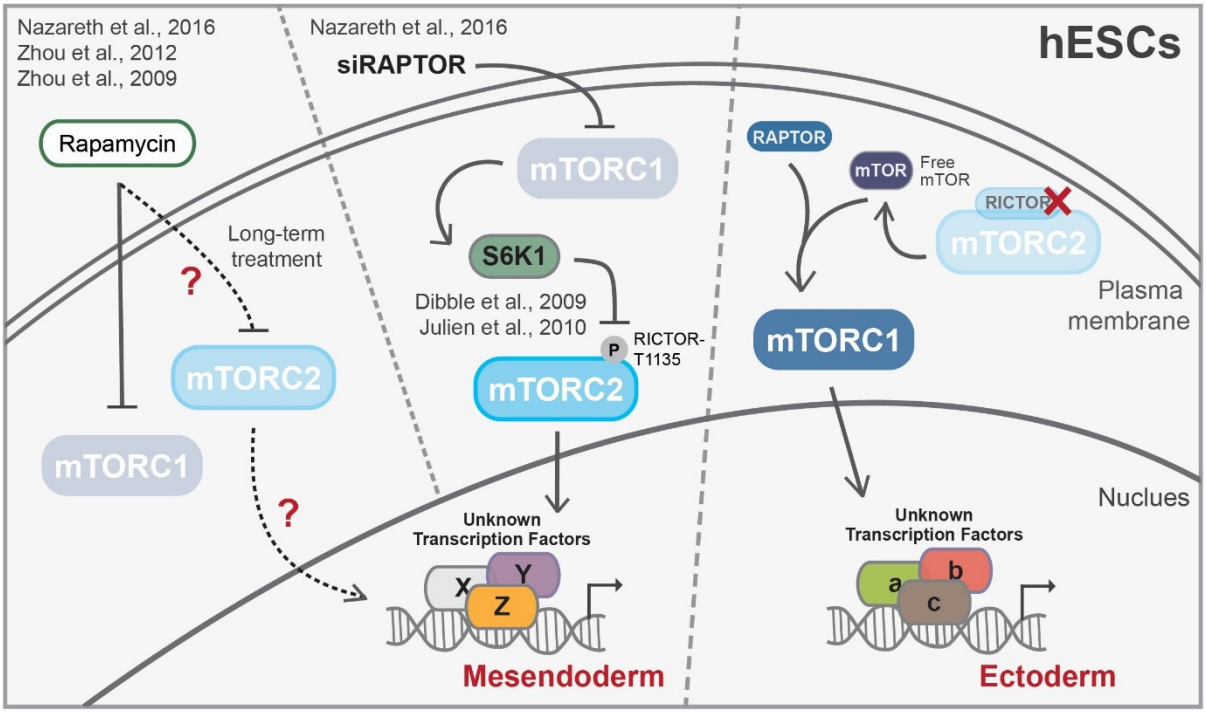


Figure 6.1 Proposed diagram of how mTOR signalling affects hESC cell-fate determination

Mesendoderm differentiation of hESCs might be induced by the dual inhibition of mTOR complexes by long-term rapamycin treatment ***(left)*** *and the activation of mTORC2* ***(middle)****. The RNAi-mediated knockdown of RAPTOR (mTORC1) subsequently inhibits the S6K1-mediated RICTOR-Thr1135 phosphorylation, and thus facilitates the activity of mTORC2. On the other hand, the disruption of mTORC2 complex assembly increases the availability of mTOR protein, which in turn promotes the assembly of mTORC1 and may enhance the ectoderm lineage differentiation* ***(Right)****.*

6.4 Future Perspective

6.4.1 RICTOR's function in mTORC2 activity: from the aspect of protein structure and cellular localisation

I. To further characterise RICTOR-PS region in the regulation of mTORC2

Results from both immunoblotting and co-immunoprecipitation (co-IP) experiments have indicated that the multiple phosphorylation sites (PS region, 1084-1188 aa) of RICTOR is not necessarily required for the formation and activity of mTORC2. To further understand the functional role of RICTOR-PS region, as such, it will be good to generate and investigate the formation and activity of mTORC2 in RICTOR-rescue cell lines which stably expressed RICTOR-full-length (WT) and RICTOR-Δ1001-1200 (mut). In detail, first, the formation efficiency of mTORC2 complex with WT-RICTOR and mut-RICTOR will be compared by co-IP, and second, the activity of mut-RICTOR/mTORC2 will be examined by *in vitro* kinase assay and immunoblotting. Finally, cellular functional assays such as cell proliferation and migration will be performed to assess whether there are any differences between these RICTOR-rescue cell lines.

II. Explore subcellular localisation of mut-RICTOR/mTORC2 under various culture conditions

Emerging evidences have demonstrated that the subcellular localisations of mTORC2 play important roles in regulating its substrates activation, and even specificity of substrate recognition (Ebner et al., 2017; Gleason et al., 2019; Liu et al., 2014). In response to growth factors stimulation, mTORC2 could be recruited to plasma membrane where it meets and phosphorylates AKT at Ser473. Recently, we have found that RICTOR, particularly its C-terminal domain, has a vital role in this process, thereby may have an important function in regulation of mTORC2 activation at plasma membrane (Xu et al., 2019). However, the exact details remain to be further investigated. Moreover, it is unclear how mTORC2 functions in the other subcellular localisations in addition to plasma membrane. Therefore, it will need to be investigated that whether RICTOR's domains have any effect on mTORC2 subcellular locations, the cellular localisation of mTORC2 complex which contained RICTOR-WT or -

Δ1001-1200 will be compared and examined by confocal microscopy under routine and different culture conditions, such as starvation or growth factor stimulation post starvation.

6.4.2 Phosphorylation of mSIN1: How is it regulated and what is the impact of it?

Whilst my current study demonstrates that the phosphorylation status of mSIN1 might differentially regulate PKCα phosphorylation, it remains unclear whether failure of mTORC2-mediated phosphorylation on hydrophobic motif of PKCα (Ser657) would affect any physiological functions of cells. Although HEK 293T cells are commonly used for studying fundamental questions in molecular cell biology, they are not a good cell model for physiological studies, such as cell migration and cell morphology. Hence, other *mSIN1*-KO cell types could be established by utilising CRISPR-Cas9 system, for instances, *mSIN1*-KO PC-3 cells. These *mSIN1*-KO cells could be used to ectopically express different mSIN1 mutants (WT and SA mutant) to assess whether there are any phenotypic differences between the cells with or without PKCα-Ser657 phosphorylation. In particular, given that mTORC2 affects cytoskeleton organisation and cell migration through modulating the activity of PKC family (Gan et al., 2012; Liu et al., 2014; Thomanetz et al., 2013), thus, the cell morphology and the underlying mechanisms will be assessed in these two types of cells by immunoblotting and cell cytoskeleton staining.

6.4.3 *mTORC2*-deficiency in differentiation: *In vitro* and *in vivo* differentiation of *RICTOR*-KO hESCs

Based on the results obtained from differentiation of hESCs via EBs formation, I have demonstrated that the *RICTOR*-KO hESCs might prefer to differentiate into ectoderm (neural) lineage. To further determine whether RICTOR/mTORC2 has a role in lineage specificity, further studies are required. Firstly, directed lineage-specific differentiation approaches can be applied to both WT and *RICTOR*-KO hESCs, particularly the differentiation toward mesodermal lineages (Mummery et al., 2012; Vazin and Freed, 2010). The resulting cells after differentiation will be subsequently assessed for their cell identity using qRT-PCR, immunoblotting and immunostaining. Secondly, to further investigate the pluripotency of

hESCs *in vivo*, teratoma formation assays will be performed by injecting either WT or *RICTOR*-KO hESCs into immunodeficient mice, and the hESC-derived teratomas will be further analysed histologically and by immunostaining for cell lineage/type identification. In addition, it is necessary to ectopically express RICTOR back into the KO cells to test whether it is able to restore the differentiation defect. These data together will produce useful information about the role of RICTOR/mTORC2 in cell fate determination and also shed a light on its role during early embryonic development.

6.4.4 Exploring the underlying mechanisms: Genetic and metabolic profiling of *mTORC2*-deficiency hESCs

RICTOR-deficiency mainly disable the mTORC2 signalling pathway and disturb the signalling network in the KO cells. These changes will ultimately bring changes in epigenetic landscape and gene expression through which they affect cell properties, functions and even metabolism. Therefore, to further explore the underlying molecular mechanisms by which RICTOR/mTORC2 affect hESC self-renewal and differentiation, it will be useful to perform transcriptome profiling by RNA- sequencing and metabolic profiling by liquid chromatography–mass spectrometry (LC-MS) and compare the gene expression/ metabolome profile between WT- and *RICTOR*-KO hESCs under both undifferentiated and differentiated states. Datasets provided by RNA-sequencing and LC-MS may contain vast information, as such, analysis will be focused on interpreting certain transcription factors, epigenetic factors and metabolites that are essential for embryonic development. By linking the gene expression profiles to metabolic diversity, the resulting information will aid further investigation to explore the function of mTORC2 in human pluripotent stem cells and human embryonic development. Although the validation might not be able to complete on all the information obtained from these assays, the datasets will help the future studies in this field beyond our laboratory.

Since our knowledge on mTORC2 is very limited so far, our current study and future work stated above will greatly contribute to the understanding of mTORC2 on its biochemical structures, signalling regulations, crosstalk with other signalling pathways and biological functions. This enriched knowledge on mTORC2 will facilitate the development of new preventive or therapeutic targets for improving human health and treating human diseases.

In summary, to evaluate the role of RICTOR on both mTORC2 assembly/activity and human development, multiple *RICTOR*-KO clonal cell types established through CRISPR-Cas9 system in order to answer different biological questions. Results obtained from *RICTOR*-KO HEK 293T cells demonstrate that both RICTOR and mSIN1 are required for the assembly and function of mTORC2. RICTOR interacts and induces mTOR-dependent phosphorylation at mSIN1-Ser260/270 to prevent mSIN1 from proteasome-mediated degradation. This auto-regulatory mechanism of mTORC2 not only stabilises mSIN1 protein but also affect mTORC2 substrate selectivity. On the other hand, the characterisation of *RICTOR*-KO hESCs reveals that the activity of RICTOR/mTORC2 may not be necessarily required for hESC self-renewal, however, it may have a role in modulating cell fate determination, which indicates that RICTOR/mTORC2 signalling has an important role in human embryonic development.

Reference

Adachi, K., Suemori, H., Yasuda, S.Y., Nakatsuji, N., and Kawase, E. (2010). Role of SOX2 in maintaining pluripotency of human embryonic stem cells. Genes Cells *15*, 455-470.

Adhikari, S., Moran, J., Weddle, C., and Hinczewski, M. (2018). Unraveling the mechanism of the cadherin-catenin-actin catch bond. PLoS Comput Biol *14*, e1006399.

Agarwal, N.K., Chen, C.H., Cho, H., Boulbes, D.R., Spooner, E., and Sarbassov, D.D. (2013). Rictor regulates cell migration by suppressing RhoGDI2. Oncogene *32*, 2521-2526.

Aimbetov, R., Chen, C.H., Bulgakova, O., Abetov, D., Bissenbaev, A.K., Bersimbaev, R.I., and Sarbassov, D.D. (2012). Integrity of mTORC2 is dependent on the rictor Gly-934 site. Oncogene *31*, 2115-2120.

Alao, J.P. (2007). The regulation of cyclin D1 degradation: roles in cancer development and the potential for therapeutic invention. Mol Cancer *6*, 24.

Alessi, D.R., Andjelkovic, M., Caudwell, B., Cron, P., Morrice, N., Cohen, P., and Hemmings, B.A. (1996). Mechanism of activation of protein kinase B by insulin and IGF-1. EMBO J *15*, 6541-6551.

Alexandropoulos, K., and Baltimore, D. (1996). Coordinate activation of c-Src by SH3- and SH2-binding sites on a novel p130Cas-related protein, Sin. Gene Dev *10*, 1341-1355.

Amita, M., Adachi, K., Alexenko, A.P., Sinha, S., Schust, D.J., Schulz, L.C., Roberts, R.M., and Ezashi, T. (2013). Complete and unidirectional conversion of human embryonic stem cells to trophoblast by BMP4. Proc Natl Acad Sci U S A *110*, E1212-1221.

Anderson, K.R., Haeussler, M., Watanabe, C., Janakiraman, V., Lund, J., Modrusan, Z., Stinson, J., Bei, Q., Buechler, A., Yu, C.*, et al.* (2018). CRISPR off-target analysis in genetically engineered rats and mice. Nat Methods *15*, 512-514.

Armstrong, L., Hughes, O., Yung, S., Hyslop, L., Stewart, R., Wappler, I., Peters, H., Walter, T., Stojkovic, P., Evans, J.*, et al.* (2006). The role of PI3K/AKT, MAPK/ERK and NFkappabeta signalling in the maintenance of human embryonic stem cell pluripotency and viability highlighted by transcriptional profiling and functional analysis. Hum Mol Genet *15*, 1894-1913.

Artus, J., Piliszek, A., and Hadjantonakis, A.K. (2011). The primitive endoderm lineage of the mouse blastocyst: sequential transcription factor activation and regulation of differentiation by Sox17. Dev Biol *350*, 393-404.

Aylett, C.H., Sauer, E., Imseng, S., Boehringer, D., Hall, M.N., Ban, N., and Maier, T. (2016). Architecture of human mTOR complex 1. Science *351*, 48-52.

Babaev, V.R., Huang, J., Ding, L., Zhang, Y., May, J.M., and Linton, M.F. (2018). Loss of Rictor in Monocyte/Macrophages Suppresses Their Proliferation and Viability Reducing Atherosclerosis in LDLR Null Mice. Front Immunol *9*, 215.

Babaie, Y., Herwig, R., Greber, B., Brink, T.C., Wruck, W., Groth, D., Lehrach, H., Burdon, T., and Adjaye, J. (2007). Analysis of Oct4-dependent transcriptional networks regulating self-renewal and pluripotency in human embryonic stem cells. Stem Cells *25*, 500-510.

Baker, D., Hirst, A.J., Gokhale, P.J., Juarez, M.A., Williams, S., Wheeler, M., Bean, K., Allison, T.F., Moore, H.D., Andrews, P.W.*, et al.* (2016). Detecting Genetic Mosaicism in Cultures of Human Pluripotent Stem Cells. Stem Cell Rep *7*, 998-1012.

Bar-Peled, L., Schweitzer, L.D., Zoncu, R., and Sabatini, D.M. (2012). Ragulator is a GEF for the rag GTPases that signal amino acid levels to mTORC1. Cell *150*, 1196-1208.

Bauer, D.E., Canver, M.C., and Orkin, S.H. (2015). Generation of genomic deletions in mammalian cell lines via CRISPR/Cas9. J Vis Exp, e52118.

Beattie, G.M., Lopez, A.D., Bucay, N., Hinton, A., Firpo, M.T., King, C.C., and Hayek, A. (2005). Activin A maintains pluripotency of human embryonic stem cells in the absence of feeder layers. Stem Cells *23*, 489-495.

Ben-Sahra, I., Howell, J.J., Asara, J.M., and Manning, B.D. (2013). Stimulation of de novo pyrimidine synthesis by growth signaling through mTOR and S6K1. Science *339*, 1323-1328.

Bentzinger, C.F., Romanino, K., Cloetta, D., Lin, S., Mascarenhas, J.B., Oliveri, F., Xia, J., Casanova, E., Costa, C.F., Brink, M.*, et al.* (2008). Skeletal muscle-specific ablation of raptor, but not of rictor, causes metabolic changes and results in muscle dystrophy. Cell Metab *8*, 411-424.

Bernardo, A.S., Faial, T., Gardner, L., Niakan, K.K., Ortmann, D., Senner, C.E., Callery, E.M., Trotter, M.W., Hemberger, M., Smith, J.C.*, et al.* (2011). BRACHYURY and CDX2 mediate BMP-induced differentiation of human and mouse pluripotent stem cells into embryonic and extraembryonic lineages. Cell Stem Cell *9*, 144-155.

Bertero, A., Madrigal, P., Galli, A., Hubner, N.C., Moreno, I., Burks, D., Brown, S., Pedersen, R.A., Gaffney, D., Mendjan, S.*, et al.* (2015). Activin/nodal signaling and NANOG orchestrate human embryonic stem cell fate decisions by controlling the H3K4me3 chromatin mark. Gene Dev *29*, 702-717.

Bhattacharya, K., Maiti, S., and Mandal, C. (2016). PTEN negatively regulates mTORC2 formation and signaling in grade IV glioma via Rictor hyperphosphorylation at Thr1135 and direct the mode of action of an mTORC1/2 inhibitor. Oncogenesis *5*, e227.

Bhaya, D., Davison, M., and Barrangou, R. (2011). CRISPR-Cas systems in bacteria and archaea: versatile small RNAs for adaptive defense and regulation. Annu Rev Genet *45*, 273-297.

Bian, Y.H., Xu, J., Zhao, W.Y., Zhang, Z.Z., Tu, L., Cao, H., and Zhang, Z.G. (2017). Targeting mTORC2 component rictor inhibits cell proliferation and promotes apoptosis in gastric cancer. Am J Transl Res *9*, 4317-4330.

Blauwkamp, T.A., Nigam, S., Ardehali, R., Weissman, I.L., and Nusse, R. (2012). Endogenous Wnt signalling in human embryonic stem cells generates an equilibrium of distinct lineage-specified progenitors. Nat Commun *3*, 1070.

Blum, B., and Benvenisty, N. (2008). The tumorigenicity of human embryonic stem cells. Adv Cancer Res *100*, 133-158.

Bording, T., Abdo, A.N., Maier, B., Gabriel, C., and Kramer, A. (2019). Generation of Human CRY1 and CRY2 Knockout Cells Using Duplex CRISPR/Cas9 Technology. Front Physiol *10*, 577.

Boulbes, D., Chen, C.H., Shaikenov, T., Agarwal, N.K., Peterson, T.R., Addona, T.A., Keshishian, H., Carr, S.A., Magnuson, M.A., Sabatini, D.M.*, et al.* (2010). Rictor phosphorylation on the Thr-1135 site does not require mammalian target of rapamycin complex 2. Mol Cancer Res *8*, 896-906.

Boyer, L.A., Lee, T.I., Cole, M.F., Johnstone, S.E., Levine, S.S., Zucker, J.P., Guenther, M.G., Kumar, R.M., Murray, H.L., Jenner, R.G.*, et al.* (2005). Core transcriptional regulatory circuitry in human embryonic stem cells. Cell *122*, 947-956.

Bratt-Leal, A.M., Carpenedo, R.L., and McDevitt, T.C. (2009). Engineering the embryoid body microenvironment to direct embryonic stem cell differentiation. Biotech Prog *25*, 43-51.

Brembeck, F.H., Rosario, M., and Birchmeier, W. (2006). Balancing cell adhesion and Wnt signaling, the key role of beta-catenin. Curr Opin Genet Dev *16*, 51-59.

Bressan, R.B., Dewari, P.S., Kalantzaki, M., Gangoso, E., Matjusaitis, M., Garcia-Diaz, C., Blin, C., Grant, V., Bulstrode, H., Gogolok, S.*, et al.* (2017). Efficient CRISPR/Cas9-assisted gene targeting enables rapid and precise genetic manipulation of mammalian neural stem cells. Development *144*, 635-648.

Brons, I.G., Smithers, L.E., Trotter, M.W., Rugg-Gunn, P., Sun, B., Chuva de Sousa Lopes, S.M., Howlett, S.K., Clarkson, A., Ahrlund-Richter, L., Pedersen, R.A., *et al.* (2007). Derivation of pluripotent epiblast stem cells from mammalian embryos. Nature *448*, 191-195.

Brown, E.J., Albers, M.W., Shin, T.B., Ichikawa, K., Keith, C.T., Lane, W.S., and Schreiber, S.L. (1994). A mammalian protein targeted by G1-arresting rapamycin-receptor complex. Nature *369*, 756-758.

Brugarolas, J., Lei, K., Hurley, R.L., Manning, B.D., Reiling, J.H., Hafen, E., Witters, L.A., Ellisen, L.W., and Kaelin, W.G., Jr. (2004). Regulation of mTOR function in response to hypoxia by REDD1 and the TSC1/TSC2 tumor suppressor complex. Gene Dev *18*, 2893-2904.

Brunn, G.J., Hudson, C.C., Sekulic, A., Williams, J.M., Hosoi, H., Houghton, P.J., Lawrence, J.C., Jr., and Abraham, R.T. (1997). Phosphorylation of the translational repressor PHAS-I by the mammalian target of rapamycin. Science *277*, 99-101.

Bulut-Karslioglu, A., Biechele, S., Jin, H., Macrae, T.A., Hejna, M., Gertsenstein, M., Song, J.S., and Ramalho-Santos, M. (2016). Inhibition of mTOR induces a paused pluripotent state. Nature *540*, 119-123.

Cameron, A.J., Linch, M.D., Saurin, A.T., Escribano, C., and Parker, P.J. (2011). mTORC2 targets AGC kinases through Sin1-dependent recruitment. Biochem J *439*, 287-297.

Cameron, A.J.M., Veeriah, S., Marshall, J.J.T., Murray, E.R., Larijani, B., and Parker, P.J. (2017). Uncoupling TORC2 from AGC kinases inhibits tumour growth. Oncotarget *8*, 84685-84696.

Cardenas-Rodriguez, M., Irigoin, F., Osborn, D.P., Gascue, C., Katsanis, N., Beales, P.L., and Badano, J.L. (2013). The Bardet-Biedl syndrome-related protein CCDC28B modulates mTORC2 function and interacts with SIN1 to control cilia length independently of the mTOR complex. Hum Mol Genet *22*, 4031-4042.

Chambers, I., Colby, D., Robertson, M., Nichols, J., Lee, S., Tweedie, S., and Smith, A. (2003). Functional expression cloning of Nanog, a pluripotency sustaining factor in embryonic stem cells. Cell *113*, 643-655.

Chan, Y.S., Goke, J., Ng, J.H., Lu, X., Gonzales, K.A., Tan, C.P., Tng, W.Q., Hong, Z.Z., Lim, Y.S., and Ng, H.H. (2013). Induction of a human pluripotent state with distinct regulatory circuitry that resembles preimplantation epiblast. Cell Stem Cell *13*, 663-675.

Chandrasekaran, S., Zhang, J., Sun, Z., Zhang, L., Ross, C.A., Huang, Y.C., Asara, J.M., Li, H., Daley, G.Q., and Collins, J.J. (2017). Comprehensive Mapping of Pluripotent Stem Cell Metabolism Using Dynamic Genome-Scale Network Modeling. Cell Rep *21*, 2965-2977.

Chen, C.H., Kiyan, V., Zhylkibayev, A.A., Kazyken, D., Bulgakova, O., Page, K.E., Bersimbaev, R.I., Spooner, E., and Sarbassov dos, D. (2013). Autoregulation of the mechanistic target of rapamycin (mTOR) complex 2 integrity is controlled by an ATP-dependent mechanism. J Biol Chem *288*, 27019-27030.

Chen, C.H., and Sarbassov dos, D. (2011). The mTOR (mammalian target of rapamycin) kinase maintains integrity of mTOR complex 2. J Biol Chem *286*, 40386-40394.

Chen, G., Hou, Z., Gulbranson, D.R., and Thomson, J.A. (2010). Actin-myosin contractility is responsible for the reduced viability of dissociated human embryonic stem cells. Cell Stem Cell *7*, 240-248.

Chen, L., Xu, B., Liu, L., Liu, C., Luo, Y., Chen, X., Barzegar, M., Chung, J., and Huang, S. (2015a). Both mTORC1 and mTORC2 are involved in the regulation of cell adhesion. Oncotarget *6*, 7136-7150.

Chen, X., Liu, M., Tian, Y., Li, J., Qi, Y., Zhao, D., Wu, Z., Huang, M., Wong, C.C.L., Wang, H.W.*, et al.* (2018). Cryo-EM structure of human mTOR complex 2. Cell Res *28*, 518-528.

Chen, Z., Yi, W., Morita, Y., Wang, H., Cong, Y., Liu, J.P., Xiao, Z., Rudolph, K.L., Cheng, T., and Ju, Z. (2015b). Wip1 deficiency impairs haematopoietic stem cell function via p53 and mTORC1 pathways. Nat Commun *6*, 6808.

Cheng, J., Zhang, D., Kim, K., Zhao, Y., Zhao, Y., and Su, B. (2005). Mip1, an MEKK2-interacting protein, controls MEKK2 dimerization and activation. Mol Cell Biol *25*, 5955-5964.

Chew, J.L., Loh, Y.H., Zhang, W., Chen, X., Tam, W.L., Yeap, L.S., Li, P., Ang, Y.S., Lim, B., Robson, P.*, et al.* (2005). Reciprocal transcriptional regulation of Pou5f1 and Sox2 via the Oct4/Sox2 complex in embryonic stem cells. Mol Cell Biol *25*, 6031-6046.

Chiu, M.I., Katz, H., and Berlin, V. (1994). RAPT1, a mammalian homolog of yeast Tor, interacts with the FKBP12/rapamycin complex. Proc Natl Acad Sci U S A *91*, 12574-12578.

Cho, H.J., Park, J., Lee, H.W., Lee, Y.S., and Kim, J.B. (2004). Regulation of adipocyte differentiation and insulin action with rapamycin. Biochem Biophys Res Commun *321*, 942-948.

Chung, J., Kuo, C.J., Crabtree, G.R., and Blenis, J. (1992). Rapamycin-FKBP specifically blocks growth-dependent activation of and signaling by the 70 kd S6 protein kinases. Cell *69*, 1227-1236.

Collier, A.J., and Rugg-Gunn, P.J. (2018). Identifying Human Naive Pluripotent Stem Cells - Evaluating State-Specific Reporter Lines and Cell-Surface Markers. BioEssays *40*, e1700239.

Collinson, A., Collier, A.J., Morgan, N.P., Sienerth, A.R., Chandra, T., Andrews, S., and Rugg-Gunn, P.J. (2016). Deletion of the Polycomb-Group Protein EZH2 Leads to Compromised Self-Renewal and Differentiation Defects in Human Embryonic Stem Cells. Cell Rep *17*, 2700-2714.

Corradetti, M.N., Inoki, K., Bardeesy, N., DePinho, R.A., and Guan, K.L. (2004). Regulation of the TSC pathway by LKB1: evidence of a molecular link between tuberous sclerosis complex and Peutz-Jeghers syndrome. Genes Dev *18*, 1533-1538.

Cradick, T.J., Fine, E.J., Antico, C.J., and Bao, G. (2013). CRISPR/Cas9 systems targeting beta-globin and CCR5 genes have substantial off-target activity. Nucleic Acids Res *41*, 9584-9592.

Cybulski, N., Polak, P., Auwerx, J., Ruegg, M.A., and Hall, M.N. (2009). mTOR complex 2 in adipose tissue negatively controls whole-body growth. Proc Natl Acad Sci U S A *106*, 9902-9907.

Czerwinska, P., Mazurek, S., Kolodziejczak, I., and Wiznerowicz, M. (2019). Gene delivery methods and genome editing of human pluripotent stem cells. Rep Pract Oncol Radiother *24*, 180-187.

Daheron, L., Opitz, S.L., Zaehres, H., Lensch, M.W., Andrews, P.W., Itskovitz-Eldor, J., and Daley, G.Q. (2004). LIF/STAT3 signaling fails to maintain self-renewal of human embryonic stem cells. Stem Cells *22*, 770-778.

Das, G., Shiras, A., Shanmuganandam, K., and Shastry, P. (2011). Rictor regulates MMP-9 activity and invasion through Raf-1-MEK-ERK signaling pathway in glioma cells. Mol Carcinog *50*, 412-423.

Dazert, E., and Hall, M.N. (2011). mTOR signaling in disease. Curr Opin Cell Biol *23*, 744-755.

Dibble, C.C., Asara, J.M., and Manning, B.D. (2009). Characterization of Rictor phosphorylation sites reveals direct regulation of mTOR complex 2 by S6K1. Mol Cell Biol *29*, 5657-5670.

Dorrello, N.V., Peschiaroli, A., Guardavaccaro, D., Colburn, N.H., Sherman, N.E., and Pagano, M. (2006). S6K1- and betaTRCP-mediated degradation of PDCD4 promotes protein translation and cell growth. Science *314*, 467-471.

Driscoll, D.R., Karim, S.A., Sano, M., Gay, D.M., Jacob, W., Yu, J., Mizukami, Y., Gopinathan, A., Jodrell, D.I., Evans, T.R.*, et al.* (2016). mTORC2 Signaling Drives the Development and Progression of Pancreatic Cancer. Cancer Res *76*, 6911-6923.

Duggal, G., Warrier, S., Ghimire, S., Broekaert, D., Van der Jeught, M., Lierman, S., Deroo, T., Peelman, L., Van Soom, A., Cornelissen, R.*, et al.* (2015). Alternative Routes to Induce Naive Pluripotency in Human Embryonic Stem Cells. Stem Cells *33*, 2686-2698.

Dutta, D., Ray, S., Home, P., Larson, M., Wolfe, M.W., and Paul, S. (2011). Self-renewal versus lineage commitment of embryonic stem cells: protein kinase C signaling shifts the balance. Stem Cells *29*, 618-628.

Easley, C.A.t., Ben-Yehudah, A., Redinger, C.J., Oliver, S.L., Varum, S.T., Eisinger, V.M., Carlisle, D.L., Donovan, P.J., and Schatten, G.P. (2010). mTOR-mediated activation of p70 S6K induces differentiation of pluripotent human embryonic stem cells. Cell Reprogram *12*, 263-273.

Ebner, M., Lucic, I., Leonard, T.A., and Yudushkin, I. (2017). PI(3,4,5)P3 Engagement Restricts Akt Activity to Cellular Membranes. Mol Cell *65*, 416-431 e416.

Eiges, R., Schuldiner, M., Drukker, M., Yanuka, O., Itskovitz-Eldor, J., and Benvenisty, N. (2001). Establishment of human embryonic stem cell-transfected clones carrying a marker for undifferentiated cells. Curr Biol *11*, 514-518.

Erard, N., Knott, S.R.V., and Hannon, G.J. (2017). A CRISPR Resource for Individual, Combinatorial, or Multiplexed Gene Knockout. Mol Cell *67*, 1080.

Farboud, B., Jarvis, E., Roth, T.L., Shin, J., Corn, J.E., Marson, A., Meyer, B.J., Patel, N.H., and Hochstrasser, M.L. (2018). Enhanced Genome Editing with Cas9 Ribonucleoprotein in Diverse Cells and Organisms. J Vis Exp.

Farhan, M., Wang, H., Gaur, U., Little, P.J., Xu, J., and Zheng, W. (2017). FOXO Signaling Pathways as Therapeutic Targets in Cancer. Int J Biol Sci *13*, 815-827.

Festuccia, N., Osorno, R., Wilson, V., and Chambers, I. (2013). The role of pluripotency gene regulatory network components in mediating transitions between pluripotent cell states. Curr Opin Genet Dev *23*, 504-511.

Fodale, V., Pierobon, M., Liotta, L., and Petricoin, E. (2011). Mechanism of cell adaptation: when and how do cancer cells develop chemoresistance? Cancer J *17*, 89-95.

Fogarty, N.M.E., McCarthy, A., Snijders, K.E., Powell, B.E., Kubikova, N., Blakeley, P., Lea, R., Elder, K., Wamaitha, S.E., Kim, D.*, et al.* (2017). Genome editing reveals a role for OCT4 in human embryogenesis. Nature *550*, 67-73.

Fong, H., Hohenstein, K.A., and Donovan, P.J. (2008). Regulation of self-renewal and pluripotency by Sox2 in human embryonic stem cells. Stem Cells *26*, 1931-1938.

Foster, K.G., Acosta-Jaquez, H.A., Romeo, Y., Ekim, B., Soliman, G.A., Carriere, A., Roux, P.P., Ballif, B.A., and Fingar, D.C. (2010). Regulation of mTOR complex 1 (mTORC1) by raptor Ser863 and multisite phosphorylation. J Biol Chem *285*, 80-94.

Frias, M.A., Thoreen, C.C., Jaffe, J.D., Schroder, W., Sculley, T., Carr, S.A., and Sabatini, D.M. (2006). mSin1 is necessary for Akt/PKB phosphorylation, and its isoforms define three distinct mTORC2s. Curr Biol *16*, 1865-1870.

Fu, Y., Foden, J.A., Khayter, C., Maeder, M.L., Reyon, D., Joung, J.K., and Sander, J.D. (2013). High-frequency off-target mutagenesis induced by CRISPR-Cas nucleases in human cells. Nat Biotechnol *31*, 822-826.

Gabriel, R., Lombardo, A., Arens, A., Miller, J.C., Genovese, P., Kaeppel, C., Nowrouzi, A., Bartholomae, C.C., Wang, J., Friedman, G.*, et al.* (2011). An unbiased genome-wide analysis of zinc-finger nuclease specificity. Nat Biotechnol *29*, 816-823.

Gafni, O., Weinberger, L., Mansour, A.A., Manor, Y.S., Chomsky, E., Ben-Yosef, D., Kalma, Y., Viukov, S., Maza, I., Zviran, A.*, et al.* (2013). Derivation of novel human ground state naive pluripotent stem cells. Nature *504*, 282-286.

Gan, X., Wang, J., Su, B., and Wu, D. (2011). Evidence for direct activation of mTORC2 kinase activity by phosphatidylinositol 3,4,5-trisphosphate. J Biol Chem *286*, 10998-11002.

Gan, X., Wang, J., Wang, C., Sommer, E., Kozasa, T., Srinivasula, S., Alessi, D., Offermanns, S., Simon, M.I., and Wu, D. (2012). PRR5L degradation promotes mTORC2-mediated PKC-delta phosphorylation and cell migration downstream of Galpha12. Nat Cell Biol *14*, 686-696.

Gangloff, Y.G., Mueller, M., Dann, S.G., Svoboda, P., Sticker, M., Spetz, J.F., Um, S.H., Brown, E.J., Cereghini, S., Thomas, G.*, et al.* (2004). Disruption of the mouse mTOR gene leads to early postimplantation lethality and prohibits embryonic stem cell development. Mol Cell Biol *24*, 9508-9516.

Gao, D., Wan, L., Inuzuka, H., Berg, A.H., Tseng, A., Zhai, B., Shaik, S., Bennett, E., Tron, A.E., Gasser, J.A.*, et al.* (2010). Rictor forms a complex with Cullin-1 to promote SGK1 ubiquitination and destruction. Mol Cell *39*, 797-808.

Garcia-Martinez, J.M., and Alessi, D.R. (2008). mTOR complex 2 (mTORC2) controls hydrophobic motif phosphorylation and activation of serum- and glucocorticoid-induced protein kinase 1 (SGK1). Biochem J *416*, 375-385.

Geest, C.R., Zwartkruis, F.J., Vellenga, E., Coffer, P.J., and Buitenhuis, M. (2009). Mammalian target of rapamycin activity is required for expansion of CD34+ hematopoietic progenitor cells. Haematologica *94*, 901-910.

Ghosh, D., Srivastava, G.P., Xu, D., Schulz, L.C., and Roberts, R.M. (2008). A link between SIN1 (MAPKAP1) and poly(rC) binding protein 2 (PCBP2) in counteracting environmental stress. Proc Natl Acad Sci U S A *105*, 11673-11678.

Gingras, A.C., Gygi, S.P., Raught, B., Polakiewicz, R.D., Abraham, R.T., Hoekstra, M.F., Aebersold, R., and Sonenberg, N. (1999). Regulation of 4E-BP1 phosphorylation: a novel two-step mechanism. Genes Dev *13*, 1422-1437.

Gkountakos, A., Pilotto, S., Mafficini, A., Vicentini, C., Simbolo, M., Milella, M., Tortora, G., Scarpa, A., Bria, E., and Corbo, V. (2018). Unmasking the impact of Rictor in cancer: novel insights of mTORC2 complex. Carcinogenesis.

Gleason, C.E., Oses-Prieto, J.A., Li, K.H., Saha, B., Situ, G., Burlingame, A.L., and Pearce, D. (2019). Phosphorylation at distinct subcellular locations underlies specificity in mTORC2-mediated activation of SGK1 and Akt. J Cell Sci *132*.

Glidden, E.J., Gray, L.G., Vemuru, S., Li, D., Harris, T.E., and Mayo, M.W. (2012). Multiple site acetylation of Rictor stimulates mammalian target of rapamycin complex 2 (mTORC2)-dependent phosphorylation of Akt protein. J Biol Chem *287*, 581-588.

Gomez-Salinero, J.M., Lopez-Olaneta, M.M., Ortiz-Sanchez, P., Larrasa-Alonso, J., Gatto, A., Felkin, L.E., Barton, P.J.R., Navarro-Lerida, I., Angel Del Pozo, M., Garcia-Pavia, P.*, et al.* (2016). The Calcineurin Variant CnAbeta1 Controls Mouse Embryonic Stem Cell Differentiation by Directing mTORC2 Membrane Localization and Activation. Cell Chem Biol *23*, 1372-1382.

Greber, B., Lehrach, H., and Adjaye, J. (2007). Fibroblast growth factor 2 modulates transforming growth factor beta signaling in mouse embryonic fibroblasts and human ESCs (hESCs) to support hESC self-renewal. Stem Cells *25*, 455-464.

Gropp, M., Itsykson, P., Singer, O., Ben-Hur, T., Reinhartz, E., Galun, E., and Reubinoff, B.E. (2003). Stable genetic modification of human embryonic stem cells by lentiviral vectors. Mol Ther *7*, 281-287.

Guertin, D.A., Stevens, D.M., Thoreen, C.C., Burds, A.A., Kalaany, N.Y., Moffat, J., Brown, M., Fitzgerald, K.J., and Sabatini, D.M. (2006). Ablation in mice of the mTORC components raptor, rictor, or mLST8 reveals that mTORC2 is required for signaling to Akt-FOXO and PKCalpha, but not S6K1. Dev Cell *11*, 859-871.

Guo, G., von Meyenn, F., Santos, F., Chen, Y., Reik, W., Bertone, P., Smith, A., and Nichols, J. (2016). Naive Pluripotent Stem Cells Derived Directly from Isolated Cells of the Human Inner Cell Mass. Stem Cell Rep *6*, 437-446.

Guo, Z., Zhou, Y., Evers, B.M., and Wang, Q. (2012). Rictor regulates FBXW7-dependent c-Myc and cyclin E degradation in colorectal cancer cells. Biochem Biophys Res Commun *418*, 426-432.

Gwinn, D.M., Shackelford, D.B., Egan, D.F., Mihaylova, M.M., Mery, A., Vasquez, D.S., Turk, B.E., and Shaw, R.J. (2008). AMPK phosphorylation of raptor mediates a metabolic checkpoint. Mol Cell *30*, 214-226.

Hagan, G.N., Lin, Y., Magnuson, M.A., Avruch, J., and Czech, M.P. (2008). A Rictor-Myo1c complex participates in dynamic cortical actin events in 3T3-L1 adipocytes. Mol Cell Biol *28*, 4215-4226.

Hanna, J., Cheng, A.W., Saha, K., Kim, J., Lengner, C.J., Soldner, F., Cassady, J.P., Muffat, J., Carey, B.W., and Jaenisch, R. (2010). Human embryonic stem cells with biological and epigenetic characteristics similar to those of mouse ESCs. Proc Natl Acad Sci U S A *107*, 9222-9227.

Hara, K., Maruki, Y., Long, X., Yoshino, K., Oshiro, N., Hidayat, S., Tokunaga, C., Avruch, J., and Yonezawa, K. (2002). Raptor, a binding partner of target of rapamycin (TOR), mediates TOR action. Cell *110*, 177-189.

Harrington, L.S., Findlay, G.M., Gray, A., Tolkacheva, T., Wigfield, S., Rebholz, H., Barnett, J., Leslie, N.R., Cheng, S., Shepherd, P.R.*, et al.* (2004). The TSC1-2 tumor suppressor controls insulin-PI3K signaling via regulation of IRS proteins. J Cell Biol *166*, 213-223.

Hay, D.C., Sutherland, L., Clark, J., and Burdon, T. (2004). Oct-4 knockdown induces similar patterns of endoderm and trophoblast differentiation markers in human and mouse embryonic stem cells. Stem Cells *22*, 225-235.

Hay, N. (2011). Interplay between FOXO, TOR, and Akt. Biochim Biophys Acta *1813*, 1965-1970.

Hayashi, T., Hatanaka, M., Nagao, K., Nakaseko, Y., Kanoh, J., Kokubu, A., Ebe, M., and Yanagida, M. (2007). Rapamycin sensitivity of the Schizosaccharomyces pombe tor2 mutant and organization of two highly phosphorylated TOR complexes by specific and common subunits. Genes Cells *12*, 1357-1370.

He, Y., Li, D., Cook, S.L., Yoon, M.S., Kapoor, A., Rao, C.V., Kenis, P.J., Chen, J., and Wang, F. (2013). Mammalian target of rapamycin and Rictor control neutrophil chemotaxis by regulating Rac/Cdc42 activity and the actin cytoskeleton. Mol Biol Cell *24*, 3369-3380.

Helliwell, S.B., Wagner, P., Kunz, J., Deuter-Reinhard, M., Henriquez, R., and Hall, M.N. (1994). TOR1 and TOR2 are structurally and functionally similar but not identical phosphatidylinositol kinase homologues in yeast. Mol Biol Cell *5*, 105-118.

Hofmann, C., Obermeier, F., Artinger, M., Hausmann, M., Falk, W., Schoelmerich, J., Rogler, G., and Grossmann, J. (2007). Cell-cell contacts prevent anoikis in primary human colonic epithelial cells. Gastroenterology *132*, 587-600.

Holz, M.K., Ballif, B.A., Gygi, S.P., and Blenis, J. (2005). mTOR and S6K1 mediate assembly of the translation preinitiation complex through dynamic protein interchange and ordered phosphorylation events. Cell *123*, 569-580.

Honda, A., Hatori, M., Hirose, M., Honda, C., Izu, H., Inoue, K., Hirasawa, R., Matoba, S., Togayachi, S., Miyoshi, H.*, et al.* (2013). Naive-like conversion overcomes the limited differentiation capacity of induced pluripotent stem cells. J Biol Chem *288*, 26157-26166.

Hornbeck, P.V., Zhang, B., Murray, B., Kornhauser, J.M., Latham, V., and Skrzypek, E. (2015). PhosphoSitePlus, 2014: mutations, PTMs and recalibrations. Nucleic Acids Res *43*, D512-520.

Hsu, P.D., and Zhang, F. (2012). Dissecting neural function using targeted genome engineering technologies. ACS Chem Neurosci *3*, 603-610.

Hsu, P.P., Kang, S.A., Rameseder, J., Zhang, Y., Ottina, K.A., Lim, D., Peterson, T.R., Choi, Y., Gray, N.S., Yaffe, M.B.*, et al.* (2011). The mTOR-regulated phosphoproteome reveals a mechanism of mTORC1-mediated inhibition of growth factor signaling. Science *332*, 1317-1322.

Hu, Q., and Rosenfeld, M.G. (2012). Epigenetic regulation of human embryonic stem cells. Front Genet *3*, 238.

Hu, Z., Wang, Y., Wang, Y., Zang, B., Hui, H., You, Z., and Wang, X. (2017). Epigenetic activation of SIN1 promotes NSCLC cell proliferation and metastasis by affecting the epithelial-mesenchymal transition. Biochem Biophys Res Commun *483*, 645-651.

Hua, H., Kong, Q., Zhang, H., Wang, J., Luo, T., and Jiang, Y. (2019). Targeting mTOR for cancer therapy. J Hematol Oncol *12*, 71.

Huang, H., and Tindall, D.J. (2007). Dynamic FoxO transcription factors. J Cell Sci *120*, 2479-2487.

Huang, J., Wu, S., Wu, C.L., and Manning, B.D. (2009). Signaling events downstream of mammalian target of rapamycin complex 2 are attenuated in cells and tumors deficient for the tuberous sclerosis complex tumor suppressors. Cancer Res *69*, 6107-6114.

Huang, T.S., Li, L., Moalim-Nour, L., Jia, D., Bai, J., Yao, Z., Bennett, S.A., Figeys, D., and Wang, L. (2015). A Regulatory Network Involving beta-Catenin, e-Cadherin, PI3k/Akt, and Slug Balances Self-Renewal and Differentiation of Human Pluripotent Stem Cells In Response to Wnt Signaling. Stem Cells *33*, 1419-1433.

Hwang, S.K., and Kim, H.H. (2011). The functions of mTOR in ischemic diseases. BMB Rep *44*, 506-511.

Hwang, Y., Kim, L.C., Song, W., Edwards, D.N., Cook, R.S., and Chen, J. (2019). Disruption of the Scaffolding Function of mLST8 Selectively Inhibits mTORC2 Assembly and Function and Suppresses mTORC2-Dependent Tumor Growth In Vivo. Cancer Res *79*, 3178-3184.

Hwang, Y.S., Chung, B.G., Ortmann, D., Hattori, N., Moeller, H.C., and Khademhosseini, A. (2009). Microwell-mediated control of embryoid body size regulates embryonic stem cell fate via differential expression of WNT5a and WNT11. Proc Natl Acad Sci U S A *106*, 16978-16983.

Hyslop, L., Stojkovic, M., Armstrong, L., Walter, T., Stojkovic, P., Przyborski, S., Herbert, M., Murdoch, A., Strachan, T., and Lako, M. (2005). Downregulation of NANOG induces differentiation of human embryonic stem cells to extraembryonic lineages. Stem Cells *23*, 1035-1043.

Ikenoue, T., Inoki, K., Yang, Q., Zhou, X., and Guan, K.L. (2008). Essential function of TORC2 in PKC and Akt turn motif phosphorylation, maturation and signalling. EMBO J *27*, 1919-1931.

Inoki, K., Li, Y., Zhu, T., Wu, J., and Guan, K.L. (2002). TSC2 is phosphorylated and inhibited by Akt and suppresses mTOR signalling. Nat Cell Biol *4*, 648-657.

Inoki, K., Ouyang, H., Zhu, T., Lindvall, C., Wang, Y., Zhang, X., Yang, Q., Bennett, C., Harada, Y., Stankunas, K.*, et al.* (2006). TSC2 integrates Wnt and energy signals via a coordinated phosphorylation by AMPK and GSK3 to regulate cell growth. Cell *126*, 955-968.

Inoki, K., Zhu, T., and Guan, K.L. (2003). TSC2 mediates cellular energy response to control cell growth and survival. Cell *115*, 577-590.

Ishino, Y., Shinagawa, H., Makino, K., Amemura, M., and Nakata, A. (1987). Nucleotide sequence of the iap gene, responsible for alkaline phosphatase isozyme conversion in Escherichia coli, and identification of the gene product. J Bacteriol *169*, 5429-5433.

Isomoto, S., Hattori, K., Ohgushi, H., Nakajima, H., Tanaka, Y., and Takakura, Y. (2007). Rapamycin as an inhibitor of osteogenic differentiation in bone marrow-derived mesenchymal stem cells. J Orthop Sci *12*, 83-88.

Itskovitz-Eldor, J., Schuldiner, M., Karsenti, D., Eden, A., Yanuka, O., Amit, M., Soreq, H., and Benvenisty, N. (2000). Differentiation of human embryonic stem cells into embryoid bodies compromising the three embryonic germ layers. Mol Med *6*, 88-95.

Jacinto, E., Facchinetti, V., Liu, D., Soto, N., Wei, S., Jung, S.Y., Huang, Q., Qin, J., and Su, B. (2006). SIN1/MIP1 maintains rictor-mTOR complex integrity and regulates Akt phosphorylation and substrate specificity. Cell *127*, 125-137.

Jacinto, E., Loewith, R., Schmidt, A., Lin, S., Ruegg, M.A., Hall, A., and Hall, M.N. (2004). Mammalian TOR complex 2 controls the actin cytoskeleton and is rapamycin insensitive. Nat Cell Biol *6*, 1122-1128.

Jansen, R., Embden, J.D., Gaastra, W., and Schouls, L.M. (2002). Identification of genes that are associated with DNA repeats in prokaryotes. Mol Microbiol *43*, 1565-1575.

Jiang, W., Bikard, D., Cox, D., Zhang, F., and Marraffini, L.A. (2013). RNA-guided editing of bacterial genomes using CRISPR-Cas systems. Nat Biotechnol *31*, 233-239.

Jinek, M., Chylinski, K., Fonfara, I., Hauer, M., Doudna, J.A., and Charpentier, E. (2012). A programmable dual-RNA-guided DNA endonuclease in adaptive bacterial immunity. Science *337*, 816-821.

Julien, L.A., Carriere, A., Moreau, J., and Roux, P.P. (2010). mTORC1-activated S6K1 phosphorylates Rictor on threonine 1135 and regulates mTORC2 signaling. Mol Cell Biol *30*, 908-921.

Jung, J.H., Kang, K.W., Kim, J., Hong, S.C., Park, Y., and Kim, B.S. (2016). CXCR2 Inhibition in Human Pluripotent Stem Cells Induces Predominant Differentiation to Mesoderm and Endoderm Through Repression of mTOR, beta-Catenin, and hTERT Activities. Stem Cells Dev *25*, 1006-1019.

Kang, H.B., Kim, J.S., Kwon, H.J., Nam, K.H., Youn, H.S., Sok, D.E., and Lee, Y. (2005). Basic fibroblast growth factor activates ERK and induces c-fos in human embryonic stem cell line MizhES1. Stem Cells Dev *14*, 395-401.

Karp, J.M., Yeh, J., Eng, G., Fukuda, J., Blumling, J., Suh, K.Y., Cheng, J., Mahdavi, A., Borenstein, J., Langer, R.*, et al.* (2007). Controlling size, shape and homogeneity of embryoid bodies using poly(ethylene glycol) microwells. Lab Chip *7*, 786-794.

Karuppasamy, M., Kusmider, B., Oliveira, T.M., Gaubitz, C., Prouteau, M., Loewith, R., and Schaffitzel, C. (2017). Cryo-EM structure of Saccharomyces cerevisiae target of rapamycin complex 2. Nat Commun *8*, 1729.

Kataoka, S., Furuita, K., Hattori, Y., Kobayashi, N., Ikegami, T., Shiozaki, K., Fujiwara, T., and Kojima, C. (2015). (1)H, (15)N and (13)C resonance assignments of the conserved region in the middle domain of S. pombe Sin1 protein. Biomol NMR Assign *9*, 89-92.

Kazyken, D., Magnuson, B., Bodur, C., Acosta-Jaquez, H.A., Zhang, D., Tong, X., Barnes, T.M., Steinl, G.K., Patterson, N.E., Altheim, C.H.*, et al.* (2019). AMPK directly activates mTORC2 to promote cell survival during acute energetic stress. Sci Signal *12*.

Keller, G. (2005). Embryonic stem cell differentiation: emergence of a new era in biology and medicine. Genes Dev *19*, 1129-1155.

Kim, D.H., Sarbassov, D.D., Ali, S.M., King, J.E., Latek, R.R., Erdjument-Bromage, H., Tempst, P., and Sabatini, D.M. (2002). mTOR interacts with raptor to form a nutrient-sensitive complex that signals to the cell growth machinery. Cell *110*, 163-175.

Kim, D.H., Sarbassov, D.D., Ali, S.M., Latek, R.R., Guntur, K.V., Erdjument-Bromage, H., Tempst, P., and Sabatini, D.M. (2003). GbetaL, a positive regulator of the rapamycin-sensitive pathway required for the nutrient-sensitive interaction between raptor and mTOR. Mol Cell *11*, 895-904.

Kim, E., Goraksha-Hicks, P., Li, L., Neufeld, T.P., and Guan, K.L. (2008). Regulation of TORC1 by Rag GTPases in nutrient response. Nat Cell Biol *10*, 935-945.

Kim, H., Wu, J., Ye, S., Tai, C.I., Zhou, X., Yan, H., Li, P., Pera, M., and Ying, Q.L. (2013). Modulation of beta-catenin function maintains mouse epiblast stem cell and human embryonic stem cell self-renewal. Nat Commun *4*, 2403.

Kim, J., and Guan, K.L. (2019). mTOR as a central hub of nutrient signalling and cell growth. Nat Cell Biol *21*, 63-71.

Kim, J., Kundu, M., Viollet, B., and Guan, K.L. (2011). AMPK and mTOR regulate autophagy through direct phosphorylation of Ulk1. Nat Cell Biol *13*, 132-141.

Kim, S., Kim, D., Cho, S.W., Kim, J., and Kim, J.S. (2014). Highly efficient RNA-guided genome editing in human cells via delivery of purified Cas9 ribonucleoproteins. Genome Res *24*, 1012-1019.

Kinoshita, M., Shimosato, D., Yamane, M., and Niwa, H. (2015). Sox7 is dispensable for primitive endoderm differentiation from mouse ES cells. BMC Dev Biol *15*, 37.

Kleinstiver, B.P., Pattanayak, V., Prew, M.S., Tsai, S.Q., Nguyen, N.T., Zheng, Z., and Joung, J.K. (2016). High-fidelity CRISPR-Cas9 nucleases with no detectable genome-wide off-target effects. Nature *529*, 490-495.

Kobayashi, T., and Cohen, P. (1999). Activation of serum- and glucocorticoid-regulated protein kinase by agonists that activate phosphatidylinositide 3-kinase is mediated by 3-phosphoinositide-dependent protein kinase-1 (PDK1) and PDK2. Biochem J *339 (Pt 2)*, 319-328.

Kumar, A., Lawrence, J.C., Jr., Jung, D.Y., Ko, H.J., Keller, S.R., Kim, J.K., Magnuson, M.A., and Harris, T.E. (2010). Fat cell-specific ablation of rictor in mice impairs insulin-regulated fat cell and whole-body glucose and lipid metabolism. Diabetes *59*, 1397-1406.

Kunz, J., Henriquez, R., Schneider, U., Deuter-Reinhard, M., Movva, N.R., and Hall, M.N. (1993). Target of rapamycin in yeast, TOR2, is an essential phosphatidylinositol kinase homolog required for G1 progression. Cell *73*, 585-596.

Kuo, C.J., Chung, J., Fiorentino, D.F., Flanagan, W.M., Blenis, J., and Crabtree, G.R. (1992). Rapamycin selectively inhibits interleukin-2 activation of p70 S6 kinase. Nature *358*, 70-73.

Kurek, D., Neagu, A., Tastemel, M., Tuysuz, N., Lehmann, J., van de Werken, H.J.G., Philipsen, S., van der Linden, R., Maas, A., van, I.W.F.J.*, et al.* (2015). Endogenous WNT signals mediate BMP-induced and spontaneous differentiation of epiblast stem cells and human embryonic stem cells. Stem Cell Rep *4*, 114-128.

Kurosawa, H. (2007). Methods for inducing embryoid body formation: in vitro differentiation system of embryonic stem cells. J Biosci Bioeng *103*, 389-398.

Lakshmipathy, U., Pelacho, B., Sudo, K., Linehan, J.L., Coucouvanis, E., Kaufman, D.S., and Verfaillie, C.M. (2004). Efficient transfection of embryonic and adult stem cells. Stem Cells *22*, 531-543.

Lamming, D.W., Ye, L., Katajisto, P., Goncalves, M.D., Saitoh, M., Stevens, D.M., Davis, J.G., Salmon, A.B., Richardson, A., Ahima, R.S.*, et al.* (2012). Rapamycin-induced insulin resistance is mediated by mTORC2 loss and uncoupled from longevity. Science *335*, 1638-1643.

Laplante, M., and Sabatini, D.M. (2012). mTOR signaling in growth control and disease. Cell *149*, 274-293.

Lee, D.F., Kuo, H.P., Chen, C.T., Hsu, J.M., Chou, C.K., Wei, Y., Sun, H.L., Li, L.Y., Ping, B., Huang, W.C.*, et al.* (2007). IKK beta suppression of TSC1 links inflammation and tumor angiogenesis via the mTOR pathway. Cell *130*, 440-455.

Lee, H.K., Kwon, B., Lemere, C.A., de la Monte, S., Itamura, K., Ha, A.Y., and Querfurth, H.W. (2017). mTORC2 (Rictor) in Alzheimer's Disease and Reversal of Amyloid-beta Expression-Induced Insulin Resistance and Toxicity in Rat Primary Cortical Neurons. J Alzheimers Dis *56*, 1015-1036.

Lee, J.E., Lim, M.S., Park, J.H., Park, C.H., and Koh, H.C. (2016a). PTEN Promotes Dopaminergic Neuronal Differentiation Through Regulation of ERK-Dependent Inhibition of S6K Signaling in Human Neural Stem Cells. Stem Cells Transl Med *5*, 1319-1329.

Lee, J.E., Lim, M.S., Park, J.H., Park, C.H., and Koh, H.C. (2016b). S6K Promotes Dopaminergic Neuronal Differentiation Through PI3K/Akt/mTOR-Dependent Signaling Pathways in Human Neural Stem Cells. Mol Neurobiol *53*, 3771-3782.

Lee, J.Y., Nakada, D., Yilmaz, O.H., Tothova, Z., Joseph, N.M., Lim, M.S., Gilliland, D.G., and Morrison, S.J. (2010a). mTOR activation induces tumor suppressors that inhibit leukemogenesis and deplete hematopoietic stem cells after Pten deletion. Cell Stem Cell *7*, 593-605.

Lee, K.C., Wong, W.K., and Feng, B. (2013). Decoding the Pluripotency Network: The Emergence of New Transcription Factors. Biomedicines *1*, 49-78.

Lee, K.W., Yook, J.Y., Son, M.Y., Kim, M.J., Koo, D.B., Han, Y.M., and Cho, Y.S. (2010b). Rapamycin promotes the osteoblastic differentiation of human embryonic stem cells by blocking the mTOR pathway and stimulating the BMP/Smad pathway. Stem Cells Dev *19*, 557-568.

Lefort, N., Feyeux, M., Bas, C., Feraud, O., Bennaceur-Griscelli, A., Tachdjian, G., Peschanski, M., and Perrier, A.L. (2008). Human embryonic stem cells reveal recurrent genomic instability at 20q11.21. Nat Biotechnol *26*, 1364-1366.

Li, J., Wang, G., Wang, C., Zhao, Y., Zhang, H., Tan, Z., Song, Z., Ding, M., and Deng, H. (2007). MEK/ERK signaling contributes to the maintenance of human embryonic stem cell self-renewal. Differentiation *75*, 299-307.

Li, M., Yu, J.S.L., Tilgner, K., Ong, S.H., Koike-Yusa, H., and Yusa, K. (2018a). Genome-wide CRISPR-KO Screen Uncovers mTORC1-Mediated Gsk3 Regulation in Naive Pluripotency Maintenance and Dissolution. Cell Rep *24*, 489-502.

Li, X., and Gao, T. (2014). mTORC2 phosphorylates protein kinase Czeta to regulate its stability and activity. EMBO Rep *15*, 191-198.

Li, X.L., Li, G.H., Fu, J., Fu, Y.W., Zhang, L., Chen, W., Arakaki, C., Zhang, J.P., Wen, W., Zhao, M.*, et al.* (2018b). Highly efficient genome editing via CRISPR-Cas9 in human pluripotent stem cells is achieved by transient BCL-XL overexpression. Nucleic Acids Res *46*, 10195-10215.

Li, X., Zhu, L., Yang, A., Lin, J., Tang, F., Jin, S., Wei, Z., Li, J., and Jin, Y. (2011). Calcineurin-NFAT signaling critically regulates early lineage specification in mouse embryonic stem cells and embryos. Cell Stem Cell *8*, 46-58.

Liang, X., Potter, J., Kumar, S., Zou, Y., Quintanilla, R., Sridharan, M., Carte, J., Chen, W., Roark, N., Ranganathan, S.*, et al.* (2015). Rapid and highly efficient mammalian cell engineering via Cas9 protein transfection. J Biotechnol *208*, 44-53.

LiCausi, F., and Hartman, N.W. (2018). Role of mTOR Complexes in Neurogenesis. Int J Mol *19*.

Liu, C., Zhang, L., Liu, H., and Cheng, K. (2017). Delivery strategies of the CRISPR-Cas9 gene-editing system for therapeutic applications. J Control Release *266*, 17-26.

Liu, P., Gan, W., Chin, Y.R., Ogura, K., Guo, J., Zhang, J., Wang, B., Blenis, J., Cantley, L.C., Toker, A.*, et al.* (2015). PtdIns(3,4,5)P3-Dependent Activation of the mTORC2 Kinase Complex. Cancer Discov *5*, 1194-1209.

Liu, P., Gan, W., Inuzuka, H., Lazorchak, A.S., Gao, D., Arojo, O., Liu, D., Wan, L., Zhai, B., Yu, Y.*, et al.* (2013). Sin1 phosphorylation impairs mTORC2 complex integrity and inhibits downstream Akt signalling to suppress tumorigenesis. Nat Cell Biol *15*, 1340-1350.

Liu, P., Guo, J., Gan, W., and Wei, W. (2014). Dual phosphorylation of Sin1 at T86 and T398 negatively regulates mTORC2 complex integrity and activity. Protein Cell *5*, 171-177.

Liu, Z., Hui, Y., Shi, L., Chen, Z., Xu, X., Chi, L., Fan, B., Fang, Y., Liu, Y., Ma, L.*, et al.* (2016). Efficient CRISPR/Cas9-Mediated Versatile, Predictable, and Donor-Free Gene Knockout in Human Pluripotent Stem Cells. Stem Cell Rep *7*, 496-507.

Loffing, J., Flores, S.Y., and Staub, O. (2006). Sgk kinases and their role in epithelial transport. Annu Rev Physiol *68*, 461-490.

Lu, M., Wang, J., Ives, H.E., and Pearce, D. (2011). mSIN1 protein mediates SGK1 protein interaction with mTORC2 protein complex and is required for selective activation of the epithelial sodium channel. J Biol Chem *286*, 30647-30654.

Luo, Y., Li, L., Zou, P., Wang, J., Shao, L., Zhou, D., and Liu, L. (2014). Rapamycin enhances long-term hematopoietic reconstitution of ex vivo expanded mouse hematopoietic stem cells by inhibiting senescence. Transplantation *97*, 20-29.

Ma, D., and Liu, F. (2015). Genome Editing and Its Applications in Model Organisms. Genomics Proteomics Bioinformatics *13*, 336-344.

Ma, X.M., Yoon, S.O., Richardson, C.J., Julich, K., and Blenis, J. (2008). SKAR links pre-mRNA splicing to mTOR/S6K1-mediated enhanced translation efficiency of spliced mRNAs. Cell *133*, 303-313.

Maji, B., Moore, C.L., Zetsche, B., Volz, S.E., Zhang, F., Shoulders, M.D., and Choudhary, A. (2017). Multidimensional chemical control of CRISPR-Cas9. Nat Chem Biol *13*, 9-11.

Makino, C., Sano, Y., Shinagawa, T., Millar, J.B., and Ishii, S. (2006). Sin1 binds to both ATF-2 and p38 and enhances ATF-2-dependent transcription in an SAPK signaling pathway. Genes Cells *11*, 1239-1251.

Mali, P., Yang, L., Esvelt, K.M., Aach, J., Guell, M., DiCarlo, J.E., Norville, J.E., and Church, G.M. (2013). RNA-guided human genome engineering via Cas9. Science *339*, 823-826.

Manning, B.D., and Cantley, L.C. (2007). AKT/PKB signaling: navigating downstream. Cell *129*, 1261-1274.

Manning, B.D., Tee, A.R., Logsdon, M.N., Blenis, J., and Cantley, L.C. (2002). Identification of the tuberous sclerosis complex-2 tumor suppressor gene product tuberin as a target of the phosphoinositide 3-kinase/akt pathway. Mol Cell *10*, 151-162.

Martin, F., Sanchez-Hernandez, S., Gutierrez-Guerrero, A., Pinedo-Gomez, J., and Benabdellah, K. (2016). Biased and Unbiased Methods for the Detection of Off-Target Cleavage by CRISPR/Cas9: An Overview. Int J Mol *17*.

Martin, G.R. (1981). Isolation of a pluripotent cell line from early mouse embryos cultured in medium conditioned by teratocarcinoma stem cells. Proc Natl Acad Sci U S A *78*, 7634-7638.

Martin, S.K., Fitter, S., Dutta, A.K., Matthews, M.P., Walkley, C.R., Hall, M.N., Ruegg, M.A., Gronthos, S., and Zannettino, A.C. (2015). Brief report: the differential roles of mTORC1 and mTORC2 in mesenchymal stem cell differentiation. Stem Cells *33*, 1359-1365.

Martina, J.A., Chen, Y., Gucek, M., and Puertollano, R. (2012). MTORC1 functions as a transcriptional regulator of autophagy by preventing nuclear transport of TFEB. Autophagy *8*, 903-914.

Martinez, R.A., Stein, J.L., Krostag, A.R., Nelson, A.M., Marken, J.S., Menon, V., May, R.C., Yao, Z., Kaykas, A., Geschwind, D.H.*, et al.* (2015). Genome engineering of isogenic human ES cells to model autism disorders. Nucleic Acids Res *43*, e65.

Masri, J., Bernath, A., Martin, J., Jo, O.D., Vartanian, R., Funk, A., and Gera, J. (2007). mTORC2 activity is elevated in gliomas and promotes growth and cell motility via overexpression of rictor. Cancer Res *67*, 11712-11720.

Masui, S., Ohtsuka, S., Yagi, R., Takahashi, K., Ko, M.S., and Niwa, H. (2008). Rex1/Zfp42 is dispensable for pluripotency in mouse ES cells. BMC Dev Biol *8*, 45.

Mathieu, J., Detraux, D., Kuppers, D., Wang, Y., Cavanaugh, C., Sidhu, S., Levy, S., Robitaille, A.M., Ferreccio, A., Bottorff, T.*, et al.* (2019). Folliculin regulates mTORC1/2 and WNT pathways in early human pluripotency. Nat Commun *10*, 632.

McDonald, P.C., Oloumi, A., Mills, J., Dobreva, I., Maidan, M., Gray, V., Wederell, E.D., Bally, M.B., Foster, L.J., and Dedhar, S. (2008). Rictor and integrin-linked kinase interact and regulate Akt phosphorylation and cancer cell survival. Cancer Res *68*, 1618-1624.

McGranahan, N., and Swanton, C. (2017). Clonal Heterogeneity and Tumor Evolution: Past, Present, and the Future. Cell *168*, 613-628.

McLean, A.B., D'Amour, K.A., Jones, K.L., Krishnamoorthy, M., Kulik, M.J., Reynolds, D.M., Sheppard, A.M., Liu, H., Xu, Y., Baetge, E.E.*, et al.* (2007). Activin a efficiently specifies definitive endoderm from human embryonic stem cells only when phosphatidylinositol 3-kinase signaling is suppressed. Stem Cells *25*, 29-38.

Mendoza, M.C., Er, E.E., and Blenis, J. (2011). The Ras-ERK and PI3K-mTOR pathways: cross-talk and compensation. Trends Biochem Sci *36*, 320-328.

Merkle, F.T., Neuhausser, W.M., Santos, D., Valen, E., Gagnon, J.A., Maas, K., Sandoe, J., Schier, A.F., and Eggan, K. (2015). Efficient CRISPR-Cas9-mediated generation of knockin human pluripotent stem cells lacking undesired mutations at the targeted locus. Cell Rep *11*, 875-883.

Mitsui, K., Tokuzawa, Y., Itoh, H., Segawa, K., Murakami, M., Takahashi, K., Maruyama, M., Maeda, M., and Yamanaka, S. (2003). The homeoprotein Nanog is required for maintenance of pluripotency in mouse epiblast and ES cells. Cell *113*, 631-642.

Mohr, J.C., Zhang, J., Azarin, S.M., Soerens, A.G., de Pablo, J.J., Thomson, J.A., Lyons, G.E., Palecek, S.P., and Kamp, T.J. (2010). The microwell control of embryoid body size in order to regulate cardiac differentiation of human embryonic stem cells. Biomaterials *31*, 1885-1893.

Mummery, C.L., Zhang, J., Ng, E.S., Elliott, D.A., Elefanty, A.G., and Kamp, T.J. (2012). Differentiation of human embryonic stem cells and induced pluripotent stem cells to cardiomyocytes: a methods overview. Circ Res *111*, 344-358.

Murakami, M., Ichisaka, T., Maeda, M., Oshiro, N., Hara, K., Edenhofer, F., Kiyama, H., Yonezawa, K., and Yamanaka, S. (2004). mTOR is essential for growth and proliferation in early mouse embryos and embryonic stem cells. Mol Cell Biol *24*, 6710-6718.

Nazareth, E.J.P., Rahman, N., Yin, T., and Zandstra, P.W. (2016). A Multi-Lineage Screen Reveals mTORC1 Inhibition Enhances Human Pluripotent Stem Cell Mesendoderm and Blood Progenitor Production. Stem Cell Rep *6*, 679-691.

Nemeth, J.A., Harb, J.F., Barroso, U., Jr., He, Z., Grignon, D.J., and Cher, M.L. (1999). Severe combined immunodeficient-hu model of human prostate cancer metastasis to human bone. Cancer Res *59*, 1987-1993.

Nichols, J., and Smith, A. (2009). Naive and primed pluripotent states. Cell Stem Cell *4*, 487-492.

Nichols, J., and Smith, A. (2011). The origin and identity of embryonic stem cells. Development *138*, 3-8.

Nichols, J., Zevnik, B., Anastassiadis, K., Niwa, H., Klewe-Nebenius, D., Chambers, I., Scholer, H., and Smith, A. (1998). Formation of pluripotent stem cells in the mammalian embryo depends on the POU transcription factor Oct4. Cell *95*, 379-391.

Nojima, H., Tokunaga, C., Eguchi, S., Oshiro, N., Hidayat, S., Yoshino, K., Hara, K., Tanaka, N., Avruch, J., and Yonezawa, K. (2003). The mammalian target of rapamycin (mTOR) partner, raptor, binds the mTOR substrates p70 S6 kinase and 4E-BP1 through their TOR signaling (TOS) motif. J Biol Chem *278*, 15461-15464.

Ogawa, T., Tokuda, M., Tomizawa, K., Matsui, H., Itano, T., Konishi, R., Nagahata, S., and Hatase, O. (1998). Osteoblastic differentiation is enhanced by rapamycin in rat osteoblast-like osteosarcoma (ROS 17/2.8) cells. Biochem Biophys Res Commun *249*, 226-230.

Oh, W.J., and Jacinto, E. (2011). mTOR complex 2 signaling and functions. Cell Cycle *10*, 2305-2316.

Ohgushi, M., Matsumura, M., Eiraku, M., Murakami, K., Aramaki, T., Nishiyama, A., Muguruma, K., Nakano, T., Suga, H., Ueno, M.*, et al.* (2010). Molecular pathway and cell state responsible for dissociation-induced apoptosis in human pluripotent stem cells. Cell Stem Cell *7*, 225-239.

Ostrow, S.L., Barshir, R., DeGregori, J., Yeger-Lotem, E., and Hershberg, R. (2014). Cancer evolution is associated with pervasive positive selection on globally expressed genes. PLoS Genet *10*, e1004239.

Park, J., Leong, M.L., Buse, P., Maiyar, A.C., Firestone, G.L., and Hemmings, B.A. (1999). Serum and glucocorticoid-inducible kinase (SGK) is a target of the PI 3-kinase-stimulated signaling pathway. EMBO J *18*, 3024-3033.

Pauklin, S., and Vallier, L. (2015). Activin/Nodal signalling in stem cells. Development *142*, 607-619.

Pearce, L.R., Huang, X., Boudeau, J., Pawlowski, R., Wullschleger, S., Deak, M., Ibrahim, A.F., Gourlay, R., Magnuson, M.A., and Alessi, D.R. (2007). Identification of Protor as a novel Rictor-binding component of mTOR complex-2. Biochem J *405*, 513-522.

Pearce, L.R., Sommer, E.M., Sakamoto, K., Wullschleger, S., and Alessi, D.R. (2011). Protor-1 is required for efficient mTORC2-mediated activation of SGK1 in the kidney. Biochem J *436*, 169-179.

Peterson, T.R., Laplante, M., Thoreen, C.C., Sancak, Y., Kang, S.A., Kuehl, W.M., Gray, N.S., and Sabatini, D.M. (2009). DEPTOR is an mTOR inhibitor frequently overexpressed in multiple myeloma cells and required for their survival. Cell *137*, 873-886.

Peterson, T.R., Sengupta, S.S., Harris, T.E., Carmack, A.E., Kang, S.A., Balderas, E., Guertin, D.A., Madden, K.L., Carpenter, A.E., Finck, B.N.*, et al.* (2011). mTOR complex 1 regulates lipin 1 localization to control the SREBP pathway. Cell *146*, 408-420.

Pettinato, G., Wen, X., and Zhang, N. (2014). Formation of well-defined embryoid bodies from dissociated human induced pluripotent stem cells using microfabricated cell-repellent microwell arrays. Sci Rep *4*, 7402.

Pieters, T., and van Roy, F. (2014). Role of cell-cell adhesion complexes in embryonic stem cell biology. J Cell Sci *127*, 2603-2613.

Polak, P., Cybulski, N., Feige, J.N., Auwerx, J., Ruegg, M.A., and Hall, M.N. (2008). Adipose-specific knockout of raptor results in lean mice with enhanced mitochondrial respiration. Cell Metab *8*, 399-410.

Populo, H., Lopes, J.M., and Soares, P. (2012). The mTOR signalling pathway in human cancer. Int J Mol *13*, 1886-1918.

Price, D.J., Grove, J.R., Calvo, V., Avruch, J., and Bierer, B.E. (1992). Rapamycin-induced inhibition of the 70-kilodalton S6 protein kinase. Science *257*, 973-977.

Ramakrishna, S., Kwaku Dad, A.B., Beloor, J., Gopalappa, R., Lee, S.K., and Kim, H. (2014). Gene disruption by cell-penetrating peptide-mediated delivery of Cas9 protein and guide RNA. Genome Res *24*, 1020-1027.

Ran, F.A., Hsu, P.D., Lin, C.Y., Gootenberg, J.S., Konermann, S., Trevino, A.E., Scott, D.A., Inoue, A., Matoba, S., Zhang, Y*., et al.* (2013a). Double nicking by RNA-guided CRISPR Cas9 for enhanced genome editing specificity. Cell *154*, 1380-1389.

Ran, F.A., Hsu, P.D., Wright, J., Agarwala, V., Scott, D.A., and Zhang, F. (2013b). Genome engineering using the CRISPR-Cas9 system. Nat Protoc *8*, 2281.

Ranganathan, V., Wahlin, K., Maruotti, J., and Zack, D.J. (2014). Expansion of the CRISPR-Cas9 genome targeting space through the use of H1 promoter-expressed guide RNAs. Nat Commun *5*, 4516.

Richter, A., Valdimarsdottir, L., Hrafnkelsdottir, H.E., Runarsson, J.F., Omarsdottir, A.R., Ward-van Oostwaard, D., Mummery, C., and Valdimarsdottir, G. (2014). BMP4 promotes EMT and mesodermal commitment in human embryonic stem cells via SLUG and MSX2. Stem Cells *32*, 636-648.

Roczniak-Ferguson, A., Petit, C.S., Froehlich, F., Qian, S., Ky, J., Angarola, B., Walther, T.C., and Ferguson, S.M. (2012). The transcription factor TFEB links mTORC1 signaling to transcriptional control of lysosome homeostasis. Sci Signal *5*, ra42.

Rogers, M.B., Hosler, B.A., and Gudas, L.J. (1991). Specific expression of a retinoic acid-regulated, zinc-finger gene, Rex-1, in preimplantation embryos, trophoblast and spermatocytes. Development *113*, 815-824.

Rogers, S., Wells, R., and Rechsteiner, M. (1986). Amino acid sequences common to rapidly degraded proteins: the PEST hypothesis. Science *234*, 364-368.

Rosner, M., Fuchs, C., Siegel, N., Valli, A., and Hengstschlager, M. (2009). Functional interaction of mammalian target of rapamycin complexes in regulating mammalian cell size and cell cycle. Hum Mol Genet *18*, 3298-3310.

Sabatini, D.M., Erdjument-Bromage, H., Lui, M., Tempst, P., and Snyder, S.H. (1994). RAFT1: a mammalian protein that binds to FKBP12 in a rapamycin-dependent fashion and is homologous to yeast TORs. Cell *78*, 35-43.

Sancak, Y., Bar-Peled, L., Zoncu, R., Markhard, A.L., Nada, S., and Sabatini, D.M. (2010). Ragulator-Rag complex targets mTORC1 to the lysosomal surface and is necessary for its activation by amino acids. Cell *141*, 290-303.

Sancak, Y., Peterson, T.R., Shaul, Y.D., Lindquist, R.A., Thoreen, C.C., Bar-Peled, L., and Sabatini, D.M. (2008). The Rag GTPases bind raptor and mediate amino acid signaling to mTORC1. Science *320*, 1496-1501.

Sancak, Y., Thoreen, C.C., Peterson, T.R., Lindquist, R.A., Kang, S.A., Spooner, E., Carr, S.A., and Sabatini, D.M. (2007). PRAS40 is an insulin-regulated inhibitor of the mTORC1 protein kinase. Mol Cell *25*, 903-915.

Sarbassov, D.D., Ali, S.M., Kim, D.H., Guertin, D.A., Latek, R.R., Erdjument-Bromage, H., Tempst, P., and Sabatini, D.M. (2004). Rictor, a novel binding partner of mTOR, defines a rapamycin-insensitive and raptor-independent pathway that regulates the cytoskeleton. Curr Biol *14*, 1296-1302.

Sarbassov, D.D., Ali, S.M., Sengupta, S., Sheen, J.H., Hsu, P.P., Bagley, A.F., Markhard, A.L., and Sabatini, D.M. (2006). Prolonged rapamycin treatment inhibits mTORC2 assembly and Akt/PKB. Mol Cell *22*, 159-168.

Sarbassov, D.D., Guertin, D.A., Ali, S.M., and Sabatini, D.M. (2005). Phosphorylation and regulation of Akt/PKB by the rictor-mTOR complex. Science *307*, 1098-1101.

Saxton, R.A., and Sabatini, D.M. (2017). mTOR Signaling in Growth, Metabolism, and Disease. Cell *169*, 361-371.

Schalm, S.S., Fingar, D.C., Sabatini, D.M., and Blenis, J. (2003). TOS motif-mediated raptor binding regulates 4E-BP1 multisite phosphorylation and function. Curr Biol *13*, 797-806.

Schmidt, K.M., Hellerbrand, C., Ruemmele, P., Michalski, C.W., Kong, B., Kroemer, A., Hackl, C., Schlitt, H.J., Geissler, E.K., and Lang, S.A. (2017). Inhibition of mTORC2 component RICTOR impairs tumor growth in pancreatic cancer models. Oncotarget *8*, 24491-24505.

Schneider, G., Schmidt-Supprian, M., Rad, R., and Saur, D. (2017). Tissue-specific tumorigenesis: context matters. Nat Rev Cancer *17*, 239-253.

Schreiber, K.H., Ortiz, D., Academia, E.C., Anies, A.C., Liao, C.Y., and Kennedy, B.K. (2015). Rapamycin-mediated mTORC2 inhibition is determined by the relative expression of FK506-binding proteins. Aging Cell *14*, 265-273.

Schroder, W., Bushell, G., and Sculley, T. (2005). The human stress-activated protein kinase-interacting 1 gene encodes JNK-binding proteins. Cell Signal *17*, 761-767.

Schroder, W., Cloonan, N., Bushell, G., and Sculley, T. (2004). Alternative polyadenylation and splicing of mRNAs transcribed from the human Sin1 gene. Gene *339*, 17-23.

Schroder, W.A., Buck, M., Cloonan, N., Hancock, J.F., Suhrbier, A., Sculley, T., and Bushell, G. (2007). Human Sin1 contains Ras-binding and pleckstrin homology domains and suppresses Ras signalling. Cell Signal *19*, 1279-1289.

Selman, C., Tullet, J.M., Wieser, D., Irvine, E., Lingard, S.J., Choudhury, A.I., Claret, M., Al-Qassab, H., Carmignac, D., Ramadani, F.*, et al.* (2009). Ribosomal protein S6 kinase 1 signaling regulates mammalian life span. Science *326*, 140-144.

Settembre, C., Zoncu, R., Medina, D.L., Vetrini, F., Erdin, S., Erdin, S., Huynh, T., Ferron, M., Karsenty, G., Vellard, M.C.*, et al.* (2012). A lysosome-to-nucleus signalling mechanism senses and regulates the lysosome via mTOR and TFEB. EMBO J *31*, 1095-1108.

Shah, O.J., Wang, Z., and Hunter, T. (2004). Inappropriate activation of the TSC/Rheb/mTOR/S6K cassette induces IRS1/2 depletion, insulin resistance, and cell survival deficiencies. Curr Biol *14*, 1650-1656.

Shao, T., and Liu, X. (2015). Identification of rictor as a novel substrate of Polo-like kinase 1. Cell Cycle *14*, 755-760.

Shimobayashi, M., and Hall, M.N. (2014). Making new contacts: the mTOR network in metabolism and signalling crosstalk. Nat Rev Mol Cell Biol *15*, 155-162.

Shiota, C., Woo, J.T., Lindner, J., Shelton, K.D., and Magnuson, M.A. (2006). Multiallelic disruption of the rictor gene in mice reveals that mTOR complex 2 is essential for fetal growth and viability. Dev Cell *11*, 583-589.

Signer, R.A., and Morrison, S.J. (2013). Mechanisms that regulate stem cell aging and life span. Cell Stem Cell *12*, 152-165.

Singh, A.M., Reynolds, D., Cliff, T., Ohtsuka, S., Mattheyses, A.L., Sun, Y., Menendez, L., Kulik, M., and Dalton, S. (2012). Signaling network crosstalk in human pluripotent cells: a Smad2/3-regulated switch that controls the balance between self-renewal and differentiation. Cell Stem Cell *10*, 312-326.

Singha, U.K., Jiang, Y., Yu, S., Luo, M., Lu, Y., Zhang, J., and Xiao, G. (2008). Rapamycin inhibits osteoblast proliferation and differentiation in MC3T3-E1 cells and primary mouse bone marrow stromal cells. J Cell Biochem *103*, 434-446.

Siuta, M.A., Robertson, S.D., Kocalis, H., Saunders, C., Gresch, P.J., Khatri, V., Shiota, C., Kennedy, J.P., Lindsley, C.W., Daws, L.C.*, et al.* (2010). Dysregulation of the norepinephrine transporter sustains cortical hypodopaminergia and schizophrenia-like behaviors in neuronal rictor null mice. PLoS Biol *8*, e1000393.

Skalecka, A., Liszewska, E., Bilinski, R., Gkogkas, C., Khoutorsky, A., Malik, A.R., Sonenberg, N., and Jaworski, J. (2016). mTOR kinase is needed for the development and stabilization of dendritic arbors in newly born olfactory bulb neurons. Dev Neurobiol *76*, 1308-1327.

Slaymaker, I.M., Gao, L., Zetsche, B., Scott, D.A., Yan, W.X., and Zhang, F. (2016). Rationally engineered Cas9 nucleases with improved specificity. Science *351*, 84-88.

Smith, C., Gore, A., Yan, W., Abalde-Atristain, L., Li, Z., He, C., Wang, Y., Brodsky, R.A., Zhang, K., Cheng, L.*, et al.* (2014). Whole-genome sequencing analysis reveals high specificity of CRISPR/Cas9 and TALEN-based genome editing in human iPSCs. Cell Stem Cell *15*, 12-13.

Smrz, D., Cruse, G., Beaven, M.A., Kirshenbaum, A., Metcalfe, D.D., and Gilfillan, A.M. (2014). Rictor negatively regulates high-affinity receptors for IgE-induced mast cell degranulation. J Immunol *193*, 5924-5932.

Son, M.Y., Choi, H., Han, Y.M., and Cho, Y.S. (2013). Unveiling the critical role of REX1 in the regulation of human stem cell pluripotency. Stem Cells *31*, 2374-2387.

Son, M.Y., Kim, H.J., Kim, M.J., and Cho, Y.S. (2011). Physical passaging of embryoid bodies generated from human pluripotent stem cells. PLoS One *6*, e19134.

Song, G., Ouyang, G., and Bao, S. (2005). The activation of Akt/PKB signaling pathway and cell survival. J Cell Mol Med *9*, 59-71.

Song, H.Y., Chien, C.S., Yarmishyn, A.A., Chou, S.J., Yang, Y.P., Wang, M.L., Wang, C.Y., Leu, H.B., Yu, W.C., Chang, Y.L.*, et al.* (2019). Generation of GLA-Knockout Human Embryonic Stem Cell Lines to Model Autophagic Dysfunction and Exosome Secretion in Fabry Disease-Associated Hypertrophic Cardiomyopathy. Cells *8*.

Stuttfeld, E., Aylett, C.H., Imseng, S., Boehringer, D., Scaiola, A., Sauer, E., Hall, M.N., Maier, T., and Ban, N. (2018). Architecture of the human mTORC2 core complex. Elife *7*.

Takahashi, S., Kobayashi, S., and Hiratani, I. (2018). Epigenetic differences between naive and primed pluripotent stem cells. Cell Mol Life Sci *75*, 1191-1203.

Tan, Y., Chu, A.H.Y., Bao, S., Hoang, D.A., Kebede, F.T., Xiong, W., Ji, M., Shi, J., and Zheng, Z. (2019). Rationally engineered Staphylococcus aureus Cas9 nucleases with high genome-wide specificity. Proc Natl Acad Sci U S A *116*, 20969-20976.

Tatebe, H., Murayama, S., Yonekura, T., Hatano, T., Richter, D., Furuya, T., Kataoka, S., Furuita, K., Kojima, C., and Shiozaki, K. (2017). Substrate specificity of TOR complex 2 is determined by a ubiquitin-fold domain of the Sin1 subunit. Elife *6*.

Tato, I., Bartrons, R., Ventura, F., and Rosa, J.L. (2011). Amino acids activate mammalian target of rapamycin complex 2 (mTORC2) via PI3K/Akt signaling. J Biol Chem *286*, 6128-6142.

Tesar, P.J., Chenoweth, J.G., Brook, F.A., Davies, T.J., Evans, E.P., Mack, D.L., Gardner, R.L., and McKay, R.D. (2007). New cell lines from mouse epiblast share defining features with human embryonic stem cells. Nature *448*, 196-199.

Theunissen, T.W., Powell, B.E., Wang, H., Mitalipova, M., Faddah, D.A., Reddy, J., Fan, Z.P., Maetzel, D., Ganz, K., Shi, L.*, et al.* (2014). Systematic Identification of Culture Conditions for Induction and Maintenance of Naive Human Pluripotency. Cell Stem Cell *15*, 524-526.

Thomanetz, V., Angliker, N., Cloetta, D., Lustenberger, R.M., Schweighauser, M., Oliveri, F., Suzuki, N., and Ruegg, M.A. (2013). Ablation of the mTORC2 component rictor in brain or Purkinje cells affects size and neuron morphology. J Cell Biol *201*, 293-308.

Thomson, J.A., Itskovitz-Eldor, J., Shapiro, S.S., Waknitz, M.A., Swiergiel, J.J., Marshall, V.S., and Jones, J.M. (1998). Embryonic stem cell lines derived from human blastocysts. Science *282*, 1145-1147.

Treins, C., Warne, P.H., Magnuson, M.A., Pende, M., and Downward, J. (2010). Rictor is a novel target of p70 S6 kinase-1. Oncogene *29*, 1003-1016.

Tsai, S.Q., Zheng, Z., Nguyen, N.T., Liebers, M., Topkar, V.V., Thapar, V., Wyvekens, N., Khayter, C., Iafrate, A.J., Le, L.P.*, et al.* (2015). GUIDE-seq enables genome-wide profiling of off-target cleavage by CRISPR-Cas nucleases. Nat Biotechnol *33*, 187-197.

Urnov, F.D., Rebar, E.J., Holmes, M.C., Zhang, H.S., and Gregory, P.D. (2010). Genome editing with engineered zinc finger nucleases. Nat Rev Genet *11*, 636-646.

Vallier, L., Mendjan, S., Brown, S., Chng, Z., Teo, A., Smithers, L.E., Trotter, M.W., Cho, C.H., Martinez, A., Rugg-Gunn, P.*, et al.* (2009). Activin/Nodal signalling maintains pluripotency by controlling Nanog expression. Development *136*, 1339-1349.

van den Berg, M.C., and Burgering, B.M. (2011). Integrating opposing signals toward Forkhead box O. Antioxid Redox Signal *14*, 607-621.

Vander Haar, E., Lee, S.I., Bandhakavi, S., Griffin, T.J., and Kim, D.H. (2007). Insulin signalling to mTOR mediated by the Akt/PKB substrate PRAS40. Nat Cell Biol *9*, 316-323.

Vanhaesebroeck, B., and Alessi, D.R. (2000). The PI3K-PDK1 connection: more than just a road to PKB. Biochem J *346 Pt 3*, 561-576.

Vazin, T., and Freed, W.J. (2010). Human embryonic stem cells: derivation, culture, and differentiation: a review. Restor Neurol Neuros *28*, 589-603.

Vezina, C., Kudelski, A., and Sehgal, S.N. (1975). Rapamycin (AY-22,989), a new antifungal antibiotic. I. Taxonomy of the producing streptomycete and isolation of the active principle. J Antibiot *28*, 721-726.

Vilarino, M., Rashid, S.T., Suchy, F.P., McNabb, B.R., van der Meulen, T., Fine, E.J., Ahsan, S., Mursaliyev, N., Sebastiano, V., Diab, S.S.*, et al.* (2017). CRISPR/Cas9 microinjection in oocytes disables pancreas development in sheep. Sci Rep *7*, 17472.

Volkers, M., Konstandin, M.H., Doroudgar, S., Toko, H., Quijada, P., Din, S., Joyo, A., Ornelas, L., Samse, K., Thuerauf, D.J.*, et al.* (2013). Mechanistic target of rapamycin complex 2 protects the heart from ischemic damage. Circulation *128*, 2132-2144.

Wahane, S.D., Hellbach, N., Prentzell, M.T., Weise, S.C., Vezzali, R., Kreutz, C., Timmer, J., Krieglstein, K., Thedieck, K., and Vogel, T. (2014). PI3K-p110-alpha-subtype signalling

mediates survival, proliferation and neurogenesis of cortical progenitor cells via activation of mTORC2. J Neurochem *130*, 255-267.

Wang, H., La Russa, M., and Qi, L.S. (2016a). CRISPR/Cas9 in Genome Editing and Beyond. Annu Rev Biochem *85*, 227-264.

Wang, L., Harris, T.E., Roth, R.A., and Lawrence, J.C., Jr. (2007). PRAS40 regulates mTORC1 kinase activity by functioning as a direct inhibitor of substrate binding. J Biol Chem *282*, 20036-20044.

Wang, Q., Zhu, J., Wang, Y.W., Dai, Y., Wang, Y.L., Wang, C., Liu, J., Baker, A., Colburn, N.H., and Yang, H.S. (2017). Tumor suppressor Pdcd4 attenuates Sin1 translation to inhibit invasion in colon carcinoma. Oncogene *36*, 6225-6234.

Wang, S., Amato, K.R., Song, W., Youngblood, V., Lee, K., Boothby, M., Brantley-Sieders, D.M., and Chen, J. (2015). Regulation of endothelial cell proliferation and vascular assembly through distinct mTORC2 signaling pathways. Mol Cell Biol *35*, 1299-1313.

Wang, X., Chu, Y., Wang, W., and Yuan, W. (2016b). mTORC signaling in hematopoiesis. Int J Hematol *103*, 510-518.

Wang, X., Lin, G., Martins-Taylor, K., Zeng, H., and Xu, R.H. (2009). Inhibition of caspase-mediated anoikis is critical for basic fibroblast growth factor-sustained culture of human pluripotent stem cells. J Biol Chem *284*, 34054-34064.

Wang, Z., Oron, E., Nelson, B., Razis, S., and Ivanova, N. (2012). Distinct lineage specification roles for NANOG, OCT4, and SOX2 in human embryonic stem cells. Cell Stem Cell *10*, 440-454.

Ware, C.B., Nelson, A.M., Mecham, B., Hesson, J., Zhou, W., Jonlin, E.C., Jimenez-Caliani, A.J., Deng, X., Cavanaugh, C., Cook, S.*, et al.* (2014). Derivation of naive human embryonic stem cells. Proc Natl Acad Sci U S A *111*, 4484-4489.

Warrier, S., Van der Jeught, M., Duggal, G., Tilleman, L., Sutherland, E., Taelman, J., Popovic, M., Lierman, S., Chuva De Sousa Lopes, S., Van Soom, A.*, et al.* (2017). Direct comparison of distinct naive pluripotent states in human embryonic stem cells. Nat Commun *8*, 15055.

Watanabe, K., Ueno, M., Kamiya, D., Nishiyama, A., Matsumura, M., Wataya, T., Takahashi, J.B., Nishikawa, S., Nishikawa, S., Muguruma, K.*, et al.* (2007). A ROCK inhibitor permits survival of dissociated human embryonic stem cells. Nat Biotechnol *25*, 681-686.

Weinberger, L., Ayyash, M., Novershtern, N., and Hanna, J.H. (2016). Dynamic stem cell states: naive to primed pluripotency in rodents and humans. Nat Rev Mol Cell Biol *17*, 155-169.

Woo, S.Y., Kim, D.H., Jun, C.B., Kim, Y.M., Haar, E.V., Lee, S.I., Hegg, J.W., Bandhakavi, S., Griffin, T.J., and Kim, D.H. (2007). PRR5, a novel component of mTOR complex 2, regulates platelet-derived growth factor receptor beta expression and signaling. J Biol Chem *282*, 25604-25612.

Wu, X., Scott, D.A., Kriz, A.J., Chiu, A.C., Hsu, P.D., Dadon, D.B., Cheng, A.W., Trevino, A.E., Konermann, S., Chen, S.*, et al.* (2014). Genome-wide binding of the CRISPR endonuclease Cas9 in mammalian cells. Nat Biotechnol *32*, 670-676.

Xiao, L., Yuan, X., and Sharkis, S.J. (2006). Activin A maintains self-renewal and regulates fibroblast growth factor, Wnt, and bone morphogenic protein pathways in human embryonic stem cells. Stem Cells *24*, 1476-1486.

Xie, J., Wang, X., and Proud, C.G. (2018). Who does TORC2 talk to? Biochem J *475*, 1721-1738.

Xiong, C., Tang, D.Q., Xie, C.Q., Zhang, L., Xu, K.F., Thompson, W.E., Chou, W., Gibbons, G.H., Chang, L.J., Yang, L.J.*, et al.* (2005). Genetic engineering of human embryonic stem cells with lentiviral vectors. Stem Cells Dev *14*, 367-377.

Xu, D., Zhu, J., Jeong, S., Li, D., Hua, X., Huang, L., Zhang, J., Luo, Y., and Xia, Q. (2018). Rictor Deficiency Aggravates Hepatic Ischemia/Reperfusion Injury in Mice by Suppressing Autophagy and Regulating MAPK Signaling. Cell Physiol Biochem *45*, 2199-2212.

Xu, R.H., Chen, X., Li, D.S., Li, R., Addicks, G.C., Glennon, C., Zwaka, T.P., and Thomson, J.A. (2002). BMP4 initiates human embryonic stem cell differentiation to trophoblast. Nat Biotechnol *20*, 1261-1264.

Xu, R.H., Sampsell-Barron, T.L., Gu, F., Root, S., Peck, R.M., Pan, G., Yu, J., Antosiewicz-Bourget, J., Tian, S., Stewart, R.*, et al.* (2008). NANOG is a direct target of TGFbeta/activin-mediated SMAD signaling in human ESCs. Cell Stem Cell *3*, 196-206.

Yang, G., Murashige, D.S., Humphrey, S.J., and James, D.E. (2015). A Positive Feedback Loop between Akt and mTORC2 via SIN1 Phosphorylation. Cell Rep *12*, 937-943.

Yang, Q., Inoki, K., Ikenoue, T., and Guan, K.L. (2006). Identification of Sin1 as an essential TORC2 component required for complex formation and kinase activity. Genes Dev *20*, 2820-2832.

Yao, C.A., Ortiz-Vega, S., Sun, Y.Y., Chien, C.T., Chuang, J.H., and Lin, Y. (2017). Association of mSin1 with mTORC2 Ras and Akt reveals a crucial domain on mSin1 involved in Akt phosphorylation. Oncotarget *8*, 63392-63404.

Yilmaz, A., and Benvenisty, N. (2019). Defining Human Pluripotency. Cell Stem Cell *25*, 9-22.

Yilmaz, A., Peretz, M., Aharony, A., Sagi, I., and Benvenisty, N. (2018). Defining essential genes for human pluripotent stem cells by CRISPR-Cas9 screening in haploid cells. Nat Cell Biol *20*, 610-619.

Yilmaz, O.H., Valdez, R., Theisen, B.K., Guo, W., Ferguson, D.O., Wu, H., and Morrison, S.J. (2006). Pten dependence distinguishes haematopoietic stem cells from leukaemia-initiating cells. Nature *441*, 475-482.

Ying, Q.L., Wray, J., Nichols, J., Batlle-Morera, L., Doble, B., Woodgett, J., Cohen, P., and Smith, A. (2008). The ground state of embryonic stem cell self-renewal. Nature *453*, 519-523.

Yu, J.S., Ramasamy, T.S., Murphy, N., Holt, M.K., Czapiewski, R., Wei, S.K., and Cui, W. (2015). PI3K/mTORC2 regulates TGF-beta/Activin signalling by modulating Smad2/3 activity via linker phosphorylation. Nat Commun *6*, 7212.

Yu, Y., Yoon, S.O., Poulogiannis, G., Yang, Q., Ma, X.M., Villen, J., Kubica, N., Hoffman, G.R., Cantley, L.C., Gygi, S.P.*, et al.* (2011). Phosphoproteomic analysis identifies Grb10 as an mTORC1 substrate that negatively regulates insulin signaling. Science *332*, 1322-1326.

Yuan, Y., Pan, B., Sun, H., Chen, G., Su, B., and Huang, Y. (2015). Characterization of Sin1 Isoforms Reveals an mTOR-Dependent and Independent Function of Sin1gamma. PLoS One *10*, e0135017.

Zaehres, H., Lensch, M.W., Daheron, L., Stewart, S.A., Itskovitz-Eldor, J., and Daley, G.Q. (2005). High-efficiency RNA interference in human embryonic stem cells. Stem Cells *23*, 299-305.

Zhang, H.H., Huang, J., Duvel, K., Boback, B., Wu, S., Squillace, R.M., Wu, C.L., and Manning, B.D. (2009). Insulin stimulates adipogenesis through the Akt-TSC2-mTORC1 pathway. PLoS One *4*, e6189.

Zhang, X., Rielland, M., Yalcin, S., and Ghaffari, S. (2011a). Regulation and function of FoxO transcription factors in normal and cancer stem cells: what have we learned? Curr Drug Targets *12*, 1267-1283.

Zhang, X., Tang, N., Hadden, T.J., and Rishi, A.K. (2011b). Akt, FoxO and regulation of apoptosis. Biochim Biophys Acta *1813*, 1978-1986.

Zhang, X., Yalcin, S., Lee, D.F., Yeh, T.Y., Lee, S.M., Su, J., Mungamuri, S.K., Rimmele, P., Kennedy, M., Sellers, R.*, et al.* (2011c). FOXO1 is an essential regulator of pluripotency in human embryonic stem cells. Nat Cell Biol *13*, 1092-1099.

Zhao, H., and Jin, Y. (2017). Signaling networks in the control of pluripotency. Curr Opin Genet Dev *46*, 141-148.

Zhao, J., Zhai, B., Gygi, S.P., and Goldberg, A.L. (2015). mTOR inhibition activates overall protein degradation by the ubiquitin proteasome system as well as by autophagy. Proc Natl Acad Sci U S A *112*, 15790-15797.

Zhao, X., Lu, S., Nie, J., Hu, X., Luo, W., Wu, X., Liu, H., Feng, Q., Chang, Z., Liu, Y.*, et al.* (2014). Phosphoinositide-dependent kinase 1 and mTORC2 synergistically maintain postnatal heart growth and heart function in mice. Mol Cell Biol *34*, 1966-1975.

Zheng, B., Wang, J., Tang, L., Shi, J., and Zhu, D. (2017). mTORC1 and mTORC2 play different roles in regulating cardiomyocyte differentiation from embryonic stem cells. Int J Dev Biol *61*, 65-72.

Zhou, C., Yang, X., Sun, Y., Yu, H., Zhang, Y., and Jin, Y. (2016). Comprehensive profiling reveals mechanisms of SOX2-mediated cell fate specification in human ESCs and NPCs. Cell Res *26*, 171-189.

Zhou, J., Li, D., and Wang, F. (2012). Assessing the function of mTOR in human embryonic stem cells. Methods Mol Biol *821*, 361-372.

Zhou, J., Su, P., Wang, L., Chen, J., Zimmermann, M., Genbacev, O., Afonja, O., Horne, M.C., Tanaka, T., Duan, E.*, et al.* (2009). mTOR supports long-term self-renewal and suppresses mesoderm and endoderm activities of human embryonic stem cells. Proc Natl Acad Sci U S A *106*, 7840-7845.

Zinzalla, V., Stracka, D., Oppliger, W., and Hall, M.N. (2011). Activation of mTORC2 by association with the ribosome. Cell *144*, 757-768.

Zwaka, T.P., and Thomson, J.A. (2003). Homologous recombination in human embryonic stem cells. Nat Biotechnol *21*, 319-321.